ISSN 0021-9673

VOL. 598 NO. 2 MAY 15, 1992

THIS ISSUE COMPLETES VOL. 598

JOURNAL OF CHROMATOGRAPHY

INCLUDING ELECTROPHORESIS AND OTHER SEPARATION METHODS

ELSEVIER

JOURNAL OF CHROMATOGRAPHY

INCLUDING ELECTROPHORESIS AND OTHER SEPARATION METHODS

Scope. The *Journal of Chromatography* publishes papers on all aspects of chromatography, electrophoresis and related methods. Contributions consist mainly of research papers dealing with chromatographic theory, instrumental development and their applications. The section *Biomedical Applications*, which is under separate editorship, deals with the following aspects: developments in and applications of chromatographic and electrophoretic techniques related to clinical diagnosis or alterations during medical treatment; screening and profiling of body fluids or tissues with special reference to metabolic disorders; results from basic medical research with direct consequences in clinical practice; drug level monitoring and pharmacokinetic studies; clinical toxicology; analytical studies in occupational medicine.

Submission of Papers. Manuscripts (in English; *four* copies are required) should be submitted to: Editorial Office of *Journal of Chromatography*, P.O. Box 681, 1000 AR Amsterdam, Netherlands, Telefax (+31-20) 5862 304, or to: The Editor of *Journal of Chromatography, Biomedical Applications*, P.O. Box 681, 1000 AR Amsterdam, Netherlands. Review articles are invited or proposed by letter to the Editors. An outline of the proposed review should first be forwarded to the Editors for preliminary discussion prior to preparation. Submission of an article is understood to imply that the article is original and unpublished and is not being considered for publication elsewhere. For copyright regulations, see below.

Publication. The *Journal of Chromatography* (incl. *Biomedical Applications*) has 39 volumes in 1992. The subscription prices for 1992 are:

J. Chromatogr. (incl. *Cum. Indexes, Vols. 551–600*) + *Biomed. Appl.* (Vols. 573–611):
Dfl. 7722.00 plus Dfl. 1209.00 (p.p.h.) (total *ca.* US$ 4880.25)

J. Chromatogr. (incl. *Cum. Indexes, Vols. 551–600*) only (Vols. 585–611):
Dfl. 6210.00 plus Dfl. 837.00 (p.p.h.) (total *ca.* US$ 3850.75)

Biomed. Appl. only (Vols. 573–584):
Dfl. 2760.00 plus Dfl. 372.00 (p.p.h.) (total *ca.* US$ 1711.50).

Subscription Orders. The Dutch guilder price is definitive. The US$ price is subject to exchange-rate fluctuations and is given as a guide. Subscriptions are accepted on a prepaid basis only, unless different terms have been previously agreed upon. Subscriptions orders can be entered only by calender year (Jan.–Dec.) and should be sent to Elsevier Science Publishers, Journal Department, P.O. Box 211, 1000 AE Amsterdam, Netherlands, Tel. (+31-20) 5803 642, Telefax (+31-20) 5803 598, or to your usual subscription agent. Postage and handling charges include surface delivery except to the following countries where air delivery via SAL (Surface Air Lift) mail is ensured: Argentina, Australia, Brazil, Canada, China, Hong Kong, India, Israel, Japan*, Malaysia, Mexico, New Zealand, Pakistan, Singapore, South Africa, South Korea, Taiwan, Thailand, USA. *For Japan air delivery (SAL) requires 25% additional charge of the normal postage and handling charge. For all other countries airmail rates are available upon request. Claims for missing issues must be made within three months of our publication (mailing) date, otherwise such claims cannot be honoured free of charge. Back volumes of the *Journal of Chromatography* (Vols. 1–572) are available at Dfl. 217.00 (plus postage). Customers in the USA and Canada wishing information on this and other Elsevier journals, please contact Journal Information Center, Elsevier Science Publishing Co. Inc., 655 Avenue of the Americas, New York, NY 10010, USA, Tel. (+1-212) 633 3750, Telefax (+1-212) 633 3990.

Abstracts/Contents Lists published in Analytical Abstracts, Biochemical Abstracts, Biological Abstracts, Chemical Abstracts, Chemical Titles, Chromatography Abstracts, Clinical Chemistry Lookout, Current Contents/Life Sciences, Current Contents/Physical, Chemical & Earth Sciences, Deep-Sea Research/Part B: Oceanographic Literature Review, Excerpta Medica, Index Medicus, Mass Spectrometry Bulletin, PASCAL-CNRS, Pharmaceutical Abstracts, Referativnyi Zhurnal, Research Alert, Science Citation Index and Trends in Biotechnology.

See inside back cover for Publication Schedule, Information for Authors and information on Advertisements.

0021-9673/92/$05.00

This issue is printed on acid-free paper.

Printed in the Netherlands

VOL. 598, NO. 2 JOURNAL OF CHROMATOGRAPHY MAY 15, 1992

CONTENTS

(Abstracts/Contents Lists published in Analytical Abstracts, Biochemical Abstracts, Biological Abstracts, Chemical Abstracts, Chemical Titles, Chromatography Abstracts, Current Contents/Life Sciences, Current Contents/Physical, Chemical & Earth Sciences, Deep-Sea Research/Part B: Oceanographic Literature Review, Excerpta Medica, Index Medicus, Mass Spectrometry Bulletin, PASCAL-CRNS, Referativnyi Zhurnal, Research Alert and Science Citation Index)

REGULAR PAPERS

Column Liquid Chromatography

Gas Chromatography

(Continued overleaf)

Contents (continued)

In articles with more than one author, the name of the author to whom correspondence should be addressed is indicated in the article heading by a 6-pointed asterisk (*).

Journal of Chromatography Library, 50

Liquid Chromatography in Biomedical Analysis

edited by **T. Hanai,** *International Institute of Technological Analysis, Health Research Foundation, Kyoto, Japan*

This book presents a guide for the analysis of biomedically important compounds using modern liquid chromatographic techniques. After a brief summary of basic liquid chromatographic methods and optimization strategies, the main part of the book focuses on the various classes of biomedically important compounds: amino acids, catecholamines, carbohydrates, fatty acids, nucleotides, porphyrins, prostaglandins and steroid hormones. The different chapters discuss specialized techniques pertaining to each class of compounds, such as sample pretreatment, pre- and post-column derivatization, detection and quantification.

1991 xii + 296 pages
Price: US $ 138.50 / Dfl. 270.00
ISBN 0-444-87451-8

Contents:

Elsevier Science Publishers

P.O. Box 211, 1000 AE Amsterdam, The Netherlands
P.O. Box 882, Madison Square Station, New York, NY 10159, USA

CHROMATOGRAPHY ABSTRACTS

by E.R. **Adlard** *and* **P.A. Sewell** .

Volume 35 (1 volume in 10 issues):
ISSN 0268-6287. Subscription price: £529.00

AUDIENCE:

Analytical, research and industrial chemists

AIMS AND SCOPE

Chromatography Abstracts are designed to provide an essential service to chromatographers throughout the world. A team of well-qualified abstractors continuously scans all the major world journals for papers reporting advances in chromatographic techniques and their application to specific problems. A feature of the Abstracts is the detailed annual subject index, helping readers to locate information on a particular topic rapidly and, if desired, transfer this information to a data base. For the convenience of readers the Abstracts are divided into three sections on Gas, Liquid and Miscellaneous methods. The latter section includes thin–layer, supercritical fluid, gel permeation and affinity chromatography as well as associated techniques such as electrophoresis and field flow fractionation.

The Abstracts are sponsored by the Chromatographic Society and reflect the expanding interests of the Society by means of a gradual extension to cover other aspects of separation science, in addition to their comprehensive coverage of the ever–increasing chromatographic literature.

Orders and requests for sample copies should be sent to:
ELSEVIER SCIENCE PUBLISHERS LTD
Crown House, Linton Road, Barking, Essex, IG11 8JU, UK
for customers in North America
Elsevier Science Publishers, Journal Information Center,
655 Avenue of the Americas, New York, NY 10010, USA

Journal of Chromatography, 598 (1992) 153–158
Elsevier Science Publishers B.V., Amsterdam

CHROM. 24 097

Reversed- and normal-phase separations by high-temperature open-tubular column liquid chromatography

G. Liu☆, N. M. Djordjevic and F. Erni*

Sandoz Pharma AG, Analytical Research and Development, CH-4002 Basle (Switzerland)

(First received February 5th, 1992; revised manuscript received February 18th, 1992)

ABSTRACT

The selectivity and stability of some commercial reversed-phase open-tubular columns were studied under high-temperature conditions. Differently substituted chlorobenzenes were used as test compounds. Graphs of ln k' *versus* the number of chlorine atoms revealed the reversed-phase nature of the separations at elevated column temperature. Normal-phase separation of some aromatic hydroxy compounds on a cyanopropyl capillary column was also examined.

INTRODUCTION

In a previous paper [1], high-temperature open-tubular column liquid chromatography (HT-OTCLC) was proposed as a new approach to high efficiency in liquid chromatography. A total efficiency of over 10^6 theoretical plates was obtained on commercial 50 μm I.D. column.

Compared with liquid chromatography carried out at room temperature and on capillary columns with small bore (I.D. < 10 μm) [2–5], HT-OTCLC is advantageous in several respects. First, the applicability of commercially available 50–100 μm I.D. columns makes the construction of the OTCLC systems easier and difficulties in handling small-bore columns are circumvented. Second, the detection of the eluted solutes is less of a problem, as on-column UV detection is feasible for columns of I.D. $\approx$ 50 μm. For small-bore columns, applications have been limited to some solutes that can only be detected electrochemically [6] or with fluorescence [7].

Owing to the reduced viscosity of the mobile phase at elevated temperatures, long columns (up to 20 m) can be used to generate high total plate numbers. Not only can a high total efficiency be obtained on long columns, but also a larger sample volume (up to 30 nl) can be injected.

Some problems arise with use of high column temperature. Commercial capillary columns, designed for application in supercritical fluid chromatography, showed limited stability at elevated temperatures when tested in our study. Further, the use of a thick film coating may be necessary in order to have retention at temperatures between 150 and 200°C. Unfortunately, however, thicker films are not always available with commercial 50 μm I.D. columns.

In this study, our objective was to separate test mixtures by reversed- and normal-phase capillary liquid chromatography at high temperatures and to examine the selectivity of different stationary phases at temperatures up to 200°C.

EXPERIMENTAL

The experimental set-up has been detailed elsewhere [1]. SB-Biphenyl-30, SB-Octyl-50, SB-Methyl-100 and SE-54 capillary columns were obtained from Lee Scientific (Salt Lake City, UT, USA), a DB-225 column from J&W Scientific (Folsom, CA, USA) and an SE-54 column from Macherey–Nagel

☆ On leave from the Southwest Research Institute of Chemical Industry, Chengdu 610047, China.

0021-9673/92/$05.00

(Oensingen, Switzerland). All columns had I.D. 50 μm and a film thickness of 0.25 μm. Bare fused-silica capillaries were obtained from Polymicro Technologies (Phoenix, AZ, USA).

Acetonitrile, methanol and hexane were of HPLC grade from Rathburn (Walkerburn, UK). Synthetic test mixtures were prepared from the pure solutes obtained from Aldrich-Chemie (Steinheim, Germany) or Fluka (Buchs, Switzerland). The elution time of tropolone was used as the column dead time (t_0).

RESULTS AND DISCUSSION

Reversed-phase separation

Commonly used reversed-phase materials in column liquid chromatography are chemically bonded octyl and octadecane phases. On these column materials the retention mechanism is mainly based on hydrophobic interaction. The retention mechanism has not been studied in OTCLC at column temperatures up to 200°C. It is reasonable to expect that the reversed-phase nature of the separation will not change under HT-OTCLC conditions. To confirm this, we studied changes in retention with increase in the number of chlorine atoms in the homologous series of chlorobenzenes. Higher halogen substitution increases the hydrophobic properties of organic molecules. The dependence of log k' (k' = capacity factor) of various chlorobenzene solutes on the number of chlorine atoms at different column temperatures and different concentrations of organic solvent (percentage of acetonitrile) in the mobile phase is depicted in Figs. 1 and 2, respectively. In both instances log k' increased linearly with increase in the number of chlorine atoms. This, together with the fact that the retention increased when concentration of acetonitrile decreased from 60 to 40%, indicates the reversed-phase nature of the separations.

In the temperature range 150–200°C, a 10% change in concentration of acetonitrile in the mobile phase produced a twofold change in k' for chlorobenzenes with $k' > 0.1$. This was in agreement with published data for chloronaphthalene [8] and alkyl phthalate solutes [9] on reversed-phase packing materials at lower column temperatures. Also, a temperature change of 50°C was needed to produce a 50% change in retention. According to the two

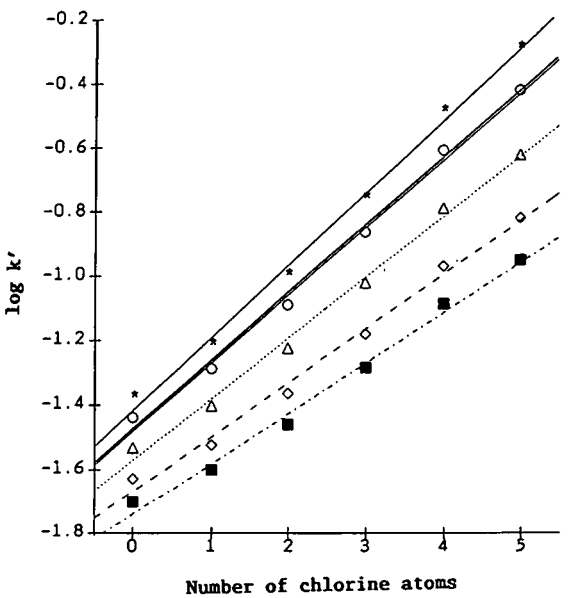

Fig. 1. Plots log k' *vs.* number of chlorine atoms at different temperatures on an SB-Octyl-50 column (9.5 m × 50 μm I.D.). Mobile phase, acetonitrile–water (50:50); test compounds, benzene, chlorobenzene, 1,4-dichlorobenzene, 1,2,4-trichlorobenzene, 1,2,4,5-tetrachlorobenzene, pentachlorobenzene. Temperature: * = 100; ○ = 120; △ = 150; ◇ = 180; ■ = 200°C.

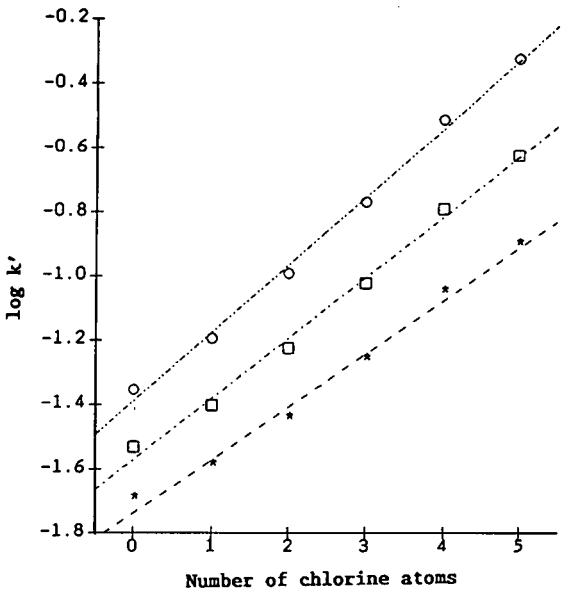

Fig. 2. Plots of log k' *vs.* number of chlorine atoms at different concentrations of acetonitrile (* = 60%; □ = 50%; ○ = 40%). Column, SB-Octyl-50 (9.5 m × 50 μm I.D.); column temperature, 150°C; test compounds as in Fig. 1.

approximations, a 1% increase in acetonitrile concentration has the same effect as a 5°C increase in column temperature in controlling solute retention. As shown in Fig. 3, equivalent separations were obtained at 150°C with 50% acetonitrile and at 200°C with 40% acetonitrile. A notable difference between the two separations was a higher column efficiency at 200°C. The plate numbers for benzene and pentachlorobenzene were 269 300 and 120 300, respectively, at 150°C and 351 500 and 185 400, respectively, at 200°C. Further, a temperature increase led to a 50% higher column efficiency for more retained solute. This indicates that retention can be controlled either by the amount of organic solvent in the mobile phase or by column temperature.

The selectivities of four different reversed-phase columns, SB-Biphenyl-30, SB-Octyl-50, SB-Methyl-100 and SE-54, were compared. A mixture of

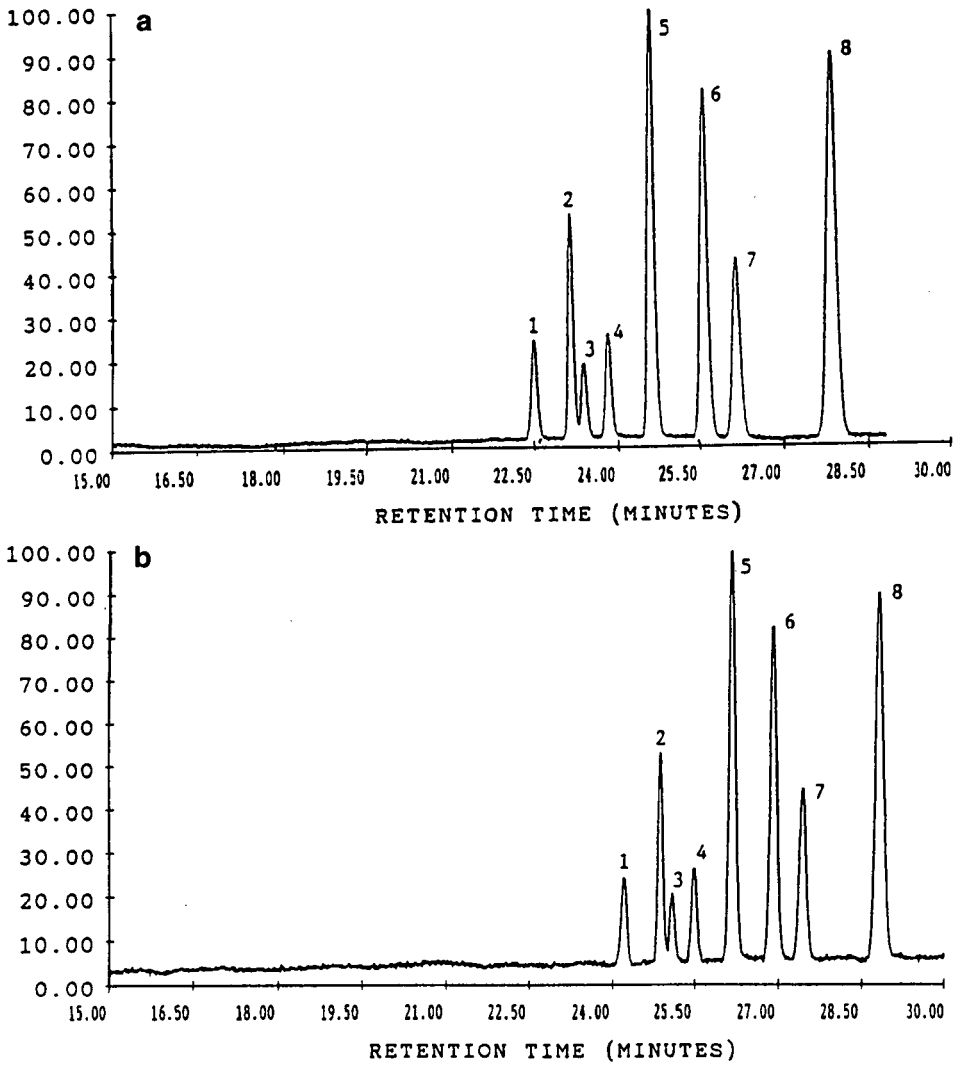

Fig. 3. (a) Separation of chlorobenzenes: 1 = tropolone; 2 = benzene; 3 = chlorobenzene; 4 = 1,4-dichlorobenzene; 5 = 1,2,4-trichlorobenzene; 6 = 1,3,5-trichlorobenzene; 7 = 1,2,4,5-tetrachlorobenzene; 8 = pentachlorobenzene. Column, SB-Octyl-50 (9.5 m × 50 μm I.D.); column temperature, 150°C; mobile phase, acetonitrile–water (50:50); flow-rate, 0.8 μl min^{-1}. (b) As (a) except column temperature 200°C and mobile phase acetonitrile–water (40:60).

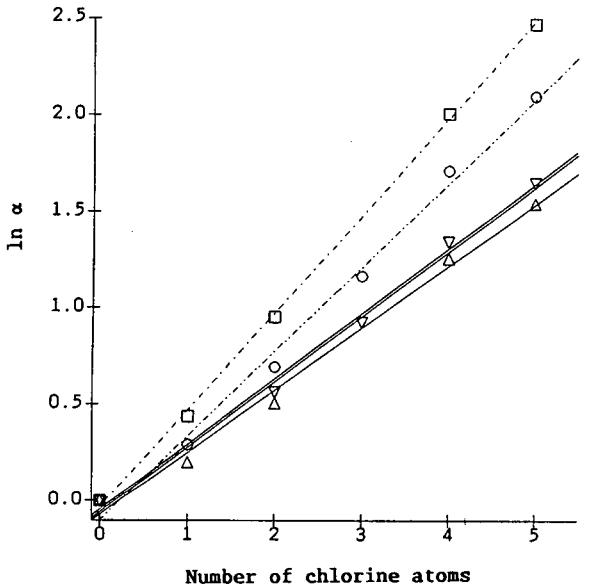

Fig. 4. Selectivity of reversed-phase columns. Column temperature, 150°C; mobile phase, acetonitrile–water (50:50); test compounds as in Fig. 1. Columns: □ = biphenyl; ○ = octyl; △ = methyl; ▽ = SE-54.

chlorobenzenes was used to study the selectivity of these columns. Retentions were measured with the same mobile phase composition [acetonitrile–water (1:1)] and column temperature (150°C). For each column, plots of ln α *vs.* number of chlorine atoms were made (Fig. 4), where $\alpha = k'/k'_0$, k' being the capacity factor of the individual chlorobenzene k'_0 the capacity factor of benzene. A linear relationship between ln α and the number of chlorine atoms indicates a hydrophobic retention mechanism for all the solutes and stationary phases tested. The slope of the curve can be used as a measure of the column selectivity. A steeper slope indicates a stronger reversed-phase character and stronger hydrophobic interaction. For the test compounds, the biphenyl column showed the highest and the methyl column the lowest selectivity. The methyl and SE-54 columns contain mainly methylpolysiloxane (SE-54 contains only 5% phenyl groups) and are expected to show similar selectivities. In fact, their lines almost overlap. The contribution of the 5% phenyl groups to solute retention was reflected in a steeper slope on the line for the SE-54 phase. It should be noted that the selectivity and efficiency of all the applied columns deteriorated with time.

The lifetime of the reversed-phase columns at 200°C was notably short owing to an accelerated dissolution of the siliceous matrix in the aqueous mobile phase. With dissolution of silica base, the stationary phase was washed off by the mobile phase. The washed-off material accumulated along

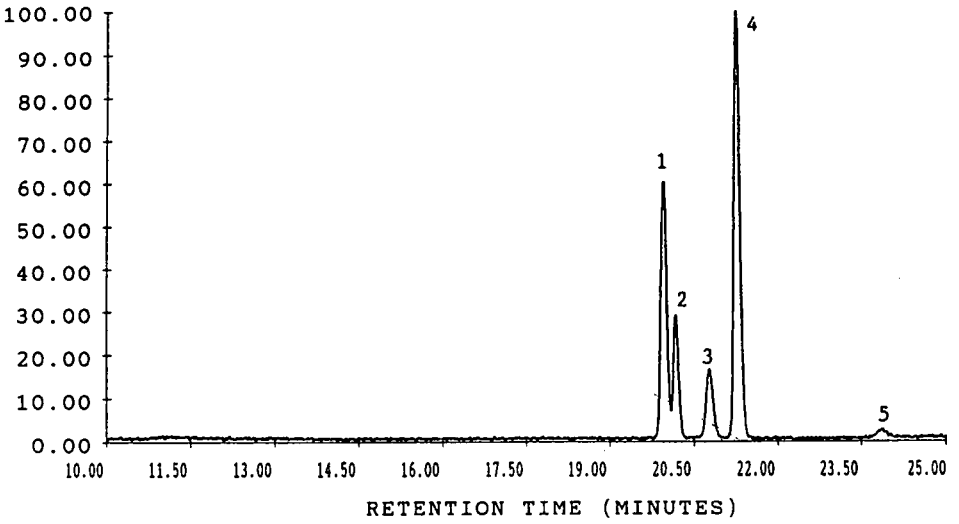

Fig. 5. Separation of aromatic hydroxy compounds. Column, DB-225 (10 m × 50 μm I.D.); column temperature, 100°C; mobile phase, *n*-hexane; flow-rate, 0.8 μl min^{-1}. Peaks: 1 = 2,6-di-*tert.*-butyl-4-methylphenol; 2 = 2,6-dimethylphenol; 3 = 1,1'-bi-2-naphthol; 4 = 1-naphthol; 5 = unknown.

the column, producing a non-uniform film thickness and reducing the column efficiency. It must be pointed out that very high column temperatures (*e.g.*, 200°C) are not always needed. At lower column temperatures, in the vicinity of 150°C, the columns tested showed satisfactory stability.

Normal-phase separation

In normal-phase separation the column lifetime is expected to be less of a problem as the mobile phase does not contain water. Fig. 5 depicts the separation of four aromatic hydroxy compounds by normal-phase OTCLC at elevated temperatures. The separation was achieved on a DB-225 column (polysiloxane backbone with 25% cyanopropyl, 25% phenyl and 50% methyl groups) with hexane as mobile phase and a column temperature of 100°C. As expected, a pure untreated fused-silica column shows selectivity towards aromatic hydroxy compounds. Fig. 6a and b display chromatograms

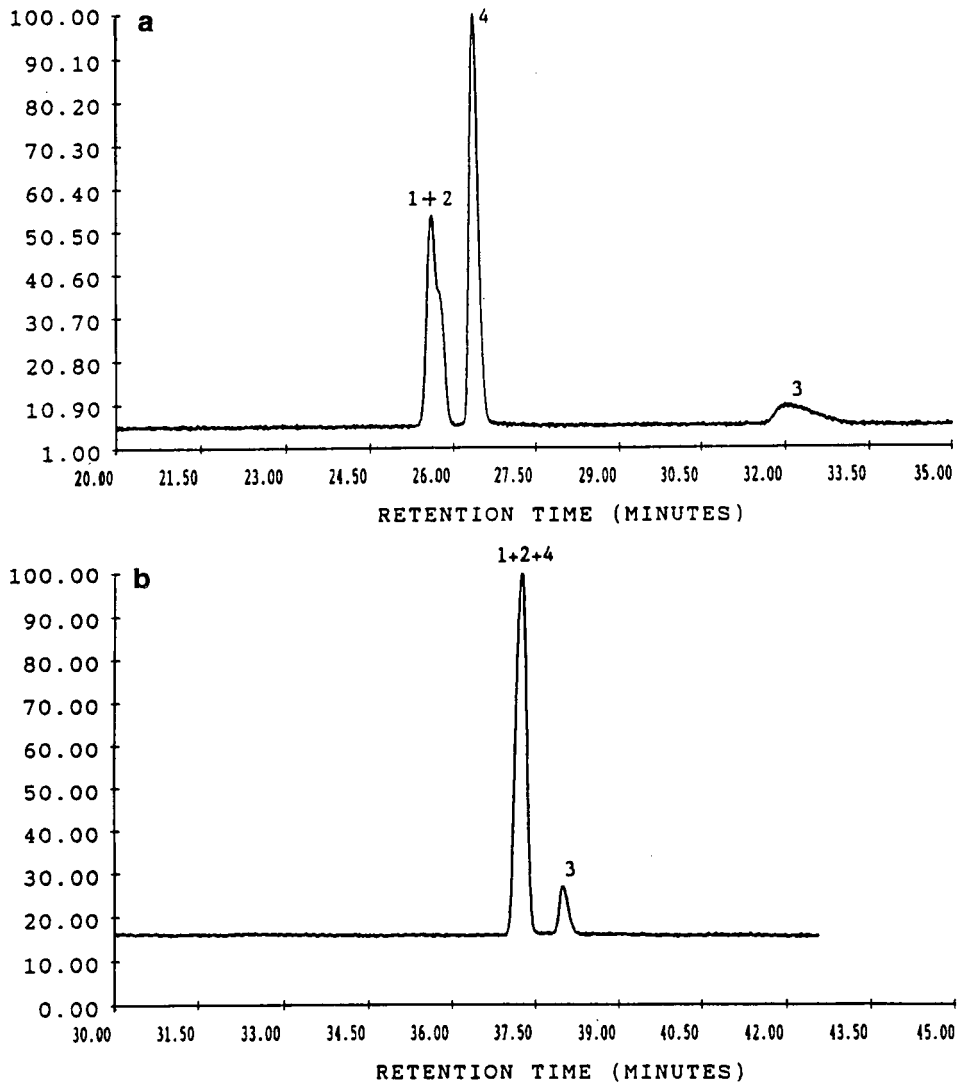

Fig. 6. Separation of aromatic hydroxy compounds on a bare fused-silica column (19.3 m × 50 μm I.D.). (a) Column temperature, 22°C; mobile phase, *n*-hexane; flow-rate, 1.4 μl min^{-1}. (b) Column temperature, 100°C; mobile phase, *n*-hexane; flow-rate, 1.0 μl min^{-1}. Peak numbers as in Fig. 5.

of the test compounds on pure fused silica at 22 and at 100°C, respectively. There was serious peak tailing at 22°C, but a nearly Gaussian peak at 100°C for 1,1'-bi-2-naphthol was observed. Tailing at room temperature caused by strong solute adsorption on the silanol groups decreased at elevated temperature. On the DB-225 column, 1,1'-bi-2-naphthol eluted before α-naphthol, whereas the opposite elution order was observed on pure fused silica. Reversal of the peak elution order indicates different selectivities on these two stationary phases.

CONCLUSIONS

The retention mechanism for substituted chlorobenzenes on the tested reversed-phase columns in the temperature range 150–200°C was based on hydrophobic interactions. Because of the short column lifetime at 200°C, commercially available columns cannot be recommended for routine application. Much has to be done in developing stable reversed-phase columns for use at temperatures above 150°C. Considering the vast choice of non-polar elution solvents in normal-phase LC and improved peak symmetry (reduced solute adsorption) at elevated temperatures, in the future more attention should be paid to normal-phase separations in HT-OCTLC.

REFERENCES

1 G. Liu, N. M. Djordjevic and F. Erni, *J. Chromatogr.*, 592 (1992) 239.
2 S. Eguchi, J. G. Kloosterboer, C. P. G. Zegers, P. J. Schoenmakers, P. P. H. Tock, J. C. Kraak and H. Poppe, *J. Chromatogr.*, 516 (1990) 301.
3 W. D. Pfeffer and E. S. Yeung, *Anal. Chem.*, 62 (1990) 2178.
4 O. van Berker, H. Poppe and J. C. Kraak, *Chromatographia*, 24 (1987) 739.
5 S. R. Mueller, W. Simon, H. M. Widmer, K. Grolimund, G. Schomberg and P. Kolla, *Anal. Chem.*, 61 (1989) 2747.
6 Y. Hirata, P. T. Lin, M. Novotny and R. M. Wightman, *J. Chromatogr.*, 181 (1980) 287.
7 S. Folestad, R. Johnson, B. Josefsson and B. Galle, *Anal. Chem.*, 54 (1984) 925.
8 J. A. Schmit, R. A. Henry, R. C. Williams and J. F. Dieckman, *J. Chromatogr. Sci.*, 9 (1971) 645.
9 J. W. Dolan, D. C. Lommen and L. R. Snyder, *J. Chromatogr.*, 535 (1990) 55.

Journal of Chromatography, 598 (1992) 159–167
Elsevier Science Publishers B.V., Amsterdam

CHROM. 24 065

Separation of the enantiomers of the 3,5-dinitrobenzamide derivatives of α-amino phosphonates on four chiral stationary phases

William H. Pirkle* and J. Andrew Burke

School of Chemical Sciences, University of Illinois, Urbana, IL 61801-3731 (USA)

(First received November 12th, 1991; revised manuscript received January 28th, 1992)

ABSTRACT

Four commercially available high-performance liquid chromatography columns containing chiral stationary phases (CSPs) have been evaluated for the separation of the enantiomers of a variety of α-amino phosphonates as the 3,5-dinitrobenzamide derivatives. The CSPs are divided into two mechanistic classes, the π-acidic N-(3,5-dinitrobenzoyl)phenylglycine / N-(3,5-dinitrobenzoyl)leucine class and the π-basic N-(2-naphthyl)alanine / N-(1-naphthyl)leucine class. As expected, the π-basic CSPs are found to be more effective for separating the enantiomers of these π-acidic analytes, separation factors being sufficiently large to make preparative or reversed-phase separations possible. A chiral recognition rationale consistent with the observed elution orders is postulated for the π-basic CSPs.

INTRODUCTION

The potential biological activity of the α-aminophosphonic acids, the phosphorus analogues of α-amino acids, has prompted the development of a variety of methods for their preparation [1]. While most of these approaches generate the racemic α-aminophosphonic acid, enantioselective procedures have been recently reported [2]. Interest in the preparation of chiral non-racemic α-aminophosphonic acids has led to a need for convenient and accurate methods for determining enantiomeric purity and absolute configuration for the members of this class of compounds. Methods reported for the assignment of absolute configuration of α-aminophosphonic acids include the relative retention of diastereomeric peptides [3] and use of the sign of the optical rotation [4]. These methods rely on having an α-aminophosphonic acid of known absolute configuration (this usually being determined by X-ray crystallography) for reference purposes.

Unlike α-amino acids and their derivatives [5], there are few data in the literature concerning separation of the enantiomers of α-aminophosphonic acids and their derivatives on chiral stationary phases (CSPs) [6]. Mechanistic rationales have been set forth for several of the CSPs developed in our laboratory and can be used to relate elution order to the absolute configurations of many analytes. From mechanistic considerations, it seemed likely that those CSPs so employed for α-amino acid derivatives might be similarly employed for α-aminophosphonic acids and their derivatives. This paper evaluates commercial versions of several of these CSPs in terms of their ability to separate the enantiomers of 3,5-dinitrobenzamides of α-aminophosphonic acid derivatives.

EXPERIMENTAL

Instrumentation

Chromatography was performed using an Anspec-Bischoff Model 2200 isocratic HPLC pump, a Rheodyne 7125 injector with 20-μl sample loop, a Milton Roy LDC UV Monitor D fixed-wavelength detector operating at 254 nm, and either an HP

0021-9673/92/$05.00

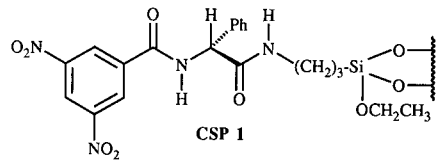

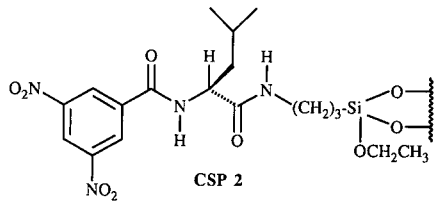

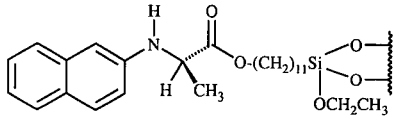

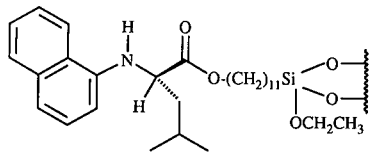

Fig. 1. Structures of CSPs.

3394A recording integrator or a Kipp & Zonen BD 41 dual-channel recorder. A Rudolph Autopol III with a 20-cm flow cell was used to monitor the sign of $[\alpha]_D$. The void volume was determined using tri-*tert*.-butylbenzene [7].

The ^1H NMR spectra were obtained using a Varian XL-200 (200 MHz) or GE GN-500 (500 MHz) spectrometers using tetramethylsilane (δ 0.00 ppm) as an internal reference. The ^{13}C NMR spectra were obtained on a GE GN-300NB (75 MHz) spectrometer using C^2HCl_3 (δ 77.0 ppm) as an internal reference. The ^{31}P NMR spectra were obtained using a GE GN-300NB (121 MHz) spectrometer with broad-band ^1H decoupling and referenced to external 85% H_3PO_4 (δ 0.00 ppm). The IR spectra were obtained on IBM IR-32 spectrometer. The mass spectra and microanalyses were obtained by the University of Illinois School of Chemical Sciences service laboratories.

Materials

· *Reagents.* The benzaldehyde, benzylamine, diphenyl phosphite and dimethyl phosphite were purchased from Aldrich and were distilled prior to use. All other reagents were used as received.

CSPs **1–4**. The CSPs **1–4** (Fig. 1) used in this study are available from Regis (Morton Grove, IL, USA).

*Diphenyl N-benzyl α-aminobenzyl phosphonate (**5**).* To a 100-ml round-bottomed flask equipped with Dean-Stark trap, reflux condenser, magnetic stir bar, and nitrogen inlet were added 3.00 g (28 mmol) of benzaldehyde, 40 ml of benzene, and 3.03 g (28 mmol) of benzylamine. The cloudy mixture was brought to reflux and, after 1 h, the benzene was removed by distillation. After the mixture cooled, the Dean-Stark trap was removed, 40 ml of dry tetrahydrofuran and 7.20 g (31 mmol) of diphenyl phosphite were added and the solution was brought to reflux under a nitrogen atmosphere. The progress of the reaction was monitored by ^{31}P NMR. After 36 h, the ratio of product (δ 16.70) to phosphite (δ 0.6) was 8:1. The solution was concentrated under reduced pressure and the residue was recrystallized from ethyl acetate–hexane (1:4, v/v) to give 7.90 g (65% yield) of colorless solid, m.p. 106–107°C. R_F (thin-layer chromatography) = 0.20 (silica/CH_2Cl_2). ^1H NMR (C^2HCl_3, 300 MHz) δ 2.50 br s 1H (exchanges with $2H_2O$) 1H; 3.75–4.0 two d (J = 54, 12.5 Hz) 2H; 4.37 d (J = 20.5 Hz) 1H; 6.80–7.6 m 20H. ^{31}P NMR (C^2HCl_3) δ 16.70. IR (KBr) 3279, 3028, 1591, 1489, 1454, 1265, 1215, 1192, 1161, 1093, 1070, 1024, 935 cm^{-1}. Mass spectrum (10 eV) *m/z* (relative intensity) 429 (0.7), 234 (100), 195 (74), 92 (52) Analysis, calculated for $C_{26}H_{24}NO_3P$: C, 72.71; H, 5.63; N, 3.23; P, 7.20; found: C, 72.71; H, 5.63; N, 3.25; P, 7.20.

*Diphenyl N-3,5-dinitrobenzoyl α-aminobenzyl phosphonate (**6**).* A solution of 0.5 g (1.16 mmol) of **5** in 10 ml of dry CH_2Cl_2 was poured into 30 ml of dry diethyl ether saturated with HCl (g) and allowed to stand at room temperature for 1 h. The cloudy suspension was then cooled to 0°C for 1 h and filtered. The collected solid, 0.494 g (m.p. 161–163 °C), was dissolved in 25 ml of dry methanol and poured over 0.1 g of 20% $Pd(OH)_2$ on carbon in a pressure bottle. The bottle was pressurized to 45 p.s.i. with hydrogen and rocked for 10 h on a Parr shaker. The catalyst was removed by filtration and

the filtrate was concentrated under reduced pressure. The ^{31}P NMR spectrum of the resulting oil has a peak at δ 11.4 ppm. The oil was dissolved in 50 ml of CH_2Cl_2 and 0.320 g (1.4 mmol) of 3,5-dinitrobenzoyl chloride was added, followed by 50 ml 1:1 water–satd. $NaHCO_3$ (1:1), and the two-phase mixture was magnetically stirred at room temperature for 1.5 h. The aqueous layer was removed and the organic layer was washed sequentially with 30-ml portions of 10% $NaHCO_3$, water, and saturated NaCl. The combined aqueous washings were extracted with two 10-ml portions of CH_2Cl_2. The combined organic layers were dried over anhydrous $MgSO_4$, filtered, and concentrated under reduced pressure. The residue was purified by chromatography on silica using CH_2Cl_2–diethyl ether (1:1), and the concentrated fractions were recrystallized from ethyl acetate–hexane (1:4, v/v) to give 420 mg (68% yield) of colorless solid, m.p. 209–210°C. R_F = 0.55 (silica/diethyl ether). ^1H NMR (C^2HCl_3, 200 MHz) δ 6.1–6.3 dd (J=21.5, 9.5 Hz) 1H; 6.6–6.7 m 2H; 7.0–7.4 m 11H; 7.6–7.7 m 2 H; 8.7–8.9 m 3H; 9.1–9.3 m 1H. ^{31}P (C^2HCl_3) δ 12.45. IR (KBr) 3279, 3080, 1643, 1542, 1489, 1344, 1210, 1183 cm^{-1}. Mass spectrum (70 eV) *m/z* (relative intensity) 440 (87), 300 (57), 195 (100), 149 (46), 140 (49), 94 (63). Analysis, calculated for $C_{26}H_{20}N_3O_8P$: C, 58.54; H, 3.78; N, 7.88; P, 5.81; found: C, 58.59; H, 3.74; N, 7.81; P, 5.72.

Diethyl N-3,5-dinitrobenzoyl α-aminobenzyl phosphonate. This compound was prepared following the procedure of Szewczyk *et al.* [8] using ethanol and **6**. Chromatographic purification and recrystallization from ethyl acetate–hexane (1:5, v/v) gives a colorless solid, m.p. 181–182°C. R_F = 0.33 (silica/diethyl ether). ^1H NMR (C^2HCl_3, 200 MHz) δ 1.1 t 3H; 1.32 t 3H; 3.6–3.8 m 1H; 3.85–4.05 m 1H; 4.1–4.35 m 2H; 5.7–5.9 two d (J=21.5, 9.5 Hz) 1H; 7.2–7.4 m 3H; 7.5–7.7 m 2H; 8.6-8.8 m 1H; 9.1–9.3 m 3H. ^{31}P NMR (C^2HCl_3) δ 20.64. IR (KBr) 3279, 3080, 2975, 1643, 1542, 1489, 1344, 1210, 1183 cm^{-1}. Mass spectrum (70 eV) *m/z* (relative intensity) 437 (1.8), 300 (73), 195 (100), 179 (20), 155 (28), 111 (38), 75 (57). Analysis, calculated for $C_{18}H_{20}N_3O_8P$: C, 49.42; H, 4.61; N, 9.61; P, 7.09; found: C, 49.66; H, 4.67; N, 9.46; P, 6.91.

Preparation of enantiomerically enriched samples

Dimethyl N-[-(S)-α-methylbenzyl]-α-aminobenzyl phosphonate. A 10:1 ratio of diasteromeric phosphonates was obtained from the procedure of Glowiak *et al.* [9] using benzaldehyde, (*S*)-α-methylbenzylamine and dimethyl phosphite. The stereochemistry of the major and minor diastereomers is known [9]. ^{31}P NMR major diastereomer (*S,R*) δ 27.28; minor diastereomer (*S,S*) δ 26.88; m.p. 83–84°C. ^1H NMR (C^2HCl_3, 200 MHz), δ 1.37 d (J=6.2 Hz) 3H; 2.12 broad s (exchanges with $2H_2O$) 1H; 3.50 d (J=10.6Hz) 3H; 3.80 m 4H; 4.12 d (J=20.7 Hz) 1H 7.25–7.5 m 10H. Analysis, calculated for $C_{17}H_{22}NO_3P$: C, 63.93; H, 6.95; N, 4.46; P, 9.70; found: C, 64.14; H, 7.15; N, 4.46; P, 9.51.

Dimethyl N-[-(S)-α-methylbenzyl]-α-aminoisobutyl phosphonate. Freshly distilled isobutyraldehyde, 5.15 g (71 mmol), was placed in a 100 ml flask with 10 g of anhydrous $MgSO_4$, 30 ml of dry CH_2Cl_2 and cooled to 0°C. The *S*-(−)-α-methylbenzylamine 8.65 g (72 mmol) was added dropwise and the mixture was stirred overnight at room temperature. Distilled dimethyl phosphite (86 mmol) was added and the resulting mixture was stirred for 72 h. The reaction mixture was filtered and the filtrate was diluted with 100 ml of CH_2Cl_2. The CH_2Cl_2 was washed with 50 ml of water and the organic layer was dried with anhydrous $MgSO_4$. After removal of the drying agent by filtration, the filtrate was concentrated under reduced pressure using a rotary evaporator to afford 19.0 g of pale yellow oil (95% yield). The diastereomeric ratio of 3:1 was determined by ^{31}P NMR analysis: major diastereomer (*S,R*) δ 33.0, minor diastereomer (*S,S*) δ 31.4. The stereochemistry of the major and minor diastereomers is known [9]. R_F = 0.28 (silica/diethyl ether). ^1H NMR (C^2HCl_3, 500 MHz), major diastereomer δ 0.84 m 3H; 0.94 m 3H; 1.32 m 3H; 1.6 broad s 1H; 2.00 m 1H; 2.57 dd (J=18.6, 6.8 Hz) 1H; 3.78 m 6H; 4.1 m 1H; 7.2–7.5 m 10H; minor diastereomer δ 1.00 d (J=7.0 Hz) 3H; 1.10 d (J=6.4 Hz) 3H; 1.6 broad s 1H; 2.2 m 1H; 2.80 dd (J=18.6, 2.7 Hz) 1H; 3.6–3.8 m 6H; 4.02 m 1H; 7.2–7.5 m 10 H. ^{13}C NMR (C^2HCl_3, 75 MHz) major diastereomer δ 17.13, 20.21, 20.41, 24.58, 28.73, 28.79, 51.70, 51.8, 56.0, 127.8, 127.12, 144.42; minor diastereomer δ 17.95, 19.99, 20.26, 23.49, 28.24, 28.30, 52.3, 52.4, 57.17, 126.0, 126.83, 144.80. IR (neat 3316, 3026, 2957, 2874, 1454, 1246, 1180, 1122, 1099, 1057 cm^{-1}. Mass spectrum 70 eV *m/z* (relative intensity) 285 (1.8), 176 (72), 120 (29), 105

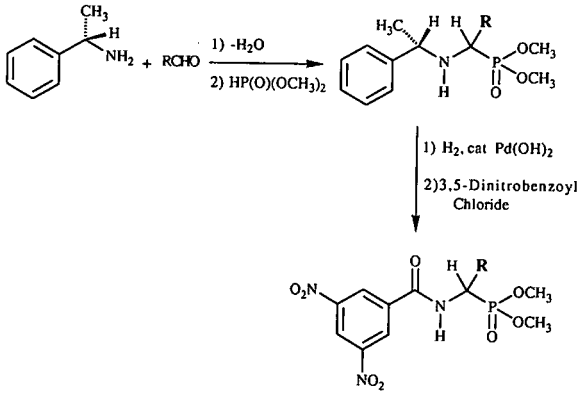

Fig. 2. Preparation of configurationally known samples. R = phenyl; isopropyl.

(93), 72 (100). Analysis, calculated for $C_{14}H_{24}NO_3P$: C, 58.93; H, 8.48; N, 4.91; P, 10.86. Found: C, 58.79; H, 8.55; N, 4.88; P, 10.73.

Preparation of (R)-enriched dimethyl N-3,5-dinitrobenzoyl α-amino phosphonates samples of known absolute configuration

The (*R*)-enriched samples were prepared from each of the preceding diastereomeric mixtures. If one uses (*S*)-α-methylbenzylamine, the major diastereomer formed has the (*R*) configuration at the stereocenter adjacent to phosphorus [9]. The ratio of diastereomers produced when (*S*)-α-methylbenzylamine was used to form the imine was monitored using ^{31}P NMR and ^{1}H NMR (Fig. 2). After hydrogenolysis of the α-methylbenzyl group using Pd $(OH)_2$ as a catalyst, N-acylation of the resulting amines with 3,5-dinitrobenzoyl chloride and analysis of the amide derivatives on a CSP, the observed enantiomeric excess was the same as the starting diastereomeric excess. These materials show the same chromatographic behavior on the CSPs and silica thin-layer plates as the corresponding racemates.

RESULTS AND DISCUSSION

A series of dimethyl esters of alkyl and aryl substituted N-(3,5-dinitrobenzoyl)-α-amino phosphonates were available from prior studies. In order to investigate the role played by the alkoxyl portion of these phosphonates in chiral recognition, a homologous series of diesters of the 3,5-dinitrobenzamide of α-aminobenzyl phosphonate was prepared by transesterification of the diphenyl phosphonate **6**. Addition of diphenyl phosphite to the imine derived from benzaldehyde and benzylamine gives N-benzyl protected diphenyl α-aminobenzyl phosphonate **5** (Fig. 3). Hydrogenolysis of **5** using $Pd(OH)_2$ on carbon gives the α-amino phosphonate which can be N-acylated with 3,5-dinitrobenzoyl chloride to give the 3,5-dinitrobenzamide of diphenyl α-aminobenzyl phosphonate **6**. The various diesters **7** were obtained from **6** following a reported procedure [8]. The elution orders of the enantiomers of α-phenyl- and α-isopropyl-substituted dimethyl α-amino phosphonates were rigorously established using the (*R*)-enriched samples.

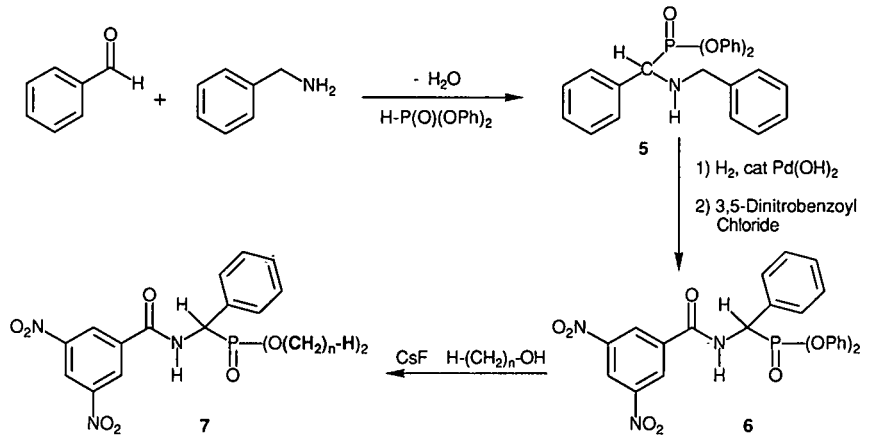

Fig. 3. Preparation of the dialkyl esters of N-(3,5-dinitrobenzoyl)-α-aminobenzyl phosphonic acid. ph = phenyl.

TABLE I

COMPARISON OF THE ABILITY OF CSPs **1** AND **2** TO SEPARATE THE ENANTIOMERS OF DIMETHYL α-AMINO-PHOSPHONATES AS THE 3,5-DINITROBENZAMIDE DERIVATIVES

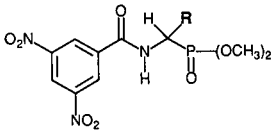

α = Chromatographic separation factor; k'_1 = capacity factor for the first eluted enantiomer using 20% (v/v) isopropyl alcohol in hexane as the mobile phase, flow-rate 2 ml/min; the detector was operating at 254 nm. The $[\alpha]_D$ column gives the sign of $[\alpha]_D$ of the second eluted enantiomer using a polarimetric detector; the letter refers to the absolute configuration of the second eluted enantiomer.

R	(*R*)-**1**			(*S*)-**2**		
	α	k'_1	$[\alpha]_D$	α	k'_1	$[\alpha]_D$
Phenyl	1.67	12.44	(−) *R*	1.40	5.14	(+) *S*
2-Tolyl	1.50	8.57	(−)	1.18	3.55	(+)
3-Tolyl	1.63	10.07	(−)	1.44	4.45	(+)
4-Tolyl	1.63	11.27	(−)	1.52	4.47	(+)
Mesityl	1.00	9.86		1.00	3.43	
p-Cymyl	1.47	7.88	(−)	1.31	3.18	(+)
4-Chlorophenyl	1.70	12.13	(−)	1.62	4.63	(+)
4-Allyloxyphenyl	1.66	16.8	(−)	1.40	6.85	(+)
α-Naphthyl	1.39	22.7	(−)	1.49	6.23	(+)
β-Naphthyl	1.88	31.4	(−)	2.61	8.82	(+)
4-Nitrophenyl	1.62	37.7	(−)	1.42	10.9	(+)
Isopropyl	1.44	6.86	(+) *R*	1.00	3.65	
Isobutyl	1.67	5.43	(+)	1.00	2.78	
tert.-Butyl	1.37	5.94	(+)	1.00	3.13	
1,1-Dimethyl-3-butenyl	1.39	5.34	(+)	1.00	2.72	

π-Acidic CSPs

The ability of π-acidic CSPs (*e.g.* **1** and **2**) to separate the enantiomers of a wide clientele of analytes has been extensively documented [10]. While these CSPs were designed to separate the enantiomers of π-basic analytes, they often suffice to separate the enantiomers of π-acidic analytes, typically with reduced levels of enantioselectivity [11]. Although not yet studied in detail, the interactions employed by these CSPs to "recognize" the stereochemistry of π-acidic analytes are not, in totality, those employed for π-basic analytes. The separation of the enantiomers of π-acidic analytes on π-acidic CSPs is frequently observed and has also been noted by Caude *et al.* [12].

After chromatographing the 3,5-dinitrobenzamides of a series of α-aryl- and α-alkyl-substituted dimethyl α-amino phosphonates on **1** and **3**, certain structure–activity relationships become apparent (Table I and Fig. 4). Perusal of the data reveals that

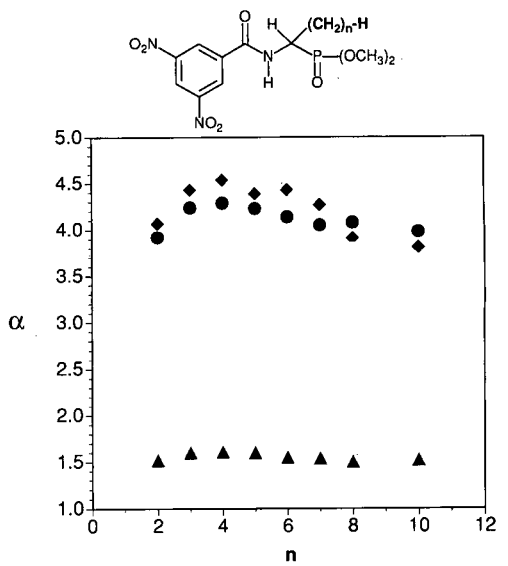

Fig. 4. The relationship between α and the number of methylene groups, *n*, in the alkyl group of dimethyl N-(3,5-dinitrobenzoyl)-α-aminoalkyl phosphonates using 20% isopropyl alcohol in hexane as the mobile phase. ◆ = CSP **3**; ● = CSP **4**; ▲ = CSP **1**.

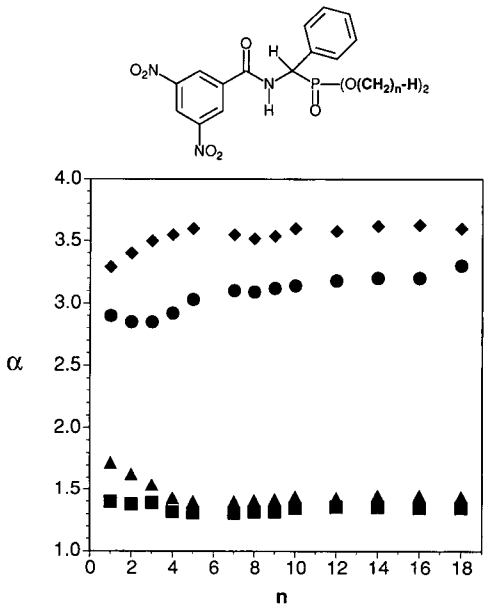

Fig. 5. The dependence of the separation factors upon the number of methylene groups, *n*, in the alkoxyl portion of N-(3,5-dinitrobenzoyl)-α-aminobenzyl phosphonates using 20% isopropyl alcohol in hexane as the mobile phase. ◆ = CSP **3**; ● = CSP **4**; ▲ = CSP **1**; ■ = CSP **2**.

1 more effectively separates these enantiomers than does **2**. Moreover, **2** is not effective for the separation of the enantiomers of 3,5-dinitrobenzamides of dimethyl α-amino-α-alkyl phosphonates. The enriched samples were used to relate the sign of the specific rotation to the absolute configuration of the dimethyl N-(3,5-dinitrobenzoyl)-α-amino phosphonates. Note from Table I that the more retained enantiomers within each of the series of 3,5-dinitrobenzamides of dimethyl α-amino phosphonates have the same sign of rotation. The more retained enantiomers in the alkyl series differ in their sign of specific rotation from their α-aryl counterparts even though they have the same absolute configuration. Using **1**, the more retained enantiomer of each member of the linear alkyl series of analytes included in Fig. 4 is dextrorotatory. The relative lack of dependence of the separation factor upon the length of alkoxyl groups of the phosphonate ester suggests that this phase has considerable generality for most esters of these analytes (Fig. 5).

Note, this CSP–analyte combination contains several possible interaction sites which may or may not be involved in the chiral recognition process. Although there are a number of plausible absorbates which may be responsible for the observed enantioselectivity, no single chiral recognition mechanism presently seems capable of rationalizing all of the structure–activity relationships observed with CSPs **1** and **2**. Even so, these CSPs are useful in determining the enantiomeric purities of members of this class of analytes.

π-Basic CSPs

The π-basic CSPs, **3** and **4**, prepared from the undecenyl esters of (*R*)-N-2-(naphthyl)alanine and (*S*)-N-1-(naphthyl)leucine respectively, effectively distinguish the enantiomers of suitably functionalized analytes [13]. For example, the separation factor for the enantiomers of the 1-adamantyl amide of N-(3,5-dinitrobenzoyl)leucine is almost 60 on **4** [14]. The chiral recognition mechanisms utilized by this class of CSPs have been extensively investigated for the N-3,5-dinitrobenzoyl α-amino amides and esters using various solution techniques such as ^{1}H NMR chemical shift non-equivalence–nuclear Overhauser effects and UV–VIS absorption studies using mixtures of the analyte and a soluble analogue of the CSP **3** [15]. X-ray crystallographic analysis of a 1:1 co-crystal of the chiral selector and an analyte shows that the interactions proposed for the more stable diastereomeric complex are also present in the solid state [16]. In the model proposed to account for the observed enantioselectivity, one of the essential interactions is a hydrogen bond between the C-terminal carbonyl oxygen of the analyte and the amino N–**H** of the selector. Since, in the phosphorus analogues of α-amino acids, one has simply replaced the C-terminal carboxyl group with the phosphonate group, one expects essentially the same chiral recognition process to operate. Since the carboxamide and phosphonate groups differ in basicity and possibly conformational disposition, the levels of enantioselectivity may differ somewhat for the two analyte classes.

The data in Table II allow one to compare the abilities of **3** and **4** to separate the enantiomers of a variety of dimethyl α-amino phosphonates as the 3,5-dinitrobenzamide derivatives and show the order of elution of the configurationally known samples. The π-basic CSPs used in this study are of opposite configurations and the elution orders observ-

TABLE II

COMPARISON OF THE ABILITY OF CSPs **3** AND **4** TO SEPARATE THE ENANTIOMERS OF DIMETHYL α-AMINOPHOSPHONATES AS THE 3,5-DINITROBENZAMIDE DERIVATIVES

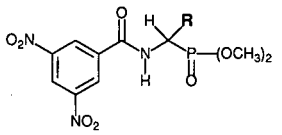

Symbols as in Table I.

R	(*R*)-**3**			(*S*)-**4**		
	α	k'_1	$[\alpha]_D$	α	k'_1	$[\alpha]_D$
Phenyl	3.29	4.34	(+) *S*	2.90	5.11	(−) *R*
2-Tolyl	3.08	3.71	(+)	3.04	3.68	(−)
3-Tolyl	3.37	3.87	(+)	3.26	4.07	(−)
4-Tolyl	3.35	3.93	(+)	2.95	4.38	(−)
Mesityl	2.03	3.16	(+)	1.92	3.28	(−)
p-Cymyl	3.04	3.14	(+)	2.28	3.52	(−)
4-Chlorophenyl	3.35	4.07	(+)	3.07	4.77	(−)
4-Allyloxyphenyl	3.11	5.00	(+)	2.87	5.25	(−)
α-Naphthyl	3.05	5.07	(+)	2.81	5.53	(−)
β-Naphthyl	3.55	5.18	(+)	3.49	5.72	(−)
4-Nitrophenyl	3.41	8.27	(+)	2.93	11.3	(−)
Isopropyl	3.33	2.94	(−) *S*	2.90	3.64	(+) *R*
Isobutyl	4.89	2.57	(−)	4.66	2.98	(+)
tert.-Butyl	2.72	2.57	(−)	3.60	2.55	(+)
1,1-Dimethyl-3-butenyl	2.82	2.43	(−)	3.83	2.52	(+)

ed are those expected from the chiral recognition mechanism. This mechanism accounts for the observation that (*R*)-**3** or **4** preferentially retains the (*R*)-enantiomer of the α-amino acid derivative [15]. Owing to Cahn–Ingold–Prelog priority sequence, the (*S*)-α-amino phosphonate derivative is mechanistically equivalent to the (*R*)-α-amino acid derivative [*i.e.*, the (*S*)-enantiomer of the α-amino phosphonate derivative would be more strongly retained on (*R*)-**3** or **4**]. This is what is observed.

Even those sterically congested analytes which contain mesityl, 2-tolyl, *tert.*-butyl, or 1,1-dimethyl-3-butenyl [17] substituents elute in the predicted order, thus providing additional evidence of the mechanistic generality of these phases. The ability of **3** and **4** to separate the enantiomers of the homologous series of alkyl substituted N-(3,5-dinitrobenzoyl)-α-amino phosphonates is shown in Fig. 4. The magnitudes of the separation factors depend only slightly upon the lengths of the α-alkyl substituents, the effect being greater for the early members of the series. Data for the series of the various alkyl diesters of N-(3,5-dinitrobenzoyl)-α-aminobenzyl phosphonate are shown in Fig. 5. Again, the separation factors depend but slightly upon the lengths of the alkoxyl groups. The relative insensitivity of the separation factors to structural changes in "non-essential" (*i.e.* those not used in chiral recognition) portions of the analyte attests to the generality of the chiral recognition process.

The recognition process utilized by these CSPs in the present instances in believed to be essentially that proposed for the 3,5-dinitrobenzamides of α-amino acid derivatives [15]. Consistent with the proposed face to face π–π interaction between the π-acidic 3,5-dinitrobenzoyl portion of the analyte and the π-basic naphthyl portion of **3** or **4** is the observation that the enantioselectivities shown by the less π-acidic *p*-nitrobenzamide derivatives are greatly diminished.

In the case of the 3,5-dinitrobenzamide derivatives, reversed-phase separation on **3** and **4** are pos-

TABLE III

COMPARISON OF THE ABILITY OF CSPs 3 AND 4 TO SEPARATE THE ENANTIOMERS OF DIMETHYL α-AMINOPHOSPHONATES AS THE 3,5-DINITROBENZAMIDE DERIVATIVES USING METHANOL–WATER (4:1) AS THE MOBILE PHASE

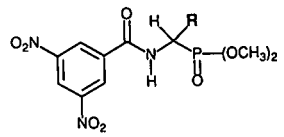

α = Chromatographic separation factor; k'_1 = capacity factor for the first eluted enantiomer using 20% water in methanol (v/v) as the mobile phase, flow-rate 2 ml/min; the detector was operating at 254 nm. In the sense column, the letter refers to the absolute configuration of the second eluted enantiomer.

R	(*R*)-3			(*S*)-4		
	α	k'_1	Sense	α	k'_1	Sense
Phenyl	1.62	1.77	*S*	1.57	2.82	*R*
2-Tolyl	1.68	1.14		1.66	3.53	
3-Tolyl	1.75	1.39		1.73	3.51	
4-Tolyl	1.68	1.41		1.60	3.56	
Mesityl	1.33	1.94		1.31	5.35	
p-Cymyl	1.75	1.89		1.59	5.48	
4-Chlorophenyl	1.71	1.37		1.64	3.76	
4-Allyloxyphenyl	1.71	1.72		1.60	4.69	
α-Naphthyl	1.73	2.37		1.70	6.16	
β-Naphthyl	1.83	2.10		1.80	5.59	
4-Nitrophenyl	1.56	1.22		1.46	3.34	
Isopropyl	1.51	0.63	*S*	1.60	1.33	*R*
Isobutyl	1.95	0.77		2.22	1.79	
tert.-Butyl	1.36	0.64		1.62	1.37	
1,1-Dimethyl-3-butenyl	1.40	0.77		1.75	1.89	

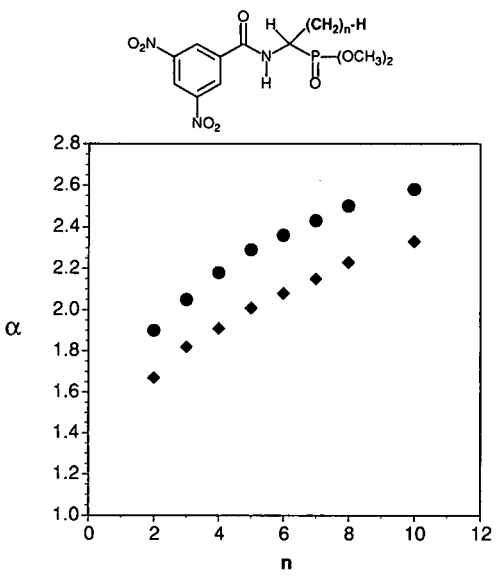

Fig. 6. The dependence of the separation factors upon the number of methylene groups, *n*, in the alkyl portion of dimethyl N-(3,5-dinitrobenzoyl)-α-aminoalkyl phosphonates using 20% water in methanol as mobile phase. ● = CSP 4; ◆ = CSP 3.

sible. Using a mobile phase of methanol–water (4:1), both retention and enantioselectivity are reduced although separation factors of the enantiomers still typically exceed 1.5 (Table III and Fig. 6). Elution orders are the same for both reversed and normal mobile phases. Notice that, for the α-alkyl series of analytes, enantioselectivity increases as the lengths of the alkyl groups on the stereogenic centers of the analytes increase. This is also observed for the corresponding phosphonic acid analytes using these phases and ion-pairing reagents. [18].

CONCLUSION

The use of four commercially available CPSs to determine enantiomeric excess and to relate elution order to the absolute configuration of the enantiomers of a variety of N-(3,5-dinitrobenzoyl)-α-amino phosphonates has been described. These phases show broad scope and levels of enantioselectivity adequate for preparative separations as well as analytical separations.

ACKNOWLEDGEMENTS

This work has been supported by research grants from the National Science Foundation, Merck, Sharp and Dohme, and Eli Lilly and Company.

REFERENCES

1 E. K. Baylis, C. D. Campbell and J. G. Dingwall, *J. Chem. Soc., Perkin Trans. 1*, (1984) 2845–2853.
2 M. Sting and W. Steglich, *Synthesis*, (1990) 132–134.
3 B. Lejczak, P. Kafarski and P. Masterlerz, *J. Chromatogr.*, 324 (1985) 455–461.
4 B. Dhawan and D. Redmore, *Phosphorus Sulfur Relat. Elem.*, 32 (1987) 119–44.
5 W. J. Lough (Editor), *Chiral Liquid Chromatography*, Blackie, London, 1989.
6 Y. P. Belov, V. A. Davankov and S. V. Rogozhin, *Izv. Akad. Nauk. SSSR., Ser. Khim.*, (1977) 1856–1860.
7 W. H. Pirkle and C. J. Welch, *J. Liq. Chromatogr.*, 14 (1991) 173–185.
8 J. Szewczyk, B. Lejczak and P. Kafarski, *Synthesis*, (1982) 409.
9 T. Glowiak, W.-S. Dobrowalska, J. Kowalik, P. Masterlerz, M. Soroka and J. Zon, *Tetrahedron Lett.*, 45 (1977) 3965–3968.
10 W. H. Pirkle and J. M. Finn, in J. D. Morrison (Editor), *Asymmetric Synthesis*, Academic Press, New York, 1983, p. 87–124..
11 W. H. Pirkle and J. A. Burke, *Chirality*, 1 (1989) 57–62.
12 M. Caude, A. Tambute and L. Siret, *J. Chromatogr.*, 550 (1991), 357–382.
13 W. H. Pirkle and T. C. Pochapsky, *Chem. Rev.*, 89 (1989) 347–362.
14 W. H. Pirkle, K. C. Deming and J. A. Burke, *Chirality*, 3 (1991) 183–187.
15 W. H. Pirkle and T. C. Pochapsky, *J. Am. Chem. Soc.*, 109 (1987) 5975–5982.
16 W. H. Pirkle, J. A. Burke and S. D. Wilson, *J. Am. Chem. Soc.*, 111 (1989), 9222–9223.
17 W. H. Pirkle and J. A. Burke, *J. Chromatogr.*, 557 (1991) 173–185.
18 W. H. Pirkle, J.-P. Chang and J. A. Burke, *J. Chromatogr.*, 479 (1989) 377–386.

Journal of Chromatography, 598 (1992) 169–180
Elsevier Science Publishers B.V., Amsterdam

CHROM. 24 030

Protein chromatography using a continuous stationary phase

Yiqi Yang☆

Textile Science, Department of Consumer Sciences and Retailing, Purdue University, West Lafayette, IN 47907 (USA)

Ajoy Velayudhan

Laboratory of Renewable Resources Engineering, Purdue University, West Lafayette, IN 47907 (USA)

Christine M. Ladisch

Textile Science, Department of Consumer Sciences and Retailing, Purdue University, West Lafayette, IN 47907 (USA)

Michael R. Ladisch*

Laboratory of Renewable Resources Engineering and Department of Agricultural Engineering, Purdue University, West Lafayette, IN 47907 (USA)

(First received April 3rd, 1991; revised manuscript received November 21st, 1991)

ABSTRACT

A continuous stationary phase consisting of yarns woven into a fabric is rolled and packed into mechanically stable liquid chromatography columns. This work utilized yarns having a characteristic width of 200–400 μm, made from 10–20-μm fibers consisting of 95% poly(*m*-phenylene isophthalamide) and 5% poly(*p*-phenylene terephthalamide). Although loadings on this stationary phase were low at 4 mg/g for bovine serum albumin and 6 mg/g for β-galactosidase, this material shows the interesting characteristic of a leveling off of plate height at mobile phase velocities of 30–80 cm/min. This phenomenon is explained on the basis of a coupling argument whereby a fraction of the mobile phase flows through the intramatrix pore space, and convective transport through the pore space dominates transport by diffusion. A modified Van Deemter expression is derived and shown to fit plate height data for polyethylene glycol standards having molecular weights of 200 and 20 000. The characteristics of this continuous stationary phase at high eluent velocities are discussed and conditions which give separation of immunoglobulin G, bovine serum albumin, insulin and β-galactosidase in 12 min are described.

INTRODUCTION

Separation costs in the manufacture of proteins and other biotechnology products are estimated to be 40% or more of the production cost [1]. Key factors which improve the cost-effectiveness of a chromatographic process are reduction of the number of steps, automation to reduce labor costs, and reduction of media costs [2,3]. Improvements are still needed in the separations technology itself, particularly in reducing residence time.

Protein–stationary phase interactions and retention behavior reflect microscopic phenomena associated directly with the chemistry of the stationary phase, and are thus an important area of study. However, a successful process-scale system must

☆ Present address: Division of Consumer Sciences, 905 South Goodwin, University of Illinois, Champaign/Urbana, IL 61801, USA.

0021-9673/92/$05.00

also provide high mass transfer rates at low pressure drop. This is equivalent to a high ratio of mass to momentum transfer. In this context, Gibbs and Lightfoot [4] suggested hollow fibers as possible chromatographic stationary phases, although they considered that problems of fabrication and flow distribution still remained. In 1989, Ding *et al.* [5] verified Gibbs and Lightfoot's suggestion by using a bundle of hollow fibers. They coated the fibers with dodecanol and trioctylphosphate–dodecane and used these systems to separate protein mixtures. Eluent pH values as high as 10 to 11 were used in order to accelerate elution; separation times of about 30 to 80 min were obtained. Ding and Cussler [6] also used such hollow-fiber systems for overloaded chromatography.

The desired characteristics of a stationary phase for liquid chromatography of proteins are well established. The sorbent should have high capacity and a well defined chemistry, and be regenerable and non-denaturing. The stationary phase structure should be rigid, and physically stable at high flow-rates. The material must also be easy to pack and scale up, with defined and reproducible characteristic dimensions. Such properties are usually associated with chromatography columns packed with particulate sorbents. We report another type of material where the stationary phase consists of phenylene phthalamide fibers which have the necessary physical characteristics, as well as separation capabilities. The fibers are assembled into yarns, which in turn are interlaced into a continuous matrix (or fabric). We refer to this as a continuous stationary phase, which when rolled into a cylindrical configuration is readily packed into standard liquid chromatography (LC) columns.

This paper reports packing properties, flow and pressure drop characteristics, protein and activity recovery, loadings for bovine serum albumin (BSA) and β-galactosidase (β-Gal), and the separation of a mixture of immunoglobulin G (IgG), BSA, β-Gal and insulin for an aramid material packed in a rolled, cylindrical configuration.

MATERIALS AND METHODS

Stationary phases

The stationary phase is an aramid fabric obtained from DuPont (Wilmington, DE, USA). It is made from a 95:5 blend of producer-colored olive green T-457 Nomex and producer-colored green Kevlar staple fiber and is finished with an antistatic resin (a mixture of polyglycol alkylamine and epoxy resin), which can be washed off under ordinary laundry conditions [7]. The structures of Nomex, poly(*m*-phenylene isophthalamide), and Kevlar, poly(*p*-phenylene terephthalamide), are shown in Fig. 1 with properties given in Table I. The average fiber length is 45 mm and the fiber width is 10–20 μm. The yarn is a ply of two single yarns with a total width of 200–400 μm.

Aramid is defined by the USA Federal Trade Commission as "a manufactured fiber in which the fiber-forming substance is a long-chain synthetic polyamide in which at least 85% of the amide (–CO–NH–) linkages are attached directly to two aromatic rings" [8]. Nomex and Kevlar are DuPont trademarks of fibers that belong to the aramid classification [9,10].

Aramid fibers are highly crystalline, do not melt, and have extremely low combustibility. Their molecular weights are equal to or greater than 60 000, *i.e.*, the degree of polymerization, DP ⩾ 250 [10]. Nomex is noted for its resistance to temperature and flame. The fiber retains useful properties at temperatures up to 370°C [8]. The chemical resistance of aramid fibers is also very good. Nomex is resistant to most alkalis except NaOH at elevated temperatures (60°C) and at concentrations above 50%. It is unaffected by most organic compounds, but is degraded by hot, concentrated acids. Typical uses for Nomex include protective suits for fire fighters and race car drivers, industrial work uniforms,

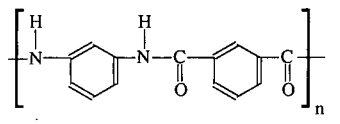

Nomex

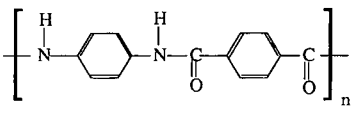

Kevlar

Fig. 1. Chemical structures of Nomex and Kevlar.

TABLE I

CHARACTERISTICS OF ARAMID FIBERS

	Nomex	Kevlar
Specific gravity	1.38	1.44
Tenacity (g/denier) dry	4.8–5.8	21.5
Moisture regain (%)	5.0	3.5–4.5
Burning characteristics	Low flammability	Low flammability
Melting point	Decomposes above 370°C	Decomposes above 260°C
Resistance to:		
Reagents	Degraded by hot, concentrated acid and alkali	Degraded by hot, concentrated acid and alkali
UV light	Degraded after prolonged exposure	Degraded after prolonged exposure

aircraft furnishings, hot gas filtration fabrics and selected components of space vehicles and apparel.

Kevlar aramid fiber has similar resistance to heat (260°C) and chemicals as Nomex. Kevlar has an extremely high tenacity, approximately 22 g/denier, which is more than five times the strength of a steel wire of the same weight and more than twice the strength of industrial nylon, polyester or fiberglass [9]. Kevlar is also flame resistant. End uses for the fiber include tire cord, bulletproof vests, conveyor belts, ropes and cable, fiber reinforcement for aircraft, space vehicles, boats, sports car bodies, and golf clubs. Selected characteristics of aramid fibers are summarized in Table I [8,11].

Packing technique

The fabric is first washed at 70°C in deionized (DI) water, and then air dried. A very small amount of starch is powdered onto the fabric to give it sufficient frictional resistance so that the layers of the fabric will "grab", thus facilitating the rolling of the fabric into a tight cylinder (Fig. 2). Once rolled, plastic ties are placed at 2- to 3-cm intervals to hold the roll in its compact cylindrical form. A hole is punched or drilled through one end of the rolled fabric, and a 10-gauge steel wire is placed through the hole, and bent into place. The wire is then threaded through the chromatography column, and the rolled fabric cylinder is gradually pulled through the column, with the plastic ties being clipped off, one at a time. The fabric is 2 to 5 cm longer than the column, so that when it is pulled through, the end can be cut flush with the column, and the section removed through which the wire was threaded.

The starch is washed out of the column during normal column operation, although some granules were evident in scanning electron micrographs taken after the column had been used.

Liquid chromatography system

To obtain high flow-rates, two pumps (Mini-Pump; Milton Roy, Riviera Beach, FL, USA) are used together in parallel to pump the solvent through an injection valve (Model 7125; Rheodyne,

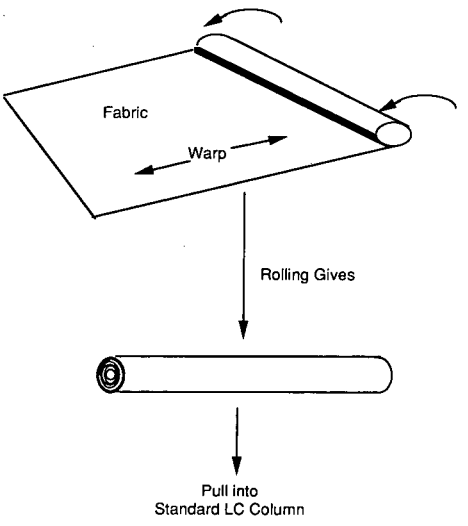

Fig. 2. Schematic representation of rolling and packing procedures.

Berkeley, CA, USA) into the column. The eluent passes into a UV–VIS detector (VARI-CHROM, Sunnyvale, CA, USA) or a refractive index detector (Refracto Monitor Model 1107, Milton Roy) and the signal is recorded on a Linear (Irvine, CA, USA) 1200 chart recorder. The flow-rate used is up to 17.5 ml/min, which is the maximum flow-rate of the combined pumps.

Operational conditions

The columns were run at ambient temperature. Column void volumes were measured with dextran (molecular weight, MW = $2 \cdot 10^6$), polyethylene glycol (PEG 20 000) (both from Sigma, St. Louis, MO, USA) and sodium chloride (from Fisher Scientific, Fair Lawn, NJ, USA). The void fraction based on PEG 20 000 (MW 20 000) was 0.22 and that based on NaCl was 0.37. These values are significantly lower than those obtained for columns packed with spherical particles, where the extra-particle void fraction ranges from 0.35 to 0.40 and the overall void fraction from 0.50 to 0.80.

In order to limit protein consumption, a small column (5 ml in volume) was used for obtaining isotherm, activity, recovery, four-protein separation, and protein loading data. A 46-ml column was also used for some separations to demonstrate the feasibility of packing and using larger columns. The characteristics of both columns are summarized in Table II. This fabric has about 90 000 fibers/g, which corresponds to an external surface area of 0.2 m^2/g.

The pressure drop as a function of flow-rate was measured using the 50-cm column. Stable operation was achieved up to the pumping limit (17.5 ml/min), where the pressure drop was 2000 p.s.i.g. A typical pressure drop curve is shown in Fig. 3.

Proteins and eluents

BSA, fraction V powder, anti-human IgG (whole molecule, developed in rabbit), insulin (from bovine pancreas) and β-Gal (grade VIII, from *E. coli*) are all from Sigma. Sodium acetate (80 m*M*, analytical-reagent grade; Mallinckrodt, Paris, KY, USA) and 80 m*M* acetic acid (reagent grade, Fisher) are mixed to give a buffer with pH of 4.7. A concentration of 5 m*M* Na_2HPO_4 (reagent grade; J. T. Baker, Phillipsburg, NJ, USA) is used with 5 m*M* KH_2PO_4 (reagent grade; Matheson, Coleman & Bell, Norwood, OH, USA) to give pH 7.0 buffer, and 10 m*M* $Na_2B_4O_7 \cdot 10H_2O$ (Matheson, Coleman & Bell) is used to adjust pH to 9.2. Ammonium sulfate (purified) is from Baker.

The porosity characteristics were determined using the following molecular probes: ^2H_2O (MW 20); NaCl (58.5); glucose (180); dextran ($2 \cdot 10^6$); and PEGs of molecular weights 200, 300, 400, 600, 1000, 1450, 3350, 8000, 10 000 and 20 000.

β-Gal activity assay

The activity of β-Gal is determined by using *o*-nitrophenyl-β-D-galactopyranoside (ONPG) as substrate. The procedure is as given by Sigma. The absorbance measurement is made 20 min after adding all the reagents.

TABLE II

COLUMN PARAMETERS

	Small	Large
Length (cm)	10	50
Diameter		
O.D. (in.)	3/8	1/2
I.D. (mm)	8.0	10.9
Volume (ml)	5.05	46.3
Stationary phase		
Dry weight (g)	2.68	21.04
Packing density $\left(\frac{\text{g dry stationary phase}}{\text{ml column volume}}\right)$	0.53	0.45

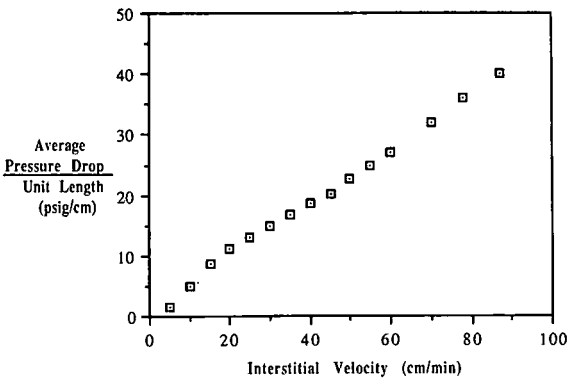

Fig. 3. Characteristic pressure drop of the rolled stationary phase in 50 cm column with aqueous mobile phase at ambient temperature. Column: 50 cm × 10.9 mm I.D., eluent: DI water.

Adsorption isotherm of BSA

The adsorption isotherm of BSA is obtained by frontal analysis [12]. The protein concentration is determined on the LC system with a zero-volume fitting substituted for the column. The concentration is calculated from the peak height using a BSA standard curve. At a concentration of above 2 mg/ml, the relation between peak height and protein concentration is no longer linear. Consequently, breakthrough curves drawn by the chart recorder cannot be used directly for the frontal analysis. In this case, samples are collected, appropriately diluted, and then measured. The adsorption isotherm for BSA in 5 m*M* phosphate buffer (pH 7.0) is monotone and concave-down, with a loading of 4 mg/g at a mobile phase concentration of 5 mg/ml (Fig. 4).

Recovery determination

A stepwise breakthrough–washing–desorption method is used to determine the recovery of protein. If the volume of the breakthrough is V_1 with initial protein concentration of C_0 and emerging concentration of C_1, and if the volume and concentration of protein in the wash step are V_2 and C_2 and in the desorption step are V_3 and C_3, the recovery (R) expressed as a percentage is

$$R(\%) = \frac{C_3 V_3}{C_0 V_1 - (C_1 V_1 + C_2 V_2)} \cdot 100 \qquad (1)$$

Protein recovery was tested with respect to BSA by loading the stationary phase to 4 mg protein/g in 5 m*M* bisodium–potassium phosphate buffer at pH 7.0. Elution was achieved by 100 m*M* NaCl (pH 7.0), and the total eluent was collected and analyzed. Protein recovery was 99%.

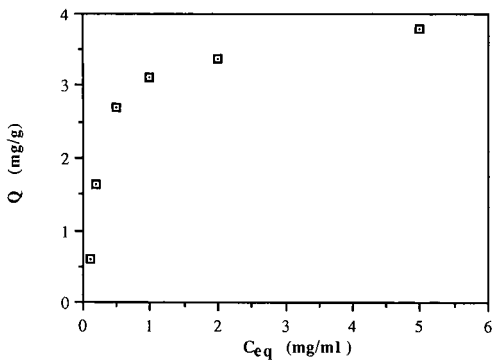

Fig. 4. Adsorption isotherm for BSA. Temperature: 25°C; column size: 10 cm × 8 mm I.D.; flow-rate: 1 ml/min; eluent: DI water.

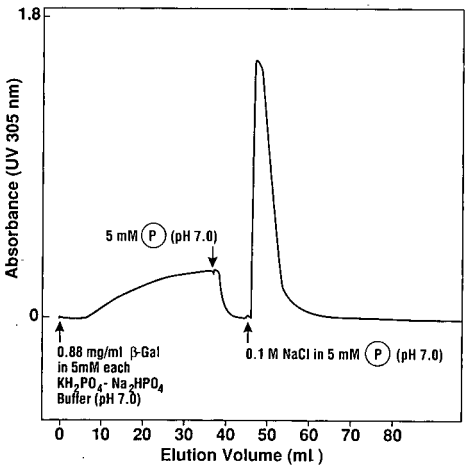

Fig. 5. Adsorption and elution profiles for β-Gal. Temperature: 25°C; column size: 10 cm × 8 mm I.D.; flow-rate: 1.1 ml/min; other conditions indicated in figure. 5 m*M* Ⓟ denotes 5 m*M* Na_2HPO_4–5 m*M* KH_2PO_4.

Retention of enzyme activity was checked by adsorbing β-Gal in 5 m*M* buffer (pH 7.0), and desorbing it at 0.1 *M* NaCl in 5 m*M* phosphate buffer (see Fig. 5). The activity was checked using an ONPG assay before adsorption and after desorption. The β-Gal was from *E. coli* and is a large multimeric protein at pH 7.0 with a molecular weight of 520 000. The adsorption of the β-Gal was much higher than that of BSA, with 0.88 mg/ml of β-Gal giving a loading of 6.1 mg/g stationary phase. The β-Gal capacity at higher concentrations was not determined because of the expense involved. Desorption of the β-Gal gave complete recovery of specific activity based on the ONPG assay.

Plate height determination

Plate heights were determined using the 50-cm column. Samples of PEG 20 000, PEG 200, or ^2H_2O (volume 100 μl) were injected and eluted from the column. Plate height was calculated directly from the chromatogram, with peak width measured at half-height.

RESULTS

Separations

This stationary phase is capable of separating both small and large proteins as indicated by the fractionation of IgG (MW 146 000–165 000), BSA (MW 60 000), insulin (MW 6100 for monomer, 12 200 for dimer), and β-Gal (MW 520 000), shown in Fig. 6. The multimodel nature of this stationary phase is related to its structure (Fig. 1) and possibly to the dye in the fiber. The polymers in the aramid fabrics have amino and/or carboxyl end groups, depending on how the polymerization was quenched, and thus exhibit ionic character. The aromatic polyamides also have many benzene rings. Hydroxylated adsorbates may therefore form π bonds with the benzene rings and adsorb.

The effect of both ionic and hydrophobic interactions between aramid fibers and proteins can be explained through Table III which summarizes retention characteristics for the four proteins in five different eluents. All four proteins studied in this paper are strongly retained in the column using DI water as eluent but unretained in 0.1 *M* NaCl. When 1 *M* $(NH_4)_2SO_4$ is the eluent, two of the proteins, insulin and β-Gal, are still strongly retained. This indicates that, in addition to ionic interactions, insulin and β-Gal exhibit hydrophobic interactions [13].

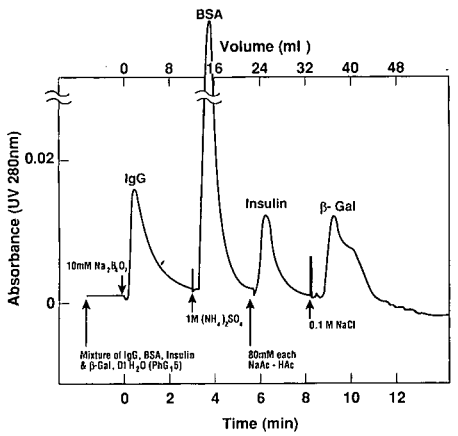

Fig. 6. Separation of four-protein mixture at flow-rate of 4 ml/min and ambient temperature (small column). Injection volume of 200 μl with the proteins at concentrations of 10 mg/ml (IgG), 10 mg/ml (BSA), saturated (insulin), and 4 mg/ml (β-Gal) (pH 7.0). Ac = Acetyl.

TABLE III

STEPWISE DESORPTION PROTOCOL

+ = Retained; − = unretained.

Eluent	Protein			
	IgG	BSA	Insulin	β-Gal
DI Water (pH 5.5)	+	+	+	+
10 m*M* $Na_2B_4O_7$ (pH 9.2)	−	+	+	+
1 *M* $(NH_4)_2SO_4$ (pH 4.5)	−	−	+	+
80 m*M* NaAc–80 m*M* HAc (pH 4.7)	−	−	−	+
0.1 *M* NaCl (pH 5.5)	−	−	−	−

Porosity

Scanning electron microscopy (SEM) compares the structures of the flat and rolled materials (Fig. 7a and b). SEM of the flat material (Fig. 7a and c) shows yarns having a diameter of 200–400 μm, with each yarn consisting of many fibers having a diameter of 10–20 μm. When rolled (Fig. 7b) a tightly packed three-dimensional matrix results. Void volumes which are accessible to eluent flow are shown in the schematic diagram of Fig. 8 and include the space between fibers, yarns and intermatrix voids.

The SEM and fiber characteristics lead to the definition of three porosities: (1) between the yarns, or the interyarn porosity with a void fraction ε_b; (2) between the fibers within a yarn or the interfiber porosity (ε_p); and (3) intrafiber void fraction (ε_i) from pores and cracks within each fiber, enclosed areas that arise when the fibers are twisted around each other to form a yarn, and from the crossing of yarns. This description is analogous to a column packed with particles possessing a macro- as well as a microporosity; ε_b, ε_p, and ε_i then correspond, respectively, to the interstitial, macroporous and microporous void fractions.

The flow porosity is about 0.22 based on the elution volume of PEG 20 000. This is low compared even to the external porosity generated by the dense packing of non-porous spherical particles, which is theoretically 0.26 [14,15], although in practice values around 0.40 are obtained. Since the

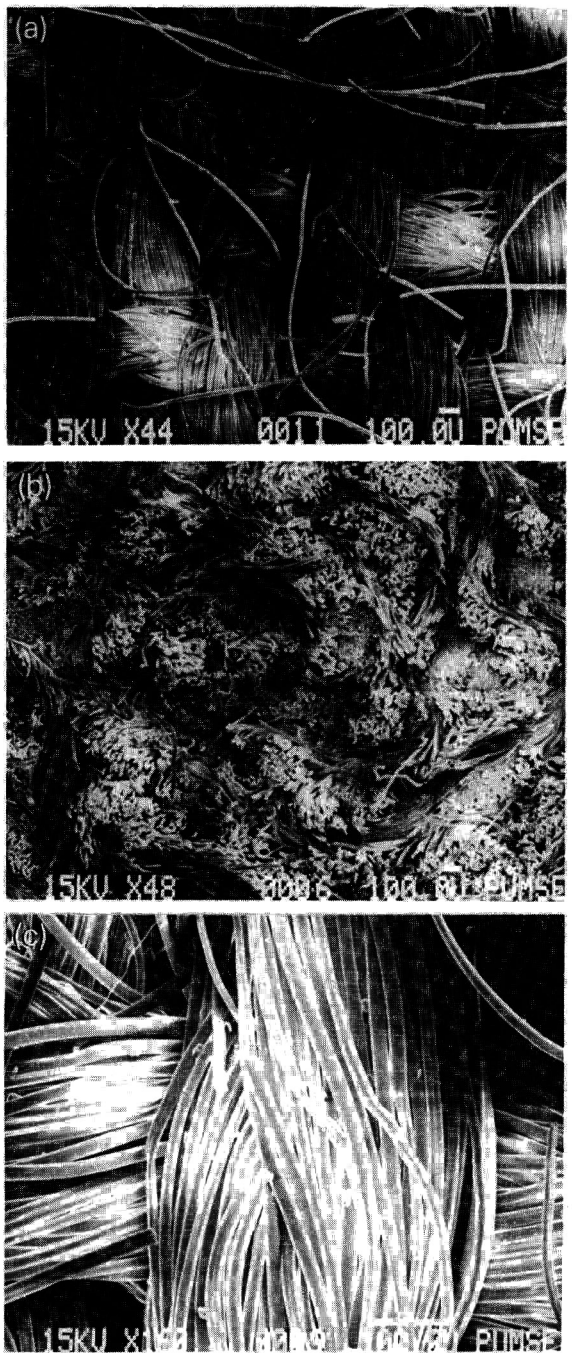

Fig. 7. Scanning electron micrographs of (a) flat fabric, (b) cross-section of rolled fabric, (c) yarn, showing individual fibers. Scale indicated at bottom of picture, bar = 100 μm.

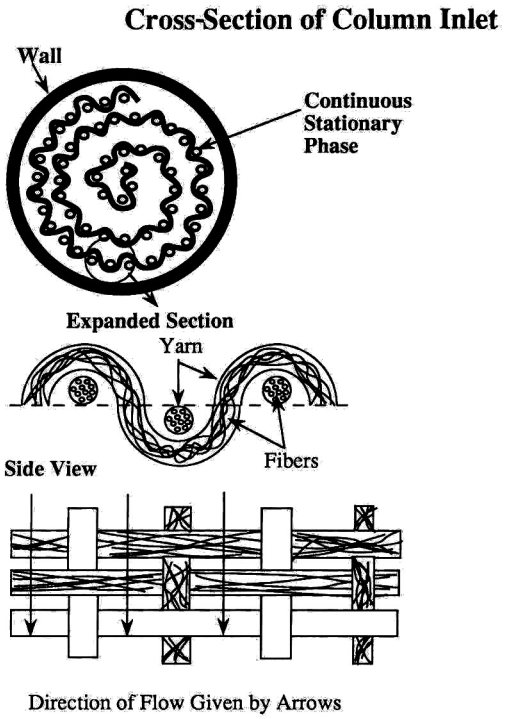

Fig. 8. Schematic of the rolled stationary phase within the column.

fabric is compressed during column packing, the measured void fraction will be lower than the overall permeabilities reported in the textile literature, which were obtained by batch measurements [16–19].

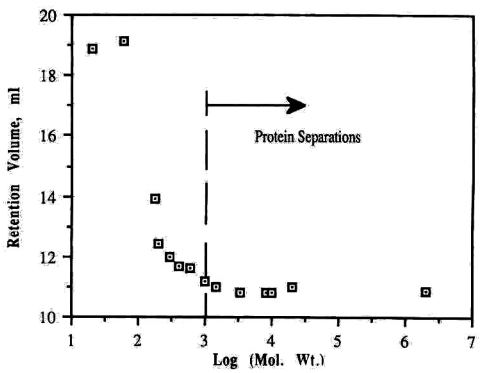

Fig. 9. Elution volume as a function of probe molecular weight. Temperature: 25°C; column size: 50 cm × 10.9 mm I.D.; flow-rate: 1.0 ml/min; eluent: DI water. The probes used were NaCl (MW 58.5); ^2H_2O (MW 20); glucose (MW 180); PEGs of molecular weight 200, 300, 400, 600, 1000, 1450, 3350, 8000, 10 000 and 20 000; and dextran (MW $2 \cdot 10^6$).

A series of molecular weight probes gave the retention behavior of Fig. 9. At molecular weights greater than 1000, the retention volume is essentially independent of molecular weight. These probes see all of the interyarn and interfiber spaces. The smaller probes (MW < 1000) also see some part of the intrafiber pore space. Because of the relatively large interfiber diameters (Fig. 7b and c), even the largest probes see all of the interfiber space, unlike in conventional chromatography with packed particles, where the macroporous space need not be completely accessible to the largest probes.

Pressure drop

Applied pressure drop is a linear function of velocity over the entire experimental range of flow-rates (Fig. 3), and follows Darcy's law (see refs. 20 and 21).

Modified Van Deemter equation

The scanning electron micrographs of Fig. 7 show relatively large interfiber spaces (on the order of micrometers). Thus convection is likely to occur through both interyarn and interfiber channels, as illustrated schematically in Fig. 10. The interfiber channels have a small cross-sectional area while the interyarn channels are large. Just as flows in parallel pipes of equal lengths distribute according to cross-sectional areas, flow through these channels are envisioned to distribute in proportion to their cross-sectional areas. Consequently, pore (*i.e.*, interfiber) velocity, v_{pore}, is a small fraction of the interyarn velocity, and therefore of the chromatographic velocity, v_{chrom}. As the eluent flow-rate increases, both the pore and the chromatographic velocity will increase proportionately (their ratio will remain constant, independent of flow-rate). At higher flow-rates, the pore velocity could become high enough to make convective transport through the interfiber space appreciable relative to diffusive transport. This would in turn affect the overall plate height expression. In order to estimate the contribution of convective intrafiber transport to band-spreading, we make the simplifying assumption of plug flow. Then the effects of convection and diffusion can be added in parallel after Guttman and DiMarzio [22]. The convective contribution to plate height for piston flow is independent of velocity; thus, the total plate height due to the "intraparticulate" pore space is given by:

$$\frac{1}{H_{pore,\,total}} = \frac{1}{H_{conv}} + \frac{1}{H_{diff}} = \frac{1}{D} + \frac{1}{C' v_{pore}} \tag{2}$$

where C' and D are empirical parameters. Eqn. 2 can be rewritten as

$$H_{pore,\,total} = \frac{DC' v_{pore}}{D + C' v_{pore}} \tag{3}$$

At high velocities, the convective term dominates the expression, while the opposite is true at low flows. The total plate count is then given by

$$H_{total} = A + \frac{B}{v_{chrom}} + \frac{DCv_{chrom}}{D + Cv_{chrom}} \tag{4}$$

which is the modified Van Deemter equation applicable to systems involving flow through the particles. Here, the pore velocity is replaced by the chromatographic velocity ($v_{pore} = f v_{chrom}$ where $0 < f < 1$). The additional constant, f, has been absorbed into C' to give C. Note that the chromatographic velocity [23] will be different for probes that see different fractions of the total mobile phase space.

Eqn. 4 gives the solid line fit to the data using non-linear regression in Figs. 11 and 12, where the reduced plate height h, given by H_{total}/d_W, is used. An average value of 300 μm was used for the characteristic particle size (yarn width) d_W. Table IV compares values of A, B, C and D for the classical and modified Van Deemter equations. The modified

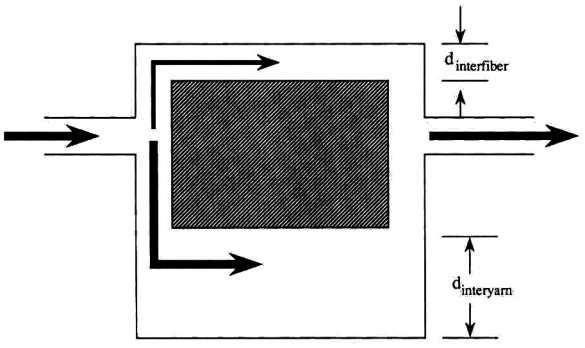

Fig. 10. Schematic of the parallel flow patterns available, representing flow through the interyarn and interfiber channels. There are numerous interfiber channels for every interyarn channel but the diagram only shows one channel of each kind, for simplicity.

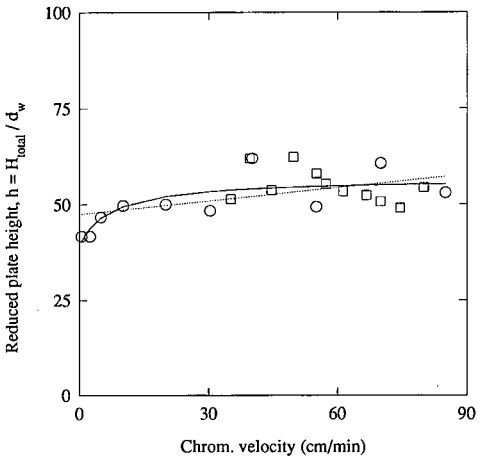

Fig. 11. Plate height as a function of chromatographic (Chrom.) velocity for PEG 20 000. The symbols ○, □ represent two different experimental runs; the dotted line represents the best-fit Van Deemter expression, and the continuous line the best-fit modified Van Deemter expression.

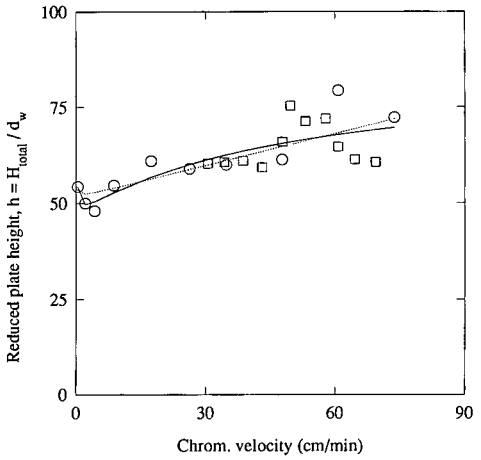

Fig. 12. Plate height as a function of chromatographic velocity for PEG 200. Symbols as in Fig. 11.

Van Deemter equation follows the trend of the data over the entire range of chromatographic velocities $[=Q/(A_x\varepsilon_i')]$.

For PEG 20 000, the contribution due to convection within the interfiber pores dominates the contribution of diffusion at high velocities, giving the flat plate height line in Fig. 11. The velocity range in which axial dispersion dominates bandspreading is lower than that used in the present experiments, and consequently the plate height data do not show a minimum. The modified Van Deemter equation fits the data well over the entire velocity range. At high enough velocities, eqn. 4 reduces to

$$H_{\text{total}} \approx A + D \tag{5}$$

which corresponds to the flat region for velocities above 30 cm/min in Fig. 11.

TABLE IV

COMPARISON OF FITTED CONSTANTS FOR CONVENTIONAL AND MODIFIED VAN DEEMTER EQUATIONS

Data in Figs. 11 and 12 fitted by non-linear regression using the Marquardt method (the NONLIN procedure in the statistical package SAS). Parentheses contain values of asymptotic standard error.

	PEG 200		PEG 20 000	
Average molecular weight	200		20 000	
Estimated D (cm^2/s)[a]	$6.3 \cdot 10^{-6}$		$8.5 \cdot 10^{-7}$	
Conventional Van Deemter ($h = A + B/v_{chrom} + Cv_{chrom}$)				
A	51.5	(2.98)	47.4	(2.36)
B	0.81	(2.69)	0.0	–
C	0.28	(0.063)	0.11	(0.045)
Modified Van Deemter (eqn. 4)				
A	46.7	(6.02)	39.3	(5.29)
B	3.0	(3.54)	0.0	–
C	0.77	(0.75)	2.5	(3.28)
D	38.5	(18.8)	17.3	(4.68)

[a] Estimated using the Wilke–Chang equation (see ref. 24).

Unlike PEG 20 000, which is too large to penetrate pores inside the fibers, PEG 200 is small enough to explore some of the intrafiber, as well as all of the interfiber and interyarn spaces. Thus, for PEG 200 the plate height increases slightly even at the highest velocities (Fig. 12). There is a plate height contribution due to microporous diffusion which, in contrast to diffusion in the interfiber space, does not act in parallel with any convective term. (There is no flow through the micropores, which are taken to be closed.) Thus the microporous diffusion contribution is linearly proportional to the velocity [25]. In addition, the smaller size of PEG 200 (and consequently its higher diffusivity) implies that the velocity range over which axial dispersion is dominant would be higher than that for PEG 20 000. In fact, this region is accessed over the experimental velocity range, and a minimum is seen in the data.

A result which did not fit either the modified Van Deemter (eqn. 4) or the classical equation was obtained for deuterated water. The ^2H_2O was found to give a decreasing plate height with increasing velocity (Fig. 13). It was expected that ^2H_2O would give a greater increase in plate height than PEG 200, since ^2H_2O is capable of exploring a bigger fraction of the microporous space.

It is not clear what causes the decreasing plate height. We hypothesize that at low flow-rates mass transfer contributes to the overall plate height due to an external boundary layer between interstitial and interfiber pores. However, at higher flow-rates, where convection becomes the dominant interfiber transport mechanism, contributions due to mass transfer across a boundary layer could be decreased, thus decreasing the overall plate height as described by Van Kreveld and Van den Hoed [25]. This would be particularly noticeable for ^2H_2O, which as a small molecule has a diffusivity on the order of $33 \cdot 10^{-6}$ cm^2/s compared to $6.3 \cdot 10^{-6}$ for PEG 200 and $8.5 \cdot 10^{-7}$ for PEG 20 000 [24].

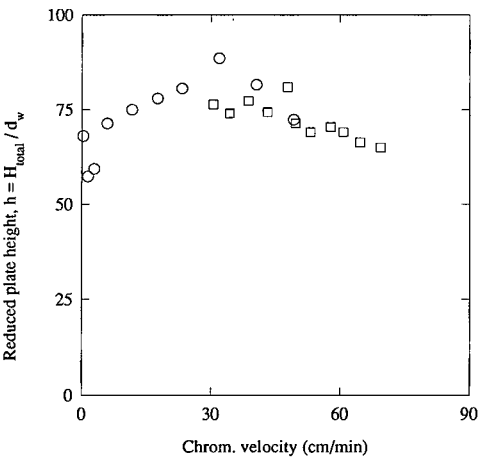

Fig. 13. Plate height as a function of chromatographic velocity for ^2H_2O. Symbols as in Fig. 11. Neither the Van Deemter nor the modified Van Deemter curves are shown because they fit the data poorly, for reasons explained in the text.

DISCUSSION

Other workers have considered analogues to the "coupling" between flow and diffusion described above. For size-exclusion chromatography, Van Kreveld and Van den Hoed [25], considered that eddy diffusion would extend from the interstitial space into the intraparticulate pores, although not necessarily fully penetrating the pore. Here the pores are not assumed to traverse the entire particle. They therefore added a velocity-dependent correction, D^*v to the pore diffusivity, D_p, to obtain an effective diffusivity:

$$D_{p,eff} = D_p + D^*v \tag{6}$$

where D^* is due to eddies. They reported a plate height expression having axial dispersion, eddy diffusion, and convective terms:

$$H_{total} = \frac{2D_m}{v} + 2A + \frac{k'}{30(1+k')^2}\left\{\frac{vd^2_{particle}}{D_p + D^*v}\right\} \tag{7}$$

This is similar in form to eqn. 4. The second term, $2A$, in eqn. 7 is due to eddy diffusion and the last term is the combined effect of flow and diffusion within the particle where the external mass-transfer contribution is neglected. At low velocities, the diffusive contribution ($2D_m/v$) predominates, and plate height is inversely proportional to the linear velocity. At high velocities, the convective term dominates, resulting in a velocity-independent plate height contribution $\{(k'/[30(1+k')^2]\}(d^2_{particle}/D^*)$.

A similar approach is described by Afeyan *et al.* [26] who report a form of chromatography where flow occurs through the particle (which they term

"perfusion chromatography"). They use a correction to the intraparticulate diffusivity analogous to eqn. 6:

$$D_{p,eff} = D_p + \frac{d_{particle}\, v_{pore}}{2} \quad (8)$$

This again results in a velocity-independent plate height contribution at high flow-rates, as in eqn. 7.

These approaches, in which two mechanisms act "in parallel," are similar to the coupling theory of Giddings [27] in which contributions from flow and diffusion act simultaneously. However, as has been pointed out by Van Kreveld and Van den Hoed [25], when flow occurs across a particle, the coupling between diffusive and convective transport across the particle becomes significant over a much higher range of flow-rates than the coupling described by Giddings.

CONCLUSIONS

The concept of LC using a continuous stationary phase, rolled and inserted into a standard LC column, is demonstrated. This stationary phase has the desirable attributes of mechanical stability and high selectivity and recovery; it is non-denaturing, and has potential for preparative protein separations if higher capacities are attained. The plate height is nearly constant at high chromatographic velocities for a solute which is small enough to pass through pore spaces which transverse the stationary phase matrix, but large enough to be excluded from the smaller dead-end pores. A coupling argument based on simultaneous flow and diffusion is used to explain this effect, and a modified Van Deemter expression is proposed which may be useful in describing other types of stationary phases with transecting pores.

ACKNOWLEDGEMENTS

The material in this work was supported by NSF Grants 8907304 and BCS 8912150. We thank R. Hendrickson, K. Kohlmann, and D. McCabe for experimental assistance. We also express our appreciation to G.-J. Tsai and A. Sarikaya and Dr. R. Dean for their helpful comments during preparation of this manuscript.

SYMBOLS

A	Eddy diffusion contribution to plate height, cm
A_x	Empty column cross-sectional area, cm^2
B	Coefficient of axial dispersion term in Van Deemter expressions (eqn. 4), cm^2/s
C	Coefficient of linear velocity term in the modified Van Deemter expression (eqn. 4), s
C'	Empirical parameter representing constant for convection through pores, s
C_1	Effluent protein concentration during breakthrough, mg/ml
C_2	Concentration of protein during wash step, mg/ml
C_3	Concentration of protein during desorption step, mg/ml
C_0	Initial protein concentration
C_{eq}	Equilibrium concentration of protein, mg/ml
D	Additional term in modified Van Deemter expression (eqn. 4), representing H_{conv}, cm
D^*	"Eddy diffusivity" corresponding to flow within particles (eqn. 6), cm
D_m	Molecular diffusivity, cm^2/s
D_p	Pore diffusivity, cm^2/s
$D_{p,eff}$	Effective pore diffusivity incorporating convective effects (eqn. 6), cm^2/s
$d_{interfiber}$	Characteristic diameter of interfiber space, cm
$d_{interyarn}$	Characteristic diameter of interyarn space, cm
$d_{particle}$	Particle diameter, cm
d_W	Characteristic distance (yarn width) for convection and diffusion in the interfiber channels, cm
f	fraction of interstitial flow-rate which passes through the pores, dimensionless
h	Reduced total plate height, H_{total}/d_W, dimensionless
H_{conv}	Contribution to plate height from convection through the interfiber channels, cm
H_{diff}	Contribution to plate height from diffusion through the interfiber channels, cm

$H_{pore,\ total}$ Net contribution from within the interfiber channels to the overall plate height, cm
H_{total} Total plate height, cm
k' Capacity factor (dimensionless)
Q Volumetric flow-rate, ml/min
R Recovery of protein
V_1 Volume of the breakthrough, ml
V_2 Volume of effluent during wash step, ml
V_3 Volume of effluent during desorption step, ml
v Linear velocity, cm/s
v_{chrom} Chromatographic velocity, cm/s
v_{pore} Interfiber velocity, cm/s
V_R Retention volume, ml

Greek symbols

ε_b Interyarn void fraction, dimensionless
ε_i Intrafiber void fraction, dimensionless
ε_i' Void fraction seen by non-interacting component i, dimensionless
ε_p Interfiber void fraction, dimensionless

REFERENCES

1 H. B. Reisman, *Economic Analysis of Fermentation Processes*, CRC Press, Cleveland, OH, 1988, p. 75.
2 G. K. Sofer and L.-E. Nystrom, *Process Chromatography*, Academic Press, San Diego, CA, 1989, p. 107.
3 P. Knight, *Bio/Technology*, 7 (1989) 777.
4 S. J. Gibbs and E. N. Lightfoot, *Ind. Eng. Chem. Fundam.*, 25 (1986) 490.
5 H. Ding, M-C. Yang, D. Schisla and E. L. Cussler, *AIChE J.*, 35 (1989) 814.
6 H. Ding and E. Cussler, *Biotech. Prog.*, 6 (1990) 472.
7 D. E. Hoffman, Industrial Products Division, Fibers and Composites Development Centers, E. I. DuPont de Nemours and Company, Wilmington, DE, personal communication, September (1989).
8 Federal Trade Commission, *Rules and Regulations Under the Textile Fiber Products Identification Act*, Washington, DC, July 9, 1986.
9 M. L. Joseph, *Introductory Textile Science*, Holt, Rinehart & Winston, New York, 5th ed., 1986, p. 110.
10 J. Preston, in M. Grayson (Editor), *Kirk-Othmer Encyclopedia of Chemical Technology*, Vol. 3, Wiley, New York, 3rd ed., 1978, p. 213.
11 P. G. Tortora, *Understanding Textiles*, Macmillan, New York, 5th ed., 1992, p. 188.
12 J. R. Conder and C. L. Young, *Physico-Chemical Measurements by Gas Chromatography*, Wiley, Chichester, 1979, Ch. 9.
13 B. F. Roettger and M. R. Ladisch, *Biotech. Adv.*, 7 (1989) 15.
14 R. M. German, *Particle Packing Characteristics*, Metal Powder Industries Federation, Princeton, NJ, 1989, pp. 32–34, 89–97.
15 D. J. Cumberland and R. J. Crawford, *The Packing of Particles*, Elsevier, Amsterdam, 1987, pp. 14–18.
16 R. McGregor, *J. Soc. Dyers Colour.*, 81 (1965) 429.
17 L. D. M. van den Brekel and E. J. de Jong, *Textile Res. J.*, 59 (1989) 433.
18 L. D. M. van den Brekel and E. J. de Jong, *Textile Res. J.*, 60 (1990) 429.
19 P. Banks-Lee, H. Peng and M. Mohammadi, *Textile Res. J.*, 60 (1990) 427.
20 A. E. Scheidegger, *The Physics of Flow Through Porous Media*, University of Toronto Press, Toronto, 3rd ed., 1974, pp. 73–79.
21 G. I. Barenblatt, V. Entov and V. M. Ryzhik, *Theory of Fluid Flows Through Natural Rocks*, Kluwer, Dordrecht, 1990, pp. 9–12.
22 C. M. Guttman and E. A. DiMarzio, *Macromolecules*, 3 (1970) 681.
23 Cs. Horváth and H.-J. Lin, *J. Chromatogr.*, 126 (1976) 401.
24 R. C. Reid, J. M. Prausnitz and T. K. Sherwood, *The Properties of Liquids and Gases*, McGraw-Hill, 3rd ed., 1977, pp. 567–590.
25 M. E. van Kreveld and N. van den Hoed, *J. Chromatogr.*, 149 (1978) 71.
26 N. B. Afeyan, N. F. Gordon, I. Maszaroff, L. Varady, S. P. Fulton, Y. B. Yang and F. E. Regnier, *J. Chromatogr.*, 519 (1990) 1.
27 J. C. Giddings, *Dynamics of Chromatography*, Part I, Marcel Dekker, New York, 1965, pp. 47–61.

Journal of Chromatography, 598 (1992) 181–187
Elsevier Science Publishers B.V., Amsterdam

CHROM. 24 007

High-performance hydrophobic interaction chromatography of proteins on reversed-phase supports coated with non-ionic surfactants of polyoxyethylene type

Purification of a fungal aspartic proteinase

Youne Lie Kong Sing, Yolande Kroviarski☆, Sylvie Cochet☆, Didier Dhermy and Olivier Bertrand*,☆

INSERM U 160 and Centre de Recherche sur les Enzymopathies de l'Association Claude Bernard, Hopital Beaujon, 92118 Clichy Cedex (France)

(First received July 19th, 1991; revised manuscript received December 20th, 1991)

ABSTRACT

On coating reversed-phase supports with polyoxyethylene-type non-ionic surfactants, proteins are no longer retained on such supports at moderate or low ionic strength, but they are retained at high ionic strength and can be desorbed by a decreasing ionic strength gradient. These reversibly modified supports were used for hydrophobic interaction chromatography (HIC). The proteins probably interact with the polyoxyethylene tail of the non-ionic surfactant while the hydrophobic part of the surfactant anchors the surfactant to the reversed-phase support by interactions with its alkane coverage. Although the interactions between non-ionic surfactant and reversed-phase support are non-covalent and the HIC mobile phases contained no surfactant, the modified columns were stable and could be used repeatedly. A surfactant-modified reversed-phase column provided a rapid, efficient, one-step purification of a fungal aspartic proteinase from a commercial crude preparation.

INTRODUCTION

Hydrophobic interaction chromatography (HIC) is a powerful method for purifying proteins. It was discovered as an adjunct to affinity chromatography when it was realized that the alkyl spacers used to immobilize affinity ligands could themselves interact with hydrophobic pockets situated on the surface of proteins and so retain them [1]. HIC columns are generally loaded with proteins at moderate to high salt concentration and the proteins are eluted with a decreasing salt concentration gradient [1–3].

HIC was initially performed with soft gels as a matrix for column preparation, but mechanically resistant supports based on a silica or a polymeric backbone can also be used [3–13]. Various ligands have been grafted to the chromatographic supports to confer the hydrophobic character needed for HIC; these ligands range from weakly hydrophobic types such as polyoxyethylene ethers [4,6,8–10,12–14] and poly(vinyl alcohols) (the name mild hydrophobic interaction was coined some years ago for this particular type of column [14]) to highly hydrophobic types such as alkane and phenyl ligands (3–5, 7, 11, 13). The influence of the nature of the ligand has been studied [4], as also have the differences between reversed-phase chromatography and HIC. The former uses strongly hydrophobic, highly

☆ Present address: INSERM U 76, INTS, 6 Rue Alexandre Cabanel, 75739 Paris Cedex 15, France.

0021-9673/92/$05.00

substituted supports and proteins lose their native structure when bound on such supports, proteins being eluted with a mobile phase containing an organic solvent [8–10]. HIC columns are less hydrophobic because they carry less hydrophobic ligands or smaller amounts of ligands, and proteins remain in their native form on such columns and no organic solvent is needed for elution.

Polyoxyethylene-type non-ionic surfactants in aqueous solution can be retained on reversed-phase supports by their alkane tails, leaving the comparatively polar parts of the surfactant molecule (*i.e.*, the polyoxyethylene part) exposed to an aqueous mobile phase [15–18]. As polyoxyethylene covalent grafting has been used to prepare HIC columns [4,6,8–10,12,13], we attempted to modify reversibly the surface properties of a reversed-phase column by coating it with a polyoxyethylene-type surfactant so as to use it for the HIC of proteins. While this paper was in the review process, we became aware that it had been noticed before that high salt conditions could promote the retention of proteins on columns prepared (for other purposes) by surfactant coating [15,17].

EXPERIMENTAL

Materials

Thermolysin and bovine trypsinogen were obtained from Merck (Darmstadt, Germany). Bovine α-chymotrypsinogen A and a fungal protease (protease from *Rhizopus* species, type XVIII) were obtained from Sigma (St. Louis, MO, USA) and bovine ribonuclease A from Boehringer (Mannheim, Germany). Proteins were used as received.

The non-ionic surfactant Brij 76 (decaethylene glycol *n*-octadecyl ether) was obtained from Sigma. All other chemicals and solvents were from Merck or Carlo Erba (Milan, Italy).

Two reversed-phase materials were purchased from SFCC (Neuilly Plaisance, France): Davisil C_{18} (irregular, mean particle diameter 20 μm, pore size 25 nm) and Ultrabase C_{18} (spherical, particle size 10 μm, pore size 30 nm).

METHODS

Chromatographic apparatus and buffers

The liquid chromatograph was a modular apparatus from Gilson. The mobile phases were 0.5 *M* ammonium acetate buffer (pH 6.0) containing 3 *M* ammonium sulphate (buffer A) and 0.5 *M* ammonium acetate buffer (pH 6.0) (buffer B).

Capacities of reversed-phase supports for non-ionic surfactant

A 150-mg amount of the reversed-phase support was slurried in a small volume of buffer B and settled in a Pharmacia 5/5 FPLC column. The column was then equilibrated with buffer B and 0.05% Brij 76 in buffer B was pumped through the column for 16 h at 1 ml/min. The column was then flushed with five column volumes of buffer B, five column volumes of water and finally twenty column volumes of methanol–isopropanol (1:1, v/v). The water and organic solvent washings were combined and dried, the residue was taken up in water and the surfactant content measured as indicated below.

Preparation of the test HIC column

Davisil C_{18} or Ultrabase C_{18} were packed into 10 cm × 4.6 mm I.D. columns by the method of Kuwata *et al.* [19]. The freshly packed columns were washed with several hundred column volumes of deionized water at 1.0 ml/min. Surfactant was adsorbed on the packing by pumping 0.05% (w/v) Brij 76 in buffer B through the column at 1.0 ml/min for 16 h. The columns were rinsed with several column volumes of buffer B, followed by buffer A.

Chromatography of model proteins

The performances of the columns were evaluated with a mixture of globular proteins dissolved in buffer A at concentrations given in the legends to Figs. 2 and 3. Sample mixture (50 μl) was injected and the columns were developed with a 20-min linear gradient from 0 to 100% B at a flow-rate of 1.0 ml/min at room temperature. The behaviour of the columns was examined by repeated chromatography of the protein mixture.

Determination of non-ionic surfactant concentration

Surfactant was assayed spectrophotometrically using Coomassie Brilliant Blue G-250 (CBBG) [20]. Briefly, aliquots of unknown or standard surfactant (40 μl) were mixed with 960 μl of CBBG reagent (BioRad Labs, Richmond, CA, USA) and the absorbance at 620 nm was read. The calibration graph

is not linear; the slope is steeper when the surfactant concentration in the assay mixture exceeds the critical micelle concentration.

Aspartic protease activity assays

Rhizopus aspartic protease was assayed by monitoring the hydrolysis of Leu–Ser–Phe(NO_2)–Nle–Ala–Leu–OCH_3 (Bachem, Bubendorf, Switzerland). The concentration of the stock substrate solution was determined spectrophotometrically [21]. The final peptide concentration in the assay mixture was 0.73 m*M* and the buffer was 25 m*M* ammonium formate (pH 3.1) containing 0.1 *M* NaCl. The peptide assay mixture also contained 20 μM 6,9-diamino-2-ethoxyacridine lactate as internal standard. Hydrolysis was allowed to proceed at 37°C for 20 min and stopped by adding one tenth of the reaction volume of 1 mg/ml Pepstatin solution in dimethyl sulphoxide. The reaction product was separated from undigested substrate by reversed-phase chromatography on a Nucleosil C_{18} (250 mm × 4.6 mm I.D.) column or on a laboratory-prepared (as indicated above) Ultrabase C_{18} column. Both columns were operated in the isocratic mode with 0.1% trifluoroacetic acid in acetonitrile–water (35:65) as the mobile phase. The absorbance of the column effluent was monitored at 280 nm. The apparatus was calibrated by injecting defined amounts of product. One enzyme unit is defined as the enzyme activity which releases 1 μmol of product per minute under the above assay conditions.

Protein assay

Proteins were determined either by dye-binding assay [22] or by measuring the absorbance at 280 nm.

Sodium dodecyl sulphate–polyacrylamide gel electrophoresis (SDS-PAGE)

SDS-PAGE was performed according to Laemmli [23] using 12.5% polyacrylamide gels under reducing conditions.

RESULTS AND DISCUSSION

Properties of the surfactant-modified reversed-phase column

A reversed-phase column loaded with non-ionic surfactant and equilibrated with a low-salt aqueous mobile phase (*e.g.*, buffer B) did not retain measurable amounts of any of the test proteins. An unloaded column retained all the proteins, and they were eluted only by adding organic solvent to the mobile phase.

This result, together with the known structure of the non-ionic surfactant, indicates that the non-ion-

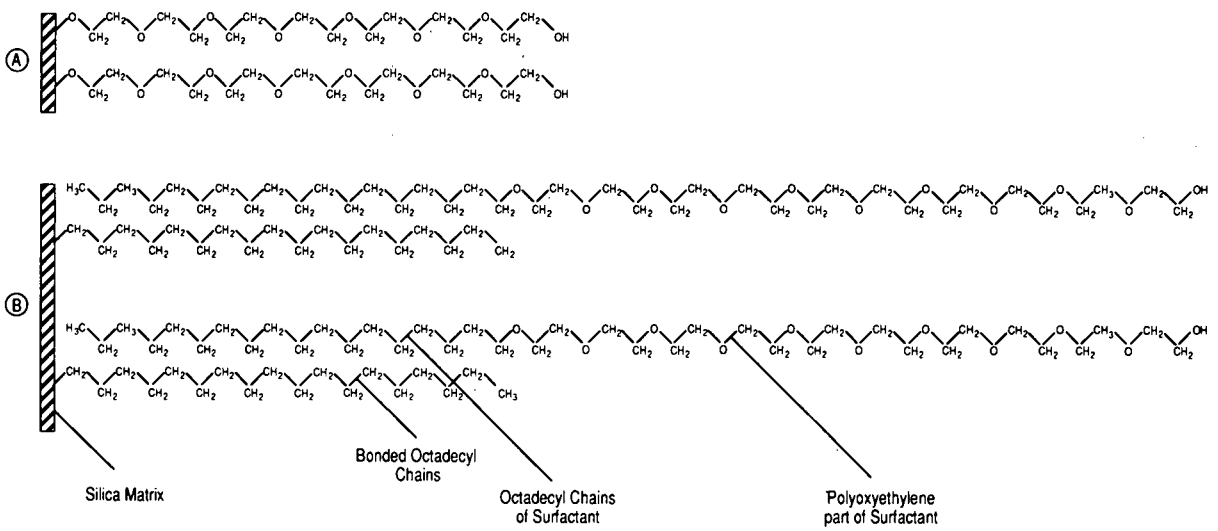

Fig. 1. Conceptual view of (A) an HIC column prepared by grafting polyoxyethylene glycol on silica and (B) the interaction between a non-ionic surfactant and a reversed-phase C_{18} support.

ic surfactant molecules are anchored to the reversed-phase support through strong hydrophobic interactions between alkane bristles of the reversed-phase support and their hydrophobic tails. The polar parts of the non-ionic surfactant molecules probably extend outwards, preventing the interaction of proteins with the buried hydrophobic layer composed of hydrophobic surfactant tails and the hydrocarbon layer grafted on to the support. This changes the surface properties of the reversed-phase support to those of the supports grafted with polyoxyethylene (as illustrated in Fig. 1).

Davisil C_{18} retained 154 μmol of surfactant per millilitre of packing and Ultrabase C_{18} retained 146 μmol/ml.

Surfactant is retained by the support only by non-covalent bonding, because of a dynamic equilibrium. It follows that some surfactant must be desorbed from the support when a surfactant-loaded column is used with a mobile phase that does not contain dissolved surfactant [18]. The extent to which this could affect the column properties was checked by measuring the surfactant load of an Ultrabase column that had been rinsed with 1000 column volumes of buffer B before eluting the surfactant with methanol–isopropanol. The value was the same as that given above, showing that surfactant leaching was indeed very low. Perhaps even more significant is the reproducibility of the chromatograms (see below), demonstrating that the column properties remained unaltered with use.

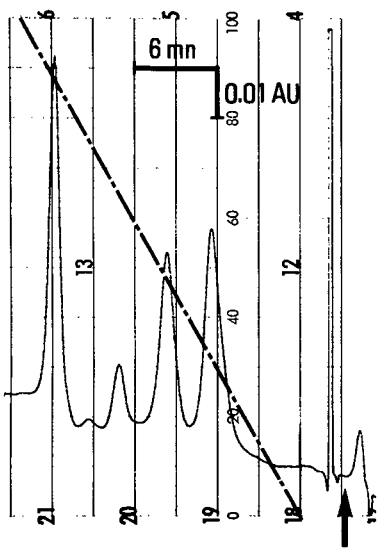

Fig. 2. Separation of a model protein mixture on a Davisil C_{18} column (10 cm × 0.46 cm I.D.) modified with Brij 76. The arrow indicates injection of the protein mixture (0.21 mg of cytochrome *c*, 0.30 mg of myoglobin, 0.15 mg of ribonuclease A and 0.18 mg of chymotrypsinogen). The peak eluting immediately after injection is a system peak; proteins are eluted through the gradient (dashed line) in the order given above. Absorbance was monitored at 280 nm. The numbers shown are from the chart paper and have no significance. mn = Minutes.

Hydrophobic interaction chromatography of a test mixture

All the test proteins were retained if dissolved in buffer A and deposited on to a surfactant-loaded column equilibrated with buffer A. Satisfactory resolution of all proteins was obtained by running a linear gradient between buffers A and B (Figs. 2 and 3). The back-pressures generated by the Davisil column were 14–24 bar and those for the Ultrabase column were 20–30 bar. A transient pressure surge to about 50 bar occasionally occurred at the time of sample injection.

Fig. 3 demonstrates that this good separation is reproducible; virtually identical chromatograms were obtained with the first and fortieth injections of the same test mixture.

Purification of an aspartyl protease from Rhizopus

Rhizopus species fungi produce several different aspartyl proteases collectively named rhizopuspepsin. Rhizopuspepsin is known to exist as several isozymic forms [24]. The commercial enzyme preparation used as the starting material for the purification showed several protein bands on SDS-PAGE. Fig. 4 shows the chromatogram obtained by running this material through a surfactant-loaded reversed-phase column and Table I gives quantitative data on the purification. About 65% of protease activity was found in pool B, and the SDS gel (Fig. 5) demonstrates that it is associated with a single band, whose molecular weight is consistent with published data [24]. Some protease activity was also found in other pools (probably corresponding to rhizopuspepsin isozymes), but the specific activity was lower than that in pool B.

Reutilization of a column in reversed-phase mode after use for HIC

The same column was used in the reversed-phase

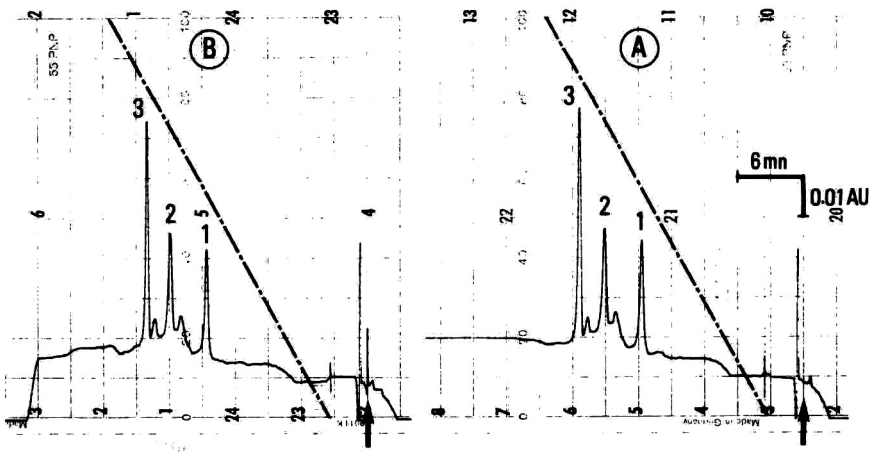

Fig. 3. Separation of a model protein mixture on an Ultrabase C_{18} column (10 cm × 0.46 cm I.D.) modified with Brij 76. The arrows indicate injections of the protein mixture (98 μg of ribonuclease A, 83 μg of trypsinogen and 53 μg of chymotrypsinogen). Peaks 1, 2 and 3 correspond to ribonuclease, trypsinogen en chymotrypsinogen, respectively, and other peaks are unidentified impurities. The dashed lines indicate the gradient profile. Absorbance was monitored at 280 nm. A and B are the recorder tracings for the first and the fourtieth injection of the same mixture, respectively.

mode for measuring protease activity (see Experimental) and then, after surfactant coating, for HIC of rhizopuspepsin (fifteen injections made as indicated above). The surfactant coverage was then removed with organic solvent and the column used again for proteolytic acitivity measurements. The chromatograms (Fig. 6) recorded before and after use in the HIC mode demonstrate that the column can be used successively in both modes. The column seemed to be more hydrophobic when used in the reversed-phase mode after the HIC mode (the k' values were higher, Fig. 6). The reason for this changed behaviour is unknown but has no significant effect on column usage.

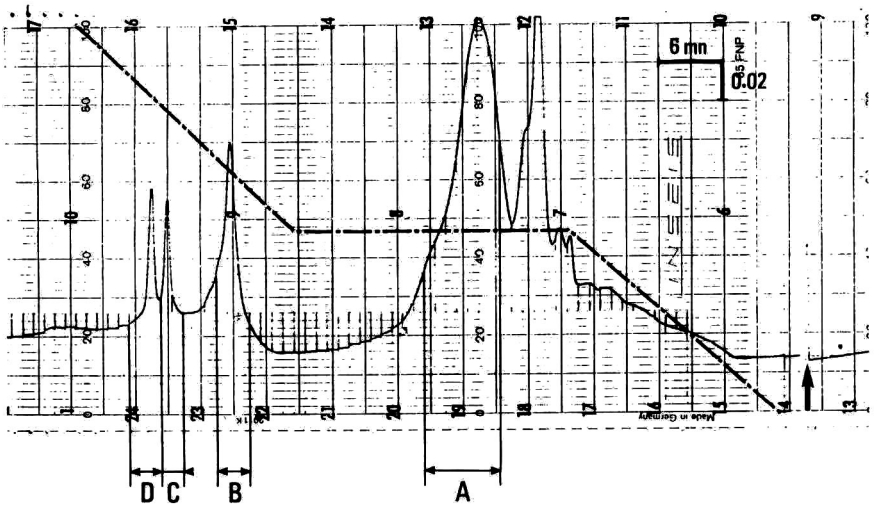

Fig. 4. Chromatogram of crude rhizopuspepsin on an Ultrabase C_{18} column (100 cm × 0.46 cm I.D.) modified with Brij 76. Crude rhizopuspepsin (1.36 mg) was injected at the arrow; the gradient profile is shown by the dashed line. Double arrows A to D indicate the pools of proteolytic activity.

TABLE I

QUANTITATIVE RESULTS FOR THE PURIFICATION OF *RHIZOPUS* ASPARTYL PROTEASE

Pool B was collected as shown in Fig. 4.

Material	Protein (mg)	Total activity (U)	Specific activity (U/mg)	Yield (%)
Starting material	1.36	14.7	10.8	100
Pool B	0.25	9.5	38.1	64.6

CONCLUSION

This study has demonstrated that a reversed-phase column is readily modified by loading it with a non-ionic surfactant, and that such a column can be used for HIC. The use of a reversed-phase support for column preparation implies that the HIC support has the mechanical resistance of the silica backbone, and is thus superior to the classical agarose-based HIC supports in terms of flow-rate. Commercial mechanically resistant HIC supports (with more or less hydrophobic ligands covalently linked to the supporting matrix) are adequate substitutes for agarose-based HIC supports and can be used for the efficient purification of a range of proteins. However, most if not all are much more expensive than reversed-phase chromatographic supports. Our approach of modifying the surface properties of reversed-phase supports provides efficient HIC columns at a reasonable cost.

Deliberate modification of the properties of a stationary phase by interaction with some mobile phase component is a long established procedure. For instance, in ion-pair chromatography, the origin of which can be traced to the early 1970s [25], one important contribution to separation seems to be the coating of the support wiht a layer of the ion-pairing agent. This even led to the extreme view that ion-pair chromatography is a form of disguised ion-exchange chromatography because of adsorp-

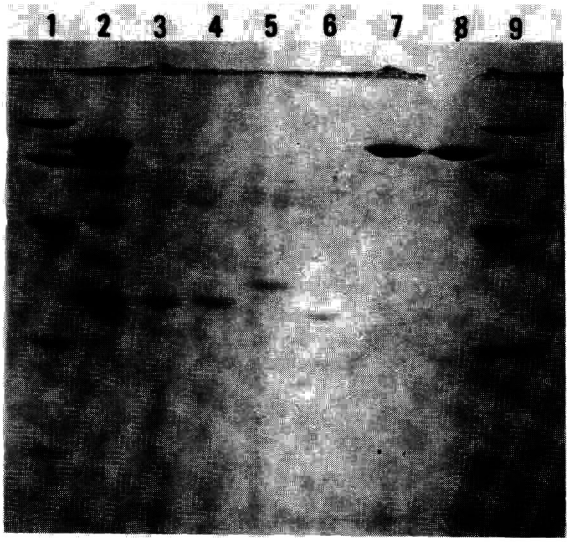

Fig. 5. SDS-PAGE of the pools obtained by chromatography of crude rhizopuspepsin on an Ultrabase C_{18} column modified with Brij 76. Starting material, lane 2; pool B, lanes 3 and 4; pool C, lane 5; pool D, lane 6; pool A, lanes 7 and 8. Molecular weight standards are on lanes 1 and 9 (from top to bottom, 94 000, 67 000, 43 000, 30 000, 20 100 and 14 400).

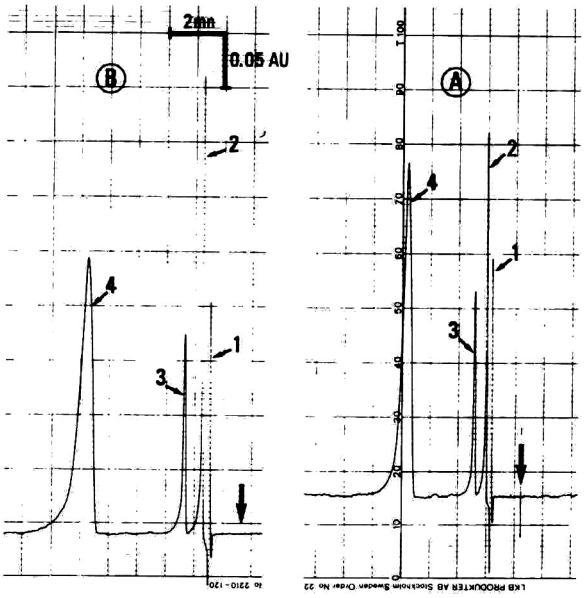

Fig. 6. Peptidolytic assay of *Rhizopus* protease activity on an Ultrabase C_{18} column (10 cm × 0.46 cm I.D.). Assay mixtures were injected at the arrows. Peak 1, 2, 3 and 4 are a system peak, reaction product [Leu–Ser–Phe(NO_2)], ethoxyacridine (internal standard) and undigested substrate, respectively. Chromatogram A was obtained with a freshly packed column and chromatogram B on the same column after use in the HIC mode and removal of the non-ionic surfactant coating.

tion of the ion-pairing agent on the stationary phase [26]. In fact, the secondary equilibria that occur in a mobile phase with an intentionally maintained concentration of ion-pairing agent are important [27]. In micellar liquid chromatography also multiple equilibria exist between the eluite, (modified) stationary phase and surfactant molecules present both as monomeric or associated (micellar) species [28]. Modification of reversed-phase support properties was also obtained by addition to the mobile phase of peculiar alcohols such as pentanol [29,30] or methoxyethanol [31] Lastly, it has been shown that the stationary phase adsorbs a certain amount of the organic component of the mobile phase in reversed-phase chromatography [32].

In all the instances cited above, the stationary phase modifier is present in the mobile phase also during chromatography. In contrast, we have used a non-ionic surfactant to modify the reversed phase before using it with pure aqueous mobile phases with no surfactant added.

The results showing that a reversed-phase column can be readily converted into a column usable for HIC provide further evidence of the versatility of reversed-phase supports used in conjunction with surfactants. Reversed-phase supports coated with non-ionic surfactants can be used for the size-exclusion chromatography of proteins [15], and reversed-phase supports can operate as ion exchangers if modified with ionic surfactants [33]. It is possible to use derivatives of non-ionic surfactants (with some suitable ligand grafted to their polar head) to convert reversed-phase columns into affinity [16] or immobilized dye chromatographic supports [18], whereas reversed-phase columns coated with non-ionic surfactants can be used as restricted access media for the chromatography of small molecules (these columns allow the analysis of small molecules by direct on-column injection of samples containing protein [17]).

All these modifications are readily performed, and might even be possible using the same reversed-phase silica backbone. Finally, the data presented above indicate that the surfactant can be stripped from the modified reversed-phase columns and the ordinary reversed phase columns thus obtained can be used thereafter in a conventional fashion.

REFERENCES

1 S. Shaltiel, *Methods Enzymol.*, 104 (1984) 69.
2 S. Hjertén, *J. Chromatogr.*, 87 (1973) 325.
3 Y. Kato, T. K. Itamura and T. Hashimoto, *J. Chromatogr.*, 298 (1984) 407.
4 S. H. Chang, K. M. Gooding and F. E. Regnier, *J. Chromatogr.*, 120 (1976) 321.
5 D. L. Gooding, M. P. Schmuck and K. M. Gooding, *J. Chromatogr.*, 296 (1984) 107.
6 N. T. Miller, B. Feibush and B. L. Karger, *J. Chromatogr.*, 316 (1984) 519.
7 J. L. Fausnaugh, E. Pfannkoch, S. Gupta and F. Regnier, *Anal. Biochem.*, 137 (1984) 464.
8 N. T. Miller and B. L. Karger, *J. Chromatogr.*, 326 (1985) 45.
9 N. T. Miller, B. Feibush, K. Corina, S. Powers Lee and B. L. Karger, *Anal. Biochem.*, 148 (1985) 510.
10 J. P. Chang, Z. E. El Rassi and Cs. Horváth, *J. Chromatogr.*, 319 (1985) 396.
11 A. J. Alpert, *J. Chromatogr.*, 359 (1986) 85.
12 Y. Shibusawa, U. Matsumoto and M. Takatori, *J. Chromatogr.*, 398 (1987) 153.
13 N. Cooke, P. Shieh and N. Miller, *LC · GC Int.*, 3 (1990) 8.
14 T. G. I. Ling and B. Mattiasson, *J. Chromatogr.*, 254 (193) 83.
15 J. P. Chang, *J. Chromatogr.*, 317 (1984) 157.
16 J. L. Torres, R. Guzman, R. G. Carbonell and P. K. Kilpatrick, *Anal. Biochem.*, 171 (1988) 411.
17 C. Desilets, M. A. Bourns and F. E. Regnier, *J. Chromatogr.*, 544 (1991) 25.
18 Y. L. Kong Sing, E. Algiman, Y. Kroviarski, D. Dhermy and O. Bertrand, *J. Chromatogr.*, 558 (1991) 43.
19 K. Kuwata, M. Uebori and Y. Yamazaki, *J. Chromatogr.*, 211 (1981) 378.
20 K. S. Rosenthal and F. Koussale, *Anal. Chem.*, 55 (1983) 1115.
21 M. N. Raymond, E. Bricas, R. Salesse, J. Garnier, P. Garnot and R. Dumas, *J. Dairy Sci.*, 56 (1973) 419.
22 M. M. Bradford, *Anal. Biochem.*, 72 (1976) 248.
23 U. K. Laemmli, *Nature (London)*, 277 (1970) 680.
24 K. Takahashi, *J. Biochem.*, 103 (1988) 162.
25 S. Eksborg and G. Schill, *Anal. Chem.*, 45 (1973) 2092.
26 P. T. Kissinger, *Anal. Chem.* 49 (1977) 883.
27 Cs. Horváth, W. Melander, I. Molnar and P. Molnar, *Anal. Chem.*, 49 (1977) 2295.
28 M. F. Borgerding, R. L. Williams, Jr., W. L. Hinze and F. H. Quina, *J. Liq. Chromatogr.*, 12 (1989) 1367.
29 K. G. Wahlund, *J. Chromatogr.*, 115 (1975) 411.
30 K. G. Wahlund and U. Lund, *J. Chromatogr.*, 122 (1976) 269.
31 W. Mönch and W. Dehnen, *J. Chromatogr.*, 147 (1978) 415.
32 R. M. McCormick and B. L. Karger, *J. Chromatogr.*, 199 (1980) 259.
33 D. E. Keller, J. L. Torres, R. G. Carbonell and P. K. Kilpatrick, *Anal. Biochem.*, 176 (1989) 191.

Journal of Chromatography, 598 (1992) 189–194
Elsevier Science Publishers B.V., Amsterdam

CHROM. 24 081

On-line continuous-flow dialysis thermospray tandem mass spectrometry for quantitative screening of drugs in plasma: rogletimide

E. van Bakergem, R. A. M. van der Hoeven, W. M. A. Niessen*, U. R. Tjaden and J. van der Greef

Division of Analytical Chemistry, Center for Bio-Pharmaceutical Sciences, P.O. Box 9502, 2300 RA Leiden (Netherlands)

G. K. Poon and R. McCague

Drug Development Section, Cancer Research Campaign Laboratory, Institute of Cancer Research, Sutton, Surrey, SM2 5NG (UK)

(First received December 17th, 1991; revised manuscript received February 5th, 1992)

ABSTRACT

The application of a continuous-flow dialysis system, consisting of a membrane dialyser and a trace enrichment column, in on-line combination with tandem mass spectrometry via a thermospray interface is described. The method is applied to the quantitation of drugs in complex biological matrices containing macromolecular interferences. The potential of the method is demonstrated by the quantitative analysis of the anti-cancer drug rogletimide in the plasma of patients after treatment.

INTRODUCTION

The quantitation of drugs in biological fluids is an important aspect of drug development and testing, *e.g.* with respect to pharmacokinetics. In many cases, mass spectrometry (MS) is involved in these studies, often in combination with separation methods such as gas or liquid chromatography (GC or LC). The major reasons for using MS are related to its sensitivity and the ability to work with stable isotopically labelled internal standards. The use of tandem mass spectrometry (MS–MS), especially triple quadrupole instruments, in this field has been advocated by Yost and co-workers [1,2]. Effective screening of drugs and metabolites by the use of soft ionization techniques and highly selective MS–MS methods can be achieved in this way [1–3]. Similar approaches were described for environmental analysis by Hunt *et al.* [4]. One of the features of these approaches is that the biological samples are analysed without significant sample pretreatment, and at any rate without chromatographic separation. However, we feel that in the routine analysis of complex biological samples some sample pretreatment is obligatory prior to MS–MS in order to avoid source contamination. Great progress has been made in the development of the on-line coupling of liquid-phase methods to MS and MS–MS via interfaces for LC–MS. In this way it is possible to perform the necessary sample pretreatment on-line.

Continous-flow membrane dialysis (CFD), *i.e.* a combination of a membrane dialyser and a trace enrichment column [5–7], has been demonstrated to be an effective sample pretreatment method in the analysis of complex samples containing macromolecular interferences, *e.g.* plasma, especially when used in combination with a selective detection method. The plasma sample is introduced in a (buffered) aqueous donor stream, which is dialysed to

0021-9673/92/$05.00

an acceptor stream. The latter is subsequently enriched onto a short trapping column. The trapping column is eluted with an appropriate solvent and the eluate is directed to an analytical LC column for separation and subsequent detection. However, in combination with a highly selective detector such as a (tandem) mass spectrometer, the trapping column can be coupled directly via an LC–MS interface, without the need for an additional analytical separation, as has been demonstrated by our group in the phase system-switching approach [8,9].

In this paper the on-line combination of CFD and MS–MS via a thermospray interface is described. The potential of the approach is demonstrated by the quantitative bioanalysis of rogletimide in plasma.

Rogletimide, 3-ethyl-3-(4-pyridyl)piperidine-2,6-dione (pyridogluthetimide, PG, **1** in Fig. 1), an analogue of aminogluthetimide, is under investigation as an aromatase inhibitor to be used in the treatment of post-menopausal women suffering from oestrogen-dependent breast carcinoma [10–12]. The human metabolism of PG has recently been elucidated with the use of thermospray LC–MS [13]. Some preliminary results regarding the detection of PG metabolites using the CFD–MS approach are reported here as well.

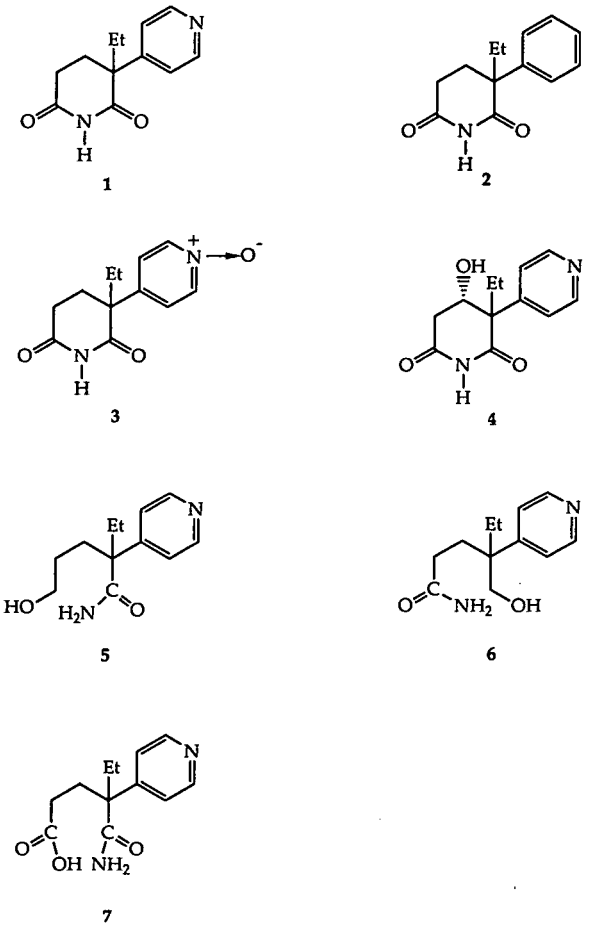

Fig. 1. Structures of the compounds investigated. **1** = Rogletimide (PG); **2** = gluthetimide; **3** = PG-N-oxide; **4** = 4-hydroxy-PG; **5** = 2-ethyl-2(4-pyridyl)-5-hydroxypentanamide; **6** = 4-ethyl-4-(4-pyridyl)-5-hydroxypentanamide; **7** = 2-ethyl-2-(4-pyridyl)-5-carboxypentanamide. Et = ethyl.

EXPERIMENTAL

Continuous-flow dialysis

The CFD system (see Fig. 2) consisted of a Skalar Analytical (Breda, Netherlands) Model 1000 autosampler, containing a Model 2002 multichannel peristaltic pump and a Model 5275 70-cm perspex dialysis block containing a cuprophan membrane (cut-off value 10 kilodaltons) coupled to two Rheodyne (Cotati, CA, USA) Model 7010 switching valves controlled by a Model 75A matrix timer (Kipp & Zonen, Delft, Netherlands). The laboratory-made trapping column (12 mm × 2 mm I.D.) was hand-packed under reduced pressure with 40–63 μm Polygosil C_8 particles (Machery-Nagel, Düren, Germany).

Plasma (1.26 ml) was introduced in an air-segmented (0.23 ml/min) donor stream (demineralized water, 0.42 ml/min) to the dialysis membrane. The non-segmented acceptor stream (demineralized water, 0.60 ml/min) was concentrated on the trapping column, which was subsequently desorbed for either liquid chromatography with UV detection, MS–MS with a thermospray interface, or LC–MS with a thermospray interface.

CFD in combination with LC and UV detection

The method was first developed and tested using a CFD system in combination with LC with UV detection. The eluate of the trapping column was directly introduced onto the analytical column. In these experiments, the LC system consisted of a Jasco (Tokyo, Japan) Model Familic 300S pump, a

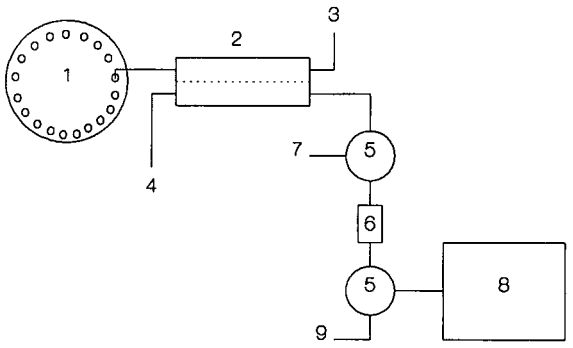

Fig. 2. Schematic diagram of the continuous-flow dialysis system coupled to tandem mass spectrometry via a thermospray interface. 1 = Autosampler; 2 = dialysis block; 3 = donor stream to waste; 4 = acceptor stream; 5 = switching valve; 6 = trapping column; 7 = desorption solvent; 8 = tandem mass spectrometer with thermospray interface; 9 = to waste.

Rheodyne Model 7125 injection valve equipped with a 20-μl injection loop, a Pye Unicam (Cambridge, UK) Model LC3 variable-wavelength UV detector operating at 254 nm and a Model BD40 flatbed recorder (Kipp & Zonen). The column was a 100 mm × 4.6 mm I.D. column slurry packed in the laboratory with 5-μm Nucleosil C_8 particles (Machery-Nagel). Isocratic elution was performed with a mobile phase of 30% methanol in 100 mmol/l ammonium acetate.

CFD in combination with a thermospray interface for LC–MS and MS–MS

The CFD system was coupled to a Finnigan MAT (San Jose, CA, USA) TSQ 70 tandem mass spectrometer equipped with a Finnigan MAT thermospray interface. The thermospray system was run with a mobile phase of 50% methanol in 50 mmol/l ammonium acetate at a flow-rate of 1.2 ml/min in discharge-on mode (1 kV). The vaporizer temperature and the repeller potential were optimized daily with respect to signal intensity and stability [14]; typical values were 100°C and 50 V, respectively. The ion source block temperature was kept at 200°C.

In MS–MS experiments, air was used as the collision gas (0.05 Pa). The collision energy was optimized at 60 eV. The effluent of the trapping column was introduced directly to the thermospray interface, bypassing the analytical column. In LC–MS experiments, the effluent of the trapping column was introduced into the analytical column, which was connected to the thermospray interface. The column and mobile phase were the same as used in the UV experiments.

Chemicals and sample treatment

Demineralized water was used throughout this study. Methanol and ammonium acetate were purchased from Baker (Deventer, Netherlands).

System development was performed using pooled plasma samples. Patients' plasma samples were collected before and 0, 0.5, 1, 2, 4, 6, 8, 12, 15, 24, 28, 32, 36 and 48 h after a single oral dose of 800 mg of PG. The samples were kept at −20°C for a prolonged period of time. Before use, they were defrosted at room temperature, diluted with demineralized water, and 10 μg of gluethetimide (Glu, **2** in Fig. 1) in 100 μl of methanol were added to 2 ml of plasma as an internal standard. Then, 1.26 ml of the sample were introduced via the autosampler without any further treatment. In quantitative studies, the plasma samples collected 0–12 h after administration were diluted twenty-fold and those collected 15–48 h after administration four-fold. In the preliminary studies with the metabolites no dilution was applied and no internal standard was added.

RESULTS AND DISCUSSION

Setting up the CFD system

In developing a CFD system for a particular application, several aspects must be taken in consideration, *e.g.* the selection of an appropriate column packing material for the enrichment of the dialysate and of a mobile phase. The latter should be capable of an efficient desorption of the compound of interest from the trapping column and should be favourable to the LC–MS interface. Furthermore, attention must be paid to the flow direction, *i.e.*, concurrent or counter-current dialysis and forward-flush or back-flush desorption from the trapping column, and to the optimization of the experimental parameters. The general importance of these parameters has been discussed by others [5–7,15,16]. In the present study, limited attention was paid to these aspects. No significant differences were observed between the various flow directions indicated above. Counter-current dialysis and forward-flush

desorption were used throughout the study. Efficient desorption of PG from the trapping column is possible with an aqueous mobile phase containing more than 20% methanol; generally 50% methanol was used. The presence of ammonium acetate had no influence on the desorption characteristics. The breakthrough volume of the trapping column for PG was found to be 10.2 ml, at a flow-rate of 0.5 ml/min, of 50 μg/ml PG in water, corresponding to a loading capacity of the trapping column for PG of *ca.* 500 μg, which is sufficient for the application at hand. PG shows poor UV characteristics; the on-column minimum detectable concentration in the CFD–LC–UV system is *ca.* 0.5 μg/ml (254 nm). Recovery after dialysis was found to be *ca.* 33%. The coefficient of variation in peak area on the UV detector was found to be 3.8% ($n=5$) at the 10 μg/ml level.

The analysis time is *ca.* 14 min per sample. Although not actually performed, the CFD–MS–MS system can be run automatically and unattended when sufficient precautions in terms of control feedback are taken (see, for example, ref. 17).

Thermospray MS of PG

The mass spectrum of PG under thermospray conditions is characterized by an intense peak of the protonated molecule at *m/z* 219; some minor fragment peaks are observed as well. The detection limit of PG in column bypass injection without the CFD system is 50 ng/ml; good linearity is observed in the range 50 ng/ml to 20 μg/ml.

The product-ion spectrum of the protonated molecule of PG under thermospray MS–MS conditions is given in Fig. 3a. The base peak of the spectrum, *m/z* 134, most likely results from a cleavage of the piperidine ring with charge retention of the pyridyl ring ($C_9H_{12}N^+$). In the CFD–MS–MS analysis of standard solutions of PG, using selected monitoring of the reaction 219 → 134, good linearity was observed over the range 5–1000 ng/ml. The detection limit was *ca.* 4 ng/ml. This detection limit indicates that despite the dilution and the poor recovery in the dialyser a significant gain in concentration detection limit, relative to column bypass injections, is achieved as a result of the trace enrichment column.

Selection of an internal standard

Although good linearity was observed for PG under thermospray conditions, for a proper quantitation of PG in patients' plasma samples and internal standard should be used. As no isotopically labelled PG was available, an analogue of PG, *i.e.* gluthetimide (Glu, **2** in Fig. 1), was selected as internal standard. The thermospray mass spectrum of Glu is characterized by an intense peak at *m/z* 218 owing to the protonated molecule; no significant fragmentation is observed. Quantitatively, and somewhat surprisingly, the responses of Glu and PG under thermospray conditions are similar. The product-ion spectrum of the protonated molecule of Glu is given in Fig. 3b. The compound shows considerable fragmentation. The peak at *m/z* 131, which will be used in selected reaction monitoring, is most likely due to a piperidine ring cleavage, leading to an ion with an elemental composition of $C_9H_7O^+$.

Glu can also be used in the CFD system under the same conditions as used for PG. The loading

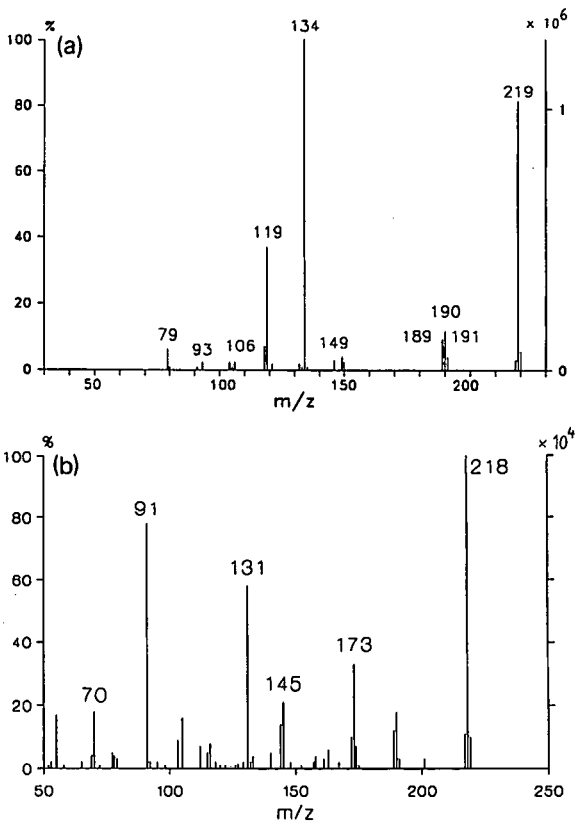

Fig. 3. Product-ion spectra of (a) rogletimide and (b) gluthetimide obtained after thermospray introduction; 200 ng injected. Right-hand scale: arbitrary units.

capacity of the trapping column for Glu was found to be *ca.* 350 μg, which is sufficient for this application.

Quantitative analysis of PG in plasma

After establishing the applicability of the method with spiked pooled plasma samples, the patient's plasma samples were analysed during the CFD–MS–MS approach in column bypass mode. Calibration of the method was done with spiked samples using the patients' plasma taken before the administration of PG. Calibration and patients' samples were measured in one series of experiments and in random order. The samples were analysed in selected reaction monitoring (219 → 134 for PG and 218 → 131 for the internal standard Glu). With spiked samples containing 1 μg/ml Glu and/or 0.8 μg/ml PG the possibility of mutual interferences in the selected reaction monitoring was experimentally excluded. Although a series of calibration samples could succesfully be measured without the addition of an internal standard, quantitation with an internal standard is preferred for the analysis of the post-treatment samples in order to correct for irregular ionization behaviour and other fluctuations in time.

With the series of calibration samples analysed with internal standard, good linearity was observed over the range 5–360 ng/ml. The determination limit of PG in plasma is found to be 5 ng/ml, indicating the effectiveness of the CFD as sample pretreatment in the analysis of real samples. The coefficient of variation in the peak area was found to be 5.2% ($n = 5$) at the 100 ng/mg level. In the post-treatment patients' samples, plasma concentrations of PG between 330 ng/ml and 40 μg/ml were observed. Therefore, dilution of the plasma samples was necessary to enable the measurement of the levels within the range of the calibration plot. A typical selected product-ion monitoring trace for a patient's plasma sample taken 36 h after administration is given in Fig. 4. The maximum plasma level found is *ca.* two-fold higher than that previously reported for PG [12] (see below).

A prerequisite of the applicability of the CFD approach is that the protein binding of the drug of interest is weak, *i.e.* readily reduced under conditions amenable to the CFD system. The plasma protein binding of PG was reported to be *ca.* 17%

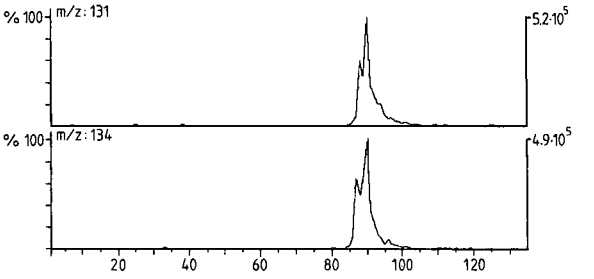

Fig. 4. Selected product-ion monitoring of the reactions for PG (*m/z* 219 → 1314) and Glu (*m/z* 218 → 131, internal standard) in CFD–MS–MS. Sample: four-fold diluted patient's plasma sample, 36 h after administration. Other conditions: see text.

and was not concentration-dependent [12]. Moreover, dilution of the plasma sample often reduces the protein binding. These effects were not further investigated for PG in this study.

Analysis of metabolites with the CFD system

In principle, the CFD approach can also be used to detect and quantitate drug metabolites in plasma. PG-N-oxide (**3** in Fig. 1) has previously been reported to be the principal metabolite of PG [11,12]. Plasma levels of PG-N-oxide up to *ca.* 2 μg/ml following a single oral dose administration of 1 g of PG have been reported [12]. The metabolism of PG was studied more extensively by Poon *et al.* [13] using thermospray LC–MS. Several metabolites were found in plasma, although some of them appeared to be present at low levels (assuming about equal response in thermospray ionization for the various metabolites). The most abundant metabolite was PG-N-oxide (**3**, molecular weight 234). Furthermore, 4-hydroxy-PG (**4**, molecular weight 234), 2-ethyl-2- and 4-ethyl-4-(4-pyridyl)-5-hydroxypentanamide (**5** and **6**, respectively, molecular weight 222) and 2-ethyl-2-(4-pyridyl)-5-carboxypentanamide (**7**, molecular weight 237) were found with significant abundance [13]. However, the last-mentioned compound is too polar to be trapped on the trapping column used in the CFD experiment.

The development of a CFD–MS system for the detection and quantitation of the metabolites of PG in plasma is hampered by the fact that several metabolites have the same molecular mass. The parent-ion spectra of the various metabolites in MS–MS also showed insufficient specificity for isomeric

discrimination by multiple reaction monitoring. Therefore, a chromatographic separation prior to the MS detection is needed. Some preliminary experiments with CFD coupled to an LC–MS system enabled the detection of two of the major metabolites, *i.e.* PG-N-oxide (**3**) and 4-hydroxy-PG (**4**). More extensive experiments, *e.g.* directed at investigating the loadability of the trapping column for these more polar metabolites and at quantitative aspects, are needed for a full assessment of the potential of the CFD approach in the quantitation of PG metabolites.

The work on the metabolites of PG revealed a possible source of overestimation of the PG level in plasma. The major metabolite, PG-N-oxide, is under thermospray conditions readily converted to PG; the intensity ratio of the peaks at *m/z* 219 and *m/z* 235 appears to be very sensitive to the conditions and not very reproducible. From this it may be concluded that part of the PG concentration measured in patients' plasma must be attributed to PG-N-oxide. In principle, this problem can obviated by the use of a short separation column between the CFD and the MS–MS, as PG and PG-N-oxide have significantly different retention characteristics. It must be emphasized that this unfavourable coincidence is typical for PG, which was chosen as the model compound for this study, but must not be considered detrimental for the CFD–MS–MS approach as such.

CONCLUSION

The method described here differs both in the experimental mode and in the field of application from the microdialysis systems which are used in the *in vivo* monitoring of, for instance, neurotransmitters [18]. Such systems have also been coupled to a mass spectrometer, either via a valve containing a loop to collect the dialysate [19] or directly to a low-flow LC–MS interface [20].

The CFD approach in on-line combination with MS and MS-MS via an LC-MS interface is an easy, rapid and versatile method for the quantitative monitoring of drug levels in biological samples. The method is useful if the presence of macromolecular compounds in the sample prohibits the direct introduction via a thermospray interface. No further sample pretreatment is necessary. The determination limits that can be achieved are compound-dependent, as is common with thermospray ionization. The method provides on-line sample preconcentration. An automatic sequential trace enrichment of dialysates system (ASTED) is commercially available from Gilson Medical Electronics (Villiers-le Bel, France).

REFERENCES

1 H. O. Brotherton and R. A. Yost, *Anal. Chem.*, 55 (1983) 549.
2 R. A. Yost, R. J. Perchalski, H. O. Brotherton, J. V. Johnson and M. B. Budd, *Talanta*, 31 (1984) 929.
3 P. Rudewicz and K. M. Straub, *Anal. Chem.*, 58 (1986) 2928.
4 D. F. Hunt, J. Shabanowitz, T. M. Harvey and M. L. Coates, *J. Chromatogr.*, 271 (1983) 93.
5 D. C. Turnell and J. D. H. Cooper, *J. Chromatogr.*, 395 (1987) 613.
6 J. D. H. Cooper, D. C. Turnell, B. Green and F. Verillon, *J. Chromatogr.*, 456 (1988) 53.
7 U. R. Tjaden, E. A. de Bruijn, R. A. M. van der Hoeven, C. Jol, J. van der Greef and H. Lingeman, *J. Chromatogr.*, 420 (1987) 53.
8 E. R. Verheij, H. J. E. M. Reeuwijk, G. F. LaVos, W. M. A. Niessen, U. R. Tjaden and J. van der Greef, *Biomed. Environ. Mass Spectrom.*, 16 (1988) 393.
9 A. Walhagen, L.-E. Edholm, C. E. M. Heeremans, R. A. M. van der Hoeven, W. M. A. Niessen, U. R. Tjaden and J. van der Greef, *J. Chromatogr.*, 474 (1989) 257.
10 A. B. Foster, M. Jarman, C.-S. Leung, M. G. Rowlands, G. N. Taylor, R. G. Plevey and P. Sampson, *J. Med. Chem.*, 28 (1985) 200.
11 A. Seago, P. E. Goss, L. J. Griggs and M. Jarman, *Biochem. Pharmacol.*, 35 (1986) 2911.
12 B. P. Haynes, M. Jarman, M. Dowsett, A. Mehta, P. E. Lønning, L. J. Griggs, A. Jones, T. Powles, R. Stein and R. C. Coombes, *Cancer Chemother. Pharmacol.*, 27 (1991) 367.
13 G. K. Poon, R. McCague, L. J. Griggs, M. Jarman and I. A. S. Lewis, *J. Chromatogr.*, 572 (1991) 143.
14 C. E. M. Heeremans, R. A. M. van der Hoeven, W. M. A. Niessen, U. R. Tjaden and J. van der Greef, *J. Chromatogr.*, 474 (1989) 149.
15 M. M. L. Aerts, W. M. J. Beek and U. A. Th. Brinkman, *J. Chromatogr.*, 500 (1990) 453.
16 D. S. Stegehuis, U. R. Tjaden and J. van der Greef, *J. Chromatogr.*, 511 (1990) 137.
17 C. Lindberg, J. Paulson and A. Blomqvist, *J. Chromatogr.*, 554 (1991) 215.
18 U. Tossman, *LC · GC Int.*, 3 (10) (1990) 40.
19 S. D. Menacherry and J. B. Justice, Jr., *Anal. Chem.*, 62 (1990) 597.
20 R. M. Caprioli and S. N. Lin, *Proc. Natl. Acad. Sci. U.S.A.*, 87 (1990) 240.

Journal of Chromatography, 598 (1992) 195–201
Elsevier Science Publishers B.V., Amsterdam

CHROM. 24 027

Reductive electrochemical detection in liquid chromatography with a zinc amalgam scrubber column

Arne Bergens*,☆

Department of Analytical Chemistry, Uppsala University, P.O. Box 531, S-751 21 Uppsala (Sweden)

(First received January 23rd, 1991; revised manuscript received January 15th, 1992)

ABSTRACT

The dissolved oxygen in an acidic mobile phase can be reduced and eliminated by a scrubber column packed with zinc amalgam particles. The zinc amalgam scrubber column is mounted between the pump and the injection device and enables sensitive amperometric detection at potentials down to −0.65 V *vs.* Ag/AgCl. The high overvoltage of hydrogen on mercury allows the use of acidic mobile phases without problems with evolution of hydrogen gas. The accessible potential range is limited by the reduction of Zn^{2+} dissolved from the scrubber column. The possibilities for trace amount determinations of nitrocompounds are demonstrated in the detection of trinitrophenyl derivatives of amino acids from reaction with trinitrobenzenesulphonic acid. The detection was focused on γ-aminobutyric acid, and a detection limit of 0.1 pmol at −0.6 V *vs.* Ag/AgCl was obtained.

INTRODUCTION

The method commonly applied for the derivatization of amino acids, for example γ-aminobutyric acid (GABA), involves reaction with *o*-phthaladehyde (OPA) [1–9]. The derivatives formed from OPA are different alkylisoindoles that can be detected either by fluorescence [1–5] or by amperometric detection [6–9]. The reaction is fast, but the stability of the derivatives formed is in some cases limited, and a half-life as short as 4.1 min has been reported for the OPA-GABA derivative [7]. In the case of amperometric detection, the amine functionality in the alkylisoindole is oxidized at +0.75 V *vs.* Ag/AgCl [7–9].

Another derivatizing agent that can be used for amino acids is trinitrobenzenesulphonic acid (TNBS) [10–13]. The reaction with TNBS is quantitative in alkaline solutions and produces stable trinitrophenyl (TNP) derivatives as exemplified for GABA in Fig. 1. TNBS was introduced as a reagent for spectrophotometric determinations because the derivatives have absorbance maxima at 335–350 nm, where TNBS and most other organic substances are transparent. The TNP derivatives also possess advantageous electrochemical reduction properties [12,13]. The TNP derivatives are reduced at moderate cathodic potentials, and the reduction of an aromatic nitro group is a four-electron process. Hence, the total process of reduction of a TNP derivative yields twelve electrons and a high current response can therefore be expected.

However, reductive amperometric detection suffers from various interferences. These are dominated by dissolved oxygen in the mobile phase, which results in large baseline offset and increased faradaic noise. The common strategies used to decrease this effect include saturation of the mobile phase with an inert gas [14,15], continuous refluxing in an

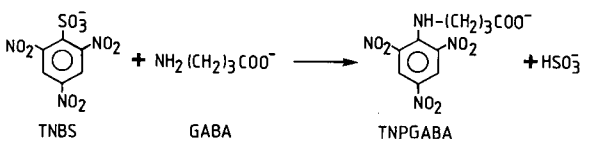

Fig. 1. Derivatization of GABA with TNBS in basic medium.

☆ Address for correspondence: Kabi Pharmacia AB, S-112 87 Stockholm, Sweden.

0021-9673/92/$05.00

inert atmosphere [16] and electrochemical reduction of the oxygen in either a scrubber cell [17] or a solvent reservoir [18]. The electrochemical reduction of oxygen seems to be a convenient and efficient technique. However, it is seldom used in practice because of the requirement for a stable high-current potentiostat. The application of an electrochemical scrubber cell seems from the literature not to have earned general use in connection with liquid chromatography (LC).

An interesting alternative to an electrochemical scrubber cell for oxygen reduction is to employ a scrubber column packed with zinc particles [19]. However, such a column would be expected to cause severe problems as a result of the evolution of microbubbles of hydrogen gas in applications that require acidic mobile phases. By treating the zinc particles with a solution of a mercuric salt, the particles become covered by a thin layer of mercury amalgam. Since hydrogen has a high overvoltage at a mercury surface, the competing reduction of H^+ is supressed. The zinc amalgam scrubber column therefore permits analysis at lower pH compared with a scrubber column packed with untreated zinc particles. The purpose of the present study was to evaluate the possibility of using a zinc amalgam scrubber column for reductive amperometric detection in LC. The application was focused on the detection and determination of trace amounts of GABA in biological samples.

EXPERIMENTAL

Apparatus

Chromatography. The high-performance LC (HPLC) system consisted of a Model 2150 (Pharmacia-LKB Biotechnology, Bromma, Sweden) double-piston pump modified with 316-grade stainless-steel connections and tubing on the inlet connectors. All tubing in the system was of 316-grade stainless steel except for a small 5 cm × 0.1 mm I.D. PTFE tube between the column and the detector cell. A three-necked round-bottomed flask was used as the mobile phase reservoir. The flask was equipped with a condenser, gas-tight connectors for the argon line and pump inlet tubing. The argon was precleaned from oxygen by passing it through a bed of copper(I) oxide catalyst (BASF, Ludwigshafen/Rhein, Germany) packed in a 42 cm × 1.2 cm glass tube. The argon was further saturated with mobile phase in a gas washing tower before entering the mobile phase reservoir. The amalgamated zinc scrubber was constructed from an empty 100 mm × 4 mm glass-lined HPLC column (SGE, Ringwood, Australia; No. 100GLE4) and mounted between the pump and the injection valve. The latter was a Valco six-port injector (Vici, Schenkon, Switzerland) with a 20-μl sample loop. All separations were performed on an RP-8 3-μm, 100 mm × 3.2 mm column obtained from Brownlee Labs. (Santa Clara, CA, USA). The column was thermostated to 35 ± 0.1°C by means of a column oven, constructed in the laboratory. The electrochemical detector was a commercially available thin-layer cell with a 50-μm gasket and a Ag/AgCl reference electrode (Bioanalytical Systems, West Lafayette, IN, USA). The potential was controlled by a Bioanalytical Systems LC-4B potentiostat. Derivatization experiments with different reaction media were performed using a Shimadzu SPD-6A (Shimadzu, Tokyo, Japan) UV detector and a Model CMA240 (Carnegie Medicin, Stockholm, Sweden) autoinjector as the injection device. All chromatograms were collected and processed with a Model SP4290 integrator (Spectra-Physics, San Jose, CA, USA).

Voltammetry. Voltammetric experiments were performed using a Model 174A polarographic analyser [EG&G Princeton Applied Research (PARC), Princeton, NJ, USA]. The electrochemical cell consisted of a 20-ml water-jacketed glass vessel with a Ag/AgCl reference electrode and a platinum-wire auxiliary electrode, all purchased from Metrohm (Herisau, Switzerland). The working electrode was a glassy carbon electrode (GCE; Metrohm, Model 6.1204.040), which could be mounted on a rotating electrode assembly (Metrohm, Model 2.628.0020), used for obtaining voltammograms under hydrodynamic conditions. The electrochemical cell was kept at 30°C by means of a conventional thermostat. The nitrogen used for deoxygenation of the supporting electrolyte was cleaned from oxygen by passing it through a washing tower containing vanadous chloride solution. Voltammograms were recorded on a Hewlett-Packard 7044B X–Y recorder.

Reagents

Zinc metal was purchased from Carl Roth (Karlsruhe, Germany) as 300-μm particles with a

specified purity of 99.99%. The mercury (II) nitrate used for the preparation of zinc amalgam was purchased from Merck (Darmstadt, Germany) and was of p.a. grade.

GABA, glycine, δ-aminovaleric acid (DAVA) and TNBS were obtained from Aldrich (Steinheim, Germany) and used as received. The amino acid standard mixture was obtained from Pierce (No. 20077; Tecator, Sollentuna, Sweden).

All organic solvents used for mobile phases were purchased from Merck and were of LiChrosolv quality. The *m*-chloroacetic acid was obtained from BDH (Poole, UK). The distilled water used in this work was further purified with a Millipore Milli-Q filtration system.

TNP derivatives of GABA, glycine and DAVA were prepared in crystalline form for use as standard substances according to Okuyama and Satake [10] and the crystals of TNP-GABA obtained showed a sharp melting point at 149–151°C, which is consistent with reported data [13].

Procedures

Preparation of the oxygen scrubber column. An 8-g portion of pure zinc particles was treated with 50 ml of 0.5 *M* nitric acid containing 2 g of mercury (II) nitrate. The mixture was stirred vigorously for 5–10 min. The solution was then removed and the zinc amalgam was washed with at least two 50-ml portions of water. The zinc amalgam was covered with water and kept in a bottle with a ground joint glass stopper to minimize exposure to oxygen. Zinc amalgam that was stored for 24 h or longer had to be treated with 2 *M* nitric acid for 2 min before use to regain maximum efficiency of the scrubber column. This precaution was taken since oxide formation on the surface of the amalgam diminished its function. The amalgam was poured in small portions into the column tube, which was filled with water and mounted in an upright position. The bottom end of the column tube was connected through its end fitting to water suction equipment, and the tube was kept filled with water throughout the packing procedure. The amalgam was sedimented on the bottom of the tube by a continuous stream of water and by vigorous knocking on the column with a spoon. With the column filled, the upper end fitting was assembled and the scrubber column was immediately mounted into the LC system.

Chromatography. The mobile phase used in the separations was a mixture of 10% (v/v) acetonitrile, 12% (v/v) 2-propanol and 78% (v/v) 0.05 *M* *m*-chloroacetic acid buffer, pH 2.7. The *m*-chloroacetic acid buffer contained 0.2 m*M* EDTA as a metal-complexing agent. Before start-up, the mobile phase was saturated with argon by vigorous bubbling for 15–30 min. The LC system was primed and running before the zinc amalgam scrubber column was prepared and mounted. Thereafter, the electrochemical detector cell was assembled and turned on. It was found necessary to leave the system running at least overnight with the mobile phase recycling at the normal flow-rate (0.70 ml/min) in order to allow the trapped oxygen in the separation column to diffuse out.

The sample solutions were deoxygenated in a 5-ml disposable syringe with a small hole made at the 5-ml mark as described previously [20]. With the injection valve in the load position and the syringe plunger above the 5-ml mark, deoxygenation of sample volumes in the range 0.5–4 ml could be made by connecting the argon to the waste tubing of the injection valve.

Voltammetry. Before any voltammetric experiments were performed, the GCE was polished with an aqueous slurry of 0.3 μm alumina powder on a damp silk cloth. The GCE was thoroughly rinsed with water in an ultrasonic bath before it was mounted on the electrode holder and inserted in the measuring cell. The supporting electrolyte was deoxygenated by saturation with nitrogen which was passed through two gas washing towers, the first containing vanadous chloride solution and the second supporting electrolyte. The electrode surface was conditioned in the deoxygenated supporting electrolyte by cycling the applied potential between −1.0 V and + 1.0 V *vs.* Ag/AgCl. The scan rate in the conditioning step was 50 mV/s, and the sweep was applied until no appreciable change in background current could be observed. After the conditioning step, the GCE was left in the supporting electrolyte and appropriate volumes of stock solutions of TNP-GABA were added. During the voltammetric experiments a 10-ml portion of supporting electrolyte was used. With the rotating electrode, the angular velocity was 157 rad/s (1500 rpm).

Derivatization. The derivatizations of GABA

standard solutions and Pierce amino acid standard solutions were performed using 1-ml Eppendorf vessels and mainly according to Caudill and Wightman [12]. The standards were prepared daily and the TNBS reagent solutions weekly with 0.05 *M* borate buffer pH 9 as solvent. All solutions were kept refrigerated when not in use. Separate experiments showed that the derivatization of a Pierce amino acid standard mixture required TNBS at an excess of 1600-fold with respect to the amount of GABA present in order to obtain the maximum yield of TNP-GABA. Therefore, the amount of TNBS used in the derivatizations was routinely 2000 times higher than the amount of GABA present in the sample. Portions of 20 μl of GABA or Pierce standard solutions were allowed to react with 200 μl of reagent solution at 40°C for 30 min. The reaction was quenched by addition of 200 μl of 4 *M* perchloric acid. The TNP derivatives were then extracted twice with 500 μl of toluene. The collected toluene phase was further re-extracted with 500 μl of borate buffer (pH 9). The 500 μl of borate buffer were finally acidified with 20 μl of 0.6 *M* perchloric acid.

RESULTS AND DISCUSSION

Introductory experiments using a similar column packed with pure zinc particles according to MacCrehan and May [19] failed because of the evolution of hydrogen gas. The microbubbels formed rendered detection at any sensitivity impossible. Attempts with back-pressure applied at the detector cell outlet also failed. Not only acidic mobile phases were tried in these experiments. Water, 0.05 *M* phosphate buffer pH 7 and the 0.025 *M* ammonium acetate buffer pH 5.4 used by MacCrehan and May were also tried with the same negative results. However, the problem of hydrogen gas evolution can be avoided if the zinc particles are treated with a mercuric salt. Amalgamated zinc is a classical reductive agent in the Jones reductor [21] for reducing, for example, Fe^{3+} to Fe^{2+} in acidic media.

The effect of the amalgamated zinc scrubber column on the background characteristics was compared with other deoxygenation techniques. The background current characteristics were studied in four different experiments. The use of an oxygen trap in the argon line was thought useful since the argon of the quality used should contain at most 5 ppm oxygen. However, the effectiveness of this oxygen trap, constructed in the laboratory, was questionable, since the background characteristics became worse when the oxygen trap was used together with argon (Fig. 2). However, a drastic improvement in the background characteristics was obtained when the zinc amalgam scrubber column was employed. The best result was obtained when the oxygen trap was used together with the zinc amalgam scrubber column. At −0.6 V, the background current decreased from 200 nA down to 30–60 nA. The background characteristics presented in Fig. 2 are typical single measurements obtained after four different preparations of the GCE. The background characteristics of a freshly polished GCE are largely dependent upon the condition of the electrode surface. A reproducible electrode treatment is therefore of great importance but difficult to obtain. The standard deviation for the data in Fig. 2 is estimated from experience to be 5–10% at a background current of 30 nA and 30% at currents higher than 100 nA. The electrode treatment also affects the faradaic noise level. In the present investigation, the levels were in the range 10–40 pA at −0.6 V. When the zinc amalgam scrubber was used the background increased sharply at potentials more negative than −0.75 V as a result of the reduction of Zn^{2+} dissolving from the scrubber column.

The lifespan of a zinc amalgam scrubber was nor-

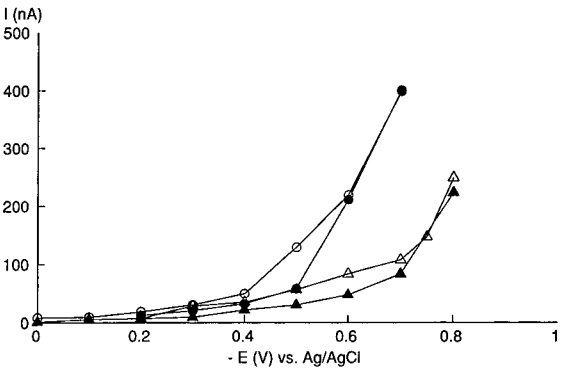

Fig. 2. Comparison of background currents for reductive detection with different methods of deoxygenation of the mobile phase: ● = saturation with argon; ○ = saturation with argon passed through an oxygen trap; △ = saturation with argon and zinc amalgam scrubber mounted; ▲ = saturation with argon passed through an oxygen trap and zinc amalgam scrubber mounted. Flow-rate 0.70 ml/min and temperature 35°C.

mally 1–3 weeks of continuous operation. It was found that the most reliable operation of the zinc amalgam scrubber was obtained if the LC system was left running at 0.70 ml/min continuously. The background current slowly increased during operation from typically 30–60 nA to 100–150 nA after approximately 1 week. Consequently, the faradaic noise became gradually worse and did not allow any measurements when the background reached 100–150 nA. The cure for these problems was to prepare a new zinc amalgam scrubber and prime the LC system with fresh mobile phase. The lifespan was prolonged if fresh mobile phase was refilled into the reservoir flask at the end of a working day.. The increasing background was expected since the function of the zinc amalgam scrubber involves dissolution of Zn^{2+}. Metal impurities present in the zinc material used must also be expected to dissolve, and recycling the mobile phase will therefore lead to enrichment of metal ions into the mobile phase.

Polarographic investigation of the zinc material used showed that the major impurities were copper ($3.8 \cdot 10^{-4}$%) and lead ($2.5 \cdot 10^{-3}$%). A polarogram of a mobile phase portion that had been used and recycled over 4 days did not show any detectable amounts of copper or lead. However, the cathodic background in the polarograms increased sharply at -0.7 V, indicating a high concentration of Zn^{2+}.

The zinc amalgam scrubber column imparts two further limitations to the LC system that should be considered. The first limitation is that the zinc amalgam scrubber column liberates Zn^{2+} ions and possibly hydrogen peroxide into the mobile phase. The presence of metal ions might catalyse reactions which consume analytes of interest, and the hydrogen peroxide, which is formed as an intermediate in oxygen reduction, might interfere with sample constituents. The second limitation is the dissolved oxygen in the sample solution. The injected solutions will acquire a higher oxygen concentration than the mobile phase since it is impossible to use a similar zinc amalgam column for the deoxygenation of sample solutions. The zinc would reduce any component of interest in the sample, and the only possible method of deoxygenating samples is therefore saturation with an inert gas in a closed compartment. As a consequence of the higher oxygen concentration, an oxygen peak at the beginning of the chromatogram cannot be avoided (Fig. 3). After 20 min of purging with argon the oxygen peak is diminished to a height of about 0.25 nA with a severe tailing during the first 4 min. Further saturation with argon results in only minor improvements.

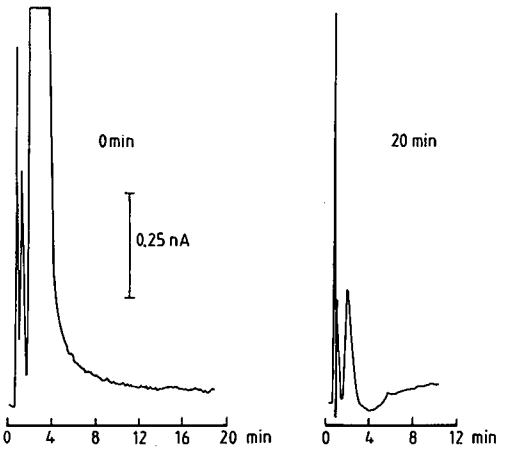

Fig. 3. Deoxygenation efficiency of the sample. A 20-μl aliquot of blank borate buffer was injected. Applied potential -0.6 V.

The electrochemical reduction of TNP-GABA has been characterized previously by Caudill and Wightman [12] as three four-electron steps with three clearly separated voltammetric waves corresponding to the reduction of each nitro group. These results could be verified with voltammetric experiments and are consistent with the commonly accepted mechanism for reduction of aromatic nitro compounds [22]. In order to find the most suitable potential setting for the amperometric detector, experiments using hydrodynamic voltammetry with a rotating GCE were performed. With the electrode rotating at 157 rad/s and the mobile phase as medium, the hydrodynamic voltammogram of TNP-GABA exhibited a maximum which was not affected by alterations in sweep rate, concentration or rotation frequency. Experiments with TNP-glycine and TNP-DAVA also showed maxima under the same hydrodynamic conditions as with TNP-GABA (Fig. 4). These maxima were most pronounced when the electrode surface was freshly polished and pretreated, which indicates that this effect is related to the condition of the electrode surface. By adding a surfactant, Triton X-100, the maxi-

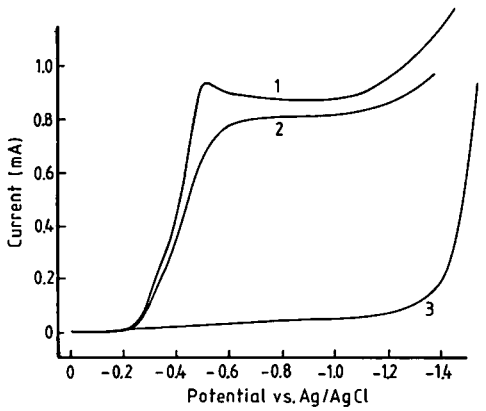

Fig. 4. Hydrodynamic voltammograms of 0.2 m*M* TNP-GABA in the chromatographic mobile phase with the electrode rotating at 1500 rpm. Curve identities are: 1 = 0.2 m*M* TNP-GABA; 2 = after the addition of one drop of 0.1% Triton X-100 solution; 3 = background current.

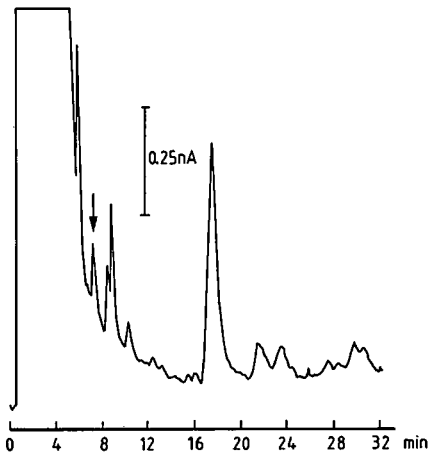

Fig. 6. Chromatogram of a Pierce amino acid standard mixture containing 0.1 pmol of each amino acid. The TNP-GABA peak is indicated by the arrow as in Fig. 7. After correction for dilution and assuming a 100% extraction efficiency, the peak corresponds to 2.6 pmol in a 10-μl sample.

mum could be suppressed, indicating that the maximum in Fig. 4 originates from differences in current density at the electrode surface. The final but most crucial conclusion that can be drawn from Fig. 4 is that a potential of at least -0.6 V *vs.* Ag/AgCl is necessary to realize a mass transport controlled current under hydrodynamic conditions. However, the potential setting needs to be verified with the amperometric detector since a different GCE was used for voltammetric experiments.

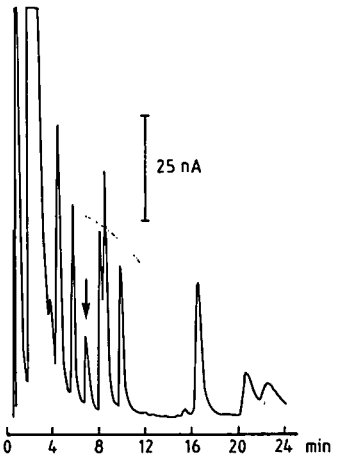

Fig. 5. Chromatogram of a Pierce amino acid standard mixture containing 10 pmol of each amino acid. Arrow indicates the TNP-GABA peak after 7.1 min. Flow-rate 0.70 ml/min and temperature 35°C.

As a first test of the deoxygenation technique developed, a Pierce amino acid standard mixture was investigated. A 20-μl aliquot of diluted standard mixture was treated with TNBS reagent solution as described in the Experimental section. The chromatograms resulting from injections of 10 and 0.1 pmol are shown in Figs. 5 and 6, respectively. The dominating peaks at the beginning of the chromatograms may be caused by picric acid, which is formed as a by-product in the derivatization procedure[11,12]. Similar peaks in the time interval 0–4 min were also found when a blank borate buffer was treated in the same procedure. The results in Fig. 6 indicate the possibility of achieving a detection limit as low as 0.1 pmol. However, the deoxygenation technique used here for sample solutions cannot be applied on sample volumes less than 500 μl. Furthermore, deoxygenation of small volumes causes severe technical problems. Experiments with deoxygenation of 10-μl samples with argon in closed 300-μl sample vials with sealing PTFE-lined silicone septa failed. The reason is probably the transfer time between the sample vial and the injection valve when the small sample volume resides in the syringe. Consequently, the limiting sample volume for a 500 μl minimum sample volume imparts a dilution factor as large as 50 on a sample of 10 μl volume.

In conclusion, it has definitely been proved that the zinc amalgam scrubber column is an efficient tool for reducing the oxygen concentration in the mobile phase to an acceptable level for analysis. It has also been shown that 0.1 pmol of GABA can be detected with TNBS derivatization and reductive mode amperometric detection. So far, the method seems to be useful in situations where the sample volume is not a limiting factor. However, for small sample volumes, as for example from microdialysis (typically 10 μl), problems with the work-up procedure occur. It is necessary to employ some procedure for the removal of the excess TNBS reagent. Extraction with toluene used in these first experiments may not be the ideal method for small sample volumes. The work-up procedure requires an internal standard since the many manipulations will influence the reproducibility. As an internal standard, DAVA has been used [12], and separate experiments have confirmed its advantages, with a retention time of about 12 min. Finally, the deoxygenation procedure needs to be modified for purging of small sample volumes.

ACKNOWLEDGEMENTS

I wish to thank Professor Bengt Nygård, University of Uppsala, and Dr. Anders Carlsson at Carnegie Medicin for many valuable discussions and reviewing the manuscript. I also acknowledge the assistance of Dr. Leif Nyholm with the polarographic experiments. Finally, I wish to thank Barbro Nelson for her assistance in preparation of the manuscript.

REFERENCES

1 B.N. Jones and J. P. Gilligan, *J. Chromatogr.*, 266 (1983) 471.
2 C. Sunol, F. Artigas, J. Ma. Tusell and E. Gelpi, *Anal. Chem.*, 60 (1988) 649.
3 B. N. Jones, S. N. Pääbo and S. Stein, *J. Liq. Chromatogr.*, 4(4) (1981) 565.
4 P. Böhlen and R. Schroeder, *Anal. Biochem.*, 126 (1982) 144.
5 D. L. Hogan, K. L. Kraemer and J. I. Isenberg, *Anal. Biochem.*, 127 (1982) 17.
6 M. H. Joseph and P. Davies, *J. Chromatogr.*, 277 (1983) 125.
7 S. M. Lasley, R. D. Greenland and I. A. Michaelson, *Life Sci.*, 35 (1984) 1921.
8 L. A. Allison, G. S. Mayer and R. E. Shoup, *Anal. Chem.*, 56 (1984) 1089.
9 J. Kehr and U. Ungerstedt, *J. Neurochem.*, 51 (1988) 1308.
10 T. Okuyama and K. Satake, *J. Biochem.*, 47 (4) (1960) 454.
11 G. E. Means, W. I. Cangdon and M. L. Bender, *Biochemistry*, 11(19) (1972) 3564.
12 W. L. Caudill and R. M. Wightman, *Anal. Chim. Acta*, 141 (1982) 269.
13 W. L. Caudill, G. P. Houck and R. M. Wightman, *J. Chromatogr.*, 227 (1982) 331.
14 L. Michel and A. Zatka, *Anal. Chim. Acta*, 105 (1979) 109.
15 M. O. Funk, M. B. Keller and B. Levison, *Anal. Chem.*, 52 (1980) 771.
16 K. Bratin and P. T. Kissinger, *Talanta*, 29 (1982) 365.
17 H. B. Hanekamp, W. H. Voogt, P. Bos and R. W. Frei, *Anal. Chim. Acta*, 118 (1980) 81.
18 W. A. MacCrehan and R. A. Durst, *Anal. Chem.*, 50 (1978) 2108.
19 W. A. MacCrehan and W. E. May, *Anal. Chem.*, 56 (1984) 625.
20 A. Bergens, *J. Chromatogr.*, 410 (1987) 437.
21 I. M. Kolthoff, E. B. Sandell, E. J. Meehan and S. Bruckenstein, *Quantitative Chemical Analysis*, Collier-Macmillan, London, 4th ed., 1969, pp. 829–832.
22 C. K. Mann and K. K. Barnes, *Electrochemical Reactions in Nonaqueous Systems*, Marcel Dekker, New York, 1970, pp. 348–352.

Journal of Chromatography, 598 (1992) 203–208
Elsevier Science Publishers B.V., Amsterdam

CHROM. 24 066

4,5-Diaminophthalhydrazide as a highly sensitive chemiluminescence derivatization reagent for α-dicarbonyl compounds in high-performance liquid chromatography

Junichi Ishida, Shinji Sonezaki and Masatoshi Yamaguchi*

Faculty of Pharmaceutical Sciences, Fukuoka University, Nanakuma Johnan-ku, Fukuoka 814-01 (Japan)

(First received November 1st, 1991; revised manuscript received February 3rd, 1992)

ABSTRACT

4,5-Diaminophthalhydrazide (DPH) was found to be a highly sensitive chemiluminescence derivatization reagent for α-dicarbonyl compounds in high-performance liquid chromatography. The reagent reacts with α-dicarbonyl compounds in dilute hydrochloric acid in the presence of β-mercaptoethanol to give highly chemiluminescent quinoxaline derivatives which produce chemiluminescence by reaction with hydrogen peroxide and potassium hexacyanoferrate(III). The DPH derivatives of five α-dicarbonyl compounds were separated on a reversed-phase column, TSKgel ODS-120T, with a mixture of acetonitrile and 10 m*M* ammonium acetate, followed by chemiluminescence detection. The detection limits are in the range 1.1–300 fmol for a 20-μl injection volume (signal-to-noise ratio 3).

INTRODUCTION

Several α-dicarbonyl compounds, such as methylglyoxal, diacetyl and 2,3-pentanedione, are present in physiological fluids [1,2] and foods [3,4]. However, despite various studies, the details of the roles of these compounds remain unknown. This might be partly due to the lack of a sensitive and specific method for the determination of α-dicarbonyl compounds. Many methods, including polarography [5], UV–visible spectrophotometry [6,7], fluorimetry [8], gas chromatography [9,10] and high-performance liquid chromatography (HPLC) with spectrophotometric [1,10] or fluorimetric detection [11,12] have been reported. Of these methods, the fluorimetric HPLC method [12] with 1,2-diamino-4,5-methylenedioxybenzene is the most sensitive.

On the other hand, chemiluminescence (CL) detection has been successfully introduced into HPLC analysis because of its high sensitivity [13–16] and several precolumn CL derivatization reagents have been reported [17,18]. No reagents, however, have been developed for α-dicarbonyl compounds.

In previous work, we developed 4,5-diaminophthalhydrazide dihydrochloride (DPH) [19] as a CL reagent for α-keto acids. Recently, it was found that α-dicarbonyl compounds also react with DPH under derivatization conditions different to those for α-keto acids to give quinoxaline derivatives (Fig.

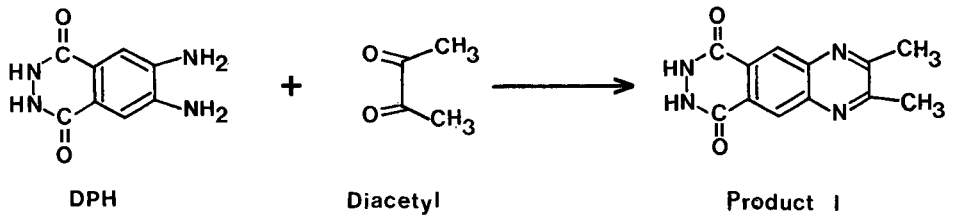

Fig. 1. Chemiluminescence derivatization reaction of diacetyl with 4,5-diaminophthalhydrazide (DPH).

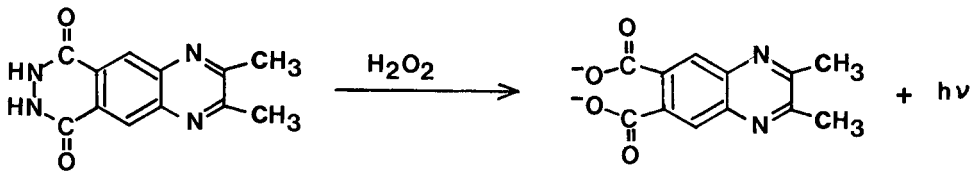

Fig. 2. Chemiluminescence reaction of the DPH derivative of diacetyl.

1). Further, the quinoxaline derivatives generated intense CL by reaction with hydrogen peroxide in the presence of potassium hexacyanoferrate(III) in alkaline media (Fig. 2), conditions which are different to those for α-keto acids. In this work, we examined the optimum derivatization and CL reaction conditions and developed a sensitive and selective method for the determination of α-dicarbonyl compounds using DPH, based on HPLC with CL detection.

EXPERIMENTAL

Chemicals and solutions

All chemicals and solvents were of analytical-reagent grade, unless stated otherwise. Distilled water, purified with a Milli-Q II system (Millipore), was used for all aquous solutions. Hydrogen peroxide (31%, v/v) was purchased from Mitsubishi Gas Kagaku (Tokyo, Japan). The α-dicarbonyl compounds listed Table I were purchased from Tokyo Kasei Kogyo (Tokyo, Japan). DPH dihydrochloride was prepared as described previously [19,20]. DPH solution (8.0 m*M*) was prepared in 0.2 *M* hydrochloric acid containing 0.2 *M* β-mercaptoethanol. This solution was used within 4 h. Hydrogen peroxide (40 m*M*) and potassium hexacyanoferrate (III) (25 m*M*) solutions were prepared in water and 2.75 *M* sodium hydroxide, respectively.

Apparatus and HPLC conditions

The time course of the CL reaction was measured with a Laboscience TD-4000 lumiphotometer. Uncorrected fluorescence spectra were measured with a Hitachi 650-60 spectrofluorimeter in a 10 × 10 mm quartz cell; a spectral bandwidth of 5 nm was used in both excitation and emission monochromators. ^{1}H nuclear magnetic resonance spectra were obtained with a Hitachi R-90H spectrometer at 90 MHz using a *ca.* 1% (w/v) solution of [$^2H_6$]dimethyl sulfoxide containing tetramethylsilane as an internal standard. Field desorption mass spectra were taken with a JEOL HX-110 spectrometer. Uncorrected melting points were measured with a Gallenkamp melting point apparatus.

Fig. 3. shows a schematic diagram of the HPLC–CL system. Chromatography was performed with a Model 655A-11 high-performance liquid chromatograph (Hitachi, Tokyo, Japan) equipped with a Rheodyne Model 7125 syringe-loading sample injector valve (20-μl loop). Chromatograms were recorded with a SIC Chromatocorder 11 (System Instruments, Tokyo, Japan). The DPH derivatives of α-dicarbonyl compounds were separated on a TSKgel ODS-120T reversed-phase column (250 × 4.6 mm I.D.; particle size 5 μm) (Tosoh, Tokyo, Japan) by isocratic elution with acetonitrile–10 m*M* ammonium acetate (27:73, v/v) as eluent. The flow-rate of the mobile phase was 1.0 ml/min. The column temperature was ambient (18–25°C).

The eluate from the HPLC column was mixed with the hydrogen peroxide and the potassium hexacyanoferrate(III) solutions delivered by two Hitachi L-6000 pumps using T-type mixing devices. The flow-rates of the hydrogen peroxide and potassium hexacyanoferrate(III) solutions were 1.0 and 2.0 ml/min, respectively. The CL generated was monitored by a Model 825-CL intelligent CL detector (Jasco, Tokyo, Japan) equipped with a 90-μl flow cell. Stainless-steel tubing (0.5 mm I.D.) was used for the HPLC system.

Preparation of chemiluminescent compound from diacetyl

DPH (0.2 g, 1.0 mmol) and diacetyl (0.1 g, 1.2 mmol) were dissolved in 15 ml of 0.2 *M* hydrochloric acid containing 0.2 *M* β-mercaptoethanol. The mixture was heated in a boiling water-bath for 1 h. The precipitate that was produced during the heating, was filtered off and then recrystallized from di-

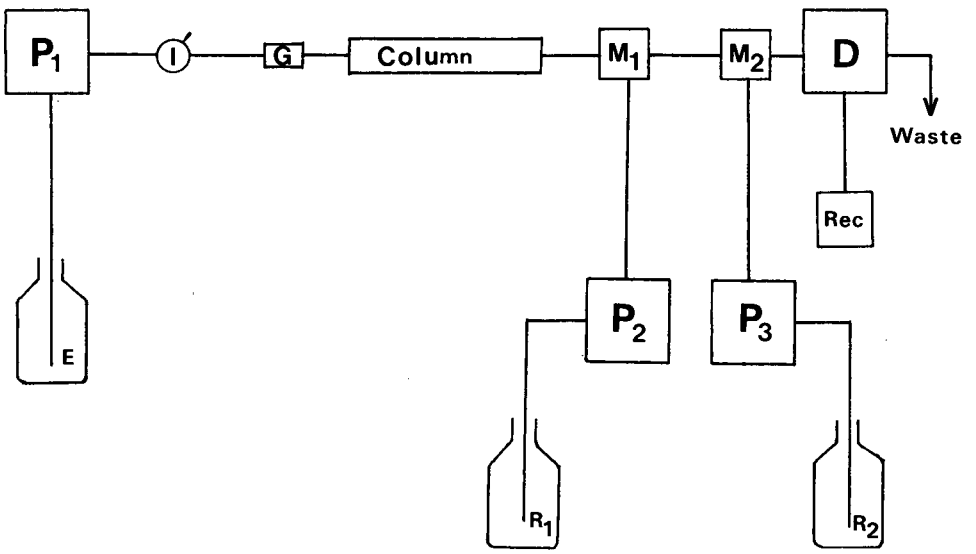

Fig. 3. Schematic flow diagram of the HPLC–CL system. P_1–P_3 = HPLC pumps; I = injector valve (20 μl); D = detector; G = guard column (TSK gel ODS-120T); Column = TSK gel ODS-120T (250 × 4.6 mm I.D.); M_1 and M_2 = mixing devices; Rec = recorder; E = mobile phase; R_1 = hydrogen peroxide solution; R_2 = potassium hexacyanoferrate(III) solution. Flow-rates: E = 1.0, R_1 = 1.0, R_2 = 2.0 ml/min.

methyl sulphoxide–water (9:1, v/v) to give product I (Fig. 1) (80 mg, 0.33 mmol) as brownish yellow needless, m.p. 330°C (decomposition). ^{1}H NMR, δ (ppm) 2.76 (6H, s, C-CH_3), 8.55 (2H, s, aromatic protons), 11.38 (2H, s, NH). Mass spectrum *m/z* 242 (M^+, base peak). Analysis: calculated for $C_{12}H_{10}N_4O_2$, C 59.50, H 4.16, N 23.13; found, C 59.73, H 4.16, N 23.00%.

Procedure

To a 100-μl aliquot of a test solution of α-dicarbonyl compounds, placed in a screw-capped tube (100 × 15 mm I.D.) were added 100 μl of the DPH solution. The tube was tightly closed and heated at 100°C for 45 min. A 20-μl aliquot of the final reaction mixture was injected into the chromatograph.

RESULTS AND DISCUSSION

HPLC conditions

A good separation of the DPH derivatives of five α-dicarbonyl compounds listed in Table I was achieved on a TSK gel ODS-120T column by isocratic elution with acetonitrile–10 m*M* ammonium acetate (27:73, v/v). A typical chromatogram obtained with a standard mixture is shown in Fig. 4. The individual α-dicarbonyl compounds gave single peaks in the chromatogram.

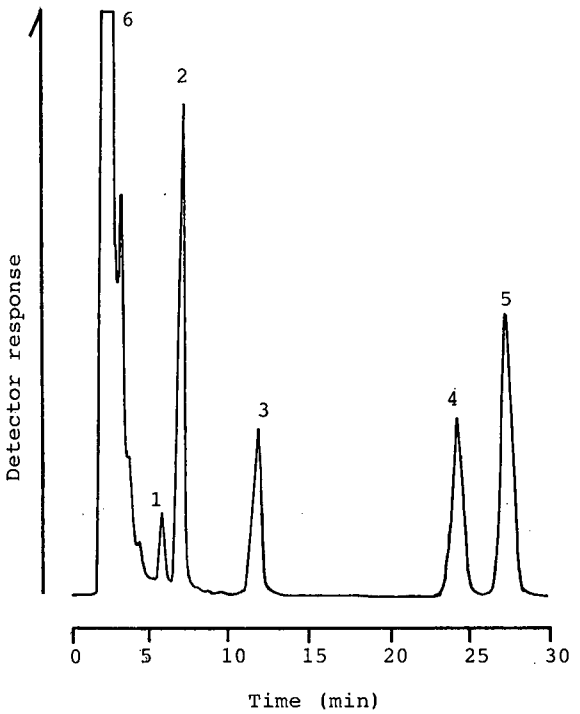

Fig. 4. Chromatogram of the DPH derivatives of five α-dicarbonyl compounds. A portion (100 μl) of a standard mixture of α-dicarbonyl compounds listed in Table I (1 mmol for 3,4-hexanedione and 10 pmol each for the other compounds per injection volume) was treated according to the procedure. Peaks: 1 = phenylglyoxal; 2 = diacetyl; 3 = 2,3-pentanedione; 4 = 3,4-hexanedione; 5 = 2,3-hexanedione; 6 = reagent blank.

Derivatization conditions

Diacetyl and 2,3-pentanedione were selected as model compounds to establish reaction conditions suitable for a more general method. α-Dicarbonyl compounds reacted with DPH in dilute hydrochloric acid, but not in neutral or alkaline solution. Hydrochloric acid at 0.18–0.30 *M* in the DPH solution gave maximum peak heights; 0.20 *M* was adopted for the preparation of the DPH solution. β-Mercaptoethanol was used to facilitate the derivatization of α-dicarbonyl compounds with DPH. The peak heights for the compounds were maximum at 0.20 *M* β-mercaptoethanol in the DPH solution. Other reductants such as sodium sulphite, sodium hydrogensulphite and sodium dithionite showed low reactivities, less than 50% of that obtained with β-mercaptoethanol.

The DPH solution gave the most intense and constant peaks at concentrations >6.0 m*M*; 8.0 m*M* was adopted. The derivatization reaction proceeded more rapidly as the reaction temperature was increased (Fig. 5). The peak heights became maximum and constant after heating at 100°C for 30 min. Therefore, heating at 100°C for 45 min was adopted in the recommended procedure.

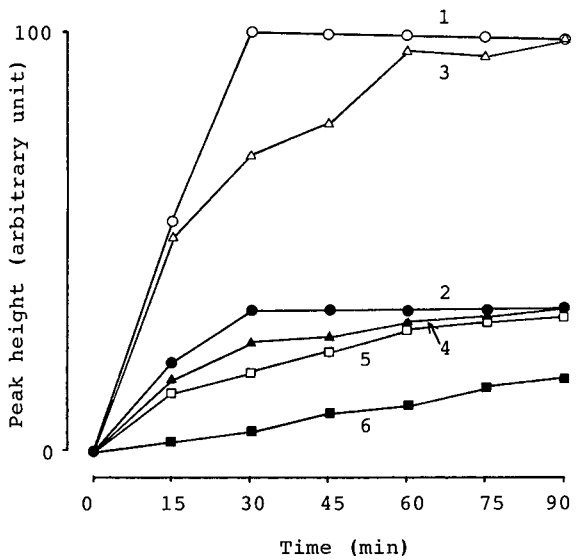

Fig. 5. Effect of reaction time and temperature on the derivatization reaction of diacetyl and 2,3-pentanedione with DPH. Temperatures: 1 and 2 = 100°C; 3 and 4 = 80°C; 5 and 6 = 50°C. Compounds: 1, 3 and 5 = diacetyl; 2, 4 and 6 = 2,3-pentanedione.

The DPH derivatives in the final solution were stable for at least 72 h in daylight at ambient temperature.

Chemiluminescence reaction

The optimum CL reaction conditions were examined by setting the flow-rates of the hydrogen peroxide and potassium hexacyanoferrate(III) solutions at 1.0 and 2.0 ml/min, respectively. The CL intensities were affected by the concentrations of hydrogen peroxide, potassium hexacyanoferrate (III) and sodium hydroxide. The concentrations of these reagents were varied one at a time to establish the maximum intensity obtainable. Based on these experiments (Fig. 6), concentrations of 40 m*M* hydrogen peroxide, 25 m*M* potassium hexacyanoferrate(III) and 2.75 *M* sodium hydroxide were selected.

The length of tubing between the second device (M_2 in Fig. 2) and the detector affected the CL response. The peak heights increased with decreasing length of the tubing; 5 cm was tentatively selected.

The extra-column dispersion caused by the post-column reaction was examined by monitoring with a UV detector set between the column and the first mixing device. The half-widths of the peaks after the postcolumn reaction were broadened about 1.2-fold.

Calibration graph, precision and detection limits

The relationships between the peak heights and the amounts of the individual α-dicarbonyl compounds were linear up to at least 5 nmol per 20-μl injection volume.

The precision was established by repeated determinations ($n = 10$) using a mixture of five α-dicarbonyl compounds (400 pmol for 3,4-hexanedione and 4 pmol each for the other compounds per 20-μl injection). The relative standard deviations did not exceed 3% for all the compounds.

The detection limits are listed in Table I; these values were determined by derivatization of trace amounts of analytes. All the compounds tested except 3,4-hexanedione can be determined at sub-femtomole levels. The sensitivities are *ca.* 20–70 times higher than those of the most sensitive fluorimetric HPLC method so far using 1,2-diamino-4,5-methylenedioxybenzene [12]. The reason for the low sensitivity with 3,4-hexanedione is unknown.

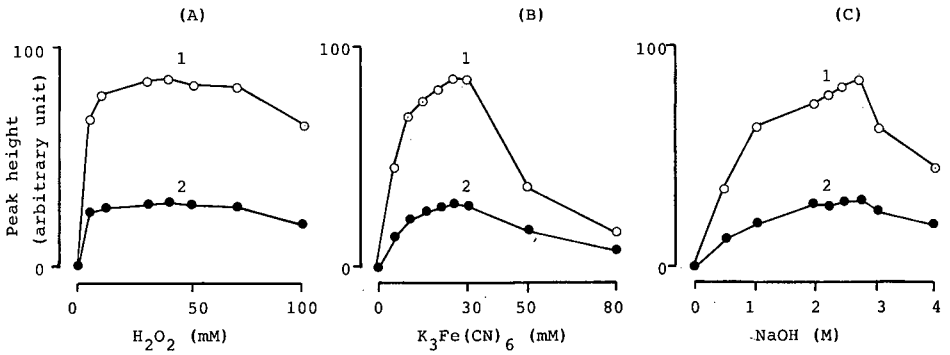

Fig. 6. Effects of (A) hydrogen peroxide, (B) potassium hexacyanoferrate(III) and (C) sodium hydroxide concentrations on the CL peak heights. Curves: 1 = diacetyl; 2 = 2,3-pentanedione.

Reaction of other substances with DPH

Glyoxal and methylglyoxal also gave single peaks at a retention time of 3.0 min for both compounds. However, the peaks were overlapped with reagents peaks under the selected HPLC conditions. α-Keto acids [19] and sialic acids [21] also react with DPH to give CL. Under the present derivatization conditions, however, α-keto acids (α-ketobutyric and phenylpyruvic acids) and sialic acids (N-acetyl- and N-glycolylneuraminic acids) gave *ca.* 1/10–1/15 of the CL intensity of α-dicarbonyl compounds (phenylglyoxal and diacetyl). None of the other physiologically important substances examined generated CL under the recommended conditions at a concentration of 10 mmol/ml. The compounds tested were seventeen L-amino acids, inositol, D-glucose, D-fructose, D-galactose, D-mannose, D-maltose, D-xylose, D-lactose, histamine, tyramine, tryptamine, 2-phenylethylamine, urea, citrulline, bilirubin, glutathione, uric acid, lactic acid, acetoacetic acid, malic acid, palmitic acid, nicotinamide, vitamin D_3, guanosine, cytosine, thymidine, adenosine, cholesterol, cortisone, epiandrosterone, aldosterone and epinephrine. The results suggest that the present derivatization method is usefully selective for α-dicarbonyl compounds.

TABLE I

RETENTION TIMES AND DETECTION LIMITS FOR DPH DERIVATIVES OF α-DICARBONYL COMPOUNDS

Compound	Retention time (min)	Detection limit (fmol)[a]
Phenylglyoxal	5.7	8.7
Diacetyl	6.8	1.1
2,3-Pentanedione	11.9	3.2
2,3-Hexanedione	27.3	1.9
3,4-Hexanedione	24.5	300.0

[a] The amount in the injection volume (20 μl) giving a signal-to-noise ratio of 3.

Chemiluminescent product in the determination of diacetyl

In order to investigate the structure of the CL products, diacetyl was employed as a model compound. The reaction products of α-dicarbonyl compounds with 1,2-diaminobezene [11] and 1,2-diamino-4,5-methylenedioxybenzene [12] have been characterized as quinoxaline derivatives. Thus the reaction product of diacetyl with DPH should be 2,3-dimethyl-7,8-dihydropyridazino[4,5-*g*]quinoxaline-6,9-dione; these identifications were based on the analytical and spectral data (see Experimental).

The time course of the CL reaction of the DPH derivative of diacetyl is shown in Fig. 7. The CL reached maximum intensity *ca.* 2 s after the reaction started, and then quenched rapidly.

With luminol, the aminophthalate ion, which was produced during the CL reaction, was proved to be a light-emitting species [22]. Therefore, the fluorescent spectra were measured after the reaction was performed using the DPH derivative. The excitation and emission maxima of the fluorescence were 370 and 433 nm, respectively. Consequently, 2,3-dimethylquinoxaline-6,7-dicarboxylic acid (Fig. 2),

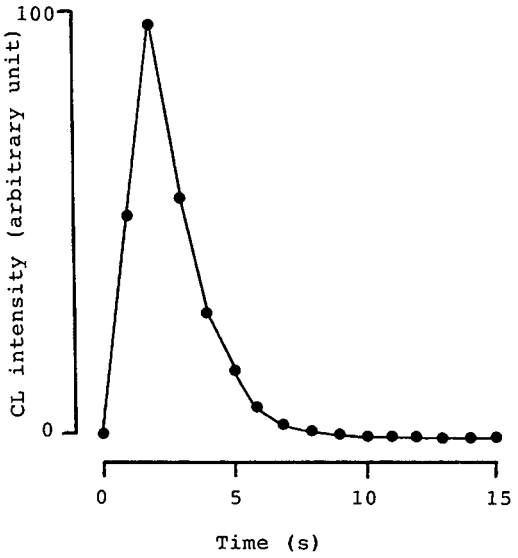

Fig. 7. Time course of the CL reaction of the DPH derivative of diacetyl. A 100-μl portion of the derivative solution ($1{:}10^{-6}$ *M*) was mixed with 100 μl of the hydrogen peroxide solution in a polystyrene tube (65 × 8 mm I.D.). The CL reaction was initiated by automatic injection of 100 μl of the potassium hexacyanoferrate(III) solution into the tube. Each point corresponds to the integrated CL intensity at 1-s intervals.

which was expected to occur in the reaction was estimated to emit light with a maximum at 433 nm.

Because this chemiluminescence reaction is similar to that of luminol, similar factors such as other oxidants and cations may affect the reaction [23,24]. Therefore, in determinations on real samples, the effects of interferents unseparated from the analyte should be considered.

The method permits the highly sensitive and selective determination of α-dicarbonyl compounds, and can be applied to the sensitive determination of biogenic α-dicarbonyl compounds in body fluids and diacetyl in foodstuffs. Further studies are in progress.

REFERENCES

1 S. Ohmori, M. Mori, M. Kawase and S. Tsuboi, *J. Chromatogr.*, 414 (1987) 149.
2 J. Mattessich and J. R. Cooper, *Anal. Biochem.*, 180 (1989) 349.
3 R. A. Baumann, C. Gooijer, N. H. Velthorst, R. W. Frei, J. Strating, L. C. Verhagen and R. C. Veldhuyzen-Doorduin, *Int. J. Environ. Anal. Chem.*, 25 (1986) 195.
4 P. Damiani and G. Burini, *J. Assoc. Off. Anal. Chem.*, 71 (1988) 462.
5 T. Wasa and S. Musha, *Bull. Chem. Soc. Jpn.*, 40 (1967) 1617.
6 R. P. Gilbert and R. B. Brandt, *Anal. Chem.*, 47 (1975) 2418.
7 D. P. Johnson, F. E. Critchfield and J. E. Ruch, *Anal. Chem.*, 34 (1962) 1389.
8 A. J. Maroulis, A. N. Voulgaropoulos and C. P. Hadjiantoniou-Maroulis, *Talanta*, 32 (1985) 504.
9 V. Medonos, V. Ruzicka, J. Kalina and A. Marhoul, *Collect. Czech. Chem. Commun.*, 33 (1968) 4393.
10 P. Moree-Testa and Y. Saint-Jalm, *J. Chromatogr.*, 217 (1981) 197.
11 T. Matsuura, K. Yoshino, E. Ooki, S. Saito, E. Ooishi and I. Tomita, *Chem. Pharm. Bull.*, 33 (1985) 3567.
12 S. Hara, M. Yamaguchi, Y. Takemori, T. Yoshitake and M. Nakamura, *Anal. Chim. Acta*, 215 (1988) 267.
13 R. L. Veazey and T. A. Nieman, *J. Chromatogr.*, 200 (1980) 153.
14 A. MacDonald and T. A. Nieman, *Anal. Chem.*, 57 (1985) 936.
15 S. Kobayashi and K. Imai, *Anal Chem.*, 52 (1980) 424.
16 O. Nozaki, Y. Ohba and K. Imai, *Anal. Chim. Acta*, 205 (1988) 255.
17 T. Kawasaki, M. Maeda and A. Tsuji, *J. Chromatogr.*, 328 (1985) 121.
18 B. Mann and M. L. Grayeski, *J. Chromatogr.*, 386 (1987) 149.
19 J. Ishida, M. Yamaguchi, T. Nakahara and M. Nakahara, *Anal. Chim. Acta*, 231 (1990) 1.
20 R. L. Williams and S. W. Shalaby, *J. Heterocycl. Chem.*, 10 (1973) 891.
21 J. Ishida, T. Nakahara and M. Yamaguchi, *Biomed. Chromatogr.*, in press.
22 E. H. White, O. Zafiriou, H. H. Kagi and J. H. M. Hill, *J. Am. Chem. Soc.*, 86 (1964) 940.
23 D. T. Bostick and D. M. Hercules, *Anal. Chem.*, 47 (1975) 447.
24 P. J. Koerner, Jr., and T. A. Nieman, *Mikrochim. Acta*, II (1987) 79.

Journal of Chromatography, 598 (1992) 209–218
Elsevier Science Publishers B.V., Amsterdam

CHROM. 24 083

High-performance liquid chromatographic separation of molecular species of neutral phospholipids

S. L. Abidi* and T. L. Mounts

Food Quality and Safety Research, National Center for Agricultural Utilization Research, Agricultural Research Service, US Department of Agriculture, 1815 N. University Street, Peoria, IL 61604 (USA)

(First received October 7th, 1991; revised manuscript received February 4th, 1992)

ABSTRACT

Molecular species of neutral phospholipids, phosphatidylcholine (PC) and phosphatidylethanolamine (PE), were resolved by reversed-phase high-performance liquid chromatography (HPLC) using mobile phases of acetonitrile–methanol–water containing tetraalkylammonium phosphates (TAAPs). Competitive interactions of TAAPs and analyte solutes with a reversed-phase HPLC column resulted in reduced retention of PC or PE with concomitant increase in detection sensitivity. The chromatographic data for PC and PE were distinctly different from those for negatively charged phospholipids where ion-pair retention mechanisms prevailed. While PC (or PE) components eluted at longer retention times with a larger size of TAAP, an increase in the TAAP concentration invariably caused a decrease in phospholipid retention times. Optimization of HPLC conditions by using high concentrations (25–100 m*M*) of tetramethylammonium phosphate in acetonitrile–methanol–water (70:22:8) facilitated elution of components with improved peak symmetry. HPLC separations of neutral phospholipids derived from animal sources were more complex than those from soybeans.

INTRODUCTION

During the course of another study on the analysis of phospholipids (PLs) in crude and degummed soybean oil, it was necessary to monitor the change in molecular species distributions of individual PL classes in the oil samples stored for various periods of time [1,2]. The four major PLs found in soybeans are phosphatidic acids (PAs), phosphatidylcholines (PCs), phosphatidylethanolamines (PEs) and phosphatidylinositols (PIs). Of these, PAs and PIs are negatively charged compounds, whereas PCs and PEs are internally neutralized molecules (Fig. 1). Although many chromatographic methods for analysis of PLs are known in the literature [3–10], reliable analytical methods for the quantification of the two ionic type of intact PL molecules have not been clearly defined. Only recently have high-performance liquid chromatographic (HPLC) methods been reported specifically for the separation of negatively charged PAs and PIs [11,12]. Subcomponents of the two classes of polar lipids can be separated only by reversed-phase ion-pair HPLC. Using the ion-pairing technique, HPLC of the phos-

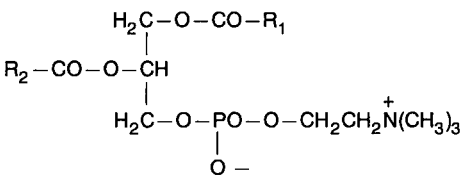

Phosphatidyl Choline

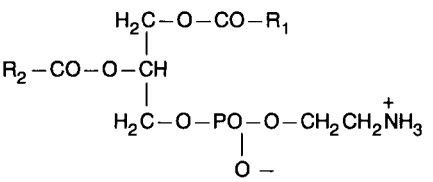

Phosphatidyl Ethanolamine

Fig. 1. Structures of phosphatidylcholine and phosphatidylethanolamine. R_1 and R_2 represent alkyl or alkenyl groups of fatty acids.

phatides leads to well-resolved molecular species with little structural disruption (especially at the glyceroyl–phosphoryl junction). On the other hand, conventional general methods [13–17] of PL analysis require conversion of PIs to derivatives of diglycerides by the removal of the phosphoryl moiety and PAs to dimethyl esters [18] prior to separation by HPLC.

In an earlier attempt to separate molecular species of PCs and PEs isolated from crude and degummed soybean oil according to a published procedure [19], it was difficult to obtain a good chromatogram for the later-eluting components due to severe peak broadening and tailing. These peaks of high hydrobicity often emerged from a HPLC column at unreasonably long retention times. In view of the success of separating negatively charged PAs and PIs by reversed-phase ion-pair HPLC, the same chromatographic methodology was applied to the analysis of samples of PCs and PEs to examine the effect of commercial ion-pairing reagents on the separation of their molecular species. Preliminary results showed that PCs and PEs in the presence of a tetraalkylammonium phosphate were less retained and had better shaped peaks than in the absence of the ammonium salt in the mobile phase. More importantly, a significant improvement in detector response was observed. Such distinct differences in the chromatographic behavior between the neutral and charged PLs are indicative of diverse retention mechanisms involved in the HPLC separation processes. The retention of neutral PLs via ion interactions with mobile phase electrolytes has not been thoroughly investigated previously. This paper reports the results of a comprehensive study of HPLC separation of molecular species of PCs and PEs under various mobile phase electrolyte conditions to demonstrate the analytical utility of the methods in practical application.

EXPERIMENTAL

Materials

PCs and PEs were purchased either from Avanti Polar Lipids (Pelham, AL, USA) or Sigma (St. Louis, MO, USA). Other PLs were obtained from Avanti. Tetramethylammonium phosphate (TMAP) and tetraethylammonium phosphate (TEAP) were prepared by treating corresponding tetraalkylammonium hydroxide (Aldrich, Milwaukee, WI, USA) with phosphoric acid (Fisher, Fair Lawn, NJ, USA) until pH 7. Tetrabutylammonium phosphate (TBAP), pentyltriethylammonium phosphate (PTAP), heptyltriethylammonium phosphate (HPTAP) and sodium pentanesulfonate (SPS) were purchased from Regis (Morton Grove, IL, USA). Tetramethylammonium sulfate (TMAS) was the high-purity product of Aldrich. HPLC-grade acetonitrile and methanol were obtained from J. T. Baker, (Phillipsburg, NJ, USA). Ultrapure water for HPLC was obtained by filtering distilled water through a Millipore (Bedford, MA) Milli-Q water purifier.

High performance liquid chromatography

All HPLC experiments were performed with a Spectra-Physics (San Jose, CA, USA) Model SP8700 liquid chromatograph interfaced to a variable-wavelength UV detector (SpectroMonitor D:LDC, Riviera Beach, FL, USA). HPLC column effluents were monitored at 208 nm. Mobile phases were prepared by adding measured amounts of tetraalkylammonium phosphates to various proportions of acetonitrile–methanol–water. These solutions were filtered, degassed and pumped through an analytical column at a flow-rate of 1–2 ml/min. Aliquots (5–10 μl) of analytical samples (10–20 mg/ml) were injected via a Rheodyne (Cotati, CA, USA) Model 7125 injector (10-μl loop) onto a reversed-phase HPLC column. All samples were freshly prepared prior to analysis. Several reversed-phase columns were used: (i) NovaPak C_{18}, 300 × 3.9 mm I.D., 4 μm (Waters Assoc., Milford, MA, USA), (ii) polymeric resins of macroporous polystyrene–divinylbenzene (MPD), PLRP-S-100, 250 × 4.6 mm I.D., 5 μm (Polymer Labs., Amherst, MA, USA), (iii) Brownlee Speri-5 RP-8, 220 × 4 mm I.D., 5 μm, (Applied Biosystems, Foster City, CA, USA), (iv) Waters Resolve C_{18}, 150 × 3.9 mm I.D., 5 μm, and (v) Alltech (Deerfield, IL, USA) Adsorbosphere HS C_{18}, 250 × 4.6 mm I.D., 5 μm.

HPLC peaks were collected and isolated molecular species were converted to fatty acid methyl esters by a known HCl–methanol procedure [20]. Fatty acid composition was determined using a Varian Model 3400 gas chromatograph equipped with a 0.25 mm × 30 m fused-silica capillary column coated with 0.2 μm SP 2330 (Supelco, Bellefonte, PA,

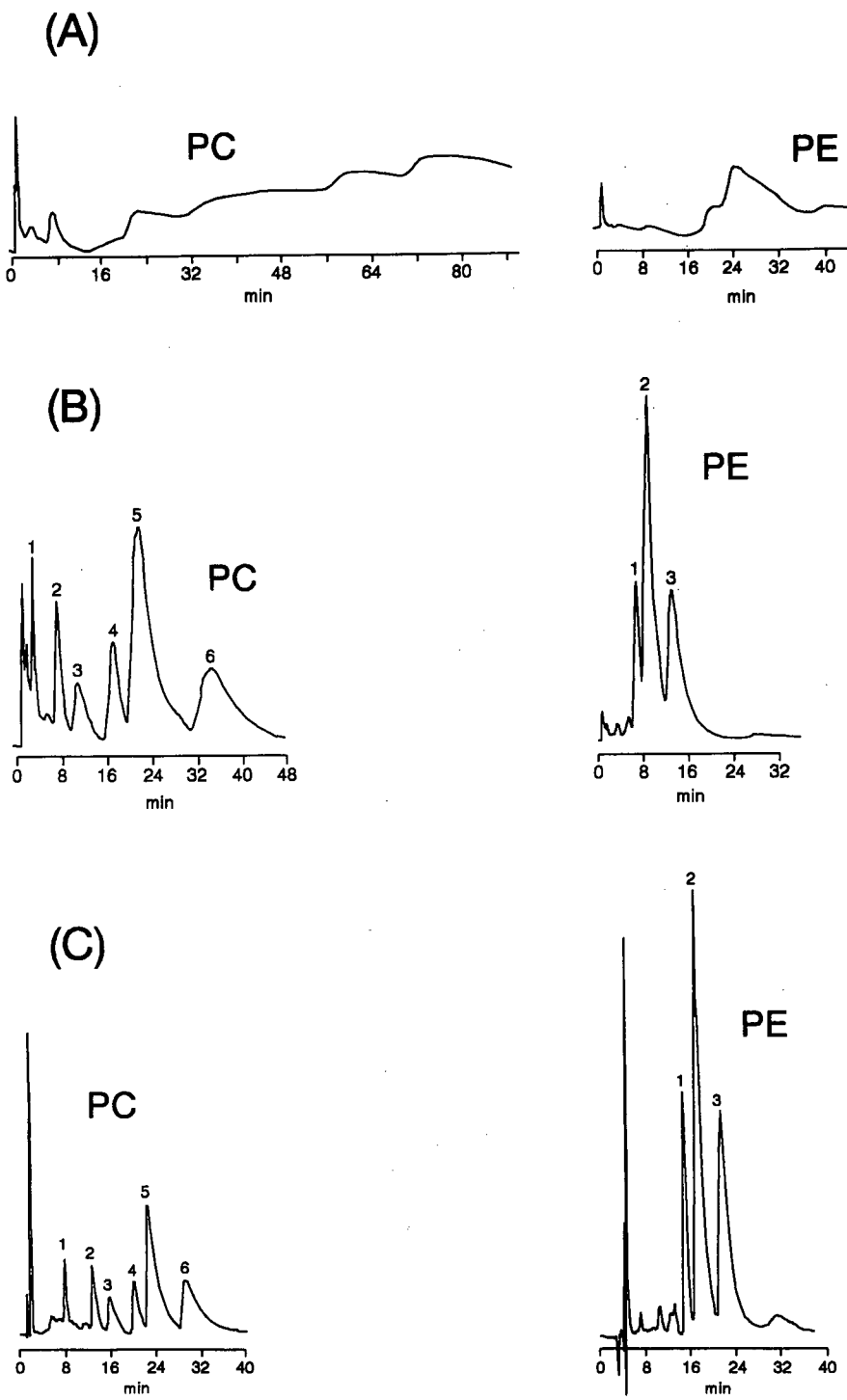

Fig. 2. HPLC separation of molecular species of soybean PCs and PEs in the absence of mobile phase salts (A) and in the presence of mobile phase salts (B, C). Columns: (A, B) Waters Resolve C_{18}, 150 × 3.9 mm, flow-rate, 2 ml/min; (C) Brownlee Spheri-5 RP-8, 220 × 4 mm, flow-rate, 2 ml/min for PCs and 1 ml/min for PEs. Mobile phases: acetonitrile–methanol–water (70:22:8) containing (A) no salt, (B) 5 m*M* HPTAP (C) 5 m*M* PTAP. UV detection at 208 nm. For peak identification, see footnote to Table I.

USA). The chromatograph was interfaced with a flame ionization detector. Helium was the carrier gas. A column temperature program was run from 200 to 220°C at 10°C/min after an initial hold of 15 min. Peak area integration was computed automatically by the data processor in the Model 3400 instrument.

RESULTS AND DISCUSSION

In an exploratory study on the HPLC separation of a pair of closely related PCs the fatty acid chains of which are interchanged at the β- and γ-carbons of the glycerol moiety, unusually long retention times of analytes having broad unsymmetrical peaks were observed. In recent reversed-phase ion-pair HPLC studies [11,12] of negatively-charged PLs, modification of mobile phases with quaternary ammonium salts produced dramatic effects on the chromatographic separation of their molecular species. A similar series of tetraalkylammonium phosphates (TAAPs) as used in those studies were employed to explore their impact on the chromatographic behavior of neutral phospholipids, PCs and PEs. The six TAAPs chosen in this study, TMAP, TEAP, TBAP, PTAP, HPTAP and TMAS, have alkyl chains considerably shorter than those used in HPLC of PIs [11] and PAs [12].

HPLC chromatograms obtained under various conditions are presented in Fig. 2 to illustrate the beneficial effect of mobile phase TAAPs on the peak characteristics of PCs and PEs. It is evident that adding TAAPs to mobile phases led to significant shortening of retention times of the lipid components with concurrent increase in peak heights. Such an improvement in peak shapes was more prominent for PCs than for PEs because of the greater degree of hydrophobicity inherent in PCs, the trimethylamino analogues of PEs (Fig. 1). Without mobile phase electrolytes in the HPLC systems, the neutral PL solutes were strongly adsorbed on a reversed-phase hydrocarbonaceous column. In other words, the amounts of injected analytes failed to elute quantitatively from the columns. The adsorption phenomenon was thwarted by incorporation of TAAPs into the mobile phases. HPLC on longer-alkyl-chain bonded silica (Resolve C_{18}) tended to give broader analyte peaks than with a shorter-alkyl-chain bonded silica (Brownlee C_8) column (Fig. 2B *vs.* C).

TABLE I

HPLC SEPARATION OF MOLECULAR SPECIES OF SOYBEAN PCs AND PEs ON A RESOLVE C_{18} COLUMN

Flow-rate 2 ml/min. Mobile phase solvents were acetonitrile–methanol–water (70:22:8). HPTAP = Heptyltriethyl ammonium phosphate.

HPTAP concentration (m*M*)	Capacity factor, *k'*					
	Component[a]					
	1	2	3	4	5	6
PCs						
5.00	2.11	6.78	11.0	18.1	23.4	37.9
2.50	2.56	7.89	12.8	22.6	29.7	49.2
1.25	3.22	9.00	17.2	29.2	38.1	63.0
0.625	3.89	12.3	21.2	35.0	45.2	76.8
0.00	Too broad to be measurable					
PEs						
5.00	6.56	8.78	13.2			
2.50	7.00	9.67	16.8			
1.25	10.6	13.7	23.0			
0.625	13.2	17.2	28.3			
0.00	23.4	28.3	45.2			

[a] Component identification: PCs: 1 = 18:3–18:3; 2 = 18:2–18:3; 3 = 18:2–18:2; 4 = 18:1–18:2; 5 = 16:0–18:2; 6 = 16:0–18:1; PEs: 1 = 18:2–18:3; 2 = 18:2–18:2; 3 = 16:0–18:2.

TABLE II

HPLC SEPARATION OF MOLECULAR SPECIES OF SOYBEAN PCs ON A BROWNLEE SPHERI-5 RP-8 COLUMN

Flow-rate 2 ml/min. Mobile phase solvents were acetonitrile–methanol–water (70:22:8). PTAP = Pentyltriethyl ammonium phosphate; SPS = sodium pentyl sulfonate. For component identification, see footnote to Table I.

Electrolyte concentration (m*M*)	Capacity factor, *k'*					
	Component					
	1	2	3	4	5	6
PTAP						
5.00	7.00	12.2	15.0	19.4	21.8	28.6
2.50	7.80	13.0	16.2	20.6	23.7	29.8
1.25	10.2	17.4	21.8	28.6	32.2	42.6
0.00	13.0	22.6	29.0	38.2	44.2	59.0
SPS						
5.00	9.80	17.4	21.8	32.2	35.8	46.6
2.50	10.6	19.4	25.0	37.4	42.6	56.2

Table I shows the concentration effect of HPTAP on the capacity factors (*k'*) of PC and PE. For both the PL classes, the *k'* values decreased with increasing HPTAP concentrations. Under the same conditions, molecular species of PCs eluted at longer retention times than PEs. Consequently, in the ab-

TABLE III

HPLC SEPARATION OF MOLECULAR SPECIES OF SOYBEAN PCs AND PEs ON A BROWNLEE SPHERI-5 RP-8 COLUMN UNDER VARIOUS MOBILE PHASE CONDITIONS

Flow-rate 1–2 ml/min. Mobile phase were solvents A–solvent B (92:8), where solvent A = acetonitrile–methanol (70:22), solvent B = 5 m*M* electrolyte in water. PTAP = Pentyltriethylammonium phosphate; TEAP = tetraethylammonium phosphate; TMAP = tetramethylammonium phosphate; TMAS = tetramethylammonium sulfate. For component identification, see footnote to Table I.

Electrolyte in solvent B	Capacity factor, *k'*					
	Component					
	1	2	3	4	5	6
PCs (2 ml/min)						
K_2HPO_4	7.00	12.2	15.4	23.0	27.0	37.0
NH_4PO_4	12.6	22.6	27.8	39.4	45.4	59.8
PTAP	9.85	16.2	19.8	26.6	29.8	37.8
TEAP	9.63	15.1	18.4	24.8	28.4	36.0
TMAP	6.19	9.38	11.4	15.0	17.8	22.9
TMAS	6.57	11.2	13.8	17.8	21.4	27.8
No salt	11.0	20.2	27.8	44.2	55.8	71.8
PE (1 ml/min)						
K_2HPO_4	1.33	1.74	2.23			
NH_4PO_4	4.20	5.21	6.98			
PTAP	3.92	4.36	5.00			
TEAP	3.24	3.61	4.58			
TMAP	2.41	2.79	3.40			
TMAS	6.40	8.63	10.2			
No salt	Too broad to be measurable					

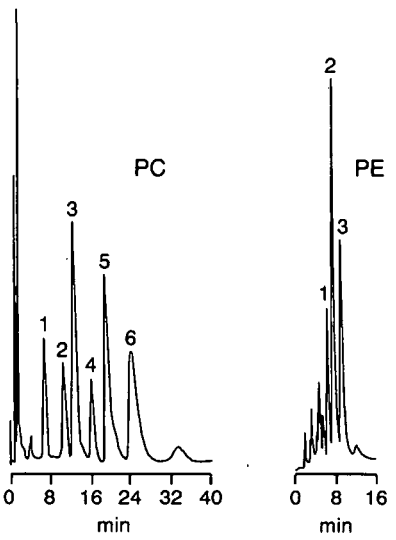

Fig. 3. HPLC separation of molecular species of soybean PC and PE on a Brownlee Spheri-5 RP-8 column. Mobile phase: [(acetonitrile–methanol) (70:22)]–(5 m*M* TMAP in water) (92:8); flow-rate, 2 ml/min for PCs and 1 ml/min for PEs. UV detection at 208 nm. For peak identification, see footnote to Table I.

sence of HPTAP in the mobile phase, the PC components were too broad to be quantifiable. Regardless of the column length, chromatographic peak characteristics were affected by the alkyl-chain length of the bonded-silica phases used. Thus, the peak separations obtained in HPLC with a Resolve C_{18} (150 × 3.9 mm) column were less compact (Table I) than those found in experiments with a Brownlee C_8 (220 × 4 mm) column (Table II). It was of interest to note that similar inverse relationships existed between the concentration effects of electrolytes PTAP and SPS on the k' values of PCs (Table II). Traditionally, both PTAP and SPS have been used as representative ion-pairing counter ions for respective anions and cations in ion-pair HPLC.

Table III shows the effect of various mobile phase electrolytes on the retention behavior of PCs and PEs on octylsilica (Brownlee). Generally solute retention was found to be stronger in HPLC with ammonium phosphate than with potassium phosphate. In comparison with the ammonium salt, the potassium salt could be more effective in alleviating analyte adsorption by way of ion suppression. With TAAPs in the mobile phases, the higher member of the electrolyte in the series gave rise to the higher k' values of the component analytes (PTAP > TEAP > TMAP). The HPLC data in Table III confirm earlier findings (Fig. 2, Tables I and II) that the presence of an electrolyte in mobile phases was es-

TABLE IV

HPLC SEPARATION OF MOLECULAR SPECIES OF SOYBEAN PCs AND PEs ON A MACROPOROUS POLYSTYRENE–DIVINYLBENZENE COLUMN

Flow-rate 1 ml/min. Mobile phase solvents were (i) acetonitrile–methanol–water (70:10:20), (ii) acetonitrile–methanol–water (70:15:15) and (iii) acetonitrile–methanol–water (70:22:8). PTAP = Pentyltriethyl ammonium phosphate. For component identification, see footnote to Table I.

Mobile phase + PTAP concentration (m*M*)	Capacity factor, k'					
	Component					
	1	2	3	4	5	6
PC						
(i) + 5.00	2.85	3.44	6.26	7.59	9.81	12.2
2.50	4.00	3.74	6.56	7.89	10.1	13.1
0.00	3.15	4.04	6.85	8.19	10.6	13.2
(ii) + 0.00	2.41	2.85	4.63	5.81	8.30	9.07
(iii) + 0.00	1.07	1.37	1.96	2.56	3.15	3.74
PEs						
(i) + 5.00	7.44	9.96	12.6			
2.50	7.59	10.4	13.4			
0.00	7.89	10.9	14.1			
(ii) + 0.00	5.67	7.40	9.52			

sential for obtaining useful chromatographic results. When the mobile phase contained no salt, component peaks had either retention times which were too long or peak shapes which were too broad to be of any analytical value. The use of sulfate in lieu of phosphate (TMAS *vs.* TMAP) in the HPLC solvent systems gave more strongly retained PL solutes, presumably due to stronger interactions of the phosphate ions with the octylsilica phase modified by the added electrolyte in the mobile phase. Some examples of chromatograms run with TMAP are shown in Fig. 3.

Separation of rat liver PC on a macroporous polystyrene–divinylbenzene (MPD) column using mobile phases without added salts has been described [21]. Our HPLC results of neutral lipids on the polymeric resins of the same MPD phase are shown in Table IV. Although the observed trends of TAAP concentration effects were similar to those found in HPLC on silica-based columns, the k' values of PCs and PEs were less sensitive to the change in the concentration of PTAP. Adsorption of the neutral PL analytes on MPD seemed to be much less likely to occur than on bonded-silica phases. In view of the low retentivity of the MPD column toward polar lipids, mobile phases normally required a higher water content than other phases to further separate the analyte peaks. The influence of mobile phase solvent compositions on the retention characteristics of PC and PE is also shown in Table IV. As usually observed in reversed-phase HPLC, higher k' values were obtained when the mobile phases contained higher percentages of water.

Table V presents HPLC data obtained with an octadecylsilica column (NovaPak C_{18}, 4 μm) which has a longer column length, but smaller particle size relative to other columns discussed. There were few differences in the number of resolved molecular species with the variation in the particle size or efficiency of the column. This observation is unlike the situation in reversed-phase ion-pair HPLC of negatively charged PAs and PIs where component reso-

TABLE V

HPLC SEPARATION OF MOLECULAR SPECIES OF SOYBEAN PCs AND PEs ON A NOVAPAK C_{18} COLUMN

Flow-rate 2 ml/min. For component identification, see footnote to Table I.

Electrolyte concentration (m*M*)	Capacity factor, k'					
	Component					
	1	2	3	4	5	6
PCs						
PTAP (acetonitrile–methanol–water) (74:23:3)						
10.0	3.44	10.1	16.8	25.7	31.9	52.3
5.00	4.33	11.4	19.4	29.7	36.3	58.6
2.50	5.67	17.7	29.2	48.8	61.7	104
Solvent B[a]						
TMAP, 5[b]	4.33	15.0	24.8	47.9	66.1	105
TMAP, 10	3.89	10.6	15.4	25.7	34.1	53.2
TMAP, 50	1.67	7.00	11.4	19.4	27.4	45.2
TMAP, 100	1.67	6.56	11.0	19.0	27.3	45.2
PEs						
PTAP (acetonitrile–methanol–water) (74:23:3)						
10.0	3.05	6.56	11.4			
5.00	4.78	8.33	12.8			
2.50	10.6	13.2	27.4			

[a] Mobile phases were solvent A–solvent B (95:5), where solvent A = acetonitrile–methanol (70:22), solvent B = various concentrations of TMAP in water.

[b] Mobile phase was solvent A–solvent B (92:8) PTAP = pentyltriethyl ammonium phosphate; TMAP = tetramethyl ammonium phosphate.

lution was notably affected by a change in column efficiency [11,12]. Since the NovaPak column is quite retentive for PCs, it is recommended to use a smaller percentage of water in the mobile phase. Examination of the data in Table V revealed similar patterns of inverse relationships for both PCs and PEs in the concentration dependence of their k' values. To obtain narrow peaks, mobile phases containing the lowest member of TAAPs (TMAP in solvent B, Table V) in the quaternary ammonium series were employed. When k' values obtained from mobile phases containing 50 mM TMAP were compared with those from mobile phases containing 100 mM of the same salt, few differences were noticeable between the corresponding retention data for PCs. The results suggest that the degree of ion interactions between PL solutes and TMAP in the HPLC processes reached a maximum at a concentration of $\leqslant$ 50 mM TMAP.

HPLC separations of molecular species of PCs and PEs from plant and egg sources are shown in Fig. 4. All of the HPLC experiments were carried out under optimized conditions. Separations of molecular species on octylsilica (Fig. 4A) are generally similar to those on octadecylsilica (Fig. 4B), but the degree of component resolution appears to be somewhat more efficient in HPLC with the octadecylsilica column. In Fig. 4B, peak profiles for the negatively charged PAs and PIs are also given with those for the neutral PLs to demonstrate the general applicability of the mobile phase quaternary ammonium electrolytes in HPLC separations of subcomponents of polar lipids. HPLC separations of molecular species of bovine brain PEs, bovine heart PCs, and platelet-activating factor are shown in Fig. 5. In comparison to plant PEs and PCs, the ether-linked species in the two bovine samples tended to have longer retention times. In general, the distribution patterns of molecular species derived from animal sources are more complex than those from plant sources.

For reversed-phase HPLC of ionic compounds (anions and cations), solute partition mechanisms have been postulated based on ion-pair, ion-exchange, and ion-interaction retionales [22]. Hence, it was logical to study the effect of mobile phase electrolytes on the chromatographic behavior of PL ions. While negatively charged PI and PA molecular species have been reported to undergo HPLC separation via ion-pairing processes [11,12], retention of neutral PL (PCs and PEs) components in the presence of counter ions appeared to follow mechanistically different pathways as each of the analytes showed less tendency to be retained by a reversed-phase HPLC column. The latter observations are reminiscent of previous studies on quanternary ammonium compounds [23] and quinoidal imminium compounds [24]. Although there are ionic charges present in both PCs and PEs, they are neutralized by intra-molecular pairing of the charges. This is

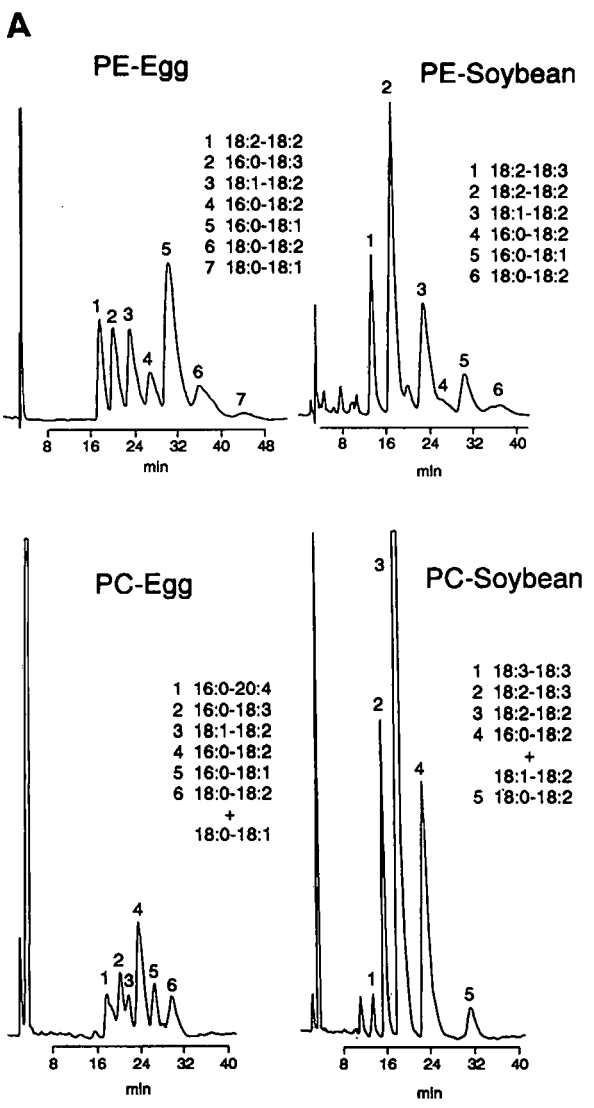

Fig. 4.

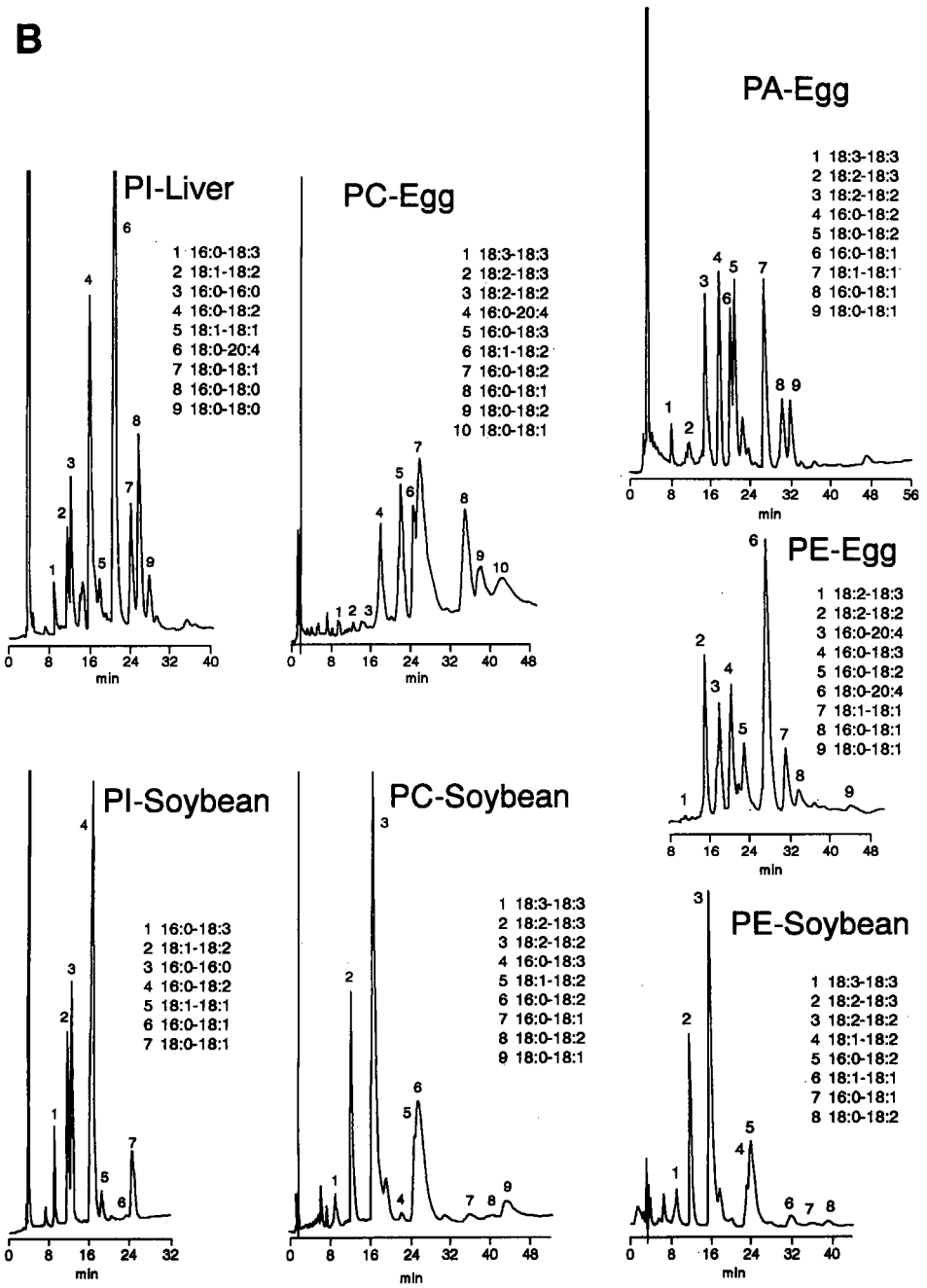

Fig. 4. (A) HPLC of animal *vs.* soybean PCs and PEs on a Brownlee Spheri-5 RP-8 column. Mobile phase: [(acetonitrile–methanol) (70:22)]–(50 m*M* TMAP in water) (92:8); flow-rate, 1 ml/min. UV detection at 208 nm. (B) HPLC of animal *vs.* soybean PAs, PCs, PEs and PIs on an Alltech Adsorbsphere HS C_{18} column. Mobile phase: acetonitrile–methanol–water (70:28:2) containing 25 m*M* TMAP; flow-rate, 2 ml/min for PCs and 1 ml/min for others. UV detection at 208 nm.

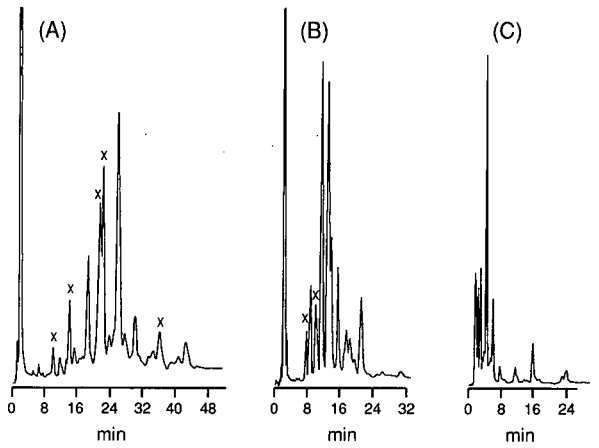

Fig. 5. HPLC of bovine heart PCs (A), bovine brain PEs (B), and platelet-activating factor (C) on a Waters NovaPak C_{18} column. Mobile phase conditions same as Fig. 4B. Flow-rate, 1 ml/min. UV detection at 208 nm. Peak components marked with × are identical with those in soybean oil. All other peak components are ether-linked species.

evidenced by the absence of ion-pairing retention characteristics observed in HPLC of negatively charged PLs (PAs and PIs). Hence, HPLC separations of molecular species of neutral PLs apparently proceeded via an ion-exchange or an ion-interaction retention mechanism.

In conclusion, the methods developed in this study are useful for direct analysis of molecular species of PCs and PEs present in various sample matrices at low levels. The method is also useful for the analysis of samples containing ether-linked aliphatic moieties at the *sn*-1 position of PEs and PCs. This is the first report documenting the mechanistically different chromatographic pathways by which separations of molecular species of neutral and charged PLs are believed to proceed. Deployment of the separation methodology in conjunction with other detection systems (mass spectrometry and nuclear magnetic resonance spectrometry) may lead to viable alternatives for characterization of molecular species. Although the methods are simplified by eliminating the need for chemical derivatization, the procedure requires peak collection and phosphorus determination for analyte quantitation. Using this technique, quantitative analysis of the neutral PLs by HPLC–evaporative light scattering detection is unsuitable because of the incompatibility of the detection systems with the mobile phase electrolytes. The limitation of HPLC-UV detection may be overcome by interfacing the HPLC system with a flame photometric detector.

ACKNOWLEDGEMENT

The authors thank Kathy A. Rennick for technical assistance.

REFERENCES

1 T. L. Mounts and A. M. Nash, *J. Am. Oil Chem. Soc.*, 67 (1990) 757.
2 T. L. Mounts, *J. Am. Oil Chem. Soc.*, in press.
3 N. A. Porter, R. A. Wolf and J. R. Nixon, *Lipids*, 14 (1979) 20.
4 B. J. Compton and W. C. Purdy, *J. Liq. Chromatogr.*, 3 (1980) 1183.
5 M. Smith and F. Jungalwala, *J. Lipid Res.*, 22 (1981) 697.
6 B. J. Compton and W. C. Purdy, *Anal. Chim. Acta*, 141 (1982) 405.
7 G. M. Patton, J. M. Fasulo and S. J. Robins, *J. Lipid Res.*, 23 (1982) 190.
8 A. Cantafora, A. DiBiase, D. Alvaro, M. Angelico, M. Martin and A. F. Attilli, *Clin. Chim. Acta*, 134 (1983) 281.
9 D. A. Kennerly, *J. Chromatogr.*, 363 (1986) 462.
10 D. A. Kennerly, *J. Chromatogr.*, 454 (1988) 425.
11 S. L. Abidi, T. L. Mounts and K. A. Rennick, *J. Liq. Chromatogr.*, 14 (1991) 573.
12 S. L. Abidi, *J. Chromatogr.*, 587 (1991) 193.
13 M. Batley, N. H. Packer and J. W. Redmond, *J. Chromatogr.*, 198 (1980) 520.
14 Y. Nakagawa and L. A. Horrocks, *J. Lipid Res.*, 24 (1983) 1268.
15 M. L. Blank, V. Fitzgerald and F. Snyder, *J. Chromatogr.*, 298 (1984) 473.
16 M. Kito, H. Takamura, H. Navita and R. Urade, *J. Biochem*, 98 (1985) 327.
17 P. J. Ryan and T. W. Honeyman, *J. Chromatogr.*, 331 (1985) 177.
18 J. Y-K. Hsieh, D. K. Welch and J. G. Turcotte, *J. Chromatogr.*, 208 (1981) 398.
19 N. Sotirhos, C. Thorngren and B. Herslof, *J. Chromatogr.*, 331 (1985) 313.
20 W. W. Christie, *Lipid Analysis*, Pergamon Press, New York, 1973, p. 85.
21 W. W. Christie and M. L. Hunter, *J. Chromatogr.*, 325 (1985) 473.
22 S. N. Deming and R. C. Kong, *J. Chromatogr.*, 217 (1981) 421; and references cited therein.
23 S. L. Abidi, *J. Chromatogr.*, 324 (1985) 209.
24 S. L. Abidi, *J. Chromatogr.*, 255 (1983) 101.

Journal of Chromatography, 598 (1992) 219–226
Elsevier Science Publishers B.V., Amsterdam

CHROM. 24 039

Analysis of sterol esters from alga and yeast by high-performance liquid chromatography and capillary gas chromatography–mass spectrometry with chemical ionization

Tomáš Řezanka

Institute of Microbiology, Vídeňská 1083, 14220 Prague (Czechoslovakia)

(First received December 2nd, 1991; revised manuscript received January 22nd, 1992)

ABSTRACT

Sterol esters from the green alga *Chlorella kessleri* and the yeast *Saccharomyces cerevisiae* were analysed by tandem high-performance liquid chromatography (HPLC–HPLC). Non-polar lipids were separated by normal-phase HPLC into individual classes and the fraction of sterol esters was subsequently separated by reversed-phase HPLC into intact molecular species. Further separation and identification of the fractions after HPLC were effected by capillary gas chromatography–mass spectrometry (cGC–MS) with positive and/or negative chemical ionization. A technique consisting of direct injection of the sample after its passage through the detector into the on-column injector of the gas chromatograph was used to transfer the sample from HPLC–HPLC to cGC–MS. By means of this method it was possible to demonstrate more than 30 sterols in both the alga and the yeast, and more than 20 new sterol esters were detected.

INTRODUCTION

Sterol esters are widely distributed in nature and have been detected in fungi, algae, plants and animals [1], in both vertebrates and invertebrates. With a few exceptions [2] (diseases of the phytosterolaemia type), mammalian and human blood only contains esters of cholesterol with acids and analysis is not complicated.

The separation of cholesterol esters and of other esters on a capillary column has been described several times using either polar or non-polar stationary phases [2–7]. Gas chromatography–mass spectrometry (GC–MS) has also been used several times [6,8–10]. However, it is much more complicated to separate sterol esters, where in a complex mixture critical pairs can be produced owing to the chromatographic behaviour of the sterols and fatty acids (FAs). A frequently used method, hydrolysis of sterol esters with subsequent identification of sterols and fatty acids, does not yield adequate results, with the exception of cholesterol. Therefore, in all sources containing more than one sterol (more FA are always present) it is necessary to separate sterol esters in their intact form.

High-performance liquid chromatography (HPLC) has been used for the separation of cholesterol esters without any problems and with excellent results [11]. On the other hand, the analysis of plant sterol esters [4] is more complicated owing to the formation of critical pairs. Capillary GC (cGC) is more advantageous. It is commonly used, often in combination with mass spectrometry. Unfortunately, electron impact (EI) mass spectra of sterol esters do not yield significant M^+ (molecular ion) or fatty acyl ions [4,8–10]. For these reasons, chemical ionization, *e.g.*, with methane, isobutane and ammonia, has been used. Ammonia was found to be most advantageous [9], especially in the negative ion scanning mode [10]. In this mode ions $[M-H_2O]^+$,

0021-9673/92/$05.00

$[M-RCO_2]^+$ and $[RCO_2]^+$ can be determined from the mass spectra.

On the basis of the above reports, we decided to use tandem HPLC–HPLC and cGC–MS with either positive (PCI) or negative chemical ionization (NCI) with natural mixtures of sterol esters from a yeast and a green alga. To our knowledge, the analysis of sterol esters in yeasts has been described only once [4] and in algae not at all.

EXPERIMENTAL

Preparation of samples and standards

The isolation of total lipids from alga (*Chlorella kessleri*) [12] and yeast (*Saccharomyces cerevisiae*) [13] has already been described.

FAs, ergosterol and thionyl chloride were obtained from Sigma (St. Louis, MO, USA) and other chemicals from Merck (Darmstadt, Germany). The standards ergosteryl palmitate, stearate and oleate were prepared by reaction of the respective acyl chloride (0.15 mmol) (synthesized from thionyl chloride) with the sterol (0.1 mmol) in a solution containing 2 ml of benzene and a few drops of pyridine, as described [9].

The samples after reversed-phase (RP) HPLC were saponified by hydrolysis with 25% KOH in 50% methanol at 90°C for 30 min. The unsaponifiable residue (sterols) was extracted and analysed by GC–MS. After acidification, free fatty acids were extracted and derivatized to methyl esters by reaction with BF_3–methanol [12,13].

Isolation of sterol ester fraction

Total lipids (100 mg) were applied to a Silica-Cart C_{18} plastic cartridge system (*e.g.*, 1-ml tube) (Tessek, Prague, Czechoslovakia) and washed with 10 ml of cyclohexane–diethyl ether (98:2). The mixture of non-polar lipids was evaporated to one tenth of its volume, dissolved in cyclohexane (10% concentration) and used for HPLC–HPLC.

HPLC

Two liquid chromatographs were used: a semipreparative Gradient LC System G-I (Shimadzu, Kyoto, Japan) with two LC-6A pumps (0.5 ml/min), an SCL-6A system controller, an SPD ultraviolet detector (206 nm), an SIL-1A sample injector and a C-R3A data processor, with an SGX (spherical silica gel) preprative column (250 mm × 8 mm I.D.; 7 μm particles) (Tessek), and a Sigma 3B analytical (Perkin-Elmer, Norwalk, CT, USA) with an analytical column (250 mm × 4 mm I.D.) packed with SGX C_{18} with 5-μm particles (Tessek).

After injection of 100 μl of solution of total lipids (50 mg/ml) a gradient of propionitrile (PCN)–methyl *tert.*-butyl ether (MTBE) (convex gradient from 100:0 to 90:10 in 20 min) was applied. Through a six-way valve the eluate from the semipreparative column was transferred directly to the second system (Sigma) and elution was then effected with acetonitrile–tetrahydrofuran–methanol using a linear gradient from 40:50:2 to 70:28:2 in 10 min and to 70:20:10 in 8 min.

Individual compounds were identified by determining fatty acid methyl esters and free sterols (by GC–MS) after hydrolysis (see above) and by direct injection of the eluate (collected in a 5-μl microsyringe) in a volume of 2.5 μl.

GC–MS

All GC–MS separations were performed by using a Finnigan MAT (San Jose, CA, USA) Model 1020 B apparatus with EI or PCI and/or NCI.

Sterols. The instrument was equipped with a splitless capillary injector heated to 260°C and a fused-silica capillary column (10 m × 0.25 mm I.D. 0.12-μm film thickness) was coated with chemically bonded, non-polar CP-SIL 5 CB liquid stationary phase (Chrompack Middelburg, Netherlands). The temperature programme was 220°C for 1 min, then increased at 5°C/min to 290°C. The linear velocity of the carrier gas (hydrogen) was 50 cm/s and the ionization energy was 70 eV (EI mode).

Fatty acids (as methyl esters). A Supelcowax 10 fused-silica capillary column (Supelco, Bellefonte, PA, USA) (30 m × 0.25 mm I.D., 0.25-μm film thickness) was used. The temperatures were as follows: splitless injection, 240°C; column, 100°C for 1 min, then increased at 20°C/min to 160°C and at 2°C/min to 220°C. The carrier gas was hydrogen at 36 cm/s and the ionization energy was 70 eV (EI mode).

Sterol esters. The injection temperature (splitless injection) was 100°C and a (Supelcowax 10) fused-silica capillary column (15 m × 0.25 mm I.D., 0.25-μm film thickness) was used. The temperature programme was 100°C for 1 min, then increased at

20°C/min to 230°C and at 2°C/min to 280°C, which was maintained for 10 min. The carrier gas was hydrogen at a linear velocity of 120 cm/s. Ammonia (0.6 Torr) was used as the CI (PCI and/or NCI mode) reagent gas. The spectra were scanned within the range m/z 200–750.

RESULTS AND DISCUSSION

Fatty acids and sterols

The content of fatty acids and sterols in yeasts and algae has been studied many times [12–15], and our results are summarized in Table I. However, intact sterol esters have been investigated only rarely. To our knowledge, only one paper [4] was concerned with the analysis of molecular species of sterol esters in yeasts, *viz.*, in wild and mutant strains. Unfortunately, more than half of the peaks remained unidentified. Esters of fatty acids with ergosterol are major sterol esters.

High-performance liquid chromatography of sterol esters

Only two studies [5,8] were concerned with the chromatographic behaviour of molecular species of both cholesteryl esters and plant sterol esters. Billheimer *et al.* [5] reported the relative retention times (RRTs) of more then 30 sterol esters related to cholesteryl oleate. Because of diversity of both the sterols and acids, the authors derived rules that make it possible to predict, at least partially, chemical structures on the basis of RRTs. In another study [8] plant sterols were chromatographed and the formation of critical pairs was observed.

The use of two different columns during HPLC–HPLC analysis, without intermediate isolation (sample concentration and subsequent injection) has not been described previously for lipids. However, the application of HPLC–cGC was highly successful, with wax and sterol esters in particular [16].

A typical HPLC profile of intact sterol esters iso-

TABLE I

CONTENTS OF FATTY ACIDS AND STEROLS IN ALGA AND YEAST

Fatty acids			Sterols		
Acid[a]	Yeast (mol%)[c]	Alga (mol%)[c]	Sterol[a]	Yeast (mol%)[c]	Alga (mol%)[c]
Lauric	0[c]	2.2±0.2	Zymosterol	13.2±1.3	0
Myristic	2.7±0.2	10.8±1.4	Ergosterol	55.7±3.1	0
Pentadecanoic	0	4.7±0.4	Ergostatetraenol	15.4±0.9	0
Palmitic	25.8±1.5	31.2±2.6	5,7-Ergostadienol	6.5±0.1	0
Palmitoleic	18.7±1.1	7.8±0.9	Cholestadienol	4.3±0.2	0
Hexadecadienoic[b]	0	3.7±0.3	8-Ergostenol	2.3±0.1	0
Hexadecatrienoic[b]	0	3.1±0.2	8(14)-Ergostenol	1.5±0.1	3.1±0.2
Stearic	3.5±0.3	4.6±0.3	Methylergostenol	1.1±0.1	0
Oleic	29.7±2.4	19.8±1.7	Ergostadienol	0	2.8±0.3
Linoleic	19.6±0.8	7.6±0.4	Fungisterol	0	53.7±3.6
Linolenic	0	4.5±0.6	Chondrillasterol	0	9.2±1.2
			Schotenol	0	28.6±2.7
			Stigmastenol	0	2.6±0.2

[a] Trivial names; systematic names are as follows: lauric = dodecanoic; myristic = tetradecanoic; palmitic = hexadecanoic; palmitoleic = 9-hexadecenoic; stearic = octadecanoic; oleic = 9-octadecenoic; linoleic = 9,12-octadecadienoic; linolenic = 9,12,15-octadecatrienoic; zymosterol = 8,24-cholestadien-3β-ol; ergosterol = 5,7,22-ergostatrien-3β-ol; ergostatetraenol = 5,7,22,24(28)-ergostatetraen-3β-ol; 5,7-ergostadienol = 5,7-ergostadien-3β-ol; cholestadienol = 5,7-cholestadien-3β-ol; 8-ergostenol = 8-ergosten-3β-ol; 8(14)-ergostenol = 8(14)-ergosten-3β-ol; methylcholestenol = 4-methyl-8-cholesten-3β-ol; ergostadienol = 7,22-ergostadien-3β-ol; fungisterol = 7-ergosten-3β-ol; chondrillasterol = 24-ethyl-7,22-cholestadien-3β-ol; schotenol = 24-ethyl-7-cholesten-3β-ol; stigmastenol = 24-ethyl-8(14)-cholesten-3β-ol.

[b] Positions of double bonds are 7,10 and 7,10,13, respectively.

[c] Each value represents the means ± S.D. from five analyses.

lated from yeasts is shown in Fig. 1 and Table II. By using the HPLC–HPLC method is was possible to separate individual classes of non-polar lipids in one analysis and by subsequently using the reversed-phase mode it was possible to separate intact sterol esters into individual molecular species. However, in several instances mixtures (critical pairs were present) (see Fig. 1 and Tables II and III).

The occurrence of 37 molecular species of sterol esters from yeast is presented as percentages in Table II. It follows from Fig. 2 that sterol esters with four double bonds and an even number of carbon atoms (44 and 46) are the most frequent. It is also apparent that the strain used tends to preserve a certain membrane fluidity which influences the composition of molecular species characterized roughly by a Gaussian distribution. The combination of polyunsaturated fatty acids with more unsaturated sterols was not found.

In the green alga *Chlorella kessleri* a total of 32 intact sterol esters were identified, of which esters of schotenol with linolenic, linoleic and oleic acids were the most frequent. Fungisterol palmitate was also highly abundant. The representation of molecular species is characterized by a much higher scattering of fungisterol esters as compared with schotenol esters.

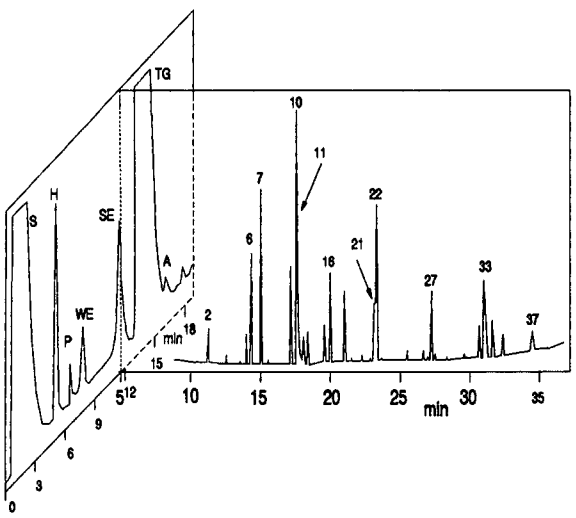

Fig. 1. Semipreparative HPLC of non-polar lipids. Left trace, normal-phase HPLC of non-polar lipids; right, RP-HPLC of sterol ester fraction. For experimental conditions, see text. Peaks: S = solvent; H = hydrocarbons; P = pigments; WE = wax esters; SE = sterol esters; TG = triglycerides; A = alcohols. Peaks 1–37 are molecular species of sterol esters (see Table II).

It follows from Tables II and III that the RRT is mainly affected by the acid moiety of the molecule but that the sterol moiety also plays a certain role (see also ref. 5). In conclusion, the results implicate several rules (see Table IV). It is of interest that individual contributions, *e.g.*, in C_{16} and C_{18} unsaturated acids, are identical. With an increase of the number of double bonds the RRT is always reduced by one quarter (the sterol moiety remains the same). On the other hand, in sterols the introduction of a second double bond (conjugated diene) results in a decrease in RRT by only one fifth (*e.g.*, 5 → 5,7 or 22 → 22,24 (28). We explain this phenomenon by a lower polarity of conjugated dienes with respect to methyl-interrupted double bonds in the fatty acid chain. However, small differences also occur in conjugated dienes, where the rigid homoannular dienes (5,7) have a higher polarity than the diene in the side-chain [22,24(28)]. Compared with the published data [5], we extended our values by further structural elements, *viz.*, the above-mentioned unsaturated acids and sterol dienes. On the basis of information about chromatographic behaviour, it is thus possible to determine at least a tentative chemical structure. However, for conclusive clarification of the structure of molecular species of sterol esters, this tentative structure must be confirmed by means of other methods.

Gas chromatography of sterol esters

Similarly to HPLC, there have been few reports of the separation and identification of intact sterol esters other than cholesterol esters by cGC.

In photosynthetic tissues (freshwater dinoflagellates [7] or celery [17]) sterol esters could be identified on non-polar capillary columns. Also in sediments sterol esters were analysed by cGC–MS with CI (methane) [6], although the shortcomings of a non-polar capillary column, *e.g.*, one chromatographic peak represents a complex mixture of sterol esters consisting of five acyl chains and four sterol moieties, were clearly demonstrated.

The separation of sterol esters on a polar column has been reported in only two papers [2,3]. In one [2], esters of plant sterols and of cholesterol with human serum fatty acids in patients suffering from phytosterolaemia were separated on a capillary col-

TABLE II

COMPOSITION OF STEROL ESTERS FROM YEAST

Peak No.[a]	Sterol ester	RRT[b,c]	Concentration (mol%)[d]
1	Ergostatetraenyl palmitoleate	0.762	0.1±0.1
2	Ergosteryl linoleate	0.789	2.3±0.2
3	Ergostatetraenyl oleate	0.833	0.7±0.1
4	Cholestadienyl oleate	0.865	0.2±0.1
5	Zymosteryl linoleate	0.880	1.5±0.2
6	Ergostatetraenyl myristate	0.891	7.4±0.3
7	Ergosteryl palmitoleate	0.914	12.5±1.2
8	Ergostadienyl linoleate	0.934	0.3±0.1
9	Ergostatetraenyl palmitate	0.988	6.9±0.3
10	Ergosteryl oleate	1.000	18.3±1.4
11	Cholestadienyl palmitoleate	1.002	1.3±0.1
12	Zymosteryl palmitoleate	1.018	2.4±0.1
13	Ergosteryl myristate	1.069	2.7±0.2
14	Ergostadienyl palmitoleate	1.081	2.1±0.1
15	Cholestadienyl oleate	1.095	2.5±0.1
16	Ergostatetraenyl stearate	1.096	3.4±0.3
17	Zymosteryl oleate	1.115	4.6±0.3
18	Ergost-8 (14)-enyl linoleate	1.130	0.2±0.1
19	Ergost-8-enyl linoleate	1.157	0.4±0.1
20	Methylergostenyl linoleate	1.175	0.2±0.1
21	Ergostadienyl oleate	1.183	3.4±0.3
22	Ergosteryl palmitate	1.186	8.0±1.2
23	Zymosteryl myristate	1.193	0.1±0.1
24	Ergostadienyl myristate	1.266	0.6±0.1
25	Cholestadienyl palmitate	1.300	0.7±0.1
26	Ergoste-8 (14)-enyl palmitate	1.310	0.2±0.1
27	Ergosteryl stearate	1.315	5.1±0.4
28	Zymosteryl palmitate	1.323	0.4±0.2
29	Methylergostenyl palmitoleate	1.360	0.2±0.2
30	Ergost-8-enyl palmitoleate	1.400	0.3±0.1
31	Ergostadienyl palmitate	1.404	0.1±0.1
32	Ergoste-8(14)-enyl oleate	1.432	1.4±0.1
33	Ergostadienyl stearate	1.441	5.1±0.7
34	Zymosteryl stearate	1.465	0.3±0.1
35	Ergost-8-enyl oleate	1.465	1.8±0.2
36	Methylergostenyl oleate	1.488	1.3±0.3
37	Ergostadienyl stearate	1.556	1.0±0.1

[a] For peak numbers, see Fig. 1.
[b] Relative retention times from RP-HPLC; ergosterol oleate has a retention time of 17.25 min.
[c] S. D. was in the range 0.0001–0.0021.
[d] Each value represents the means ± S. D. from six analyses.

umn. In the other only cholesterol esters were separated.

Gas chromatography–mass spectrometry of sterol esters

The only method suitable for the identification of sterol esters after cGC is MS. During EI ionization the M^+ (molecular ion) is not recognizable and, therefore, either PCI or NCI is used. Wakeham and Frew [6] used PCI (methane) and individual sterol esters were identified on the basis of split ions ($[RCOOH_2]^+$, $[M-RCOO]^+$ and $[M-RCOO-H_2O]^+$). Unfortunately, M^+ could not be identified even with PCI (methane).

TABLE III

COMPOSITION OF STEROL ESTERS FROM ALGA

Sterol ester	RRT[a,b]	Concentration (mol%)[c]
Fungisteryl hexadecatrienoate	0.554	6.6±0.2
Schotenyl hexadecatrienoate	0.598	2.9±0.1
Fungisteryl linolenate	0.617	0.4±0.1
Ergostadienyl palmitoleate	0.762	0.1±0.1
Schotenyl linolenate	0.665	19.1±2.3
Chondrillasteryl linoleate	0.723	1.3±0.2
Ergostadienyl linoleate	0.723	0.4±0.1
Fungisteryl hexadecadienoate	0.738	4.0±0.2
Schotenyl hexadecadienoate	0.797	1.1±0.1
Fungisteryl linoleate	0.822	1.3±0.1
Schotenyl linoleate	0.887	13.9±2.6
Ergostadienyl oleate	0.928	0.5±0.2
Chondrillasteryl oleate	0.928	1.6±0.1
Fungisteryl palmitoleate	0.947	2.8±0.2
Schotenyl palmitoleate	1.022	1.0±0.1
Ergostenyl oleate	1.044	0.4±0.1
Fungisteryl pentadecanoate	1.052	4.5±0.3
Fungisteryl oleate	1.054	0.5±0.1
Schotenyl laurate	1.083	0.6±0.1
Fungisteryl myristate	1.110	6.8±0.4
Stigmastenyl oleate	1.128	0.5±0.1
Schotenyl pentadecanoate	1.134	0.4±0.1
Schotenyl oleate	1.139	15.0±2.7
Chondrillasteryl palmitate	1.168	2.7±0.3
Stigmastenyl myristate	1.187	0.3±0.2
Schotenyl myristate	1.198	1.1±0.1
Ergostenyl palmitate	1.217	0.5±0.1
Fungisteryl palmitate	1.237	15.5±3.4
Stigmastenyl palmitate	1.325	0.8±0.1
Schotenyl palmitate	1.328	3.3±0.3
Fungisteryl stearate	1.375	1.5±0.2
Schotenyl stearate	1.479	3.3±0.5

[a] See Table II.
[b] S.D. was in the range 0.0001–0.0021.
[c] Each value represents the mean ± S.D. from five analyses.

In another study [9] different ionization gases and different ionization temperatures were compared and ammonia was found to be the gas of choice. When using PCI with ammonia, pseudo-molecular $[M+NH_4]^+$ ions could be detected. Therefore, it is advantageous to use NCI [10] with ammonia, during which three major ions, *viz.*, $[M - RCO_2H - H]^-$, $[RCOO]^-$ and $[RCO_2 - H_2O]^-$, are produced.

For GC–MS analysis the peaks were always collected in a microsyringe at the elution maximum from the reversed-phase column. Table V presents retention times and important ions of the identified molecular species of sterol esters. It was found that on the polar capillary column with Supelcowax 10 it is possible to separate even critical pairs that are not separated by RP-HPLC. This is due primarily to different interactions [*e.g.*, hydrogen bonds between the stationary phase (polyethylene glycol) and polar groups of the sterol ester]. From the chromatographic data for all the sterols (not shown), it was possible, similarly to RP-HPLC, to derive rules of chromatographic behaviour even for cGC on a polar column (Table IV). Mass spectra of sterol esters were measured in both the positive and negative modes. PCI was selected according to ref. 9. As shown in Table V, pseudo-molecular ions were always identified, roughly with an intensity of 40–70% of the base peak $[M+NH_4-RCO_2H]$. In the NCI mode three major ions were detected (Table V and Fig. 3) [8,9].

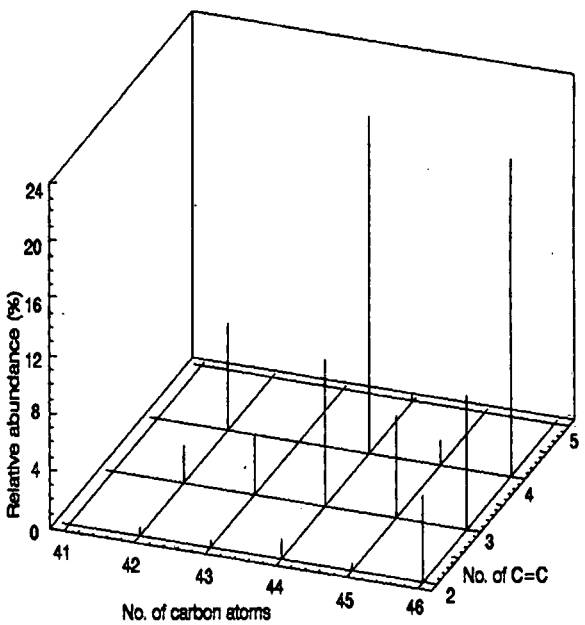

Fig. 2. Relationship between number of double bonds, total carbon atoms and relative abundance of intact steryl esters from yeast. The data were calculated from Table II.

TABLE IV

CONTRIBUTION OF UNSATURATION IN THE FATTY ACID AND STEROL AND OF ADDITIONAL METHYLENE GROUP IN THE FATTY ACID OR STEROL ON THE RETENTION TIMES OF STERYL ESTERS BY MEANS RP-HPLC AND CGC

No. of C=C	Fatty acid[a]	
	RP-HPLC	cGC
0	1.00	1.00
1	0.77±0.02	1.07±0.02
2	0.60±0.01	1.18±0.03
3	0.43±0.01	1.31±0.05

No. of C=C	Position of C=C	Sterol	
		RP-HPLC	cGC
0	–	1.00	1.00
1	5	0.84±0.02	1.08±0.01
1	8	0.84±0.01	1.06±0.02
1	8(14)	0.81±0.01	1.07±0.01
1	22	0.83±0.02	1.11±0.01
2	5,7	0.67±0.03	1.34±0.00
2	22,24(28)	0.70±0.01	1.27±0.00

Difference in CH_2	Fatty acid		Sterol	
	RP-HPLC	cGC	RP-HPLC	cGC
0	1.00	1.00	1.00	1.00
1	1.15±0.03	1.09	1.08±0.03	1.06

[a] *cis*, Methylene interrupted.

TABLE V

GC–MS OF STEROL ESTERS AFTER RP-HPLC (FROM 16 TO 19 min) (FIG. 1) ON POLAR CAPILLARY COLUMN

Sterol ester	*m/z*				
	RRT[a]	$[M+NH_4]^{+b}$	$[M-RCO_2H_2]^{-c}$	$[RCO_2]^{-c}$	$[RCO_2-18]^{-c}$
Ergosteryl myristate	0.874	624	377	227	209
Zymosteryl palmitoleate	0.895	638	365	253	235
Cholestadienyl palmitoleate	0.902	638	365	253	235
Ergostadienyl palmitoleate	0.930	652	379	253	235
Ergostatetraenyl palmitate	0.943	650	375	255	237
Ergosteryl oleate	1.000	678	377	281	263

[a] Relative to ergosteryl oleate (retention time 12.48 min).
[b] PCI-MS.
[c] NCI-MS.

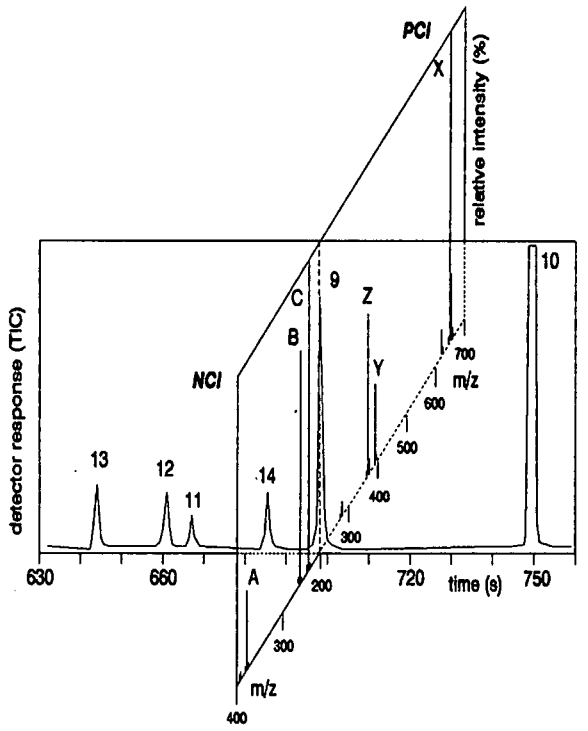

Fig. 3. cGC–MS with PCI and NCI. Trace from left to right, total ion current of partial chromatogram. Front mass spectrum, NCI; rear mass spectrum, PCI. Numbers represent molecular species in Table II. Letters are peaks of the following structures (relative abundance to base peak, in %): A = $[M-RCOOH]^-$ (25); B = $[RCOO]^-$ (80); C = $[RCOO-H_2O]^-$ (100); X = $[M+NH_4]^+$ (100); Y = $[M+NH_4-RCOOH]^+$ (25); Z = $[M+H-RCOOH]^+$ (56).

CONCLUSIONS

By using HPLC–HPLC and cGC–MS with PCI and/or NCI it was possible to identify 32 and 37 sterol esters in green alga and yeast, respectively.

The rules for RP-HPLC and cGC of sterol esters were derived by a combination of HPLC–HPLC and cGC–MS (with PCI and/or NCI). For the first time sterol esters in green algae were demonstrated and the spectrum of known sterol esters in the yeasts was greatly extended. By means of HPLC–HPLC it is possible to identify at least tentatively molecular species of sterol esters; occassional critical pairs can then be further separated and their structure can be fully verified by cGC–MS (with PCI and/or NCI). In a few hours it is thus possible to identify completely even complex mixtures such as sterol esters from microorganisms.

REFERENCES

1 W. R. Nes and M. McKean, *Biochemistry of Steroid and Other Isoprenoids*, University Park Press, Baltimore, MD, 1977.
2 A. Kuksis, J. J. Myher, L. Marai, J. A. Little, R. G. McArthur and D. A. K. Roncari, *Lipids*, 21 (1986) 371.
3 N. B. Smith, *J. Chromatogr.*, 254 (1983) 195.
4 G. P. Fenner and L. W. Parks, *Lipids*, 24 (1989) 625.
5 J. T. Billheimer, S. Avart and B. J. Milani, *Prog. Lipid Res.*, 24 (1983) 1646.
6 S. Wakeham and N. M. Frew, *Lipids*, 17 (1982) 831.
7 P. A. Cranwell, N. Robinson and G. Eglinton, *Lipids*, 20 (1985) 645.
8 R. P. Evershed, V. L. Male and L. J. Goad, *J. Chromatogr.*, 400 (1987) 187.
9 W. R. Lusby, M. J. Thompson and J. Kochansky, *Lipids*, 19 (1984) 888.
10 R. P. Evershed and L. J. Goad, *Biomed. Environ. Mass Spectrom.*, 14 (1987) 131.
11 E. G. Perkins, D. S. Hendren, J. E. Bauer and A. H. El-Hamdy, *Lipids*, 16 (1981) 609.
12 T. Řezanka, L. Doležalová, O. Vyhnálek and Č. Novotný, *Folia Microbiol.*, 30, (1985) 501.
13 T. Řezanka, O. Vyhnálek and M. Podojil, *Folia Microbiol.*, 31 (1986) 44.
14 J. B. M. Rattray, in C. Ratledge and S. G. Wilkinson (Editors), *Microbial Lipids*, Vol. 1, Academic Press, London, 1988, p. 555.
15 Y. Fujino and M. Ohnishi, *Lipids*, 14 (1979) 663.
16 K. Grob, M. Lanfranchi and C. Mariani, *J. Am. Oil Chem. Soc.*, 67 (1990) 626.
17 L. Dyas, M. C. Prescott, R. P. Evershed and L. J. Goad, *Lipids*, 26 (1991) 536.

Journal of Chromatography, 598 (1992) 227–236
Elsevier Science Publishers B.V., Amsterdam

CHROM. 24 029

Simultaneous assay for amatoxins and phallotoxins in *Amanita phalloides* Fr. by high-performance liquid chromatography

F. Enjalbert*

Laboratoire de Botanique, Phytochimie et Mycologie, Faculté de Pharmacie, Avenue Charles Flahaut, 34060 Montpellier (France)

C. Gallion, F. Jehl and H. Monteil

Institut de Bactériologie, 3 Rue Koeberlé, 67000 Strasbourg (France)

H. Faulstich

Max-Planck-Institut für Medizinische Forschung, Jahnstrasse 29, W-6900 Heidelberg (Germany)

(First received July 9th, 1991; revised manuscript received January 22nd, 1992)

ABSTRACT

A reversed-phase high-performance liquid chromatographic method is described that allows the simultaneous determination of up to eight amatoxins and phallotoxins. The method identifies both neutral toxins (α- and γ-amanitin, phalloidin, phallisin and phalloin) and acidic toxins (β-amanitin, phallacidin and phallisacin). Toxins were separated, identified and determined by gradient elution with 0.02 *M* aqueous ammonium acetate–acetonitrile and simultaneous monitoring of the absorbances at 214 and 295 nm. The assay was successfully applied to the analysis of the toxins in a crude extract of *Amanita phalloides*. The limit of detection for each toxin was 10 ng/ml of extraction medium. The assay was further validated by analysing the toxin content in *Galerina marginata*, a species containing only amatoxins. This relatively simple method should be suitable for the detection of amatoxins and phallotoxins in almost any species of mushrooms.

INTRODUCTION

The isolation and complete chemical characterization of the bicyclic peptide toxins from *Amanita phalloides* Fr. has led to the identification of two major classes of peptides, known as amatoxins and phallotoxins [1]. The amatoxins are a family of bicyclic octapeptides which bind and inhibit eukaryotic RNA polymerase II and are considered to be the principal agents responsible for human poisoning by this mushroom. The phallotoxins, bicyclic heptapeptides, block depolymerization of filamentous F-actin to globular G-actin [2,3].

Various chromatographic methods have been used to determine the toxic peptides in mushrooms. The most reliable of these approaches is column chromatography, followed by the identification of single toxic compounds using spectrophotometric or colorimetric methods [4–6]. Although this technique allows the determination of single components, it is time consuming and laborious. Other analytical attempts are based on thin-layer chromatography (TLC) or high-performance TLC (HPLTC) [7–11]. In these procedures, chromatographic spots on thin-layer plates, coloured for amatoxins and fluorescent for phallotoxins, were measured spectrophotometrically. Most of these investigations have been reviewed [1].

0021-9673/92/$05.00

Small amounts of biologically active toxic peptides can be determined by bioassays and binding assays using either the target proteins or antibodies. A binding assay employing the affinity of muscle rabbit actin for a labelled phallotoxin derivative, [^{3}H]demethylphalloin, has been reported [12]. A more sensitive assay is based on the protective effect of phalloidin on the inhibition of a pancreatic desoxyribonuclease by actin [13]. For the determination of amatoxins, a technique using the specific inhibition of the DNA-dependent RNA polymerase II has been developed [14,15]. It is obvious that only the sum of all phallotoxins or amatoxins can be determined using bioassays; the same is true for radioimmunoassays (RIA). First, Fiume *et al.* [16] succeeded in raising antibodies against β-amanitin in rats. In rabbits also, amatoxin-specific antibodies could be obtained when conjugates of α-amanitin with fetuin [17,18], or detoxified amanitin derivatives [19] are used as antigens. RIA methods, permitting the detection of amanitins in the range of nanograms per millilitre, have mostly been applied to the detection of amatoxins in biological fluids from patients [18,19].

For the same purpose, high-performance liquid chromatographic (HPLC) methods for amatoxins have been developed by several laboratories [20–25]. These methods are fairly sensitive and can therefore quickly provide information on the severity of an intoxication from *A. phalloides* or from other amatoxins containing fungi or on the effectiveness of the detoxication treatment. Although HPLC can be extremely useful for the determination of toxic components in mushroom extracts [10,23], so far only a few papers have been published reporting applications of this technique. Moreover, no detailed quantification of amatoxins and phallotoxins has been reported.

Here we present a method based on reversed-phase HPLC for the simultaneous determination of up to eight amatoxins and phallotoxins in *A. phalloides* and other mushroom extracts.

EXPERIMENTAL

Standard solutions and chemicals

α-Amanitin (α-Ama), β-amanitin (β-Ama), phalloidin (PHD) and phallacidin (PCD) were provided by Sigma (St. Louis, MO, USA). γ-amanitin (γ-Ama), phalloin (PHN), phallisin (PHS) and a mixture of phallacidin (PCD) and phallisacin (PSC) were prepared according to previously published procedures [26–29] and in our laboratory [5].

Stock solutions of 500 μg/ml of each toxin were prepared in doubly distilled water and stored at −20°C. Methanol, hydrochloric acid, acetonitrile, ammonium acetate and acetic acid were of analytical-reagent grade (Merck, Darmstadt, Germany). Water was obtained daily from a Milli-Ro–Milli-Q system (Millipore, Molsheim, France).

Extraction procedure

A fresh, fruiting body (18.4 g) of *A. phalloides* consisting of three organs (cap, stipe and volva) was chopped into small pieces. Each fragment of about 2 g was introduced in a cartridge of a Model 6700 freezer-mill (SPEX Industries, Edison, NJ, USA), crushed for 1–2 min and extracted with 3 ml of extraction medium [methanol–water–0.01 *M* hydrochloric acid (5:4:1, v/v/v)]. Overall, 30 ml of extraction medium were utilized. The mixed extracts were incubated overnight at 4°C, then centrifuged at 1000 *g* for 10 min. The supernatant was collected and preserved at 4°C and the pellet was mixed again with 8 ml of the extraction medium and incubated for other 12 h at 4°C. The mixture was centrifuged again at 1000 *g* for 10 min and the supernatant was pooled with the other. A 20-μl aliquot of the combined supernatants was used for the separation and determination of the main toxins. The same procedure was used to prepare extracts from *Galerina marginata* (Batsh) Kühn. and *Amanita pantherina* (D.C.: Fr.) Krombh.

Apparatus and chromatographic conditions

Chromatographic separation of different toxins was carried out by gradient elution. The HPLC apparatus was composed of the following units: a Model 114 M solvent-delivery module, a Model 210 A sample injection valve with a 20-μl loop and a Model 168 variable-wavelength UV diode-array detector (all from Beckman, Fullerton, CA, USA). This detector allows the monitoring of the eluate at two wavelengths simultaneously and the recording of absorbance spectra at definite time intervals (from 1 spectrum per 2 s to 16 spectra/s). In this work, the system was set at 1 spectrum/s. Chromatograms were processed with a System GOLD chromatographic data system (Beckman).

Separations were performed at ambient temperature on a reversed-phase 5-μm Ultrasphere ODS column (250 × 4.6 mm I.D.) (Beckman). The mobile phase was a mixture of two solvents: solvent A was 0.02 *M* aqueous ammonium acetate–acetonitrile (90:10, v/v) and solvent B was 0.02 *M* aqueous ammonium acetate–acetonitrile (76:24, v/v). The pH of mixtures A and B was adjusted to 5 with filtered glacial acetic acid. The gradient profile was as follows: 100% A for 4 min, then 57% B for 16 min, then 100% B for 10 min and finally 100% A. The mobile phase flow-rate was 1 ml/min. The absorbance of the eluate was monitored simultaneously at 214 and 295 nm.

Quality control parameters of the method

A calibration graph was prepared in the extraction medium with increasing amounts of each of the eight toxins yielding concentrations of 1, 50 and 100 μg/ml (except for PCD: 1, 5 and 10 μg/ml). The limit of detection was defined as the lowest concentration of each toxin resulting in a signal-to-noise ratio of 4. The accuracy of the method was investigated for each toxin at three concentrations (1, 50 and 100 μg/ml) by comparing the amount of toxin added to the extraction medium with that actually measured. The precision was determined by calculating the within- and between-day relative standard deviations (R.S.D.) (n = 10) at the same levels.

RESULTS

Chromatographic parameters of toxins

The chromatographic parameters of the toxins are shown in Table I. The values of the capacity factors are in agreement with the currently accepted values. The selectivity factors for two neighbouring peaks, defined as the ratio of their capacity factors, k'_2/k'_1, are 1.15, 1.21, 1.06, 1.18, 1.20, 1.34 and 1.59. A good resolution of each toxin was obtained (Fig. 1).

Amatoxins eluted earlier than phallotoxins. Within each of the two families the toxins eluted as a function of lipophilicity: acidic toxins eluted earlier than neutral toxins (β-amanitin before α- and γ-amanitin; phallisacin and phallacidin before phallisin, phalloidin and phalloin), and toxins having a higher number of hydroxy groups eluted earlier than those with a smaller number (α-amanitin before γ-amanitin; phallisacin before phallacidin; phallisin before phalloidin before phalloin).

TABLE I

CHROMATOGRAPHIC CHARACTERISTICS OF TOXINS

Results are means ± S.E.M.; n = 4.

Toxin	Retention time (min)	Capacity factor (k')	Absorbance ratio (214/295 nm)
β-Ama	8.12 ± 0.09	1.86 ± 0.03	2.68 ± 0.03
α-Ama	8.87 ± 0.02	2.14 ± 0.03	2.81 ± 0.05
PSC	10.18 ± 0.04	2.61 ± 0.03	2.30 ± 0.06
γ-Ama	10.64 ± 0.06	2.77 ± 0.04	2.65 ± 0.01
PCD	12.04 ± 0.18	3.27 ± 0.1	2.52 ± 0.15
PHS	13.89 ± 0.18	3.94 ± 0.09	2.73 ± 0.05
PHD	17.66 ± 0.31	5.28 ± 0.14	2.72 ± 0.18
PHN	26.57 ± 0.16	8.44 ± 0.13	2.63 ± 0.04

The 214/295 nm absorbance ratios were established for each toxin with pure standards and are reported in Table I.

Quality control

The limit of detection for both groups of toxins was 10 ng/ml of extraction medium, corresponding to a detection limit of 0.5 ng/g of fungal matrix. Quantification of toxins, based on peak areas, was linear between 1 and 100 μg/ml (correlation coefficient 0.9987). This concentration range includes the concentration of toxins usually found in fresh mushroom extracts. The accuracy of the measurements of α-amanitin and phalloidin is shown in Table II. Similar values were obtained for other toxins. The precision was evaluated by calculating intra- and inter-day R.S.D. values which ranged from 1.1 tot 4.2% (n = 10).

Assay

The chromatogram illustrated in Fig. 2 shows the analysis of the toxins in an *A. phalloides* extract. The eight toxins are completely resolved from endogenous peaks. The purity of each peak was monitored by comparison of its 214/295 nm absorbance ratio and the superimpostion of its UV absorption spectrum with those of the standards. The maxima for the phallotoxins and the amatoxins are located

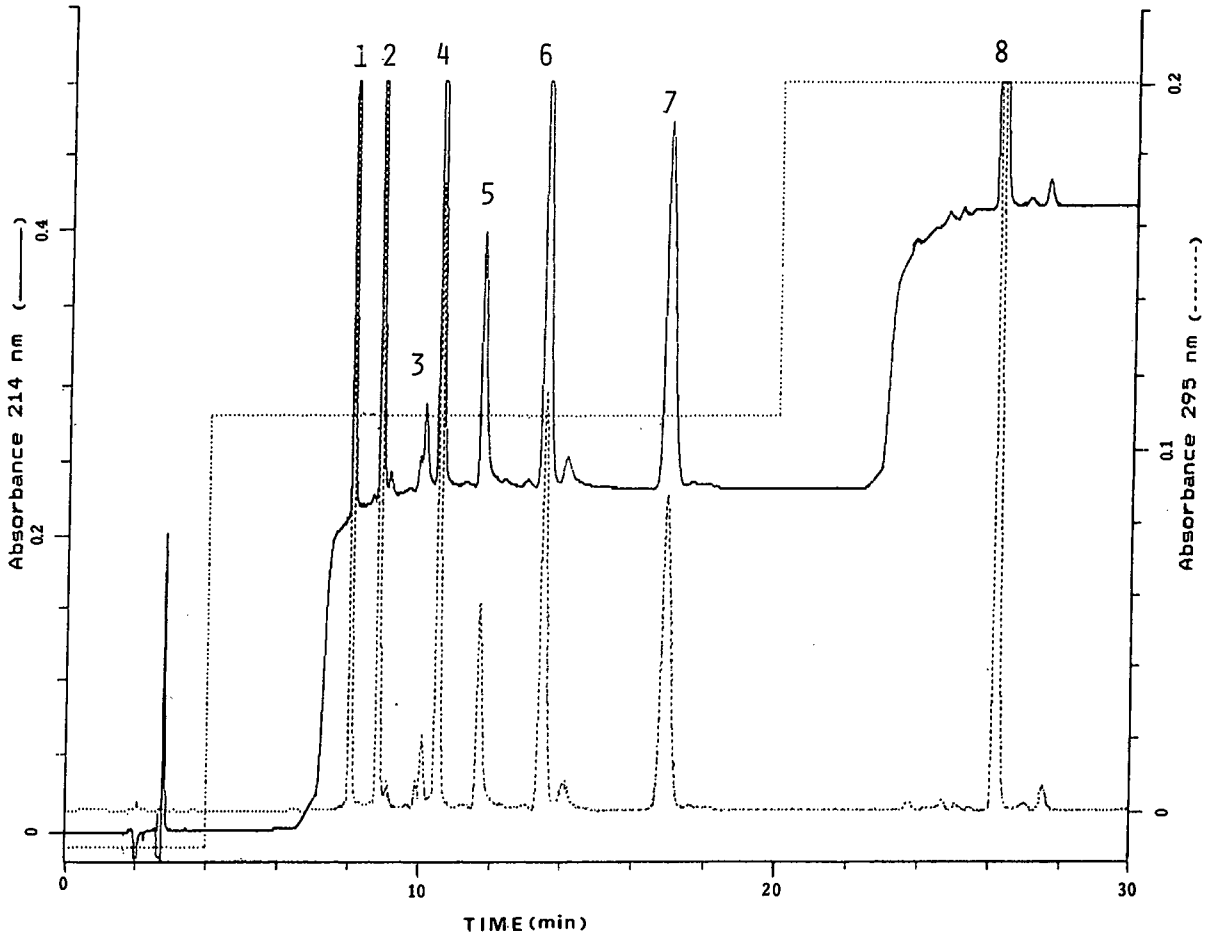

Fig. 1. Chromatogram resulting from the analysis of the standard mixture of the eight toxins. Concentrations were 100 μg/ml (except for phallisacin, 10 μg/ml). Peaks: 1 = β-Ama; 2 = α-Ama; 3 = PSC; 4 = γ-Ama; 5 = PCD; 6 = PHS; 7 = PHD; 8 = PHN.

TABLE II

RECOVERY OF α-AMANITIN AND PHALLOIDIN IN THE EXTRACTION MEDIUM

Compound	Toxin added (μg/ml)	Toxin measured (μg/ml)[a]	R.S.D. (%)
α-Amanitin	1	0.95 ± 0.05	5.0
	50	50.90 ± 0.91	1.8
	100	98.00 ± 1.96	2.0
Phalloidin	1	1.05 ± 0.05	5.0
	50	51.20 ± 1.22	2.4
	100	103.00 ± 3.10	3.0

[a] Mean ± S.D. (n = 3).

at wavelengths 285 and 305 nm, respectively (Fig. 3).

The content of toxic peptides in a single sample of *A. phalloides* was 0.07% of the fresh tissue and is reported in Table III. The amatoxin content was found to be 291 μg/g of fresh tissue and is in good agreement with the amount of amatoxins assayed by RIA (200–400 μg/g of fresh tissue [30]; acidic amatoxins represented 16% and neutral amatoxins represented 25.4%. The phallotoxin content was found to be 412.2 μg/g of fresh tissue, which corresponds to 5.15 mg/g dry weight. This value is very close to those obtained by spectrophotometry, *i.e.*, 3.95–5.1 mg/g dry weight [6]. Acidic phallotoxins

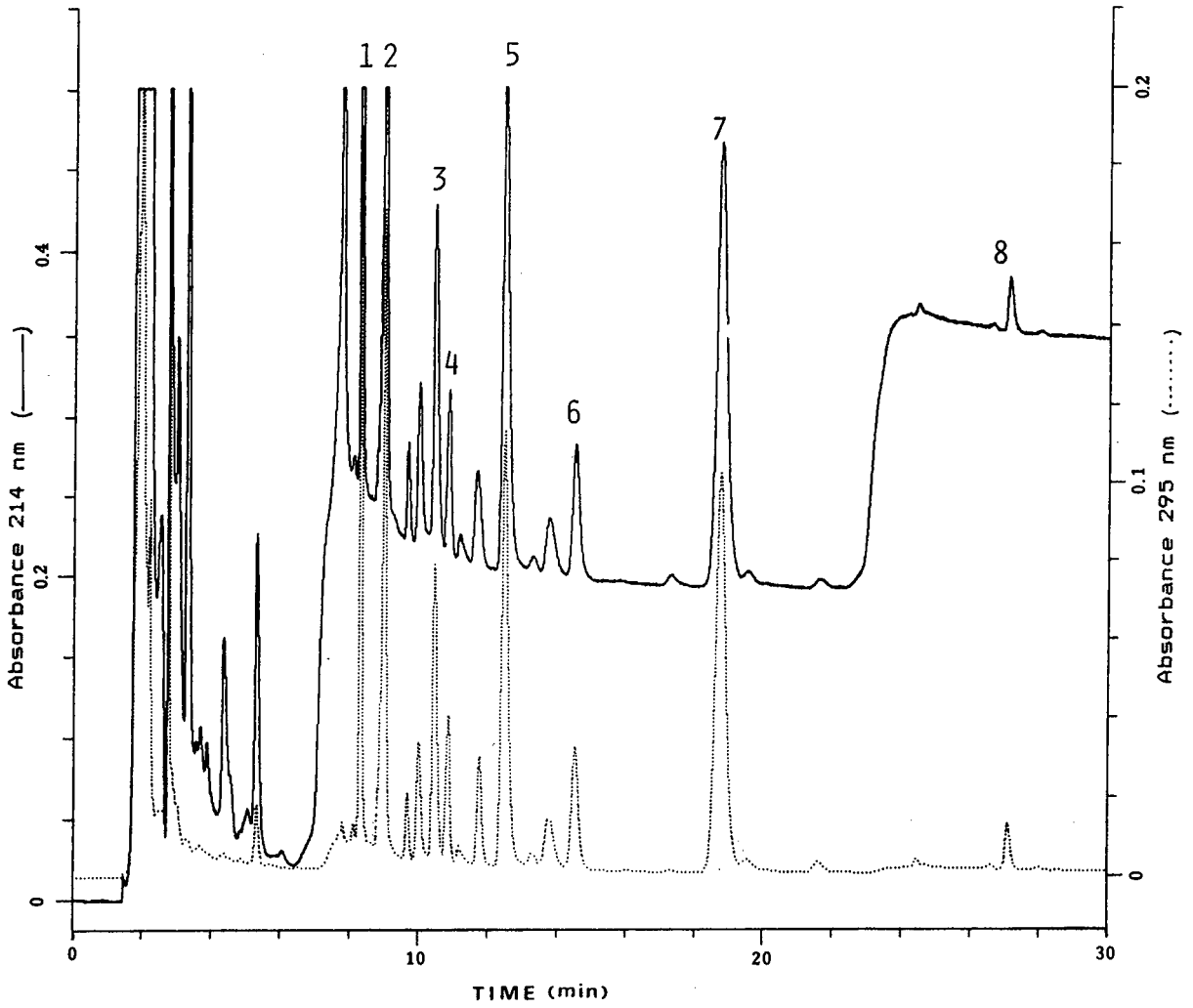

Fig. 2. Chromatogram of an *Amanita phalloides* extract. Peaks as in Fig. 1.

represented 41.3% of the toxin content and neutral phallotoxins 17.3%.

This method was successfully applied to the assay of amatoxins in *Galerina marginata*. This species does not belong to the genus *Amanita*, but it contains amatoxins. Good resolution of the three amatoxins (β-, α- and γ-Ama) was observed (Fig. 4). The amatoxin in this mushroom was 54.3 μg/g of fresh tissue; α-Ama represented 46%, β-Ama 45.3% and γ-Ama 8.7%. Phallotoxins were not detected in this species; these results confirm those reported in the literature [31].

Lastly, this procedure was applied to an *A. pantherina* extract. The chromatogram displayed in Fig. 5 shows the analysis of this specimen. The retention time of the major peak (8.5 min) was very close to that of β-Ama, but its scan analysis revealed that it was different from this toxin. The comparison of its 214/295 nm absorbance ratio with that of β-Ama confirms this result. In an attempt to detect amatoxins and phallotoxins, we prepared a concentrated extract. Even under these conditions, neither of the toxic cyclopeptides could be found.

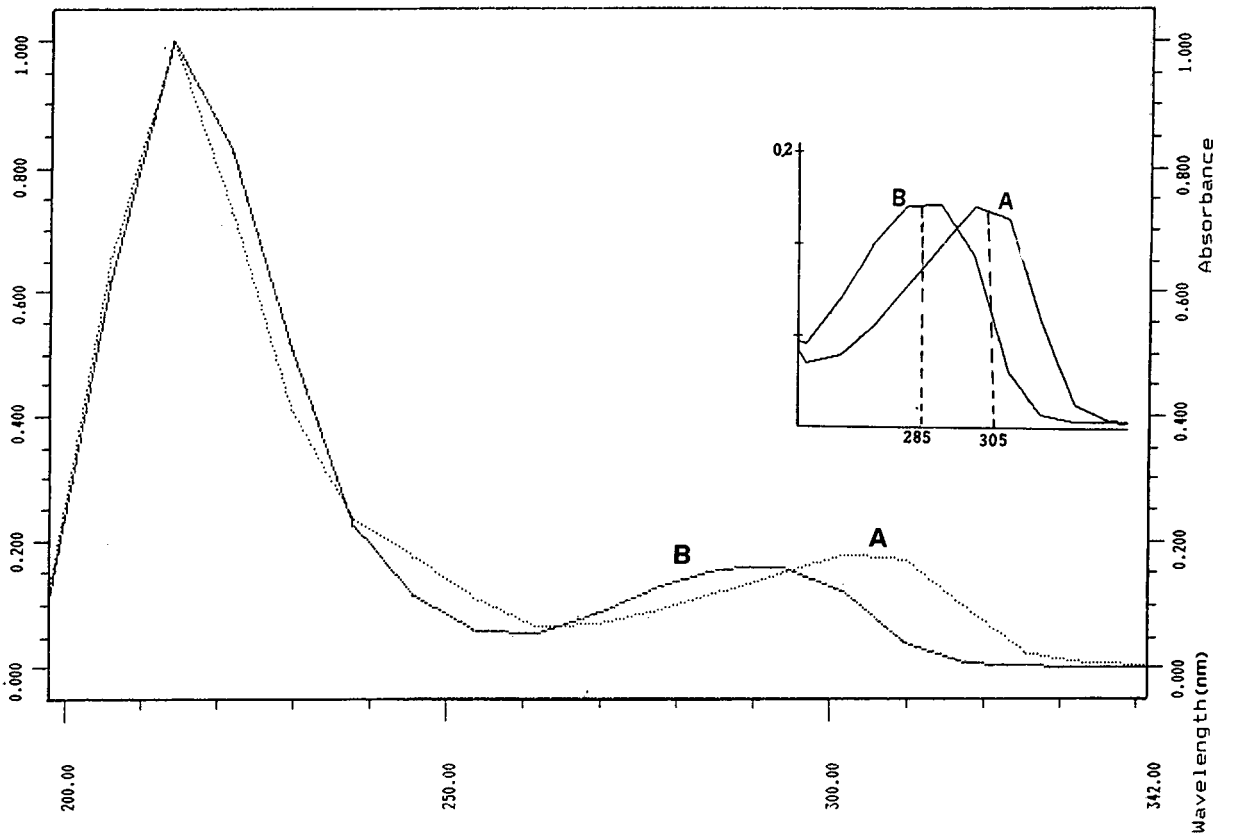

Fig. 3. Absorbance spectra (200–342 nm) of (A) amatoxins and (B) phallotoxins, measured on-line with the diode-array detector. Expanded: comparison between spectra of amatoxins and phallotoxins at 285 and 305 nm.

TABLE III

TOXIN CONCENTRATIONS (μg/g OF FRESH TISSUE) IN A SINGLE SPECIMEN OF *AMANITA PHALLOIDES*, TOTAL CONTENT (mg) OF THE WHOLE MUSHROOM (FRESH WEIGHT 18.4 g) AND DISTRIBUTION OF TOXINS

Toxin	Concentration (μg/g)	Total amount (mg)	Distribution (%)
β-Ama	112.5	2.07	16
Total acidic amatoxin	112.5	2.07	16
α-Ama	123	2.26	17.5
γ-Ama	55.6	1.02	7.9
Total neutral amatoxins	178.6	3.28	25.4
Total amatoxins	291.1	5.36	41.4
PSC	104.8	1.93	14.9
PCD	185.7	3.41	26.4
Total acidic phallotoxins	290.5	5.34	41.3
PHS	11.3	0.20	1.6
PHD	105.5	1.94	15
PHN	4.9	0.09	0.7
Total neutral phallotoxins	121.7	2.23	17.3
Total phallotoxins	412.2	7.59	58.6
Total toxins	703.3	12.94	

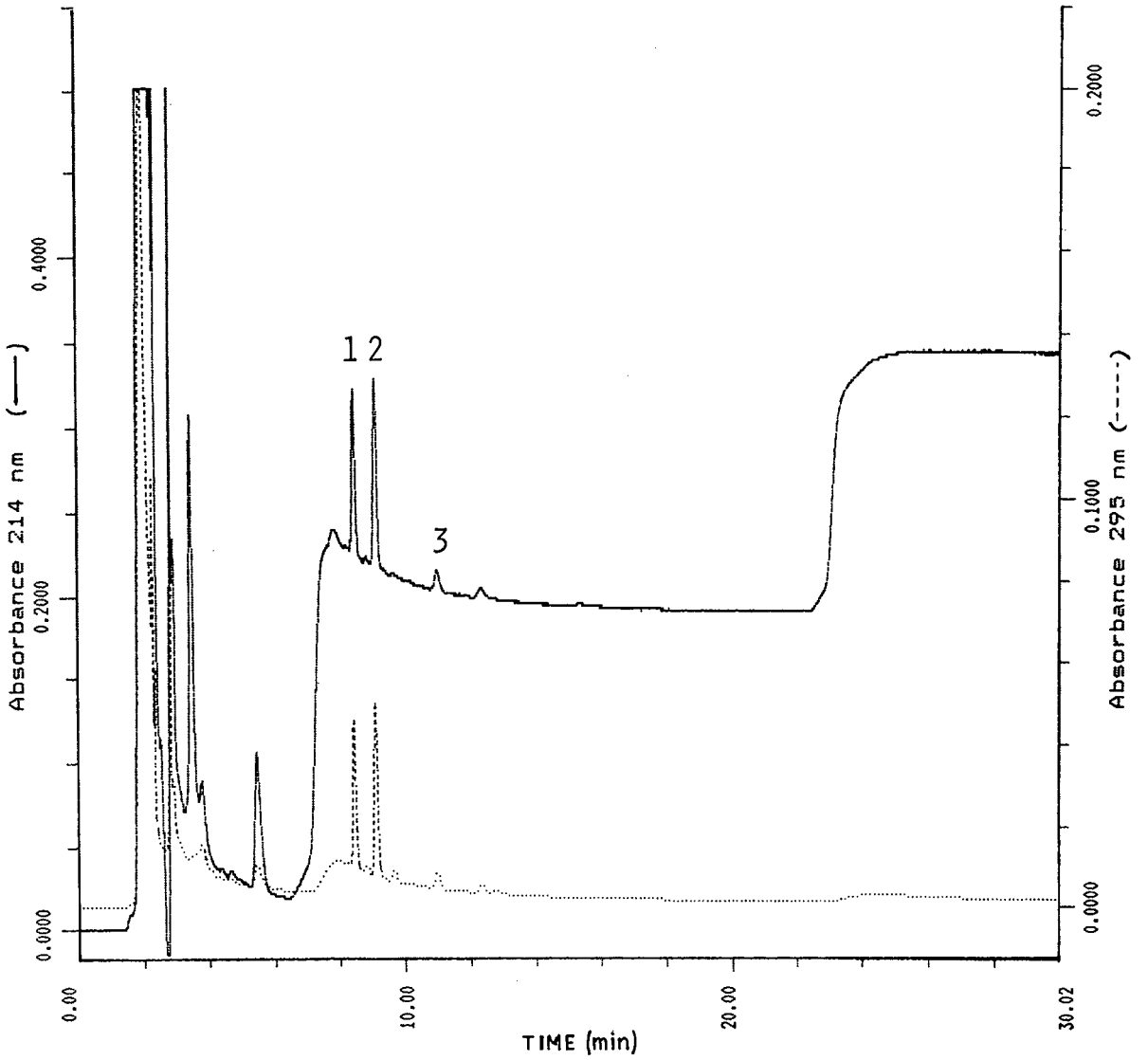

Fig. 4. Chromatogram of a *Galerina marginata* extract. Peaks: 1 = β-Ama; 2 = α-Ama; 3 = γ-Ama.

DISCUSSION

Sample preparation procedure

Significant variations in the amounts of toxins present in *A. phalloides* have been reported [8,32]. For this reason, we analysed an individual carpophore instead of pooled material. The advantage of carrying out these assays on fresh material has been reported [8,11], as drying causes degradation of toxins and chiefly phallotoxins. The extraction medium methanol–water–0.01 *M* hydrochloric acid (5:4:1, v/v/v) was preferred to methanol–water (1:1, v/v), as a slightly acidic pH appears to enhance the stability of molecules [6] and to increase the recovery of toxins. Most of the extraction procedures reported in the literature were carried out using a Soxhlet apparatus [8,13,15], by stirring with a magnetic stirrer [4,6,7,10] or by ultrasonication [11]. The tissues

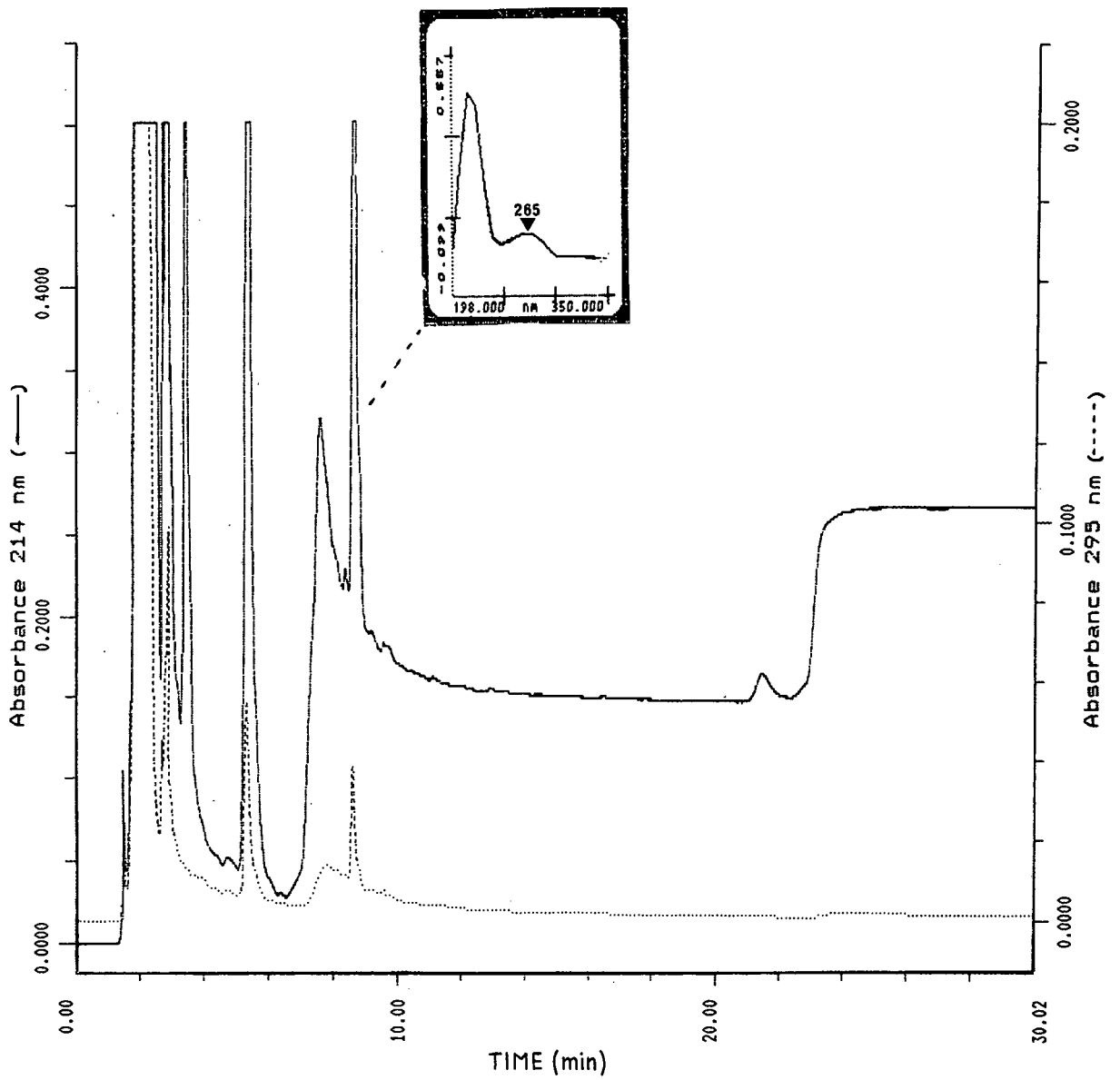

Fig. 5. Chromatogram of an *Amanita pantherina* extract. Expanded: spectrum of the peak (retention time = 8.5 min) located at 265 nm.

were crushed with a freezer-mill to avoid heating of the samples [11]. A rapid and almost complete extraction was achieved by this procedure, as additional operations with the same extraction medium did not lead to the recovery of detectable amounts of residual toxins. Moreover, when small volumes of extraction medium are used no concentration step is needed.

HPLC method

The HPLC technique described here proved to be highly efficient for assaying toxins in mushroom extracts. To our knowledge, this is the first description of an assay for the simultaneous determination of eight toxins. Comparison of this method with existing methods reveals two advantages: first, peak identification is carried out by means of the super-

imposition of its scan analysis with that of the standard, followed by comparison of its 214/295 nm absorbance ratio with the reference value previously established with the pure toxin (Table I). As shown in Fig. 3, the maximum wavelengths of the UV absorption spectra for phallotoxins (285 nm) and amatoxins (305 nm) are sufficiently different to allow their spectral discrimination. The second advantage is the limit of detection, down to the nanogram range. In fact, TLC and HPTLC methods with staining of toxins by cinnamaldehyde/HCl, diazotized sulfanilic acid or p-dimethylaminobenzaldehyde/H_2SO_4 are of limited sensitivity [7,8,11]. Bioassays, such as protein-binding assay, RIA or enzyme inhibition assay are able to measure small amounts of toxins in the nanogram range [12–14,18,19]. But they cannot be used to determine the amounts of the individual toxins in each family because of varying degrees of crossreactivity of the binding protein [12] and the antibodies [18]. Moreover, a crude mushroom extract may contain compounds that interfere with bioassays [31].

The HPLC method was able to resolve simultaneously the main amatoxins and phallotoxins with acceptable sensitivity. In fact, an acidic and two neutral amatoxins (β-, α- and γ-amanitin) together with three neutral phallotoxins (PHS, PHD and PHN) and two acidic phallotoxins (PCD and PSC) could be assayed. Phallacin (PCN), another acidic phallotoxin, could not be analysed because the toxin standard was not available. However, in our *A. phalloides* sample, examination of the UV spectra of all peaks did not reveal any molecule having a maximum UV absorption around 285 nm that might be attributed to PCN; either the PCN content was very low or this toxin was not present in the mushroom.

In papers on the determination of cyclopeptides of *Amanita* species from the northeastern USA, by means of UV absorption or direct spectrophotometry [6,10], only the amounts of three phallotoxins (PHN, PHD and PCD) were reported. A more detailed analysis has been described, using a combination of chromatographic separation with spectrophotometric determination. In a single *A. phalloides* mushroom, up to eleven toxic compounds can be identified, but this method is time consuming and unsuitable for application to large numbers of specimens [5]. On the other hand, the advantages of the present procedure are selectivity, sensitivity and rapidity.

The determination of the toxin content in *Galerina marginata* shows that the proposed method can be used to measure the amounts of amatoxins in species other than *A. phalloides*. Overall, the results indicate that this novel HPLC method can be used to determine amatoxins and phallotoxins in many mushroom species. Furthermore, it should be possible to scale it up to a preparative level. Finally, this approach has proved its effectiveness for diagnostic purposes in clinical toxicology [20–25].

ACKNOWLEDGEMENT

We thank Dr. S. L. Salhi for help in preparing the manuscript.

REFERENCES

1 T. Wieland and H. Faulstich, in R. F. Keller and A. T. Tu (Editors), *Handbook of Natural Toxins*, Vol. I, Marcel Dekker, New York, 1983, Ch. 18.
2 T. Wieland, *Int. J. Pept. Protein Res.*, 22 (1983) 257.
3 T. Wieland, *Naturwissenschaften*, 74 (1987) 367.
4 H. Faulstich, D. Georgopoulos and M. Blocking, *J. Chromatogr.*, 79 (1973) 257.
5 H. Faulstich, D. Georgopoulos, M. Blocking and T. Wieland, *Z. Naturforsch., C: Biosci.*, 29 (1974) 86.
6 R. R. Yocum and D. M. Simons, *Lloydia*, 40 (1977) 178.
7 C. Andary, F. Enjalbert, G. Privat and B. Mandrou, *J. Chromatogr.*, 132 (1977) 525.
8 T. Stijve and R. Seeger, *Z. Naturforsch., C: Biosci.*, 34 (1979) 1133.
9 R. Seeger and T. Stijve, *Z. Naturforsch., C: Biosci.*, 34 (1979) 330.
10 J. A. Beutler and A. H. Marderosian, *J. Nat. Products*, 44 (1981) 422.
11 F. Enjalbert, M. J. Bourrier and C. Andary, *J. Chromatogr.*, 462 (1989) 442.
12 J. A. Schäfer and H. Faulstich, *Anal. Biochem.*, 83 (1977) 720.
13 J. E. Mullersman and J. F. Preston, *Anal. Biochem.*, 119 (1982) 266.
14 M. Cochet-Meilhac and P. Chambon, *Biochim. Biophys. Acta*, 353 (1974) 160.
15 J. F. Preston, H. J. Starck and J. W. Kimbrough, *Lloydia*, 38 (1975) 153.
16 L. Fiume, C. Busi, G. Campadelli-Fiume and C. Franceschi, *Experientia*, 31 (1975) 1233.
17 H. Faulstich, H. Trischmann and S. Zobeley, *FEBS Lett.*, 56 (1975) 312.
18 H. Faulstich, S. Zobeley and H. Trischmann, *Toxicon*, 20 (1982) 913.
19 R. Y. Andres, W. Frei, K. Gautschi and D. J. Vonderschmitt, *Clin. Chem.*, 32 (1986) 1751.
20 L. Pastorello, D. Tolentino, M. D'Alterio, R. Paladino, A. Frigerio, N. Bergamo and A. Valli, *J. Chromatogr.*, 233 (1982) 398.

21 F. Belliardo and G. Massano, *J. Liq. Chromatogr.*, 6 (1983) 551.
22 F. Jehl, C. Gallion, P. Birckel, A. Jaeger, F. Flesch and R. Minck, *Anal. Biochem.*, 149 (1985) 35.
23 G. Caccialanza, C. Gandini and R. Ponci, *J. Pharm. Biomed. Anal.*, 3 (1985) 179.
24 W. Rieck and D. Platt, *J. Chromatogr.*, 425 (1988) 121.
25 F. Tagliaro, G. Schiavon, G. Bontempelli, G. Carli and M. Marigo, *J. Chromatogr.*, 563 (1991) 299.
26 T. Wieland and C. Dudensing, *Justus Liebigs Ann Chem.*, 600 (1956) 156.
27 T. Wieland and K. Mannes, *Angew. Chem.*, 69 (1957) 389.
28 T. Wieland, D. Rempel, U. Gebert, A. Buku and H. Boehringer, *Justus Liebigs Ann. Chem.*, 704 (1967) 226.
29 T. Wieland and H. W. Schnabel, *Justus Liebigs Ann Chem.*, 657 (1962) 218.
30 H. Bodenmuller, H. Faulstich and T. Wieland, in G. Witzstrock (Editor), *Amanita Toxins and Poisoning*, Lubrecht Cramer, New York, 1980, p. 18.
31 T. Wieland, in A. Rich (Editor), *Peptides of Poisonous Amanita Mushrooms*, Springer, New York, Berlin, 1986, p. 10.
32 F. Enjalbert, G. Cassanas and C. Andary, *Mycologia*, 81 (1989) 266.

Journal of Chromatography, 598 (1992) 237–241
Elsevier Science Publishers B.V., Amsterdam

CHROM. 24 048

Determination of inorganic anions in salt solutions by ion chromatography using C_{18} reversed-phase columns coated with cetyltrimethylammonium

Kazuaki Ito* and Yasunobu Ariyoshi

Department of Environmental Science, Faculty of Engineering, Hiroshima University, 1–4–1 Kagamiyama, Higashi-Hiroshima 724 (Japan)

Hiroshi Sunahara

Department of Industrial Chemistry, Faculty of Engineering, Kinki University, 1-Umenobe, Takaya, Higashi-Hiroshima 729–17 (Japan)

(First received October 2nd, 1991; revised manuscript received January 20th, 1992)

ABSTRACT

A simple and sensitive method using ion chromatography is described for the determination of I^-, SCN^-, NO_2^- and $S_2O_3^{2-}$ as impurities in inorganic analytical-reagent grade chemicals. Aqueous solutions of individual salts containing matrix anions (5–20 g/l) were prepared and analyzed directly for trace impurities. Good chromatograms of trace anions were obtained without interference by matrix ions. C_{18} reversed-phase columns coated with cetyltrimethylammonium (CTA^+), with either high or low capacity, a mobile phase mixture (pH 5.8) of sodium chloride (0.1 *M*) and sodium phosphate buffer (0.005 *M*), and ultraviolet (225 nm) and amperometric (+1.0 V *vs.* Ag/AgCl) detection systems were used. The detection limits for different impurities in the solutions were 0.002–0.06 mg/l.

INTRODUCTION

Recently, efforts have been made to develop an improved method for the separation and detection of trace anions in concentrated salt solutions by ion chromatography (IC). For the separation of anions, the use of C_{18} reversed-phase columns has become of increasing interest not only because of their good chromatographic efficiency but also the flexibility in choosing eluents and ion-pair reagents [1–6]. Especially columns coated permanently with ion-pair reagents such as cationic surfactants can be used as "fixed-site" anion-exchange columns. The anion-exchange capacity can be adjusted by controlling the conditions of column coating for practical applications. An increase in exchange capacity improved the mutual separation between anions without any changes to the elution order [5,6]. When using coated columns, however, the selection of the mobile phase and the detection method are the most important features and are being improved continuously.

In a previous paper [7], we reported the determination of μg/l levels of iodide in 100 μl of sea water using a conventional IC column, 0.1 *M* NaCl solution as eluent, and UV and amperometric (with a glassy carbon electrode) detection, without interference from excess of anions, especially chloride. NaCl is UV-transparent and electroinactive on a glassy carbon electrode and the separation of different anions was in accordance with the theoretical predictions for ion-exchange reactions [8]. However, the IC column could not be applied to μg/l levels of nitrite and nitrate in sea water (100 μl), because of incomplete separations owing to the low exchange capacity of the column. Separation was

0021-9673/92/$05.00

successfully achieved using a C_{18} reversed-phase column (silicone-coated silica packing) coated with cetyltrimethylammonium (CTA^+), which has a high exchange capacity (0.25 mequiv. per column) [5]. The silicone-coated C_{18} reversed-phase column is resistant to alkaline samples (*e.g.*, sea water, pH *ca.* 8) and retains the chromatographic efficiency of the silica-based packings [9]. The observed anion-exchange capacity of a coated column (150 mm × 4.6 mm I.D.) was in the range 0–0.4 m*M* depending on the amount of CTA^+ attached [5]. Thus, iodide in sea water was also determined using a CTA^+-coated column with low capacity [6].

In this study, the determination of anionic impurities in the presence of various matrix anions was examined by direct ultraviolet (UV) and amperometric detection; the anionic impurities examined included iodide, thiocyanate, nitrite and thiosulfate in analytical reagent-grade inorganic salts such as $NaIO_3$, KCN, Na_2SO_4, NaBr and $NaNO_3$. CTA^+-coated C_{18} (AG 120) reversed-phase columns with high and low capacities were employed for the separation of various analyte anions. As the matrix anions, IO_3^-, NO_3^- and Br^-, have UV absorption, complete separation of the analyte anions is essential. With the exception of Br^-, a glassy carbon electrode is electroinactive for matrix ions whereas a silver electrode is electroactive for Cl^- present in the mobile phase and Br^- and CN^- in the matrix [10].

EXPERIMENTAL

Apparatus

The IC system consisted of a Tosoh Model CCPM pump, a Rheodyne Model 7125 injector with a 100-μl sample loop, a Hitachi Model L-4200 UV detector, Yanagimoto Models VMD-101A and P-1000 amperometric detectors with a glassy carbon working electrode and a Tosoh Model CP-8000 chromato-processor.

Column

A Shiseido Capcellpak C_{18} (AG 120) reversed-phase column (150 × 4.6 mm I.D., particle size 5 μm, octadecyl-bonded silica gel already precoated with silicone polymer) was used. The column was equilibrated with 1 m*M* cetyltrimethylammonium chloride (CTAC) in water–methanol mixtures (80:20 and 56:44, v/v) at 20°C. The CTA^+-coated columns were employed for the separation of analyte anions. CTAC and high-performance liquid chromatographic grade methanol, both obtained from Katayama Chemical, were used as received.

Sample and mobile phase preparation

Inorganic salts of analytical-reagent grade were obtained from Katayama Chemical and were used without treatment. Ion-free distilled water was used throughout for preparing solutions. The concentration of matrix anions in the stock solutions prepared was IO_3^- 20 g/l ($NaIO_3$), CN^- 10 g/l (KCN), SO_4^{2-} 40 g/l (Na_2SO_4), Br^- 20 g/l (NaBr) and NO_3^- 20 g/l ($NaNO_3$). Dilute sample solutions both with and without the added analyte (0.01–0.5 mg/l) were analyzed directly. Mobile phase (pH 5.8) consisting of 0.1 *M* NaCl and 0.005 *M* sodium phosphate buffer (0.5 m*M* Na_2HPO_4 and 4.5 m*M* NaH_2PO_4) was prepared from stock solutions.

RESULTS AND DISCUSSION

Use of CTA^+-coated column with low capacity

Anionic impurities in analytical reagent-grade chemicals such as $NaHCO_3$, NaOH and Na_2CO_3 have been determined by IC with conductivity detection [11,12]. After removing Na^+ by the "dual ion-exchange method", anionic impurities in the resulting solutions (H_2CO_3, H_2O) with lower conductivity were determined. However, it is difficult to remove the matrix anions effectively, together with Na^+ or K^+, for the present samples by chemical pretreatment. Recycle IC (also known as the reinjection method) is capable of separating a small impurity peak from a large sample peak. Anionic impurities in inorganic acids have been determined by recycle IC with conductivity detection after their dilution with ion-free distilled water followed by neutralization with NaOH [13]. Similarly, the determination of sub-mg/l levels of nitrite in sea water has been achieved using recycle IC with conductivity detection [14]. This system, however, requires valve switching during analysis, which causes a decrease in the detectability owing to peak broadening by reinjection and long retention times of the analyte anions. In this study, a direct and sensitive method for the detection of anionic impurities in various salt solutions was examined using UV and amperometric detection methods.

Analytical reagent-grade sodium iodate and potassium cyanide usually contain iodide and thiocyanate, respectively, as impurities. Figs. 1 and 2 show the separation of I^- and SCN^- in their respective reagents (IO_3^-, 10 g/l; SCN^-, 5 g/l) on a CTA^+-coated C_{18} reversed-phase column with low capacity (0.06 mequiv. per column). The coating solution employed was 1 m*M* CTA^+ solution in water–methanol (56:44, v/v) [6]. The retention times for I^- and SCN^- were identical with those obtained for solutions spiked with 0.2 mg/l of I^- and SCN^-, respectively (dashed line). The use of 0.1 *M* NaCl as mobile phase eliminated the interference of faster eluting species. Further, 0.1 *M* NaCl stabilized the sorbed CTA^+ and improved the long-term use of the coated column [5,15]. The chromatograms were obtained by UV (225 nm) and amperometric (+1.0 V *vs.* Ag/AgCl) detection as reported [6]. The iodate peak with UV absorptivity did not interfere with I^- and separate peaks were observed. Similarly, with amperometric detection only the I^- peak was observed (Fig. 1B) and IO_3^-, which is amperometry inactive, was eliminated.

Good chromatograms were obtained for SCN^- in KCN solution even though the sensitivity of

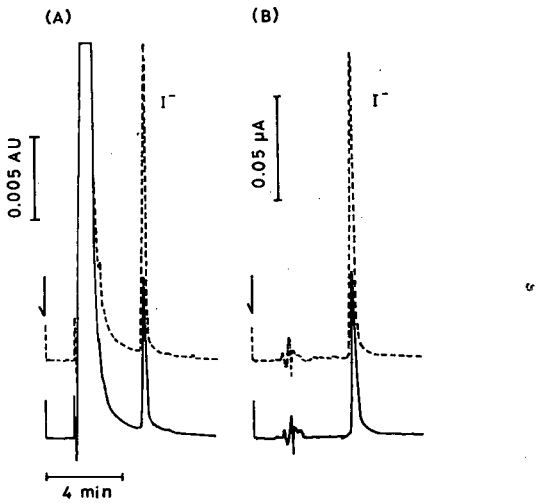

Fig. 1. Ion chromatograms of sodium iodate solution (10 g/l IO_3^-, solid line) and the solution spiked with 0.2 mg/l of I^- (dashed line). Column, Capcellpak C_{18} coated with 1 m*M* CTA^+ in water–methanol (56:44, v/v); mobile phase, 0.1 *M* NaCl–0.005 *M* sodium phosphate buffer (pH 5.8); detection (A) UV, 225 nm; (B) amperometry, +1.0 V (*vs.* Ag/AgCl); flow-rate, 1.0 ml/min; sample volume, 100 μl.

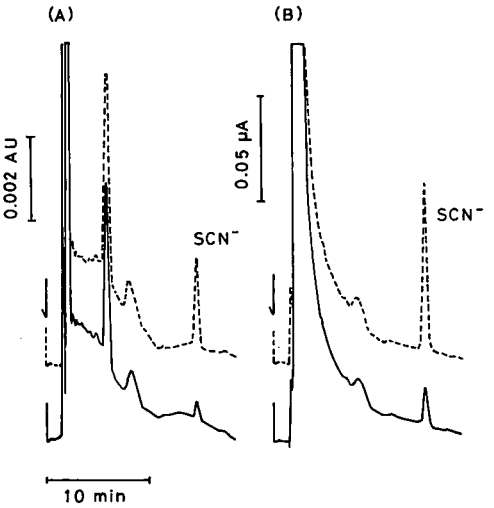

Fig. 2. Ion chromatograms of potassium cyanide solution (5 g/l CN^-, solid line) and the solution spiked with 0.2 mg/l of SCN^- (dashed line). Conditions as in Fig. 1.

SCN^- for amperometric detection was increased with multiple injection of the sample. This may be due to the activation of the glassy carbon electrode surface by CN^-. Determination of the analytes was effected using calibration graphs (0–1 mg/l) and the standard addition (0.1–0.5 mg/l) method using peak areas. Peak areas of the analyte ions remained constant on addition of salts whereas the peak heights decreased rapidly [5,6].

The results are summarized in Table I. With good agreement between the two detection methods, detection limits of 0.005 mg/l for I^- and 0.015 mg/l for SCN^- (signal-to-noise ratio 2) were observed.

Use of CTA^+-coated column with high capacity

The presence of nitrite and thiosulfate as impurities in inorganic salts such as sodium sulfate, sodium nitrate and sodium bromide was examined. A column coated with 1 m*M* CTA^+ in water–methanol (80:20, v/v) (anion-exchange capacity 0.25 mequiv. per column) was used as reported [5] for the separation of NO_2^- and $S_2O_3^{2-}$. Fig. 3 shows chromatograms of Na_2SO_4 solutions (SO_4^{2-} 20 g/l) unspiked (solid line) and spiked (dashed line) with 0.05 mg/l of NO_2^- and 0.1 mg/l of $S_2O_3^{2-}$. Compared with $S_2O_3^{2-}$, NO_2^- was relatively more sensitive for both UV and amperometric detection. The detection conditions were as reported [5]. The presence of

TABLE I

RESULTS FOR IMPURITIES IN INORGANIC SALT SOLUTIONS

Mean results ± standard deviations for five determinations. The results were obtained using a calibration graph and (in parentheses) by the standard addition method.

Reagent	I^- (mg/l)		SCN^- (mg/l)	
	UV	Amperometry	UV	Amperometry
$NaIO_3$, (10 g/l IO_3^-)	0.18 ± 0.01[a] (0.18 ± 0.01)	0.18 ± 0.01 (0.22 ± 0.01)	–	–
KCN (5 g/l CN^-)	–	–	0.043 ± 0.010 (0.054 ± 0.010)	0.043 ± 0.002 (0.046 ± 0.002)

[a] The certificate value of I^- in the solution was < 0.23 mg/l.

large amounts of SO_4^{2-} did not interfere with NO_2^-.

Figs. 4 and 5 show chromatograms of unspiked NaBr and $NaNO_3$ (Br^- 5 g/l, NO_3^- 5 g/l; solid line) and spiked (dashed line) solutions containing 0.05 mg/l of NO_2^- and 0.1 mg/l of $S_2O_3^{2-}$, respectively. Altough Br^- showed a response in UV and amperometric detection, it did not interfere in the detection of the analyte anions. The sensitivity of NO_2^- in $NaNO_3$ solution was high and remained unaffected by the presence of matrix NO_3^-. The peak height of NO_2^- added to Na_2SO_4 solution was lower than those in NaBr and $NaNO_3$, presumably owing to the difference in concentration of the matrix ions. Detection limits in NaBr solution (Br^- 5 g/l), for example, were 0.004 mg/l (UV) and 0.002 mg/l (amperometric detection) for NO_2^- and 0.06 mg/l (UV) and 0.01 mg/l (amperometric detection) for $S_2O_3^{2-}$. Only NO_2^- (0.004 mg/l, UV and amperometric detection) in $NaNO_3$ solution (NO_3^- 5 g/l) was determined.

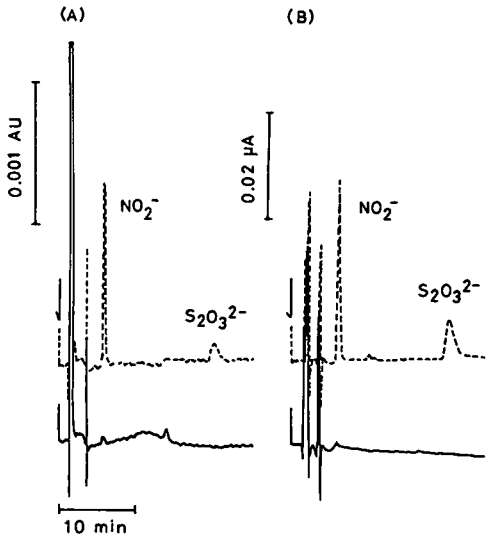

Fig. 3. Ion chromatograms of sodium sulfate solution (20 g/l SO_4^{2-}, solid line) and the solution spiked with 0.05 mg/l NO_2^- and 0.1 mg/l $S_2O_3^{2-}$ (dashed line). Column, Capcellpak C_{18} coated with 1 m*M* CTA^+ in water–methanol (80:20, v/v). Other conditions as in Fig. 1.

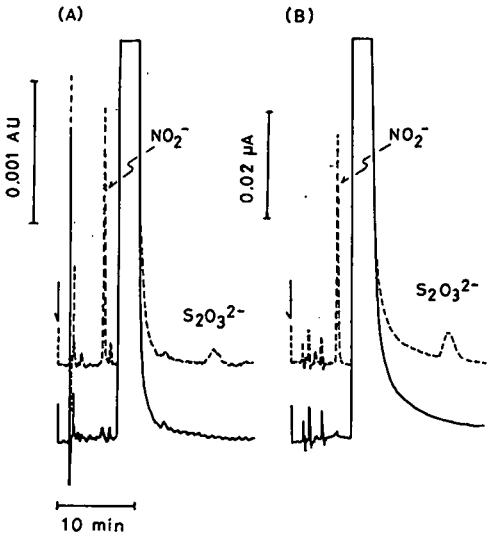

Fig. 4. Ion chromatograms of sodium bromide solution (5 g/l Br^-, solid line) and the solution spiked with 0.05 mg/l NO_2^- and 0.1 mg/l $S_2O_3^{2-}$ (dashed line). Conditions as in Fig. 3.

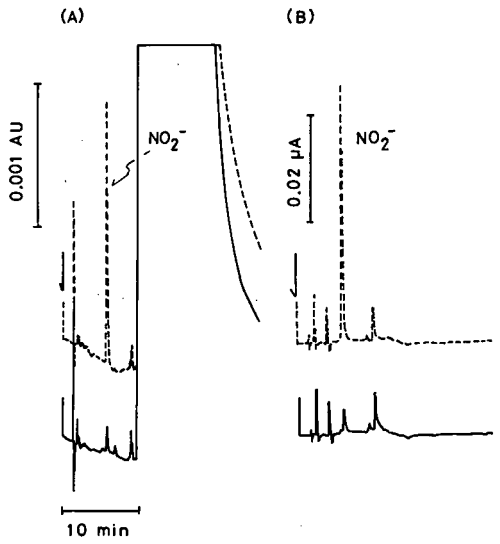

Fig. 5. Ion chromatograms of sodium nitrate solution (5 g/l NO_3^-, solid line) and the solution spiked with 0.05 mg/l NO_2^- (dashed line). Conditions as in Fig. 3.

ACKNOWLEDGEMENTS

This work was partially supported by a Grant-in-Aid for Scientific Research, No 63740316 (K. I.), from the Ministry of Education, Science and Culture of Japan. The authors thank Imdadullah of the Department of Chemistry, Hiroshima University, for his help in preparing the manuscript.

REFERENCES

1 P. K. Dasgupta, in J. G. Tarter (Editor), *Ion Chromatography*, Marcel Dekker, New York, 1987, p. 253; and references cited therein.
2 D. J. Barkley, T. E. Dahms and K. N. Villeneuve, *J. Chromatogr.*, 395 (1988) 631.
3 G. Müller and H.-U. Meisch, *J. Chromatogr.*, 483 (1989) 145.
4 B. A. Bidlingmeyer, C. T. Santasania and F. V. Warren, Jr., *Anal. Chem.*, 59 (1987) 1843.
5 K. Ito, Y. Ariyoshi, F. Tanabiki and H. Sunahara, *Anal. Chem.*, 63 (1991) 273.
6 K. Ito, E. Shoto and H. Sunahara, *J. Chromatogr.*, 549 (1991) 265.
7 K. Ito and H. Sunahara, *J. Chromatogr.*, 502 (1990) 121.
8 Marheni, P. R. Haddad and A. R. McTaggart, *J. Chromatogr.*, 546 (1991) 221.
9 Y. Ohtsu, H. Fukui, T. Kanda, K. Nakamura, M. Nakano, O. Nakata and Y. Fujiyama, *Chromatographia*, 24 (1987) 380.
10 R. D. Rocklin and E. L. Johnson, *Anal. Chem.*, 55 (1983) 4.
11 J. A. Cox and N. Tanaka, *Anal. Chem.*, 57 (1985) 383.
12 J. A. Cox and N. Tanaka, *Anal. Chem.*, 57 (1985) 385.
13 M. Murayama, M. Suzuki and S. Takitani, *J. Chromatogr.*, 466 (1989) 355.
14 P. F. Subosa, K. Kihara, S. Rokushika, H. Hatano, T. Murayama, T. Kubota and Y. Hanaoka, *J. Chromatogr. Sci.*, 27 (1989) 680.
15 A. Berthod, I. Girard and C. Gonnet, *Anal. Chem.*, 58 (1986) 1362.

Journal of Chromatography, 598 (1992) 243–250
Elsevier Science Publishers B.V., Amsterdam

CHROM. 24 053

Relationship between gas chromatographic retention indices and molecular connectivity indices of chlorinated pesticides and structurally related compounds

Vilma E. F. Heinzen and Rosendo A. Yunes*

Department of Chemistry, Universidade Federal de Santa Catarina, Florianópolis, Santa Catarina (Brazil)

(First received September 3rd, 1991; revised manuscript received January 24th, 1992)

ABSTRACT

The ability of the molecular connectivity model to predict retention indices using both statistical correlation coefficients and correctly predicted elution sequences as criteria of fitness was tested. The tests were performed with chlorinated pesticides and some structurally related compounds. The effect on the retention index of increasing replacement by chlorine of hydrogen atoms bonded to one carbon of the aliphatic part of the molecule was excellently correlated by $^1\chi^v$, the first-order valence molecular connectivity index, using a quadratic polynomial equation. This equation also fits $^1\chi^v$ with the retention indices of halobenzenes and halobiphenyl compounds. On the other hand, $^1\chi^v$ was the most significant connectivity index, using a single linear regression equation to correlate the retention indices of all the compounds. However, $^1\chi^v$ alone was not sufficient to distinguish significantly some isomers and the correct elution sequence giving a relatively low correlation coefficient. Therefore, other connectivity indices and the consequent use of multiple linear regression equations were necessary in order to represent more completely the molecules and to obtain more accurate results.

INTRODUCTION

Studies of topological indices, such as molecular connectivity indices, were first introduced by Randic [1] and were further developed and extensively used by Kier [2]. This method gives a quantitative description of the molecular structure by attributing numerical values to the atoms. The importance of this method was demonstrated by the excellent correlations obtained between the theoretical indices and the experimental values of physico-chemical properties [3–5], biological activity [6–9] and chromatographic retention indices [10–14].

Correlations of chromatographic retention with the physico-chemical and structural characteristics of substances are the basis for the choice of appropriate chromatographic systems and are of great significance for solving problems involving the identification of components of complex mixtures, *e.g.*, giving supplementary information to gas chromatographic–mass spectrometric results for the identification of individual components.

The correlation between the retention indices and the structural parameters is based on the assumption of additivity of the free energies of interaction of the sorbates with the stationary phase, which may be calculated by adding up the structural parts of the molecule.

This work was carried out in order to test the ability of connectivity indices to predict the retention indices, on polar and non-polar stationary phases, of DDT and related compounds. These compounds were selected because they and other chlorinated benzenes and hydrocarbons constitute an important group of environmentally hazardous compounds, because they provide a challenge to the molecular connectivity model owing to the effect of chlorine substitution (shown by Haken and Korhonen [15] to be non-linear) and because of the complexity of their molecular structures.

0021-9673/92/$05.00

Sabljic [16] showed that frequently the criterion used to test the fitness between the observed and calculated retention indices in investigations is the statistical correlation coefficient. This criterion is insufficient to test the usefulness of the topological approach for predicting retention indices, as a high correlation coefficient does not necessarily imply a correct elution sequence. Hence a high correlation coefficient and a correctly predicted elution sequence are prerequisites for the prediction of retention indices.

These aspects were examined in order to find the best linear regression equation and molecular connectivity parameters to permit the prediction of the gas chromatographic retention indices of the compounds studied.

EXPERIMENTAL

Method of calculation

The molecular connectivity indices used were $^{1}\chi$, $^{1}\chi^{v}$, $^{3}\chi_{p}$, $^{3}\chi_{c}$, $^{3}\chi_{c}^{v}$, $^{4}\chi_{pc}$ and $^{4}\chi_{pc}^{v}$, which were calculated according to Kier [1].

The compounds used were 1,1-diphenylethane (DDO_H), 1,1-bis(4-chlorophenyl)ethane (DDO), 1,1-bis(4-chlorophenyl)-2-chloroethane (DDM), 1,1-diphenyl-2,2-dichloroethane (DDD_H), 1,1-bis(4-methylphenyl)-2,2-dichloroethane (DDD_{CH_3}), 1,1-bis(4-ethylphenyl)-2,2-dichloroethane ($DDD_{C_2H_5}$), 1-(2-chlorophenyl)-1-(4-chlorophenyl)-2,2-dichloroethane ($DDD_{o,p'\text{-Cl}}$), 1,1-bis(4-chlorophenyl)-2,2-dichloroethane (DDD), 1,1-bis(4-methoxyphenyl)-2,2-dichloroethane (DDD_{OCH_3}), 1,1-bis(4-bromophenyl)-2,2-dichloroethane (DDD_{Br}), 2,2-diphenyl-1,1,1-trichloroethane (DDT_H), 2,2-bis(4-methylphenyl)-1,1,1-trichloroethane (DDT_{CH_3}), 2-(2-chlorophenyl)-2-(4-chlorophenyl)-1,1,1-trichloroethane ($DDT_{o,p'\text{-Cl}}$), 2,2-bis(4-chlorophenyl)-1,1,1-trichloroethane (DDT), 2,2-bis(4-hydroxyphenyl)-1,1,1-trichloroethane (DDT_{OH}), 1,2-bis(4-chlorophenyl)-1-chloroethane (DDMF), 2,2-bis(4-chlorophenyl) ethanoic acid (DDA), 1,1-bis(4-chlorophenyl)-2-hydroxyethane (DDOH), 1,1-diphenyl-2-chloroethylene ($DDMU_H$), 1,1-bis(4-chlorophenyl)-2-chloroethylene(DDMU), 1,1-diphenylethylene ($DDNU_H$), 1,1-bis(4-chlorophenyl)ethylene (DDNU), 1,1-diphenyl-2,2-dichloroethylene (DDE_H), 1,1-bis(4-methylphenyl)-2,2-dichloroethylene(DDE_{CH_3}), 1-(2-chlorophenyl)-1-(4-chlorophenyl)-2,2-dichloroethylene ($DDE_{o,p'\text{-Cl}}$), 1,1-bis(4-chlorophenyl)-2,2-dichloroethylene (DDE), 1,1-bis(4-methoxyphenyl)-2,2-dichloroethylene (DDE_{OCH_3}), 1,2-diphenylethylene (DCS_H), 1,2-bis(4-methylphenyl)ethylene (DCS_{CH_3}) and 1,2-bis(4-chlorophenyl)ethylene (DCS).

The retention indices (I) of the above compound were reported by Zanette [17] and were obtained using a nickel column (5.5 m × 3.2 mm I.D.) and a glass column (1.8 m × 3.2 mm I.D.) packed with 3% OV-17 on Chromosorb W AW DMCS (80–100 mesh) as a polar stationary phase and a glass column (1.8 m × 3.2 mm I.D.) with 15% Apiezon L (ApL) on Chromosorb W as a non-polar stationary phase, with a column temperature of 215°C.

All calculations in single and multiple linear regression analyses were carried out on an IBM PC/XT computer.

RESULTS AND DISCUSSION

Study of the additivity of the effect of the increase in chlorine substitution

The effect of multiple chlorine replacement of hydrogen atoms was first studied considering the compounds containing one, two or three chlorine atoms bonded to one carbon of the aliphatic part of the molecule. The $^{1}\chi$ and $^{1}\chi^{v}$ connectivity indices give a good linear correlation (eqn. 1) and a correct elution sequence. The correlation coefficients are indicated in Table I.

$$I_i = A + B\chi_i \quad (1)$$

In spite of this good correlation, the increase in the retention indices with increase in the number of chlorine atoms showed that the values were not additive. For this reason, the experimental values of I were tested using other equations, and the best results, with both polar and non-polar phases, were obtained with the quadratic polynomial equation

$$I_i = A + B\chi_i + C(\chi_i)^2 \quad (2)$$

It is interesting that for groups of compounds with increasing chlorine substitution on the aliphatic carbon, but with some structural differences, such as DDO, DDM, DDD and DDT with respect to DDO_H, DDM_H, DDD_H and DDT_H, when the retention indices corresponding to each group are correlated with $^{1}\chi^{v}$ by the quadratic polynomial eqn.

TABLE I

EFFECT OF CHLORINE SUBSTITUTION ON THE RETENTION INDICES OF PESTICIDES AND THEIR CORRELATION WITH CONNECTIVITY INDICES

Compounds	Linear equation	Quadratic polynomial equation	Stationary phase
DDO, DDM, DDD, DDT	$I = 286.0699\,^1\chi - 213.6038$ $n = 4, r = 0.9654, r^2 = 0.9320$	$I = 3776.687\,^1\chi - 211.4237\,(^1\chi)^2 - 14576.87$ $n = 4, r = 0.9987, r^2 = 0.9974$	ApL
	$I = 373.1168\,^1\chi - 644.9431$ $n = 4, r = 0.9810, r^2 = 0.9623$	$I = 3767.867\,^1\chi - 205.6175\,(^1\chi)^2 - 14613.7$ $n = 4, r = 0.9999, r^2 = 0.9998$	OV-17
	$I = 231.0055\,^1\chi^v + 591.7717$ $n = 4, r = 0.9672, r^2 = 0.9355$	$I = 2032.495\,^1\chi^v - 133.8105\,(^1\chi^v)^2 - 5428.305$ $n = 4, r = 0.9999, r^2 = 0.9998$	ApL
	$I = 310.1502\,^1\chi^v + 406.4995$ $n = 4, r = 0.9823, r^2 = 0.9649$	$I = 2042.253\,^1\chi^v - 129.3253\,(^1\chi^v)^2 - 5411.773$ $n = 4, r = 0.9999, r^2 = 0.9998$	OV-17
DDO_H, DDM_H, DDD_H, DDT_H	$I = 250.4838\,^1\chi - 94.3365$ $n = 4, r = 0.9968, r^2 = 0.9937$	$I = 964.4149\,^1\chi - 47.7967\,(^1\chi^v)^2 - 2750.295$ $n = 4, r = 0.9991, r^2 = 0.9982$	ApL
	$I = 395.1449\,^1\chi - 938.9389$ $n = 4, r = 0.9848, r^2 = 0.9698$	$I = 3305.604\,^1\chi - 194.8507\,(^1\chi^v)^2 - 11766.44$ $n = 4, r = 0.9999, r^2 = 0.9999$	OV-17
	$I = 210.5761\,^1\chi^v + 624.6025$ $n = 4, r = 0.9972, r^2 = 0.9943$	$I = 531.5087\,^1\chi^v - 28.8874\,(^1\chi^v)^2 - 308.1047$ $n = 4, r = 0.9992, r^2 = 0.9984$	ApL
	$I = 318.146\,^1\chi^v + 194.3096$ $n = 4, r = 0.9856, r^2 = 0.9713$	$I = 1721.411\,^1\chi^v - 122.863\,(^1\chi^v)^2 - 3772.679$ $n = 4, r = 0.9999, r^2 = 0.9999$	OV-17
DDO, DDM, DDD, DDT, DDO_H, DDM_H, DDD_H, DDT_H	$I = 357.6265\,^1\chi - 855.8640$ $n = 8, r = 0.9545, r^2 = 0.9107$	$I = 143.358\,^1\chi - 13.5728\,(^1\chi)^2 - 15.1131$ $n = 8, r = 0.9546, r^2 = 0.9107$	ApL
	$I = 449.4493\,^1\chi - 1314.5$ $n = 8, r = 0.9793, r^2 = 0.9590$	$I = 969.4059\,^1\chi - 32.9382\,(^1\chi)^2 - 3354.61$ $n = 8, r = 0.9803, r^2 = 0.9610$	OV-17
	$I = 284.1314\,^1\chi^v + 187.317$ $n = 8, r = 0.9607, r^2 = 0.9229$	$I = 166.5885\,^1\chi^v - 9.3840\,(^1\chi^v)^2 - 549.9678$ $n = 8, r = 0.9612, r^2 = 0.9240$	ApL
	$I = 355.8\,^1\chi^v + 4.3818$ $n = 8, r = 0.9833, r^2 = 0.9668$	$I = 600.2858\,^1\chi^v - 19.4215\,(^1\chi^v)^2 - 725.309$ $n = 8, r = 0.9843, r^2 = 0.9690$	OV-17

2, excellent correlation coefficients are obtained (Table I). However, when the two groups are considered together, the correlation coefficient is smaller because each group clearly follows a separate distinct curve, as can be seen in Fig. 1.

A lack of additivity is observed for the increase in the retention indices produced by chlorine substitutions on the aromatic ring (mono-, di-, tri-, tetra-, penta- and hexachlorobenzenes) according to the values given by Sabljic [18].

The correlations were also done with the retention values given by Hasan and Jurs [19] for polyhalogenated biphenyls. The compounds utilized were those with one or more chlorine atoms as substituents on one of the aromatic rings, such as 2-chlorobiphenyl, 2,3-dichlorobiphenyl, 2,3,4-trichlorobiphenyl, 2,3,4,5-tetrachlorobiphenyl, or on both of the aromatic rings, such as decachlorobiphenyl. The best results are observed when the quadratic polynomial equation is used (Table II).

Correlation between chromatographic retention indices and connectivity indices for all compounds

Different molecular connectivity indices and experimental retention indices of the 30 compounds examined are shown in Table II.

The best correlation of the retention indices on both stationary phases (ApL and OV-17) was ob-

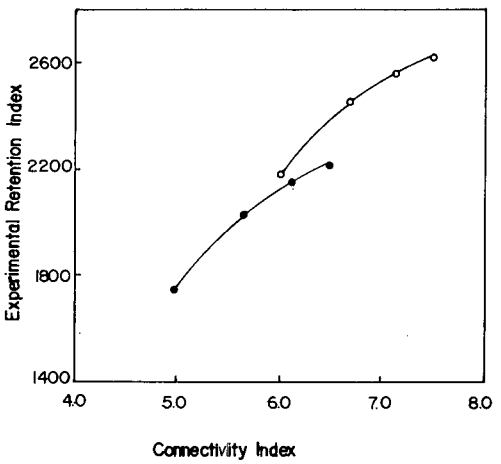

Fig. 1. Correlation between experimental retention indices (polar stationary phase, OV-17) and molecular connectivity index $^1\chi^v$ by the quadratic polynomial eqn. 2. ○ = DDO, DDM, DDD and DDT; ● = DDO_H, DDM_H, DDD_H and DDT_H.

tained using the one-variable eqn. 1 with the first-order and valence first-order molecular connectivity indices, $^1\chi$ and $^1\chi^v$.

The $^1\chi^v$ index is more selective than $^1\chi$, considering that it distinguishes the degree of unsaturation and the presence of heteroatoms. Thus, $^1\chi$ (as $^3\chi_p$, $^3\chi_c$ and $^4\chi_{pc}$) cannot distinguish between a group of six compounds, three groups of three compounds and five groups of two compounds, whereas $^1\chi^v$ indices cannot distinguish significantly only between the isomers $DDE_{o,p\text{-Cl}}$ and DDE, $DDD_{o,p'\text{-Cl}}$ and DDD and $DDT_{o,p'\text{-Cl}}$ and DDT (Table III).

For the *I* value of the 30 compounds on OV-17, the correlation coefficient with $^1\chi^v$ was 0.8393 and with $^1\chi$ 0.8599. For the *I* value of 23 compounds for which experimental determinations exist, on the non-polar stationary phase (ApL) the correlation coefficient with $^1\chi^v$ was 0.8071 and on the polar stationary phase (OV-17) it was 0.8454. Figs. 2 and 3 show the plots of *I* as a function of $^1\chi^v$ on the two stationary phases. The correlation coefficients are relatively low. However, the *t*-test (90% confidence) is significant.

Correlation between retention indices on a polar phase (OV-17) and a single connectivity index

The compounds that have a larger dispersion on the polar stationary phase (OV-17) with the connectivity index ($^1\chi^v$) are DDT_{OH}, DDD_{OH}, $DDD_{C_2H_5}$, DDA, DDE_{OCH_3}, DDD_{OCH_3} and DCS (Fig. 1).

For $DDD_{C_2H_5}$, the value of the $^1\chi^v$ increases significantly relative to that of DDD owing to the larger numbers of substructures by the addition of

TABLE II

EFFECT OF CHLORINE SUBSTITUTION ON THE RETENTION INDICES OF BENZENE AND BIPHENYL AND THEIR CORRELATION WITH CONNECTIVITY INDICES

Compounds	Linear equation	Quadratic polynomial equation	Stationary phase[a]
Mono-, 1,2-di-, 1,2,3-tri, 1,2,3,4-tetra-, penta-, hexachlorobenzene	$I = 421.3038^1\chi - 61.6637$ $n = 6, r = 0.9849, r^2 = 0.9700$	$I = 1366.585^1\chi - 106.7444\ (^1\chi)^2 - 2101.229$ $n = 6, r = 0.9965, r^2 = 0.9930$	C-20M
	$I = 418.4995^1\chi - 545.593$ $n = 6, r = 0.9973, r^2 = 0.9945$	$I = 833.3634^1\chi - 46.8479\ (^1\chi)^2 - 1440.71$ $n = 6, r = 0.9995, r^2 = 0.9990$	SE-30
	$I = 337.9849^1\chi^v + 519.3046$ $n = 6, r = 0.9853, r^2 = 0.9707$	$I = 851.1492^1\chi^v - 67.5898\ (^1\chi^v)^2 - 402.3637$ $n = 6, r = 0.9965, r^2 = 0.9930$	C-20M
	$I = 335.67^1\chi^v + 31.7508$ $n = 6, r = 0.9974, r^2 = 0.9949$	$I = 553.687^1\chi^v - 28.7154\ (^1\chi^v)^2 - 359.8143$ $n = 6, r = 0.9995, r^2 = 0.9990$	SE-30
2-Chlorobiphenyl, 2,3-di-, 2,3,4-tri-, 2,3,4,5-tetra-, decachlorobiphenyl	$I = 324.2829^1\chi^v + 283.1577$ $n = 5, r = 0.9969, r^2 = 0.9938$	$I = 546.4355^1\chi^v - 15.7442\ (^1\chi^v)^2 - 447.2039$ $n = 5, r = 0.9985, r^2 = 0.9970$	DB-210-CB

[a] C-20M = Carbowax 20M polar stationary phase; SE-30 = non-polar stationary phase; DB-210-CB = polar stationary phase (capillary column).

TABLE III

MOLECULAR CONNECTIVITY INDICES AND OBSERVED RETENTION INDICES OF PESTICIDES AND RELATED COMPOUNDS ON NON-POLAR (APIEZON L) AND POLAR (OV-17) STATIONARY PHASES AT 215°C

Compound	$^1\chi$	$^1\chi^v$	$^3\chi_p$	$^3\chi_c$	$^3\chi_c^v$	$^4\chi_{pc}$	$^4\chi_{pc}^v$	I^a	
								ApL	OV-17
DDO_H	6.8760	4.9750	4.7860	0.5258	0.3368	1.5400	0.8430	1620	1750
DDO	7.6620	5.9970	5.6080	1.1032	0.7352	2.3560	1.3030	1950	2184
DDM	8.2000	6.6730	5.8030	1.0469	0.6930	2.2360	1.2720	2168	2460
DDD_H	7.7860	6.1100	5.1570	0.7777	0.7520	1.7780	1.2960	1854	2156
DDD_{CH_3}	8.5720	6.9340	5.9790	1.3551	1.0854	2.5940	1.6810	–	2335
$DDD_{C_2H_5}$	9.6500	8.0540	6.7880	1.1859	0.9877	2.7630	1.8040	2232	2524
$DDD_{o,p'\text{-Cl}}$	8.5880	7.1340	6.0440	1.2716	1.1108	2.6980	1.8900	2184	2502
DDD	8.5720	7.1320	5.9790	1.3551	1.1504	2.5940	1.7560	2272	2572
DDD_{OCH_2}	9.6500	7.1580	6.7880	1.1859	0.8881	2.7630	1.5890	–	2775
DDD_{Br}	8.5720	7.9330	5.9790	1.0664	1.4187	2.5940	2.0660	–	2820
DDT_H	8.0870	6.4800	5.3140	1.5069	1.9432	2.0580	1.6650	1926	2224
DDT_{CH_3}	8.8740	7.3040	6.1360	2.0843	2.2770	2.8740	2.0500	2124	2436
$DDT_{o,p'\text{-Cl}}$	8.8910	7.5060	6.2070	2.1694	2.3019	2.9820	2.2600	–	2563
DDT	8.8740	7.5000	6.1340	2.0843	2.3416	2.8740	2.1250	2284	2632
DDT_{OH}	8.8740	6.7540	6.1360	2.0843	2.0923	2.8740	1.8360	–	2783
DDMF	8.1440	6.5830	5.7050	1.1839	0.8565	2.2130	1.3620	2196	2400
DDA	8.5720	6.1340	5.9790	1.3551	0.7158	2.5940	1.1560	1933	2475
DDOH	8.2000	6.1430	5.8030	1.0468	0.6930	2.2360	1.1960	2186	2517
$DDMU_H$	7.4140	5.2990	4.9810	0.4694	0.1555	1.4200	0.6240	1704	1960
DDMU	8.2000	6.3190	5.8030	1.0468	0.6372	2.2360	1.0850	2132	2384
$DDNU_H$	6.8760	4.6740	4.7860	0.5258	0.2550	1.5400	0.5970	1634	1760
DDNU	7.6620	5.6940	5.6080	1.1032	0.6534	2.3560	1.0580	1972	2166
DDE_H	7.7860	5.7650	5.1570	0.7777	0.5862	1.7780	1.0090	1754	2062
DDE_{CH_3}	8.5720	6.5900	5.9790	1.3551	0.7526	2.5940	1.3940	1974	2274
$DDE_{o,p'\text{-Cl}}$	8.5880	6.7900	6.0440	1.2716	0.9473	2.6980	1.5820	–	2396
DDE	8.5720	6.7880	5.9790	1.3551	0.9846	2.5940	1.4690	2180	2452
DDE_{OCH_3}	9.6500	6.8140	6.7880	1.1859	0.8219	2.7630	1.3020	–	2670
DCS_H	6.9480	4.7310	4.4310	0.4082	0.1925	0.8670	0.3330	1778	1972
DCS_{CH_3}	7.7340	5.5550	5.2520	0.9856	0.5258	1.6830	0.7180	2003	2177
DCS	7.7340	5.7510	5.2520	0.9856	0.5909	1.6830	0.7930	2217	2450

[a] Observed retention indices of pesticides are those reported in ref. 17.

the ethyl group to the molecule, but the increase in the experimental retention index is relatively smaller because the ethyl group is non-polar.

DCS has an experimental I value that shows a large positive deviation from the correlation line. The cause is unknown. However, the very high deviation observed also on the non-polar phase (ApL) suggests that the I value might depend strongly on the surface area and size of the molecule. It is observed that the values of the connectivity indices for DCS and DDNU, similar to those for DCS_H and $DDNU_H$, are close because the molecules have the same number of subgraphs, but the I values are different. DCS and DCS_H show larger I values than $DDNU_H$ and DDNU, possibly because in the former compounds the aromatic rings are bonded to different carbon atoms of the ethylene group, and in this way the molecule has a larger contact surface, thereby increasing the interaction with the stationary phase and consequently the retention time in the column.

The compounds that have polar groups such as the "OH" and "OCH_3" compounds show higher I values than those calculated through the connectivity index ($^1\chi^v$). This result may be due in part to the method of calculation.

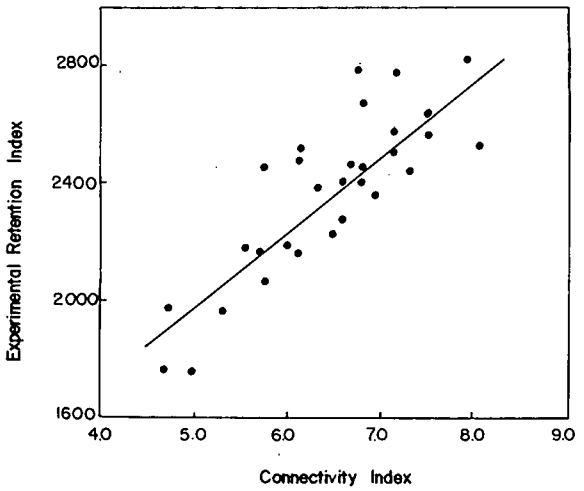

Fig. 2. Correlation between experimental retention indices (polar stationary phase, OV-17) and molecular connectivity index $^1\chi^v$ for 30 compounds.

It is known that the values of the connectivity index $^1\chi^v$ refer to subgraphs consisting of two adjacent and consecutive vertices (atoms). The vertices are described by their valence delta values (δ^v) according to the expression

$$\delta^v = Z^v - h \tag{3}$$

for atoms beyond the first row of the Periodic Table (*e.g.*, for oxygen $\delta^v = 6$), where Z^v is the number of valence electrons in the atom (vertex) and h is the number of hydrogen atoms bonded to the same atom. For atoms beyond the second row in the Periodic Table, the relationship which leads to appropriate δ^v is

$$\delta^v = \frac{Z^v - h}{Z - Z^v} \tag{4}$$

where Z is the atomic number.

The compounds studied have only chlorine and oxygen as heteroatoms in the molecule. The value of δ^v of the chlorine atom calculated through the eqn. 4 is 0.7. As this value is less than 1 it contributes to increasing the $^1\chi^v$ value, according to the increase that occurs in the experimental I value due to the presence of the polar chlorine atom.

However, with oxygen, eqn. 3 gives a value of $\delta^v = 5$ for "OH", which contributes to a decrease in the value of $^1\chi^v$, whereas the experimental I value increases in the presence of a polar OH group.

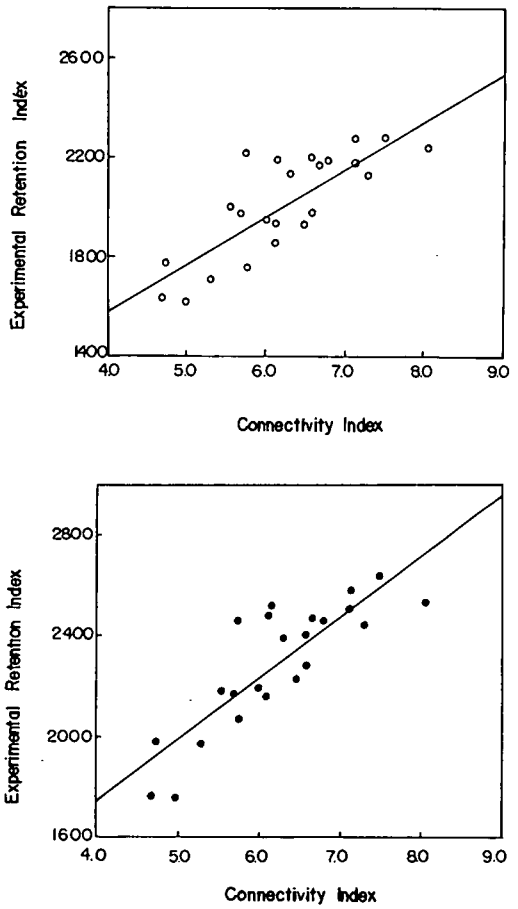

Fig. 3. Correlation between experimental retention indices and molecular connectivity index $^1\chi^v$ for 23 compounds. O = Non-polar stationary phase (ApL); ● = polar stationary phase (OV-17).

If eqn. 4 is utilized to calculate the value of δ^v for the oxygen atom of OH, OCH_3 and C=O groups, smaller values are obtained. In this instance, the final values of $^1\chi^v$ increase like the experimental I values. Thus, if the $^1\chi^v$ values of compounds having oxygen in the molecule (DDOH, DDA, DDT_{OH}, DDE_{OCH_3}, DDD_{OCH_3}) are calculated using eqn. 4 for δ^v of oxygen, a better correlation coefficient with the I values ($r = 0.8781$) is obtained.

Correlation between retention indices on a non-polar stationary phase (Apiezon L)

With the non-polar stationary phase ApL the

compounds that show the largest dispersion in the correlation between I and $^1\chi^v$ are DCS, DDOH, $DDD_{C_2H_5}$, DDO_H and DDE_H (Fig. 2).

The $^1\chi^v$ value of DCS (which has one chlorine atom in each aromatic ring) and DCS_{CH_3} (which has one methyl group in each aromatic ring) are very close, in spite of the consideration of the value of $\delta^v = 0.7$ for the chlorine atom and $\delta^v = 1$ for the methyl group compared with the difference existing between the values of the retention indices.

For compounds with polar groups such as OH and OCH_3, the same results as for the polar phase (OV-17) were obtained.

Correlation between chromatographic retention indices and connectivity indices by multiple linear correlation equations

The analyses by the single linear regression method demonstrate that correlations with only one variable are not sufficient to discriminate clearly the compounds or their correct elution sequence. This led us to test multi-variable regression equations with indices that were able to give a better representation of the molecules. To select the connectivity indices, a correlation matrix between them was applied, and to define the type of function that relates the retention indices with each connectivity index, the scatter plot method was used. From this exploratory data analysis we selected as independent variables $^1\chi$ or $^1\chi^v$; $^3\chi_p$; $^3\chi_c$ or $^3\chi_c^v$; and $^4\chi_{pc}$ or $^4\chi_{pc}^v$.

In spite of the fact that the best correlation coefficient with two variables was obtained with $^1\chi$ and $^3\chi_c$ ($r = 0.8909$), the best result with two-variable equations was obtained with $^1\chi^v$ and $^3\chi_p$ ($r = 0.8729$), considering that these last two variables are able to distinguish significantly all the compounds (see eqns. 5, 6 and 7).

$$I = 265.4079\,{}^1\chi^v + 652.0186 \qquad (5)$$

$r = 0.8393 \qquad F = 66.70 \qquad (P > 0.0001)$

where P is the level of probability indicated by the sample;

$$I = 244.2217\,{}^1\chi + 177.3415\,{}^3\chi_c + 120.8026 \qquad (6)$$

$r = 0.8909 \qquad F(^1\chi) = 31.87 \qquad (P > 0.0001)$

$F(^3\chi_c) = 7.11 \qquad (P > 0.0128)$

$$I = 133.80\,{}^1\chi^v + 229.20\,{}^3\chi_p + 182.80 \qquad (7)$$

$r = 0.8729 \qquad F(^1\chi^v) = 79.88 \qquad (P > 0.0001)$

$F(^3\chi_p) = 6.55 \qquad (P > 0.0166)$

The correlation coefficient is better than with a single linear regression equation ($^1\chi^v$) owing the existence of other factors besides correspondence with $^1\chi^v$ (which distinguish the degree of unsaturation and the presence of heteroatoms) participating in the physico-chemical process of retention of the compounds. In this case, $^3\chi_p$ is a topological description that includes the size and degree of branching of the molecules.

Equations with three or more connectivity indices show that the third or fourth variables do not meet the 0.15 significance level for entry into the statistical analysis model.

CONCLUSIONS

The increase in the values of the retention indices with increase in the number of chlorine atoms in the molecule is non-linear. The correlation by a single linear regression equation of the retention indices and the molecular connectivity indices ($^1\chi^v$) is good because it takes only a first relatively linear part of a curve. For this reason, the correlation by a quadratic polynomial equation gives the best results with chlorinated pesticides, chlorinated aromatic compounds and halogenated biphenyls.

The molecular connectivity indices do not entirely predict, by a single linear regression equation, the chromatographic retention indices and the correct elution sequence of the different chlorinated pesticides and related compounds. Using two connectivity indices, it is possible to represent more aspects of the structure of the molecules that are important in their interaction with the stationary phase, and therefore the multiple linear regression equation gives better results.

ACKNOWLEDGEMENTS

The authors thank CNPq (Brazil) for financial support and also Professors Pedro A. Barbetta and José Francisco Fletes of the Departamento de Ciencias Estatísticas e da Computaçao (UFSC) for useful discussions of the statistical methods.

REFERENCES

1 M. Randić, *J. Am. Chem. Soc.*, 97 (1975) 6609.
2 L. B. Kier, in S. H. Yakowsky, A. Sinkula and S. C. Valvani (Editors), *Physical Chemical Properties of Drugs*, Marcel Dekker, New York, 1980, Ch. 9, p. 277.
3 L. H. Hall, L. B. Kier and W. J. Murray, *J. Pharm. Sci.*, 64 (1975) 1974.
4 J. Bermejo, J. S. Canga, O. M. Gayol and M. D. Guillén, *J. Chromatogr. Sci.*, 22 (1984) 252.
5 A. Sabljic and H. Güsten, *Environ. Sci. Technol.*, 24 (1990) 1321.
6 L. B. Kier and R. L. Hall, *J. Med. Chem.*, 20 (1977) 1631.
7 R. Koch, *Toxicol. Environ. Chem.*, 6 (1983) 87.
8 A. Sabljic and M. Protic, *Chem.-Biol. Interact.*, 42 (1982) 301.
9 A. Sabljic, *Z. Gesamte Hyg.*, 33 (1987) 10.
10 A. Robbat, Jr., G. Xyrafas and D. Marshall, *Anal. Chem.*, 60 (1988) 982.
11 K. Héberger, *Chromatographia*, 25 (1988) 725.
12 V. A. Gerasimenko and V. M. Nabivach, *J. Chromatogr.*, 498 (1990) 357.
13 M. Kuchar, H. Tomková, V. Rejholec and O. Skalicka, *J. Chromatogr.*, 333 (1985) 21.
14 O. Papp, Gy. Szász, M. Farbas, G. Simon and I. Hermecz, *J. Chromatogr.*, 403 (1987) 19.
15 J. R. Haken and I. O. D. Korhonen, *J. Chromatogr.*, 265 (1983) 322.
16 A. Sabljic, *J. Chromatogr.*, 314 (1984) 1.
17 D. R. Zanette, *Thesis (M.Sc.), Pós-graduaçao em Fisico-Química*, UFSC, Florianópolis, Santa Catarina, Brazil, 1983.
18 A. Sabljic, *J. Chromatogr.*, 319 (1985) 1.
19 M. N. Hasan and P. C. Jurs, *Anal. Chem.*, 62 (1990) 2316.

Journal of Chromatography, 598 (1992) 251–265
Elsevier Science Publishers B.V., Amsterdam

CHROM. 24 089

Some novel homochiral derivatizing agents for the gas chromatographic analysis of enantiomeric secondary alcohols

Duncan A. Rimmer

Health and Safety Executive, O.M.H.L. 3, 403-5 Edgware Road, Cricklewood, London NW2 6LN (UK)

Malcolm E. Rose*

Department of Chemistry, The Open University, Walton Hall, Milton Keynes MK7 6AA (UK)

(Received December 12th, 1991)

ABSTRACT

Some novel homochiral derivatizing agents for the determination of enantiomeric composition of chiral alcohols have been synthesised. The reactions of the reagents with alkan-2-ols and the gas chromatographic behaviour of the resulting diastereoisomeric derivatives have been examined. The most promising reagents are (*S*)-(+)-tetrahydro-5-oxo-2-furanmethyl chloromethyl ether, and (*S*)-(+)-2-methylcarboxypropyl chloromethyl ether. Despite having five bonds between chiral centres in their diastereoisomeric derivatives, resolution was readily achieved on common, conventional stationary phases.

INTRODUCTION

Chromatographic and electrophoretic methods for separating the enantiomers of chiral compounds depend on creating an asymmetric environment. This is achieved with (i) a homochiral derivatizing reagent, (ii) a homochiral stationary phase [1–5] or (iii) a mobile phase containing homochiral additives. Each of these approaches has both advantages and disadvantages. For gas chromatography and approach (i), many achiral derivatization agents, developed primarily to enhance the volatility of analytes, have been adapted for use as homochiral reagents so as to form diastereoisomers from enantiomers. The derivatization reaction most commonly employed in diastereoisomer formation involves the use of chiral acid chlorides. For example, homochiral acid chlorides include (+)-*trans*-chrysanthemoyl chloride which has enabled the quantification of enantiomers of pheromones [6], terpenes such as menthol [7] and triazole alcohols [8] and various amines (*e.g.*, amphetamine) [7] by gas chromatography (GC). Another, prepared from the cheap and readily available amino acid (*S*)-proline, is N-trifluoroacetyl-(*S*)-prolyl chloride. This reagent has been used widely for the separation of enantiomers of numerous alcohols and amines by GC [6,9–12] as well as by high-performance liquid chromatography [13,14]. Use of N-heptafluorobutyl-(*S*)-prolyl chloride has also been reported [15]. Conversely, homochiral alcohols that can be employed for the derivatization of enantiomers of acids (via their acid chlorides) for GC analysis include (−)-menthol [16–18], (+)-3-methyl-2-butanol [19, 20] and enantiomerically pure 2-alcohols [21–23]. Many other derivatization reactions applicable to the formation of diastereoisomers are known. Examples of homochiral reagents for these reactions are listed in several texts [24–26].

The advantages of homochiral derivatization are

0021-9673/92/$05.00

also several fold: (a) the reagents are usually obtained from cheap and readily available starting materials; (b) the separations can be achieved on conventional, relatively cheap achiral columns; (c) the order of elution of the diastereoisomeric products can be changed readily by using the optical antipode of the homochiral reagent; (d) different analogues of the homochiral reagents can be synthesised in order to enhance factors such as volatility of the reagent or to improve the sensitivity or selectivity of the analysis.

While GC analysis of diastereoisomers has produced some very good separations, the technique has several well known drawbacks such as: (i) the reagent used needs to be 100% optically pure; (ii) racemization of the reagent can occur under certain reaction conditions; (iii) kinetic resolution may occur (*i.e.*, one enantiomer may react more rapidly than its antipode with an asymmetric reagent), giving misleading results if the derivatization does not go to completion; (iv) where there are more than four bonds between the two chiral centres of the diastereoisomers unsatisfactory separations are said [1] to be produced; (v) different classes of analytes require different reagents (*i.e.*, many metho ds are specific to just one class of compound); and (vi) an enantiomerically enriched sample of the analyte must be obtainable in order to determine the order of elution of the diastereoisomers (it does not always follow that the elution order will be the same for different homologues [27]). The work reported here seeks to overcome some of the disadvantages associated with the gas chromatographic determination of enantiomeric compositions following derivatization with a homochiral reagent.

The use of homochiral haloalkanes as derivatizing agents forming diastereoisomeric ethers from chiral alcohols

$$R^*OH + R\text{–}X \rightarrow R^*\text{–}O\text{–}R + HX \qquad (1)$$

(where X = Cl, Br, I) has received little attention. For example, alcohols and related nucleophilic compounds react with simple haloalkanes under the mild, though basic, conditions of solid KOH in dimethyl sulphoxide (DMSO) [28]. This procedure would appear to be adaptable to chiral analysis. However, it was found [29] that, when more complex haloalkanes were employed (with β-branching to create a chiral centre), hydrolysis and/or dehydrohalogenation (elimination) predominated over the required substitution according to eqn. 1. Barluenga *et al.* [30,31] have effected the reaction in eqn. 1 under mild and neutral conditions. Mercury tetrafluoroborate in dichloromethane was utilized to enhance the reactivity of the haloalkane. We have applied this procedure to homochiral reagents as a means of derivatizing chiral alcohols prior to GC separation. The procedure has the advantage of being compatible with base-sensitive functions in the analyte or in the reagent.

If the reagent haloalkane molecule does not contain a C–H unit in the β-position, dehydrohalogenation is prevented from occurring. Chloromethyl ethers offer this feature:

$$R^*OH + R\text{–}OCH_2\text{–}Cl \xrightarrow[CHCl_3/\text{reflux}]{EtN^iPr_2} R^*O\text{–}CH_2OR + HCl \qquad (2)$$

(where Et = ethyl and ^{i}Pr = isopropyl). In addition, these reagents are very reactive because the oxygen atom is able to stabilize the transition state and/or intermediate in the substitution reaction.

We have developed two derivatization procedures, one based on homochiral iodoalkanes **1** and **2**, the other on homochiral chloromethyl ethers **3**–

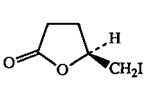

1

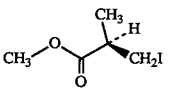

2

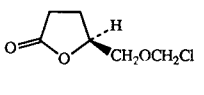

3

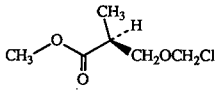

4

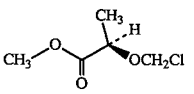

5

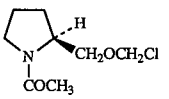

6

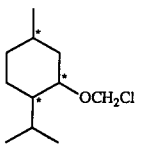

7 (* = chiral centres:1S,2R,5S)

7, for determining enantiomeric compositions of alcohols by GC. The efficiency of the methods is assessed by comparison with established derivatization schemes using homochiral acyl chlorides:

$$R^*OH + RCO\text{–}Cl \rightarrow R^*O\text{–}COR + HCl \quad (3)$$

An unexpected variation of resolution with the number of bonds between the chiral centers in the resulting diastereoisomeric ethers was observed and is also described herein.

EXPERIMENTAL

Apparatus and chemicals

The following gas chromatographs were used: (a) Carlo-Erba, GC6000 Vega Series 2 fitted with an on-column injector and flame ionization detector (250°C), the data being processed with a Milton Roy Cl-10CB integrator; (b) Hewlett-Packard 5890 fitted with a split injector (275°C) and flame ionization detector (270°C), the data being processed with a Hewlett-Packard HP5895A work station. GC–mass spectrometry (MS) was effected with a Hewlett-Packard 5890 gas chromatograph coupled to a VG 20-250 quadrupole mass spectrometer in the electron ionization (EI) mode. Typically, the ion source was maintained at 200°C, the electron beam energy was 70 eV and the emission current 100–200 μA. Spectra were recorded repetitively every second. The various columns and temperature programmes used for GC are given in the legends to the figures and tables. Helium carrier gas inlet pressures were in the range 30–40 KPa.

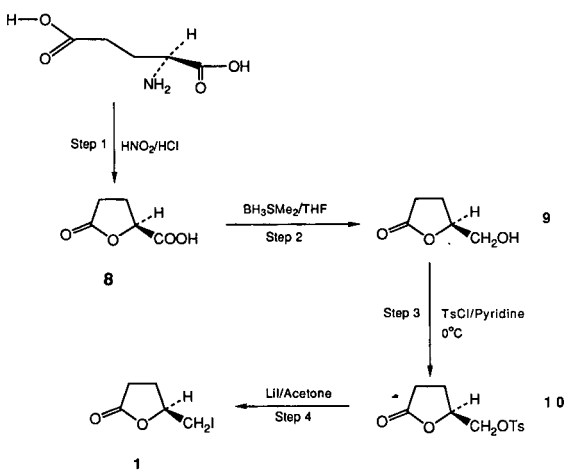

Fig. 1. Preparation of reagent **1**. Me = Methyl; Ts = tosyl.

Other instruments utilized during the preparation of the derivatizing agents: Jeol FX90Q FT NMR (90 MHz) for ^{13}C and ^{1}H NMR spectroscopy; Perkin-Elmer 1420 ratio recording spectrophotometer for infrared spectroscopy; a half-shadow polarimeter (Lippich type) for measuring optical rotations. Elemental analyses were performed by Medac, Brunel University, Uxbridge, UK.

All chemicals were purchased from either Aldrich or Sigma.

Synthesis of the homochiral derivatizing agents

Reagent ***1****: (S)-(−)-tetrahydro-5-oxo-2-furanmethyl iodide*

This compound was prepared according to Fig. 1 as follows [32–34]:

Step 1. A solution of sodium nitrite (126 g; 1.83 mol) in water (270 ml) was added dropwise to a mixture of (*S*)-(+)-glutamic acid (180 g; 1.22 mol) in water (480 ml) and concentrated (37%) hydrochloric acid solution (180 ml) at 0–5°C in a 2-l flask fitted with a mechanical strirrer. On addition, the stirred solution cleared and effervesced. After three hours stirring, the mixture was allowed to stand overnight at 0°C, then at room temperature for 5 h. The water was removed by freeze drying to yield a pale yellow oil and colourless fine crystals. Hot acetone was added (600 ml) until all the oil was dissolved, leaving a fine suspension of sodium chloride. This was filtered off and the filtrate was concentrated to 300 ml. Anhydrous magnesium sulphate was added and the mixture was allowed to stand overnight at 3°C. The solids were removed by filtration and the solvent was removed. The oily residue was taken up in ethyl acetate (500 ml), and any further insoluble material was removed by filtration. The solvent was removed and the residue was taken up in a minimum of warm ethyl acetate (200 ml). An equal volume of benzene was added and the mixture was allowed to crystallize in a freezer (after seeding). The crystalline product was filtered and washed with anhydrous diethyl ether. The combined filtrates were again seeded and cooled to give a further crop of crystals.

The total yield of acid **8** was 80 g (50%); m.p. 55°C (lit. 70–72°C [32]); $[\alpha]_D^{20}$ +14.6° (*c* = 2.0, C_2H_5OH)

(lit. +15.6°); IR: ν_{max} (nujol) 3600–2350 (OH_{STR}, acid[a]), 1765 ($C{=}O_{STR}$, lactone), 1720 ($C{=}O_{STR}$, acid), 1180 cm^{-1} ($C{-}O_{STR}$); NMR: δ_H ($C^2H_3O^2H$) 2.2–2.7 ($CH_2{-}CH_2$, m, 4H), 5.0 (CH, m, 1H) 5.4 ppm (OH, s, 1H); NMR: δ_c ($C^2H_3O^2H$) 28.5 and 29.5 ($CH_2{-}CH_2$), 79.0 (CH–O), 175.1 and 180.8 ppm (C=O lactone and acid).

Step 2. To a three-necked 500-ml round-bottomed flask, set up with a magnetic stirrer, septum, stopper and reflux condenser connected to an argon bubbler, was added acid **8** (21.6 g, 0.166 mol), followed by 140 ml of tetrahydrofuran (THF). After flushing the system with argon, a 2 *M* solution of borane methyl sulphide complex (95 ml, 0.19 mol) in THF was injected slowly (over 1 h). After 3 h stirring, the mixture was quenched by cautious addition of anhydrous methanol (60 ml). Most of the solvent was removed by rotary evaporation and a further portion of methanol (200 ml) was added then removed. Vacuum distillation (125–135°C/0.6 mmHg) yielded 16.7 g (87%) of alcohol **9** as a clear oil. $[\alpha]_D^{20}$ +25.5° (c = 2.0, C_2H_5OH) [lit. [32] $[\alpha]_D^{20}$ +29.6° (c = 0.4, C_2H_5OH)]. IR: ν_{max} (thin film) 3400 ($O{-}H_{STR}$), 1765 cm^{-1} ($C{=}O_{STR}$, lactone); NMR: δ_H (C^2HCl_3) 2.25 and 2.6 ($CH_2{-}CH_2$, m, 4H), 3.75 (CH_2–O, m, 2H), 4.1 (O–H, s, 1H), 4.6 ppm (CH, m, 1H); NMR: δ_C (C^2HCl_3) 23.0 (C–CH_2–C), 28.4 ($O_2C{-}CH_2{-}C$), 63.6 (O–CH–C), 80.9 (CH_2–OH), 178 ppm (C=O).

Step 3. *p*-Toluenesulphonyl chloride (tosyl chloride) (42 g, 0.22 mol) was added to a stirred solution of alcohol **9** (15 g, 0.13 mol) in dry pyridine (100 ml) at 0°C. After 30 min stirring the mixture was left to stand at 0°C for 22 h. The mixture was then filtered and the filtrate was poured into cold 5% sodium hydrogen carbonate solution (180 ml). The product was extracted into ethyl acetate (2 × 100 ml), and the combined extracts were washed with 5% sodium hydrogen carbonate solution (100 ml), water (100 ml) and brine (100 ml). After drying with anhydrous magnesium sulphate and filtering, the solvent was removed to yield an orange oil which was crystallized twice from benzene/hexane to yield 16.2 g (47%) of tosylate **10** as fine white needles. M.p. = 83°C (lit. = 85–87°C [32]). $[\alpha]_D^{20}$ +43° (c = 1, $CHCl_3$) [lit. [32] $[\alpha]_D^{20}$ +47° (c = 1.6, $CHCl_3$)]. IR: ν_{max} (KBr disc) 1760 ($C = O_{STR}$, lactone), 1355 (S=O), 1170 (S=O), 975 cm^{-1} (S–O–C); NMR: δ_H (C^2HCl_3) 2.0–2.6 (CH_2CH_2, m, 4H), 2.45 (CH_3, s, 3H), 4.15 (CH_2–O, dd, 2H), 4.65 (CH–O, m, 1H), 7.25 and 7.8 ppm (aromatic CH, 2 × d, 4H); NMR: δ_c (C^2HCl_3) 21.6 (CH_3), 23.4 and 27.8 ($CH_2{-}CH_2$), 69.9 (CH–O), 76.3 (CH_2–O), 127 and 130 (aromatic CH), 132.2 (C–CH_3), 145.3 (C–S), 175.9 ppm (C=O).

Step 4. Lithium iodide (24 g, 0.18 mol) was added to a solution of tosylate **10** (12 g, 0.044 mol) in acetone (150 ml). The mixture was stirred and heated under reflux for 5 h, when the reaction was seen to be complete by thin-layer chromatography (on silica plates using methanol or chloroform as solvent). The acetone was removed by rotary evaporation and the orange-brown residue was dissolved in water (20 ml). The product was extracted twice with ethyl acetate (15 ml), and the combined extracts were washed with sodium thiosulphate and brine solutions. After drying with anhydrous magnesium sulphate and filtering, the ethyl acetate was removed by rotary evaporation to yield 9.3 g (94%) of iodide **1** as a pale orange oil; $[\alpha]_D^{20}$ −15.4° (c = 1.75, $CHCl_3$); IR: ν_{max} (thin film) 1760 cm^{-1} ($C{=}O_{STR}$, lactone); NMR: δ_H (C^2HCl_3) 2-3 ($CH_2{-}CH_2$, m, 4H), 3.5 (CH–CH_2–I, d, 2H), 4.65 ppm (CH–O, m, 1H); NMR: δ_c ($C^2H_3O^2H$) 7.9 (CH_2–I), 28.0 and 28.8 ($CH_2{-}CH_2$), 78.4 (CH–O), 176.2 ppm (C=O).

Reagent 2: methyl (S)-(+)-3-iodo-2-methylpropanoate

This compound was prepared from methyl (*S*)-(+)-3-hydroxy-2-methylpropanoate **11** according to Fig. 2 by effecting steps 3 and 4 as above.

Thus, methyl (*S*)-(+)-3-hydroxy-2-methylpropanoate (1.534 g, 13 mmol), pyridine (10 ml) and tosyl chloride (4.2 g, 22 mmol) were used. The work-up, scaled accordingly, gave 2.4 g (68%) of compound **12** as a pale orange oil (pure by GC). Found: C, 52.88; H, 5.92 ($C_{12}H_{16}O_5S$ requires C, 52.93; H,

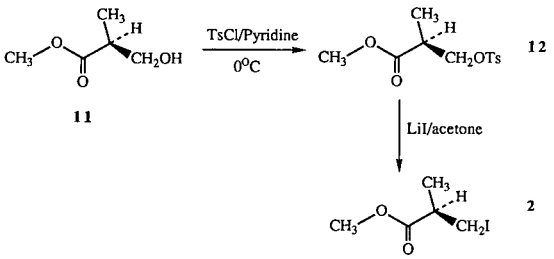

Fig. 2. Preparation of reagent **2**.

[a] STR = stretching.

5.92). $[\alpha]_D^{20}$ +9.0° (*c* = 2.0 CH_3OH); IR: ν_{max} (thin film) 1745 (C=O_{STR}, ester), 1600/1495 (aromatic C=C_{STR}), 1365 (S=O), 1210 [C(=O)–O–C_{STR}], 1180 (S=O), 975 (S–O–C), 750 (C–H_b)[a], 670 cm^{-1} (C=C_b); NMR: δ_H (C^2HCl_3) 1.15 (CH_3CH, d, 3H), 2.4 [aromatic group (Ar)–CH_3, s, 3H], 2.85 (CH, q, 1H), 3.6 (CH_3–O, s, 3H), 4.1 (CHCH_2O, 2H), 7.35 and 7.8 ppm (aromatic CHs, 2 × d, 4H); NMR: δ_C (C^2HCl_3) 13.6 (CH_3CH), 21.6 (Ar–CH_3), 39.2 (CH), 52.0 (CH_3O), 70.8 (CH_2O), 127.9 and 129.9 (aromatic CH), 132.8 (aromatic C–CH_3), 145.0 (aromatic C–S), 173.0 ppm (C=O); EI-MS: *m/z* 272 (8%, $M^{+\bullet}$), 241 (2%, $[M - CH_3O^{\bullet}]^+$), 187 (10%), 172 (12%, $TsOH^{+\bullet}$), 155 (80%, $CH_3(C_6H_4)\dot{S}O_2$), 117 (57%, $[M - CH_3(C_6H_4)SO_2^{\bullet}]^+$), 91 (100%, $C_7H_7^+$), 85 (30%, $CH_3OC\dot{O}C{=}CH_2$) and 69 [20%, $O{=}C{=}C(CH_3)CH_2^+$].

The iodide **2** was prepared from tosylate **12** on a 5-mmol scale. Thus, lithium iodide (2.74 g, 20.5 mmol), tosylate **12** (1.35 g, 5 mmol) and acetone (20 ml) were used. The work-up, also scaled accordingly, gave 0.76 g (63%) of iodide **2** as a pale yellow liquid (pure by GC). Found: C, 26.68; H, 4.05 ($C_5H_9IO_2$ requires C, 26.34; H, 3.98). $[\alpha]_D^{20}$ +21° (*c* = 2.0, CH_3OH); IR: ν_{max} (thin film) 1740 (C=O_{STR}, ester), 1210 and 1160 cm^{-1} [C(=O)–O–C_{STR}]; NMR: δ_H (C^2HCl_3) 1.25 (CH_3–CH, d, 3H), 2.80 (CH, m, 1H), 3.3 (CH_2–I, m, 2H), 3.7 ppm (CH_3–O, s, 3H); NMR: δ_C (C^2HCl_3) 6.8 (CH_2–I), 18.1 (CH_3–CH), 42.2 (CH), 52.0 (CH_3–O), 173.7 ppm (C=O); EI-MS: *m/z* 228 (28%, $M^{+\bullet}$), 197 (8%, $[M - CH_3O^{\bullet}]^+$), 169 (26%, $[M - {}^{\bullet}COOCH_3]^+$), 127 (9%, I^+), 101 (100%, $[M - I^{\bullet}]^+$), 73 (20%), 59 (75%, $CH_3OC{\equiv}O^+$) and 41 (30%).

Reagents 3–7: chloromethyl ethers

These reagents were prepared from the corresponding alcohol via their methylthiomethyl (MTM) ether derivatives:

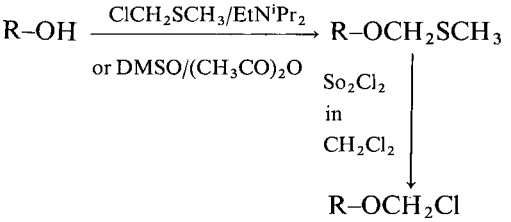

[a] b = bending.

General synthesis of MTM ethers. To the homochiral alcohol (20 mmol) in ethanol-free chloroform (60 ml) was added diisopropylethylamine (12.9 g, 100 mmol) and chloromethyl methyl sulphide (5.8 g, 60 mmol) under an argon atmosphere. The mixture was refluxed for 3–4 h until the reaction mixture contained a maximun quantity of product (typically 60–70%) with respect to the starting material and by-products (as monitored by GC). The cooled reaction mixture was washed with 1 *M* hydrochloric acid (100 ml) and water (200 ml) then dried ($MgSO_4$). The solvent was removed and the product purified by distillation. The yields and analytical data were as follows.

(S)-(+)-Tetrahydro-5-oxo-2-furanmethyl methylthiomethyl ether. Prepared from (*S*)-(+)-tetrahydro-5-oxo-2-furanmethyl alcohol **9** (2.32 g, 20 mmol). Distillation (130°C/0.15 mmHg) afforded 1.625 g (46%) MTM ether as a pale yellow liquid. Found: C, 47.65; H, 7.01; S, 18.08 ($C_7H_{12}O_3S$ requires C, 47.71; H, 6.86; S, 18.18%). $[\alpha]_D^{20}$ +20° (*c* = 1.0, C_2H_5OH); IR: ν_{max} (thin film) 1780 (C=O_{STR}, lactone), 1180 (C(=O)–O–C_{STR}, ester), 1080 cm^{-1} (C–O–C_{STR}, ether); NMR: δ_H (C^2HCl_3) 2.0–2.7 (CH_2–CH_2, m, 4H), 2.15 (S–CH_3, s, 3H), 3.6 (CH_2–O, m, 2H), 4.6 ppm (O–CH_2–S, s, 2H and CH, m, 1H); NMR: δ_C (C^2HCl_3) 14.1 (S–CH_3), 24.3 (CH_2–CH_2–CH), 28.6 (CH_2C=O), 69.5 (O–CH), 75.9 (O–CH_2–S), 79.0 (CH_2–O), 177.6 ppm (C=O); EI-MS: *m/z* 176 (28%, $M^{+\bullet}$), 146 (43%, $[M - CH_2O]^{+\bullet}$), 129 (57%, $[M - CH_3S^{\bullet}]^+$), 114 (16%, $[M - CH_3SCH_3]^{+\bullet}$), 99 (100%, $[M - CH_3SCH_2O^{\bullet}]^+$), 85 (83%, $[M - {}^{\bullet}CH_2OCH_2SCH_3]^+$) and 61 (1%, $CH_2{=}\dot{S}CH_3$).

(S)(+)-2-Methylcarboxypropylmethylthiomethyl ether. Prepared from methyl (*S*)-(+)-3-hydroxy-2-methylpropanoate **11** (2.36 g, 20 mmol). Distillation (50–55°C/0.25 mmHg) afforded 0.9 g (25%) MTM ether as a clear liquid. Found: C, 47.14; H, 8.11; S, 17.89 ($C_7H_{14}O_3S$ requires C, 47.17; H, 7.92; S, 17.9%). $[\alpha]_D^{20}$ +27° (*c* = 0.6, CH_3OH); IR: ν_{max} (thin film) 1720 (C=O_{STR}, ester), 1190 (C(=O)–O–C_{STR}, ester), 1060 cm^{-1} (C–O–C_{STR}, ether); NMR: δ_H (C^2HCl_3) 1.1 (CH_3CH, d, 3H), 2.1 (S–CH_3, s, 3H), 2.7 (CH, m, 1H), 3.7 (CH_3OCO and CH_2–O, s and m, 5H), 4.6 ppm (O–CH_2–S, s, 2H); NMR: δ_C (C^2HCl_3) 13.73 (CH_3–CH), 14.02 (S–CH_3), 39.92 (CH), 51.76 (CH_3OCO), 69.74 (CH_2–O), 75.37 (O–CH_2–S), 175.1 ppm (C=O).

(S)-(−)-1-Methylcarboxyethyl methylthiomethyl ether. Prepared from (*S*)-(−)-methyl lactate (2.08 g, 20 mmol). Distillation (68°C/5.5 mmHg) afforded 1.29 g (40%) MTM ether as a clear liquid. Found: C, 43.84; H, 7.37; S, 19.28 ($C_6H_{12}O_3S$ requires C, 43.88; H, 7.37; S, 19.51%). $[\alpha]_D^{20}$ −158° (*c* = 2.0, $CHCl_3$); IR: ν_{max} (thin film) 1730 (C=O_{STR}, ester), 1200 (C(=O)–O–C_{STR}, ester), 1100 cm^{-1} (C–O–C_{STR}, ether); NMR: δ_H (C^2HCl_3) 1.4 (CH_3–CH, d, 3H), 2.15 (S–CH_3, s, 3H), 3.75 (CH_3–OCO, s, 3H), 4.35 (CH, q, 1H), 4.7 ppm (O–CH_2–S, s, 2H); NMR: δ_C (C^2HCl_3) 13.9 (S–CH_3), 18.4 (CH_3–CH), 51.9 (CH_3OCO), 71.1 (CH–O), 74.3 (O–CH_2–S), 173.3 ppm (C=O); EI-MS: *m/z* 117 (100%, $[M-CH_3S^{\bullet}]^+$), 89 (95%, $CH_3OCOCH=\overset{+}{O}H$), 70 (30%), 61 (42%, $CH_2=\overset{+}{S}CH_3$), 59 (49%, $^+COOCH_3$) and 45 (55%).

N-Acetyl-(S)-(−)-2-pyrrolidinemethyl methylthiomethyl ether. Prepared from N-acetyl-(*S*)-(−)-2-pyrrolidinemethanol (2.86 g, 20 mmol). Distillation (140°C/0.1 mmHg) afforded 1.04 g (26%) MTM ether as a pale yellow oil. $[\alpha]_D^{20}$ −80° (*c* = 0.35, C_2H_5OH); IR: ν_{max} (thin film) 1650 (C=O_{STR}, amide), 1420 (C–N_{STR}, amide), 1070 cm^{-1} (C–O–C_{STR}, ether); NMR: δ_H (C^2HCl_3) 1.6–2.1 (CH_2–CH_2, m, 4H), 2.05 (CH_3C=O, s, 3H), 2.15 (S–CH_3, s, 3H), 3.2–3.75 (CH_2–O and CH_2–N, m, 4H), 4.25 (CH, m, 1H), 4.6 ppm (O–CH_2–S, s, 2H); NMR: δ_C (C^2HCl_3) 14.0/14.39 (S–CH_3), 22.4 and 22.8/22.9 (CH_2–CH_2), 27.86/28.95 (CH_3C=O), 45.6/48.5 (CH_2–N), 56.1/57.6 and 68.1/69.1 (CH_2–O and CH–N), 75.6 (O–CH_2–S), 169.4 ppm (C=O); EI-MS: *m/z* 188 (1%, $[M-{}^{\bullet}CH_3]^+$), 156 (3%, $[M-CH_3S^{\bullet}]^+$), 142 (24%, $[M-{}^{\bullet}CH_2SCH_3]^+$), 127 (34%, $[M-CH_3SCH=O]^{+\bullet}$), 112 (40%, $[M-{}^{\bullet}CH_2OCH_2SCH_3]^+$), 100 (13%), 84 (16%), 70 (100%, $[M-(CH_2C=\overset{+}{O}+{}^{\bullet}CH_2OCH_2SCH_3)]^+$) and 61 (13%, $CH_2=\overset{+}{S}CH_3$).

(1S, 2R, 5S)-(+)-Menthyl methylthiomethyl ether. This compound was prepared with a different, literature procedure [35]. To (1*S*, 2*R*, 5*S*)-(+)-menthol (1.872 g, 12 mmol) in a round-bottomed flask, was added DMSO (60 ml) and acetic anhydride (60 ml). The reaction was stirred at room temperature for 30 h (monitoring by GC) before pouring into water (200 ml). The product mixture was extracted into chloroform (100 ml), which was then washed 5 times with water (100 ml). After drying ($MgSO_4$), the solvent and acetic anhydride were removed by rotary evaporation. Applying a high vacuum and warming the flask removed the last traces of any remaining menthol to leave 2.15 g (78%) as a clear liquid. $[\alpha]_D^{20}$ +199° (*c* = 2.0, C_2H_5OH); IR: ν_{max} (thin film) 1050 cm^{-1} (C–O–C_{STR}, ether); NMR: δ_H (C^2HCl_3) 0.7–2.7 (CH_3, CH_2 and CH, 18H), 2.15 (S–CH_3, s, 3H), 3.5 (CH–O, dt, 1H), 4.6 ppm (O–CH_2–S, s, 2H); NMR: δ_C (C^2HCl_3) 12 signals observed as expected; diagnostic signals at 14.1 (SCH_3), 72.3 (CHO), 75.9 ppm (OCH_2S); EI-MS: *m/z* 216 (1.5%, $M^{+\bullet}$), 169 (18%, $[M-CH_3S^{\bullet}]^+$), 139 (24%, $[M-{}^{\bullet}CH_2OCH_2SCH_3]^+$), 111 (5%, $C_8H_{15}^+$), 97 (18%, $C_7H_{13}^+$), 83 (100%, $CH_2=CH-\overset{+}{C}H-CH(CH_3)_2$), 69 (27%, $C_5H_9^+$), 61 (22%, $CH_2-\overset{+}{S}CH_3$), 55 (25%, $C_4H_7^+$) and 41 (10%, $C_3H_5^+$).

General procedure for the preparation of chloromethyl ethers 3–7. The chloromethyl ethers were prepared in small quantities from the corresponding MTM ethers when required. Sulphuryl chloride (0.34 g, 2.5 mmol) in dichloromethane (5 ml) was added dropwise to a stirred solution of the homochiral MTM ether (2.5 mmol) in dichloromethane (8 ml). A small amount of effervescence (SO_2) was observed on addition. After stirring for 30 min at room temperature, the solvent and methanesulphenyl chloride by-product were removed by rotary evaporation and high vacuum. The products were used in the derivatization reactions without further purification. Yields and analytical data are presented as follows.

(S)-(+)-Tetrahydro-5-oxo-2-furanmethyl chloromethyl ether 3. Prepared from (*S*)-(+)-tetrahydro-5-oxo-2-furanmethyl MTM ether (0.44 g, 2.5 mmol). Yield: 0.39 g (95%) as a clear liquid. $[\alpha]_D^{20}$ +23° (*c* = 1.0, $CHCl_3$); IR: ν_{max} (thin film) 1780 (C=O_{STR}, lactone), 1180 (C(=O)–O–C_{STR}, ester), 1070 (C–O–C_{STR}, ether), 650 cm^{-1} (C–Cl_{STR}); NMR: δ_H (C^2HCl_3) 2.0–2.8 (CH_2–CH_2, m, 4H), 3.8 (CH_2–O, m, 2H), 4.65 (CH, m, 1H), 5.45 ppm (O–CH_2–S, s, 2H); NMR: δ_C (C^2HCl_3) 23.7 (CH_2–CH_2–CH), 28.2 (CH_2C=O), 69.2 (O–CH), 78.6 (CH_2–O), 95.4 (O–CH_2–Cl), 177.0 ppm (C=O); EI-MS: *m/z* 129 (7%, $[M-Cl^{\bullet}]^+$), 114 (7%, $[M-CH_3Cl]^{+\bullet}$), 99 (7%, $[M-ClCH_2O^{\bullet}]^+$), 85 (100%, $[M-{}^{\bullet}CH_2OCH_2Cl]^+$), 49/51 (6%, CH_2Cl^+) and 36/38 (4%, HCl^+).

(S)-(+)-2-Methylcarboxypropyl chloromethyl ether 4. Prepared from (*S*)-(+)-2-methylcarboxypropyl MTM ether (0.44 g, 2.5 mmol). Yield: 0.39 g

(93%) as a pale yellow liquid. IR: ν_{max} (thin film) 1745 (C=O_{STR}, ester), 1200 (C(=O)–O–C_{STR}, ester), 1125 (C–O–C_{STR}, ether), 640 cm^{-1} (C–Cl_{STR}); NMR: δ_H (C^2HCl_3) 1.2 (CH_3CH, d, 3H), 2.7 (CH, m, 1H), 3.7 (CH_3–OCO and CH_2–O, s and d, 5H), 5.4 ppm (O–CH_2-Cl, s, 2H); NMR: δ_C (C^2HCl_3) 13.84/14.0 (CH_3–CH), 39.5/40.1 (CH), 51.78/51.9 (CH_3OCO), 69.7/71.9 (CH_2–O), 82.8 (O–CH_2–Cl), 175.1 ppm (C=O).

(S)-(−)-1-Methylcarboxyethyl chloromethyl ether **5**. Prepared from (*S*)-(−)-1-methylcarboxyethyl MTM ether (0.41 g, 2.5 mmol). Yield: 0.36 g (95%) as a pale yellow liquid. Found: C, 39.49; H, 6.10 ($C_5H_9O_3Cl$ requires C, 39.36; H, 5.95%). $[\alpha]_D^{20}$ −129° (*c* = 1.0, $CHCl_3$); IR: ν_{max} (thin film) 1730 (C=O_{STR}, ester), 1200 (C(=O)–O–C_{STR}, ester), 1100 cm^{-1} (C–O–C_{STR}, ether); NMR: δ_H (C^2HCl_3) 1.45 (CH_3CH, d, 3H) 3.8 (CH_3–OCO, s, 3H), 4.45 (CH, q, 1H), 5.55 ppm (O–CH_2–Cl, s, 2H); NMR: δ_C (C^2HCl_3) 18.0 (CH_3–CH), 52.0 (CH_3OCO), 72.7 (CH–O), 80.8 (O–CH_2–Cl), 172 ppm (C=O).

N-Acetyl (S)-(−)-2-pyrrolidinemethyl chloromethyl ether **6**. Prepared from N-acetyl-(*S*)-(−)-2-pyrrolidinemethyl MTM ether (0.51 g, 2.5 mmol). Yield: 0.46 g (97%) as a clear oil. IR: ν_{max} (thin film) 1640 (C=O_{STR}, amide), 1420 (C–N_{STR}, amide), 1040 (C–O–C_{STR}, ether), 640 cm^{-1} (C–Cl_{STR}); NMR: δ_H (C^2HCl_3) 1.8–2.2 (CH_2–CH_2, m, 4H), 2.2 (CH_3CO, s, 3H), 3.5 (CH_2–N, t, 2H), 3.75 (CH_2–O, d, 2H), 4.25 (CH, m, 1H), 5.4 ppm (O–CH_2–Cl, s, 2H); EI-MS: *m/z* 191/3 (1%, $M^{+\bullet}$), 156 (13%, $[M-Cl]^+$), 126 (28%, $[M-ClCH_2O^{\bullet}]^+$), 112 (95%, $[M-{}^{\bullet}CH_2OCH_2Cl]^+$), 70 (100%, $[M-(CH_2C=O+{}^{\bullet}CH_2OCH_2Cl)]^+$) and 36/38 (20%, HCl^+).

(1S, 2R, 5S)-(+)-Menthyl chloromethyl ether **7**. Prepared from (1*S*,2*R*,5*S*)-(+)-menthyl MTM ether (0.54 g, 2.5 mmol). Yield: 0.47 g (91%) as a clear liquid. $[\alpha]_D^{20}$ +31° (*c* = 1.0, $CHCl_3$); IR: ν_{max} (thin film) 1115 (C–O–C_{STR}, ether), 640 cm^{-1} (C–Cl); NMR: δ_H (C^2HCl_3) 0.7–2.3 (CH_3, CH_2 and CH, 18H), 3.55 (CH–O, dt, 1H), 5.55 ppm (O–CH_2-Cl, s, 2H); NMR: δ_C (C^2HCl_3) 15–48 (9 signals from the menthyl unit), 78.97 (CH–O), 81.2 ppm (O–CH_2–Cl).

Reagents **13** *and* **14**: *acyl chlorides*

(S)-(+)-Tetrahydro-5-oxo-2-furancarbonyl chloride **13**. Acid **8** (5 g; 0.038 mol) was heated with oxalyl chloride (6.71 ml; 0.077 mol) in dry benzene (10 ml) at 60–70°C for 5 h. Benzene and excess oxalyl chloride were removed under vacuum and the residual oil was distilled under vacuum (110–120°C/0.2 mmHg (lit. [36] 76–82°C/0.02 mmHg)) to yield 4.97 g (87%) of **13** as a clear oil; $[\alpha]_D^{20}$ +4.0° (*c* = 2, $CHCl_3$); IR: ν_{max} (thin film) 1800 (C=O_{STR}, lactone and acid chloride), 1170 and 1140 (C–O), 970 and 910 cm^{-1} (C–Cl); NMR: δ_H (C^2HCl_3) 2.3–2.8 (CH_2–CH_2, m, 4H), 5.1 ppm (CH, m, 1H); EI-MS: *m/z* 148/150 (1.2%, $M^{+\bullet}$), 85 (100%, $[M-{}^{\bullet}COCl]^+$), 36/38 (13%, HCl^+).

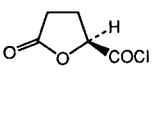

13

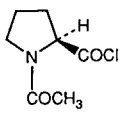

14

N-Acetyl-(S)-(−)prolyl chloride **14**. (*S*)-(−)-Proline (4 g; 0.035 mol) was dissolved in 2 *M* NaOH (15 ml). The stirred solution was cooled in ice while acetic anhydride (20 ml) was added dropwise. The reaction was left to stand for 18 h before acidifying with 2 *M* H_2SO_4. The product was extracted into chloroform (2 × 150 ml) which was then dried ($MgSO_4$). After filtering, the solvent was removed by rotary evaporation. Ethyl acetate (40 ml) was added to the residue and the white crystalline product was filtered then washed with cold ethyl acetate. The product was dried in an oven at 40°C yielding 3.61 g (66%) of N-acetyl-L-proline as a white solid. M.p. 116–118°C (lit. = 118°C [37]). $[\alpha]_D^{20}$ −101° (*c* = 2.0, H_2O) [commercial N-acetyl-L-proline $[\alpha]_D^{20}$ −100° (*c* = 2.0, H_2O)]. Lit. [37] $[\alpha]_D^{20}$ = −115° (*c* = 2.0, H_2O); IR: ν_{max} (KBr disc) 3600–2300 (O-H_{STR}, acid), 1720 (C=O_{STR}, acid) and 1600 cm^{-1} (C=O_{STR}, amide); NMR; δ_H (C^2HCl_3) 2.1 (CH_3CO, s, 3H), 1.8–2.3 (CH_2–CH_2, m, 4H), 3.5 (N–CH_2, m, 2H), 4.4 (CH, dt, 1H) and 8.5 ppm (COOH, s, 1H); NMR; δ_C (C^2HCl_3) 22.0/22.8 and 24.6 (CH_2–CH_2), 28.7 (CH_3CO), 46.6/48.3 (CH_2–N), 59.3/60.4 (CH), 171.7 and 173.6 ppm (C=O, acid and C=O, amide); EI-MS: *m/z* (probe) 157 (2%, $M^{+\bullet}$), 113 (28%), 112 (25%, $[M-{}^{\bullet}COOH]^+$), 85 (16%), 70 (100%, $[M-({}^{\bullet}COOH + CH_2CO)]^+$), 43 (63%, CH_3CO^+).

To a stirred solution of N-acetyl-(*S*)-(−)-proline

(1.56 g, 10 mmol) in dry, ethanol-free dichloromethane (40 ml) was added dropwise thionyl chloride (2.3 g, 20 mmol). The reaction was stirred for 1 h at room temperature before removing the solvent and excess thionyl chloride under vacuum. The N-acetyl-(S)-(−)-prolyl chloride product was a light orange viscous oil with a yield of 1.83 g (104%) indicating that some thionyl chloride was still present (trapped in the oil). IR: ν_{max} (thin film) 1798 (C=O$_{STR}$, acid chloride) and 1650 cm^{-1} (C=O$_{STR}$, amide); NMR: δ_H (C^2HCl_3) 1.8–2.4 (CH_2–CH_2, m, 4H), 2.15 (CH_3CO, s, 3H), 3.65 (–CH_2–N, dt, 2H) and 4.75 ppm (CH, t, 1H); NMR: δ_C 21.8/22.3 and 24.5 (CH_2–CH_2), 28.8/31.2 (CH_3CO), 47.0/48.0 (–CH_2–N), 67.3/69.1 (CH), 170.3 and 173.5 ppm (C=O, amide and C=O, acid chloride); EI-MS: *m/z* 139 (18%, $[M-HCl]^{+\bullet}$), 112 (48%, $[M-{}^{\bullet}COCl]^+$) 70 (100%, $[M-(CH_2CO+{}^{\bullet}COCl)]^+$), 43 (22%, CH_3CO^+) and 36/38 (3:1, 5%, HCl^+).

General derivatization procedures for the secondary alcohols

*Homochiral iodides **1** and **2** as reagents*

The $Hg(BF_4)_2$ reagent was prepared from yellow mercury(II) oxide according to a literature method [38]. A solution of alkan-2-ols (0.5 mmol) and the iodide (1 mmol) in dichloromethane (2 ml) were added to dry mercury(II) tetrafluoroborate (0.19 g; 0.5 mmol). The mixture was stirred for 2 h at room temperature before being treated with 3 *M* potassium hydroxide until basic [31,32]. The regenerated mercury(II) oxide was filtered off and the organic layer was separated and dried before undergoing GC and GC–MS analyses.

*Homochiral chloromethyl ethers **3–7** as reagents*

To a solution containing alkan-2-ols (0.125 mmol) in dichloromethane (0.5 ml) under an argon atmosphere was added diisopropylethylamine (80 mg, 0.62 mmol) and one of the chloromethyl ethers (0.377 mmol) in dichloromethane (0.5 ml). The mixture was allowed to react for 5 h before taking a sample (0.2 ml). The solvent was removed from the sample (argon gas) and the product was extracted from hydrochloric acid (2 ml of a 0.5 *M* solution) into ethyl acetate (1 ml). After washing with water and drying, the sample underwent GC–MS and/or GC analysis.

*Homochiral acyl chloride **13** as reagent*

Derivatizations with (*S*)-(+)-tetrahydro-5-oxo-2-furancarbonyl chloride followed a literature method [39]. The alkan-2-ol (0.14 mmol) was added to pyridine (80 μl) and the mixture was stirred and cooled to 0°C. A 2 *M* solution of acid chloride **13** in dichloromethane (100 μl; 0.2 mmol) was added and the reaction mixture was allowed to warm to room temperature. Two drops of 1 *M* hydrochloric acid solution was added followed by hexane (2 ml). The layers were separated and the organic phase was dried by passing through anhydrous magnesium sulphate. This solution was then analysed directly by GC and GC–MS. The mass spectrum for the product obtained from heptan-2-ol contained the following diagnostic ions: EI-MS: *m/z* 229 $[M+H]^+$, 213 $[M-{}^{\bullet}CH_3]^+$, 185 $[M-C_3H_7]^+$, 157 $[M-C_5H_{11}]^+$, 143 $[M-C_6H_{13}]^+$ and 85 $[M-{}^{\bullet}COOC_7H_{15}]^+$.

*Homochiral acyl chloride **14** as reagent*

To N-acetyl-(*S*)-(−)-prolyl chloride (0.35 g, 2 mmol) in toluene (15 ml) was added the alkan-2-ol mixture (27 mg, 0.25 mmol). The reaction was stirred at room temperature for 1 h. A 1-ml sample was taken and the solvent was removed. Ethyl acetate was added and the sample washed with water. This was dried ($MgSO_4$) and filtered, then analysed by GC and GC–MS.

RESULTS AND DISCUSSION

Extent of the derivatization reactions

The derivatization of alkan-2-ols [$RCH(OH)CH_3$] with the homochiral chloromethyl ethers **3–7** and with the two acyl chlorides **13** and **14** proceeded rapidly, with little or none of the alkanol analytes remaining at the end of the stated reaction time. In the presence of mercury(II) tetrafluoroborate, the same alcohols reacted with the iodide reagents **1** and **2** to a much lesser extent. Even after extending the reaction time from 2 to 24 h, yields were typically 10% in our hands. Whilst GC separation of the resulting diastereoisomeric ethers was successful (see below), the low yield of this reaction undermines its application. Detection limits of the method would be poor and kinetic resolution could occur, leading to erroneous results.

TABLE I

SEPARATION FACTORS (α) AND RESOLUTION VALUES (R_s) FOR DIASTEREOISOMERIC DERIVATIVES OF OCTAN-2-OL

t_R = Retention time; NR = Not resolved; * = not sufficiently resolved to calculate R_s.

Derivatizing agent	t_R (min)	α	R_s
1[a]	10.02/10.22	1.021	1.57
2[b]	16.28/16.73	1.028	1.10
3[c]	19.41/19.76	1.019	1.36
4[d]	23.77/24.20	1.019	1.25
5[e]	17.50/17.71	1.012	*
6[f]	14.41/14.55	1.010	*
7[g]	13.37	NR	NR
13[h]	10.71	NR	NR
14[i]	12.20/12.90	1.060	1.73

[a] BP-1, 12 m × 0.22 mm I.D. fused-silica column with 0.25 μm film thickness [80°C (2 min) to 220°C (at 10°C min^{-1})].

[b] BP-5, 12 m × 0.33 mm I.D. fused-silica column with 0.5 μm film thickness (isothermal 103°C). In this case the somewhat better separation factor of 1.036 was obtained with a BP-20 column (12 m × 0.32 mm I.D., 0.5 μm film thickness at 93°C).

[c] DB-1701, 30 m × 0.25 mm I.D. fused-silica column with 0.2 μm film thickness (isothermal 180°C).

[d] DB-1701 column as above[c] but isothermal 130°C.

[e] BP-5 as above[b] but isothermal 113°C.

[f] FFAP-CB 25 m × 0.32 mm I.D. fused-silica column with 0.3 μm film thickness (isothermal 200°C).

[g] BP-5 as above[b] but 120 to 220°C (at 5°C min^{-1}).

[h] The result shown is for the heptan-2-ol derivatives chromatographed on the BP-1 column[a]. Various temperature programs and columns were tried but separation was not achieved. The octan-2-ol derivatives have been reported to be inseparable on all but very polar columns [39].

[i] BP-5 column as above[b] but isothermal 170°C.

Separations of the diastereoisomeric derivatives

Undoubtedly, quantitative application of any of the reagents prepared in this study would require further purification to remove traces of the unwanted enantiomer. However, for the initial assessment of the efficiency of each "homochiral" reagent, the compounds were used without such purification. To illustrate results that are typical for alkan-2-ols, the case of octan-2-ol is described first.

The diastereoisomers produced from racemic octan-2-ol after derivatization with each of the various reagents were analysed by GC and/or by GC–MS. The results, giving both the separation factors (α) and resolutions (R_s), are summarized in Table I. In each case, the results shown are for separations obtained under conditions that were optimized in terms of stationary phase and column temperature.

Baseline separations were achieved for the ethers resulting from reaction of octan-2-ol with iodides **1** and **2**, and near-baseline separations resulted from derivatization with chloromethyl ethers **3** and **4**. Typical chromatograms are shown in Figs. 3 and 4b for the derivatives **15** and **16** arising from the furan-based reagents **1** and **3**, respectively. The elution order for the octan-2-ol diastereoisomeric derivatives was determined by separate analysis of commercially available, enantiomerically pure (*R*)- and (*S*)-octan-2-ols. MS confirmed the identity of the separated diastereoisomers. For each pair of diastereoisomers, **15** and **16**, the two EI spectra were virtually identical (Figs. 5 and 6, respectively).

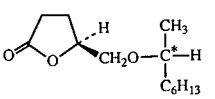

15

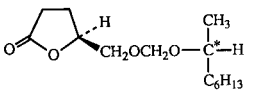

16

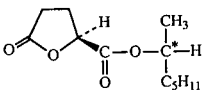

17

It is noteworthy from Table I that the chloromethyl ether derived from menthol, **7**, failed to give a separation when reacted with alkan-2-ols, and that the lactate-derived reagent **5** and proline-based reagent **6** barely caused the resulting diastereoisomers to separate by GC. On the other hand, the proline-based acyl chloride, **14**, produced esters from racemic octan-2-ol that were well separated, whereas the furan-based acyl chloride, **13**, did not induce resolution of the corresponding diastereoisomeric esters, **17**, on the columns tested. This latter observation is in agreement with literature [39] that suggests that diastereoisomers produced from the reagent **13** only separate on very polar stationary phases. This behaviour of the diastereoisomeric esters, **17**, should be contrasted with that of the diastereoisomeric ethers, **15**, derived from reagent **1**. The ethers **15** are well separated even on a non-polar

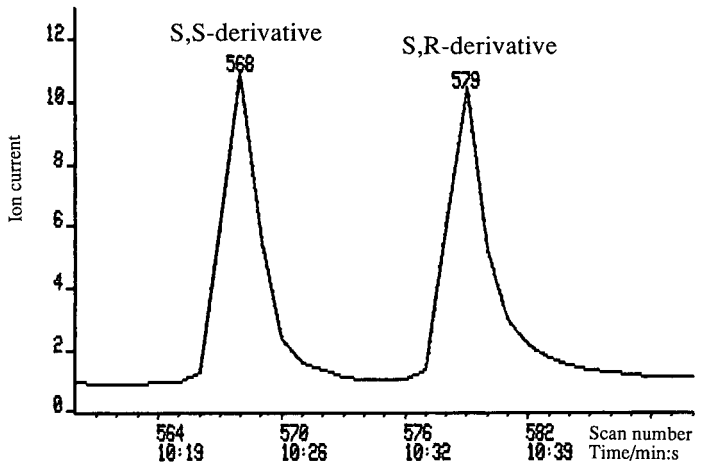

Fig. 3. Part of the total ion current chromatogram obtained by GC–MS after reacting reagent **1** with racemic octan-2-ol to give diastereoisomers **15**. The diastereoisomer from (*S*)-octan-2-ol eluted before that from the (*R*)-isomer. GC conditions: 12 m × 0.22 mm I.D. BP-1; film thickness, 0.25 μm; column temperature, 80–220°C at 10°C min^{-1}.

BP-1 column. Presumably, when the COO ester functionality of **17** is replaced by a CH_2O group in **15**, the reduction in polarity favours separation on less polar stationary phases.

These results are typical for a range of alkan-2-ols. It is instructive to examine the separation factors and resolutions across a range of alkan-2-ols following reaction with one of the homochiral derivatizing agents because it was generally observed that separation improved with increasing chain-length. For example, Table II shows the separations obtained for $CH_3(CH_2)_nCH(OH)CH_3$ (n = 2–5) after derivatization with chloromethyl ether **3** on a DB-1701 column at different temperatures, such that all five alkan-2-ol derivatives elute in the range 9.77–9.97 min. Notably, at a fixed retention time, the resolution (R_s) of the diastereoisomers increases markedly with increasing carbon chain length. The same trend, of slight increases in α and large increases in R_s with increasing chain length, was noted following derivatizations with acyl chloride reagent **14**, (+)-*trans*-chrysanthemoyl chloride [40] and chloromethyl ethers **4** and **5**. For example, at a constant retention time, the separation factors and resolutions of the diastereoisomeric (+)-*trans*-chrysanthemate esters [6] of racemic alkan-2-ols analysed on an SE-30 column (33 m × 0.25 mm) were: hexan-2-ol, α = 1.022, R_s = 0.79; heptan-2-ol, 1.036, 1.23; octan-2-ol, 1.041, 1.52 [40]. Such improvements in resolution with increasing carbon chain length may be rationalized by considering the structures of the compounds, say, **18**. It is assumed that the two hydrophobic chains in a given pair of diastereoisomers (*i.e.* the CH_3 and the $(CH_2)_nCH_3$ group) interact with the non-polar stationary phase and are involved in the chiral recognition mechanism. Then, the greater the dissimilarity of the two groups (*i.e.* as n increases), the more easily the stationary phase is able to differentiate them, and so the greater is the separation of the diastereoisomeric pair. Thus, when n = 0, structures **18a** and **18b** are identical molecules, but as n increases, the binding sites are increasingly able to differentiate a methyl group and a larger chain. This is reflected by the increase in the resolution values, as observed in Fig. 7, showing data from Table II in graphical form. The trend is most marked amongst the lower alkan-2-ol homologues. As the carbon chain length continues to increase, increasing n by one among the higher homologues gives little extra potential for molecular

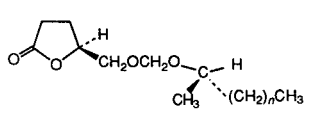

18a

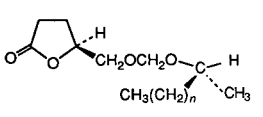

18b

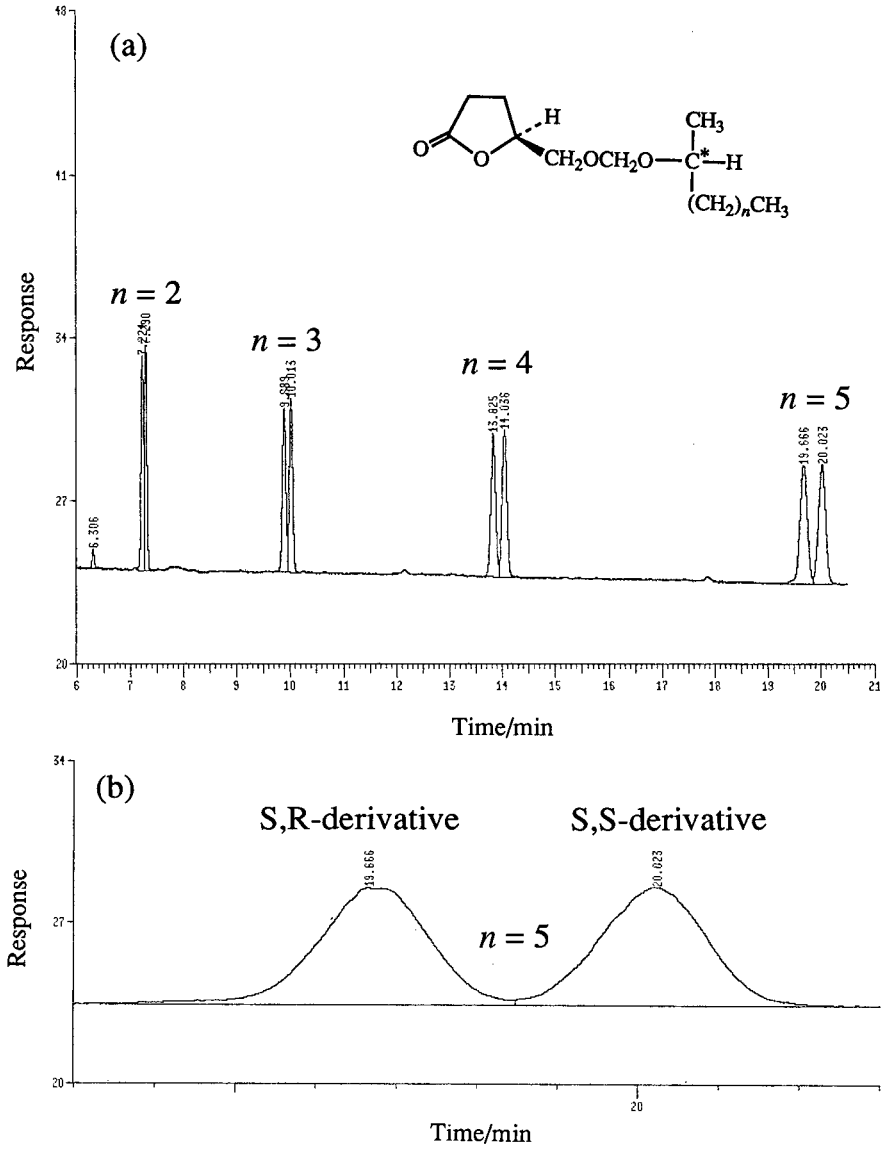

Fig. 4. (a) Chromatogram showing the GC resolution of a mixture of racemic pentan-2-ol, hexan-2-ol, heptan-2-ol and octan-2-ol after derivatization with chloromethyl ether **3**. (b) Close-up of the same chromatogram showing the separation of the enantiomers of octan-2-ol as diastereoisomeric derivatives, **16**. The diastereoisomer from (*R*)-octan-2-ol eluted before that from the (*S*)-isomer. GC conditions: 30 m × 0.25 mm I.D. DB-1701; film thickness, 0.25 μm; column temperature, 180°C.

recognition by the binding site. Hence, the resolution values would be expected to become almost constant with larger values of *n*. Accordingly, Fig. 7 shows a levelling off of the resolution values consistent with this hypothesis. The view that such diastereoisomers are separated most effectively when there is a large difference in size between the two hydrophobic chains receives strong support from the (+)-*trans*-chrysanthemate esters of heptan-2-ol and heptan-3-ol. On an SE-30 column, the R_s value for the diastereoisomeric derivatives of heptan-2-ol, where the stationary phase must differentiate C_1 and

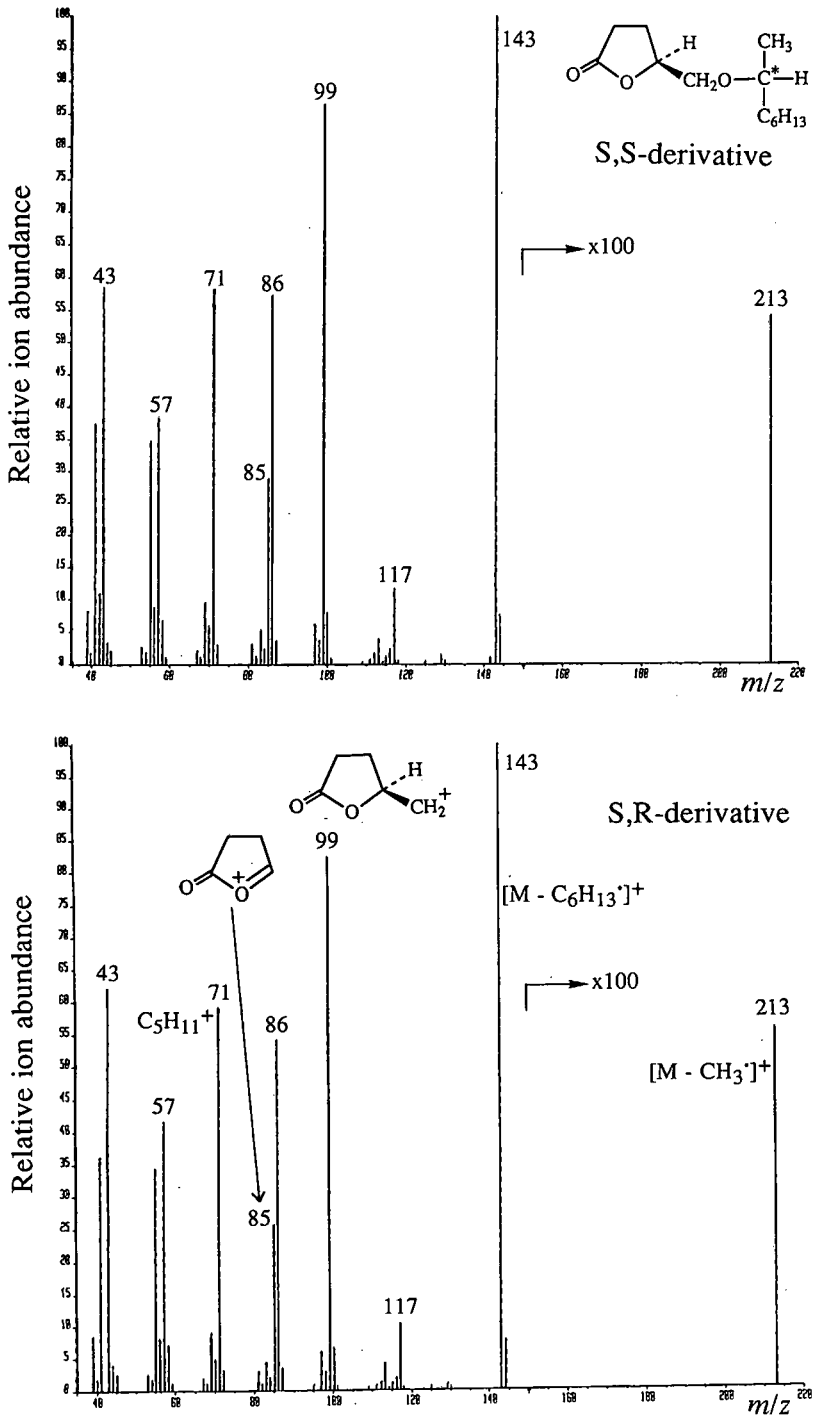

Fig. 5. EI Mass spectra of the resolved diastereoisomers from octan-2-ol, **15**. Top: *S,S*-isomer; bottom: *S,R*-isomer of derivative **15**.

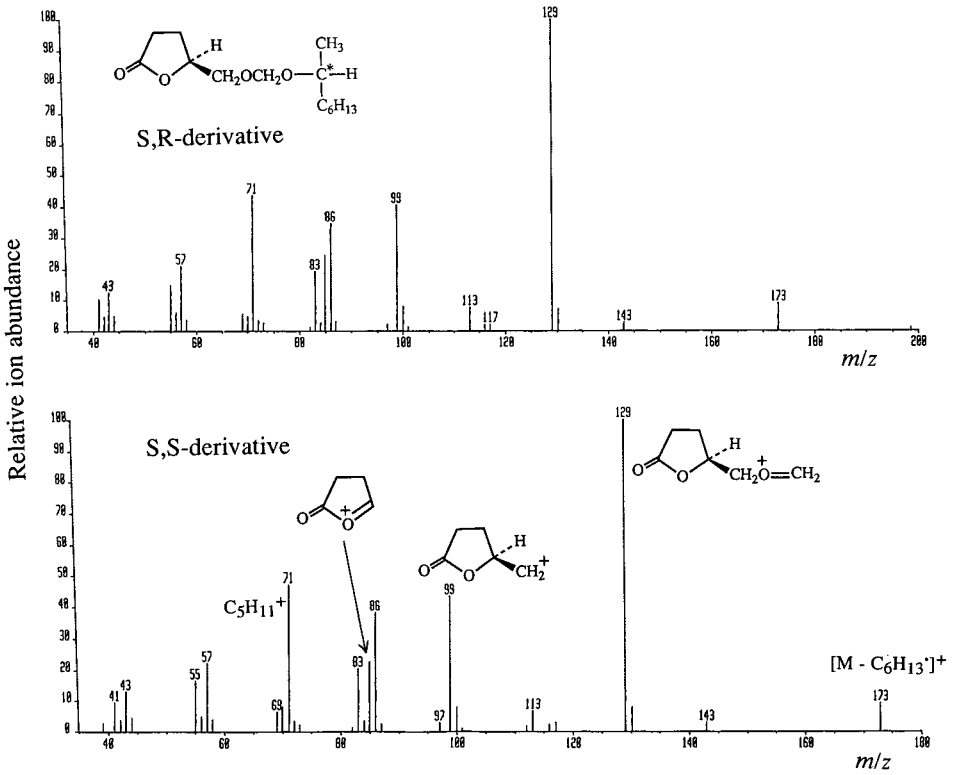

Fig. 6. EI Mass spectra of the resolved diastereoisomers from octan-2-ol, **16**. Top: *S,R*-isomer; bottom: *S,S*-isomer of derivative **16**.

C_5 chains, was measured to be 2.5 times greater than that of the heptan-3-ol derivatives, where the more demanding differentiation of C_2 and C_4 chains is required [40]. The dependence of separation factors on the relative bulk of side-chains in diastereoisomers has been noted previously (see, for example, ref. 41).

Another interesting trend becomes apparent when the octan-2-ol derivatives from reagents **2**, **5** and **4** are compared. The structures of the products (**19**, **20** and **21**, respectively) are similar except for the number of bonds between the chiral centre derived from the original analyte and that from the homochiral reagent in the resulting diastereoisomers. The number of bonds separating the chiral centres is 3, 4 and 5, respectively. Separation factors for these derivatives on a range of stationary phases are given in Table III. It would be expected that diastereoisomers with fewer bonds between chiral centres would be separated more efficiently. In fact, it has been assumed that diastereoisomers with 4 or more

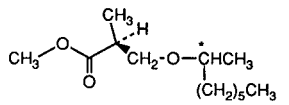

19

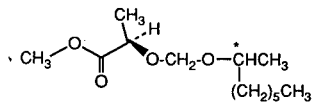

20

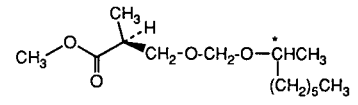

21

bonds between the chiral centres are indistinguishable by gas chromatography [1,3,42]. This concept is not compatible with the differences in the separation

TABLE II

RETENTION TIMES AND R_s VALUES FOR THE DIASTEREOISOMERIC DERIVATIVES **18** FOR A RANGE OF ALKAN-2-OLS FOLLOWING DERIVATIZATION WITH CHLOROMETHYL ETHER, **3**

These analyses were performed on a DB-1701 fused-silica column (30 m × 0.25 mm; 0.2 μm film thickness).

Alcohol	n	Oven temp. (isothermal, °C)	t_R (min)	R_s
2-Pentanol	2	170	9.77/9.88	0.77
2-Hexanol	3	180	9.77/9.90	0.93
2-Heptanol	4	190	9.84/9.97	1.00
2-Octanol	5	200	9.77/9.89	1.04

efficiencies shown in Table III. As expected, the best separations across the range of stationary phases were obtained for derivatives **19**, with three bonds between chiral centres, but the diastereoisomers with 5 bonds between chiral centres (**21**) were separated to a greater extent than those containing 4 bonds between the chiral centres (**20**). This result may be explained if it is assumed that interactions between the chiral centres are significant to the separation mechanism. This fits with the theory that generally the fewer bonds between the chiral centres, the closer their proximity, the greater their interactions and the greater is the separation of the diastereoisomers. However, if more distant chiral centres can be brought into close proximity by intramolecular interactions then separations could also be improved. In other words, chiral centres that have a large through-bond distance could take up conformations that bring them close through space. It is likely that the chiral centres of diastereoisomers **21**, with 5 bonds between them, can approach closer in space than the chiral centres of diastereoisomers **20**, with only 4 bonds between them. This may lead to stronger interactions in products **21** than in products **20**. However, the relevance of any such conformations at the high temperatures experienced in GC and in the presence of an interactive stationary phase are unclear.

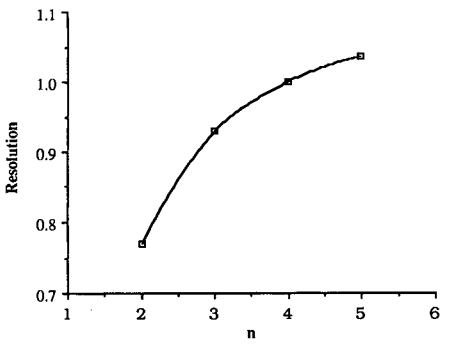

Fig. 7. The variation of GC resolution with carbon chain length for diastereoisomeric derivatives, **18**. See structures **18** for definition of n. When $n = 2$, the original analyte was pentan-2-ol; $n = 3$, hexan-2-ol; $n = 4$, heptan-2-ol; $n = 5$, octan-2-ol. The GC column used was coated with DB-1701, and the column temperature was adjusted in different analyses so that each had approximately the same retention time.

TABLE III

THE α VALUES FOR DIASTEREOISOMERS **19**, **20** AND **21** RESULTING FROM DERIVATIZATION OF OCTAN-2-OL WITH REAGENTS **2**, **5** AND **4**, RESPECTIVELY

Retention times (min) are given in parentheses, and the isothermal column temperatures on a range of different columns are also stated. NR = Not resolved.

Diastereoisomers	α		
	BP-1[a]	BR-5[b]	BP-20[c]
19	1.026 (18.15/18.62) 105°C	1.028 (16.28/16.73) 103°C	1.036 (18.72/19.40) 93°C
20	NR (19.25) 115°C	1.012 (17.50/17.71) 113°C	NR (17.38) 115°C
21	1.012 (15.86/16.06) 130°C	1.018 (16.79/17.09) 125°C	NR (19.45) 123°C

[a] 12.5 m × 0.32 mm, 1.0 μm film thickness.
[b] 12 m × 0.33 mm, 0.5 μm film thickness.
[c] 12 m × 0.32 mm, 0.5 μm film thickness.

CONCLUSIONS

Some new homochiral derivatizing agents have been prepared and initial investigations suggest that (*S*)-(−)-tetrahydro-5-oxo-2-furanmethyl iodide **1**, (*S*)-(+)-tetrahydro-5-oxo-2-furanmethyl chloromethyl ether **3**, and (S)-(+)-2-methylcarboxypropyl chloromethyl ether **4** are the most promising reagents. To be useful, conditions for the complete reaction of iodide **1** with nucleophilic analytes have

yet to be found. Chloromethyl ethers **3** and **4** are highly reactive electrophiles under very mild conditions so their reactions with alcohols go rapidly to completion, thus avoiding the potential effects of kinetic resolution. Being very reactive, these reagents may be applicable to a broad range of chiral nucleophilic analytes. When reacted with alkan-2-ols, the resulting diastereoisomers have five bonds between chiral centres. This could be considered a disadvantage, unlikely to allow resolution by GC [1,3,42]. However, good resolutions have been observed and these are superior to those achieved with diastereoisomers with similar structures but having four bonds between chiral centres.

ACKNOWLEDGEMENT

We gratefully acknowledge the SERC for the award of a studentship (to D.A.R.).

REFERENCES

1 W. A. König, *The Practice of Enantiomer Separation by Capillary Gas Chromatography*, Hüthig, Heidelberg, 1987.
2 A. M. Krstulović, *Chiral Separations by HPLC: Applications to Pharmaceutical Compounds*, Ellis Horwood, Chichester, 1989, pp. 27–28.
3 S. G. Allenmark, *Chromatographic Enantioseparations*, Ellis Horwood, Chichester, 1988, pp. 31–33.
4 V. Schurig, *Kontakte (Darmstadt)*, 1 (1986) 3–22.
5 C. H. Lochmüller and R. W. Souter, *J. Chromatogr.*, 113 (1975) 283–302.
6 A. B. Attygalle, E. D. Morgan, R. P. Evershed and S. J. Rowland, *J. Chromatogr.*, 260 (1983) 411–417.
7 C. J. W. Brooks, M. T. Gilbert and J. D. Gilbert, *Anal. Chem.*, 45 (1973) 896–902.
8 R. S. Burden, A. H. B. Deas and T. Clark, *J. Chromatogr.*, 391 (1987) 273–279.
9 L. Addadi, S. Weinstein, E. Gati, I. Weissbush and M. Lahav, *J. Am. Chem. Soc.*, 104 (1982) 4610–4617.
10 B. Halpern and J. W. Westley, *J. Chem. Soc., Chem. Commun.*, (1966) 34–35.
11 R. W. Souter, *J. Chromatogr.*, 108 (1975) 265–274.
12 R. H. Liu, W. W. Ku and M. P. Fitzgerald, *J. Assoc. Off. Anal. Chem.*, 66 (1983) 1443–1446.
13 J. Hermansson and E. von Bahr, *J. Chromatogr.*, 221 (1980) 109–117.
14 B. Silber and J. Riegelman, *J. Pharm. Exp. Ther.*, 215 (1980) 643–648.
15 S. D. Roy and H. K. Lim, *J. Chromatogr.*, 431 (1988) 210–215.
16 M. Hasegawa and I. Matsubara, *Anal. Biochem.*, 63 (1975) 308–320.
17 R. Klein, *J. Chromatogr.*, 170 (1979) 468–472.
18 M. Horiba, H. Kitaharo, H. Takahashi, S. Yamamota, A. Muramo and N. Oi, *Agric. Biol. Chem.*, 43 (1979) 2311–2316.
19 W. A. König, W. Rahn and J. Eyem, *J. Chromatogr.*, 133 (1977) 141–146.
20 W. A. König, *The Practice of Enantiomer Separation by Capillary Gas Chromatography*, Hüthig, Heidelberg, 1987, p. 71.
21 F. Raulin and B. N. Khare, *J. Chromatogr.*, 75 (1973) 13–18.
22 J. P. Kamerling, M. Duran, G. J. Gerwig, D. Ketting, L. Bruinvis, J. F. G. Vliegenthart and S. K. Wadman, *J. Chromatogr.*, 222 (1981) 276–283.
23 H. Schweer, *J. Chromatogr.*, 243 (1982) 149–152.
24 S. G. Allenmark, *Chromatographic Enantioseparations*, Ellis Horwood, Chichester, 1988, pp. 51–61.
25 K. Blau and G. S. King, *Handbook of Derivatives for Chromatography*, Heyden, London, 1978.
26 W. A. König, *The Practice of Enantiomer Separation by Capillary Gas Chromatography*, Hüthig, Heidelberg, 1987, p. 71–83.
27 W. Deger, G. Gessner, G. Heusinger, G. Singer and A. Mosandl, *J. Chromatogr.*, 366 (1986) 385–390.
28 R. A. W. Johnstone and M. E. Rose, *Tetrahedron*, 35 (1979) 2169–2173.
29 D. A. Rimmer, *Ph.D. Thesis*, The Open University, Milton Keynes, 1990.
30 J. Barluenga, L. Alonso-Cires, P. J. Campos and G. Asensio, *Synthesis*, (1983) 53–55.
31 J. Barluenga, L. Alonso-Cires, P. J. Campos and G. Asensio, *Synthesis*, (1983) 649–651.
32 U. Ravid, R. M. Silverstein and L. R. Smith, *Tetrahedron*, 34 (1978) 1449–1452.
33 K. Mori, *Tetrahedron*, 31 (1975) 3011–3012.
34 J. P. Vigneran and R. Meric, *Tetrahedron Lett.*, 23 (1982) 5051–5054.
35 K. Yamada, K. Kato, H. Nagase and Y. Hirato, *Tetrahedron Lett.*, (1976) 65–66.
36 R. E. Doolittle, J. M. Tumlinson, A. T. Proveaux and R. R. Heath, *J. Chem. Ecol.*, 6 (1980) 473–485.
37 *Dictionary of Organic Compounds*, Chapman & Hall, London, 5th ed., 1982, p. 4773.
38 J. Barluenga, L. Alonso-Cires and G. Asensio, *Synth. Commun.*, (1979) 962–964.
39 R. E. Doolittle and R. R. Heath, *J. Org. Chem.*, 49 (1984) 5041–5050.
40 S. Lowes and M. E. Rose, unpublished results.
41 B. Feibush, *J. Chromatogr.*, 436 (1988) 517–519.
42 H. C. Rose, R. L. Stern and B. L. Karger, *Anal. Chem.*, 38 (1966) 469–472.

Journal of Chromatography, 598 (1992) 267–276
Elsevier Science Publishers B.V., Amsterdam

CHROM. 24 014

Novel long-chain *anteiso*-alkanes and *anteiso*-alkanoic acids in Antarctic rocks colonized by living and fossil cryptoendolithic microorganisms

Genki I. Matsumoto*,☆

Department of Chemistry, College of Arts and Sciences, University of Tokyo, Komaba, Meguro-ku, Tokyo 153 (Japan)

E. Imre Friedmann

Polar Desert Research Center, Department of Biological Science, Florida State University, Tallahassee, FL 32306 (USA)

Kunihiko Watanuki

Department of Chemistry, College of Arts and Sciences, University of Tokyo, Komaba, Meguro-ku, Tokyo 153 (Japan)

Roseli Ocampo-Friedmann

Department of Biology, Florida A&M University, Tallahassee, FL 32307 (USA)

(First received September 11th, 1991; revised manuscript received January 14th, 1992)

ABSTRACT

Saponified extracts of rock samples colonized by cryptoendolithic microbial communities from the McMurdo Dry Valleys of Southern Victoria Land, Antarctica, were separated into hydrocarbon and fatty acid fractions by silica gel column chromatography. Hydrocarbons and methyl esters of fatty acids were analyzed by capillary gas chromatography–mass spectrometry. Unusually, a suite of long-chain *anteiso*-alkanes (*a*-C_{20} to *a*-C_{30}) and *anteiso*-alkanoic acids (*a*-C_{20} to *a*-C_{30}) were detected in many samples, together with straight-chain, branched and/or cyclic and acyclic isoprenoid compounds. These novel compounds are probably derived from unidentified heterotrophic bacteria or symbiotic processes in a unique microbial community in the Antarctic cold desert and suggest the occurrence of a special biosynthetic pathway. Long-chain *anteiso*-alkanes are probably formed through microbial decarboxylation of corresponding *anteiso*-alkanoic acids. They may serve as new biomarkers in environmental and geochemical studies.

INTRODUCTION

Most of Antarctica is covered by an ice sheet approximately 2450 m thick, but ice-free areas are sparsely distributed in coastal regions and inland mountains. The Ross Desert (the McMurdo Dry Valleys) of Southern Victoria Land is the largest ice-free area in Antarctica and covers 2500 km^2. The Ross Desert environment is extremely cold and dry, and the surface is virtually abiotic. Cryptoendolithic microbial communities colonize the near-surface layers of porous rocks, where the rock is warmed by insolation to temperatures above the ambient [1–3]. Several distinct cryptoendolithic microbial communities exist. The most common ones

* Present address: Environmental Information Studies Course, School of Social Information Studies, Ohtsuma Women's University, Kamioyamada-cho 9–1, Tama, Tokyo 206, Japan.

0021-9673/92/$05.00

are the lichen-dominated communities consisting of lichen-forming fungi and green algae, parasymbiotic fungi, free-living fungi and green algae and cyanobacteria, the red *Gloeocapsa* communities (several *Gloeocapsa* species and other cyanobacteria) and the *Hormathonema–Gloeocapsa* communities (formed by several cyanobacteria). All these communities harbor a number of (largely unidentified) heterotrophic bacteria [4]. In the Ross desert, organisms exist near the temperature limit below which life is impossible, and even slight changes in the environment result in death and extinction [5]. Communities in various stages of fossilization occur [6] and are common on Mt. Fleming (unpublished results), which is partly surrounded by the Antarctic ice sheet.

Hydrocarbons and fatty acids are two of the most widely distributed groups of organic compounds in living organisms and natural environments. In geological settings from the Holecene to the Precambrian, these compounds can be used to evaluate sources, maturation, alteration and sedimentary conditions of organic matter in various environments [7–10]. Long-chain *n*-alkanes ($>C_{19}$) with a predominance of odd carbon numbers are believed to originate from the waxes of vascular plants. *Iso*- and/or *anteiso*-alkanes are reported to occur in ancient sediments [11], coals [12] and air–sea interface samples [13]. Their proposed sources are the waxes of vascular plants and/or bacteria [11,12]. Short-chain *n*-alkanoic acids ($<C_{20}$) occur in most living organisms, and long-chain *n*-alkanoic acids (*n*-C_{20} to *n*-C_{34}) are abundant in the waxes of vascular plants [14,15]. Although short-chain *iso*- and *anteiso*-alkanoic acids are major lipids of certain bacteria [16], little is known about the occurrence of long-chain *anteiso*-alkanoic acids ($>C_{19}$) in the natural environment. Here we report capillary gas chromatographic–mass spectrometric (GC–MS) results of the discovery of a series of novel long-chain *anteiso*-alkanes (*a*-C_{20} to *a*-C_{30}) and long-chain *anteiso*-alkanoic acids (*a*-C_{20} to *a*-C_{30}) in rock samples colonized by cryptoendolithic microbial communities of the Ross Desert in Southern Victoria Land, Antarctica, and discuss their possible sources and geochemical and biological significance.

EXPERIMENTAL

Apparatus and chemicals

Care was taken to avoid contamination of samples; glassware rather than plastics was used throughout. Liquid chromatographic-grade organic solvents [hexane, benzene and ethyl acetate (Wako)] were used without any treatment. Silica gel (100 mesh) (Mallinckrodt) was used after heating at 500°C for 2 h to remove organic contaminants. Platinum dioxide (Wako) was used without any treatment. Boron-trifluoride methanol (51:49) (GL Science) was diluted to 14:86 with methanol. Authentic alkanes and alkanoic acids (99%) were purchased from GL Science. The GC–MS measurements were carried out with Shimadzu GCMS QP1000 gas chromatograph–mass spectrometer equipped with a cooled on-column injector.

Sampling sites and samples

The Beacon Supergroup, a Gondwanaland sediment, mainly composed of sandstone, forms the dominant rock type at higher elevations throughout the region [17]. It provides a favorable habitat for cryptoendolithic microorganisms. Rock (sandstone) samples colonized by cryptoendolithic microbial communities were collected from Linnaeus Terrace (77°36′S, 161°05′E, elevation 1600–1650 m) in the Asgard Range and Mount Fleming (77°33′S, 160°07′E, elevation 2200 m) and other localities in the Ross Desert of Southern Victoria Land, Antarctica, during the austral summers of 1977–1986 by E.I.F. and R.O.-F. All samples were kept frozen (−30°C) until analyzed in 1988–1991 by G.I.M. and K.W. The sandstone samples were crushed into particles of the original sand size in an agate mortar.

Analytical procedures

The analytical methods for hydrocarbons and fatty acids have been described elsewhere [18]. Briefly, the crushed rock samples (10–50 g) were refluxed with 0.5 *M* potassium hydroxide in methanol (80°C, 2 h) and extracted with ethyl acetate after acidification. Hydrocarbon and fatty acid fractions were obtained through a silica gel column (160 × 5 mm I.D., 100 mesh, 5% water). Fatty acids were methylated with boron trifluoride–methanol (14:86) (80°C, 2 h). Normal alkenes were identified after

hydrogenation with hydrogen and platinum dioxide in hexane [19]. Hydrocarbons and fatty acids were analyzed by GC–MS.

GC–MS was operated with a DB-5 fused-silica capillary column (30 m × 0.32 mm I.D., film thickness 0.25 μm) (J&W Scientific). The column temperature was programmed from 70 to 120°C at 25°C/min and then from 120 to 310°C at 6°C/min. Fatty acids were analyzed by GC–MS with a DB-225 fused-silica capillary column (J&W Scientific) of the same size as the DB-5 column to resolve the degree of unsaturation of the alkenoic acids. The columm temperature was programmed from 70 to 120°C at 25°C/min and then from 120 to 240°C at 5°C/min. The molecular separator and ion source were maintained at 320 and 250°C, respectively. The flow-rate of helium carrier gas was 4.3 ml/min. Mass spectra (*m/z* 50–600) were taken continuously at intervals of 1.3 s at 70 eV. The hydrocarbons and fatty acid methyl esters were identified by comparision of the retention sequences and mass spectra with those of authentic compounds and published data [18–21]. The determination of hydrocarbons and fatty acids was performed by measurement of peak heights on the gas chromatograms (TIC) and/or mass chromatograms (*m/z* 71 for alkanes; *m/z* 74 for alkanoic acids).

RESULTS AND DISCUSSION

Identification

A series of long-chain *anteiso*-alkanes from *a*-C_{20} to *a*-C_{30}, with a peak at *a*-C_{26}, were found in the capillary gas chromatogram of the hydrocarbon fraction of a rock sample colonized by cryptoendolithic lichen-dominated microbial communities from the Ross Desert of Antarctica, toghether with a suite of *n*-alkanes (*n*-C_{15} to *n*-C_{36}), isoprenoid alkanes (pristane and phytane) and/or *n*-$C_{17:1,2}$ alkenes (Fig. 1). The mass spectra of *anteiso*-alkanes showed a strong peak at $M^+ - 29$ duo to α-cleavage, whereas those of *iso*-alkanes revealed a strong peak at $M^+ - 15$ (Fig. 2 [20]). Thus *anteiso*-alkanes are easily distinguished from *n*- and *iso*-alkanes and can be identified.

A series of *n*-alkanoic acids are detected in the

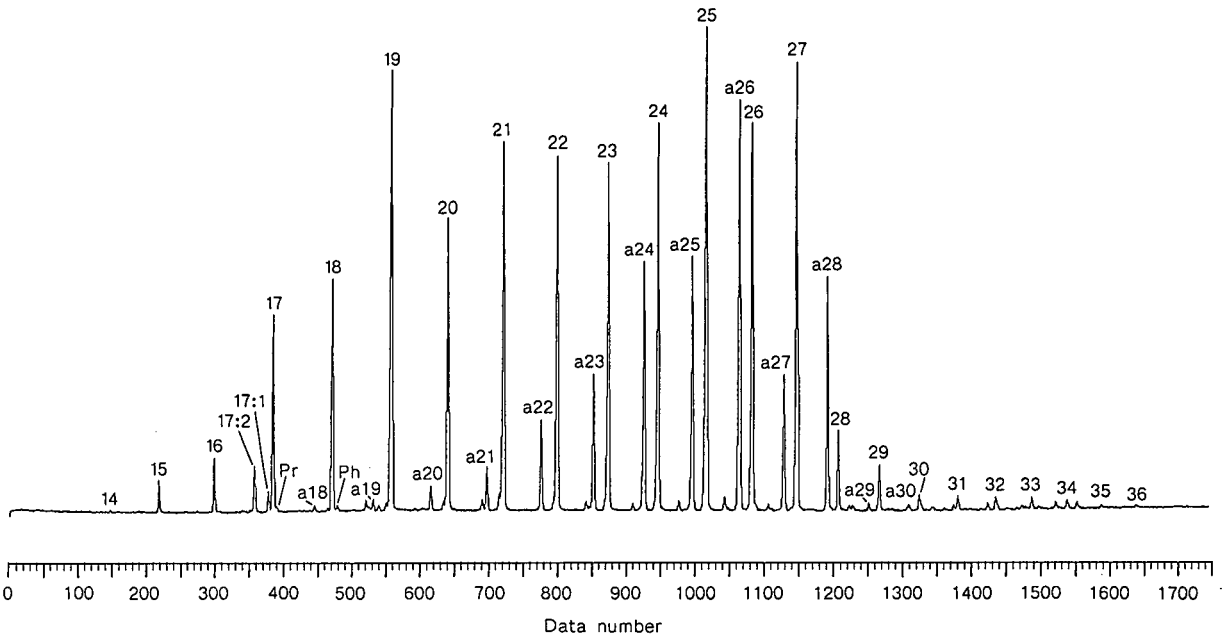

Fig. 1. Capillary gas chromatogram of the hydrocarbon fraction from a rock sample colonized by cryptoendolithic lichen-dominated microbial communities of the Ross Desert in Southern Victoria Land, Antarctica (A856-100). Arabic figures on the peaks denote carbon chain length of *n*-alkanes. Pr, Ph, and a are pristane, phytane and *anteiso*-alkanes, respectively. *m*:*n* = carbon chain length: number of double bonds.

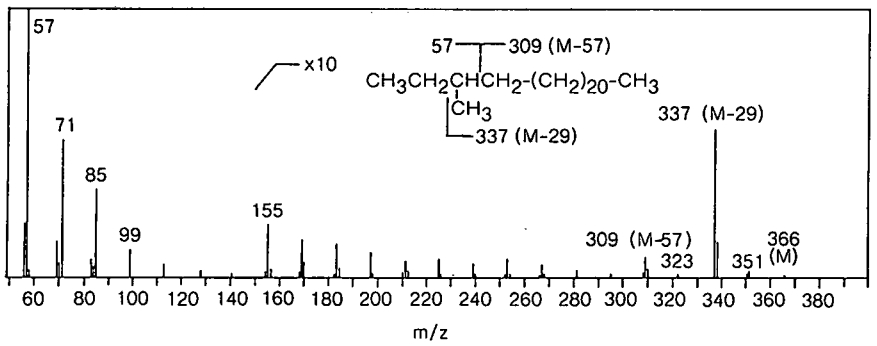

Fig. 2. Mass spectrum of long-chain *anteiso*-$C_{26:0}$ alkane found in a rock sample colonized by cryptoendolithic lichen-dominated microbial communities, Antarctica (A856-100).

capillary gas chromatogram of the fatty acid fraction of the above rock sample, together with short-chain *iso*- and *anteiso*-alkanoic and *n*-alkenoic acids (Fig. 3). Of special interest is the occurrence of a series of long-chain unidentified compounds. The mass spectra of these unknown compounds were similar to those of *n*-alkanoic acid methyl esters, so they probably cannot be distinguished from long-chain *n*- and/or *iso*-alkanoic acid methyl esters by mass spectra alone (Fig. 4). However, the *m/z* 57

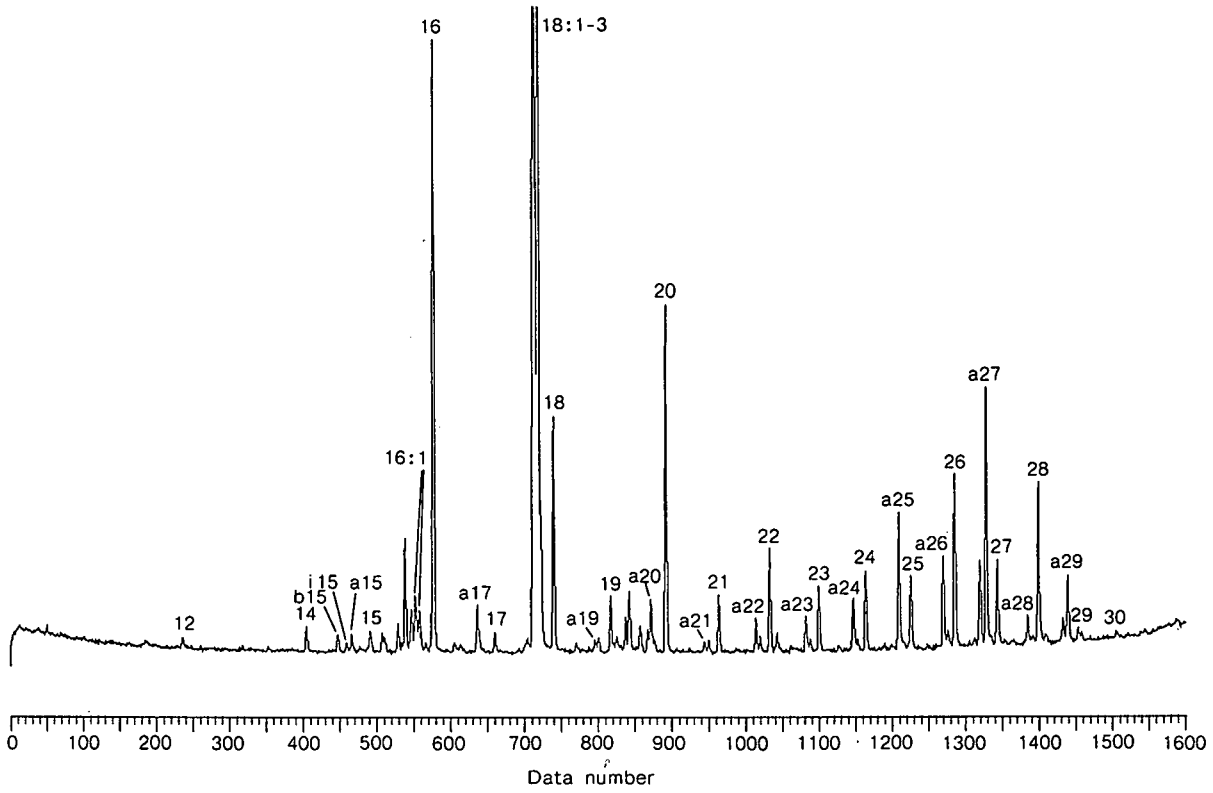

Fig. 3. Capillary gas chromatogram of the fatty acid fraction from a rock sample colonized by cryptoendolithic lichen-dominated microbial communities, Antarctica (A856-100). Arabic figures on the peaks denote carbon chain length of *n*-alkanoic acids; i and a are *iso*- and *anteiso*- alkanoic acids, respectively. *m*:*n* = carbon chain length:number of double bonds.

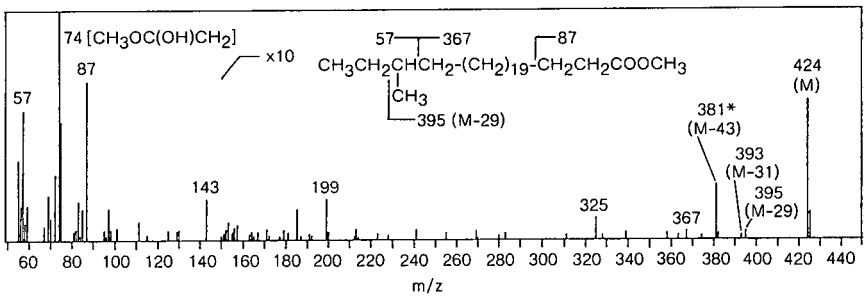

Fig. 4. Mass spectrum of the methyl ester of long-chain *anteiso*-$C_{27:0}$ alkanoic acid found in a rock sample colonized by cryptoendolithic lichen-dominated microbial communities, Antarctica (A856-100). The peak marked with an asterisk may be due to loss of a propyl group.

intensities of the unknown compounds are approximately 1.61 ± 0.15 (standard deviation) times greater than those of *n*-alkanoic acid methyl esters. The excess *m/z* 57 peak may be due to α-cleavage of methyl branch at the *anteiso*-position of the unknown compounds (Fig. 4). Equivalent carbon-chain length (ECL) values for the DB-5 column were also calculated from *iso*- and *anteiso*-C_{12}–C_{19} acid methyl esters found in the same chromatograms. The ECL values of *anteiso*-alkanoic acid methyl esters (n-C_{n-1} + 0.73 ± 0.01) were much greater than those of *iso*-alkanoic acid methyl esters (n-C_{n-1} + 0.63 ± 0.01). Generally the ECL values of a series of these unidentified peaks fit within the *anteiso*-alkanoic acid methyl esters (Table II). Also, a series of long-chain *anteiso*-alkanes with the same range were detected in these samples. These compounds were therefore identified to be long-chain *anteiso*-alkanoic acids.

Characteristics of hydrocarbons and fatty acids

Long-chain *anteiso*-alkanes were found in 40% of the 55 rock samples analyzed. Long-chain *anteiso*-alkanes were detected in some lichen-dominanted communities (*e.g.*, A856-100), fossils of lichen-dominated communities (*e.g.*, A867-110, A834-576, A845-523 and A856-82f), red *Gloeocapsa* communities and *Hormathonema–Gloeocapsa* communities, but were not found in any pure lichen communities, algal and cyanobacterial communities or uncolonized samples. The analytical results for long-chain *anteiso*-alkanes in five selected typical samples are shown in Table I, together with those for normal and isoprenoid hydrocarbons. Long-chain *anteiso*-alkanes are major hydrocarbons in the A856-100, A834-576, A845-523 and A856-82f samples (20.44–25. 95%). The predominant long-chain *anteiso*-alkane was *a*-C_{26} in all these samples (*e.g.*, Table I). Even-carbon-numbered long-chain *anteiso*-alkanes were predominant, as shown by the low odd/even carbon ratios (0.52–0.78). No one has reported such hydrocarbon distributions anywhere in the world. Interestingly, long-chain *n*-alkanes, were abundant in these samples (40.38–78.33%), although their odd/even carbon ratios were near unity (0.99–1.6).

Long-chain *anteiso*-alkanoic acids were found in 51% of the 55 rock samples. The analytical results for long-chain *anteiso*-alkanoic acids in five selected samples are shown in Table II. These samples contained *n*-alkanoic (n-C_9 to n-C_{32}), *n*-alkenoic (u-C_{16} to u-C_{18}) and short-chain *iso*- and *anteiso*- alkanoic acids (i,a-C_{12} to i,a-C_{18}), in addition to unidentified branched acids (b-C_{15} to b-C_{19}). A series of long-chain *anteiso*-alkanoic acids from a-C_{20} to a-C_{30} were detected in rock samples colonized by the lichen-dominated communities, the red *Gloeocapsa* communities and the *Hormathonema–Gloeocapsa* communities, and also in rocks containing fossil lichen-dominated communities, but were not detected in any pure lichen communities or in uncolonized rocks. Generally, long-chain *anteiso*-alkanoic acids were detected together with long-chain *anteiso*-alkanes. The most predominant *anteiso*-alkanoic acids was a-C_{27} in all samples (*e.g.*, Table II). Odd-carbon-numbered long-chain *anteiso*-alkanoic acids were predominant in all samples, as shown by the low even/odd carbon ratios (0.19–0.92). In addition, long-chain *anteiso*-alkanes are abundant acids in all samples shown in Table II (21.55–35.78%).

The total concentration of hydrocarbons and fat-

TABLE I

HYDROCARBON COMPOSITIONS AND CONTENTS FOR ROCK SAMPLES COLONIZED BY CRYPTOENDOLITHIC LICHEN-DOMINATED MICROBIAL COMMUNITIES, ANTARCTICA

The lichen-dominated microbial communities consist of lichen-forming fungi and green algae, parasymbiotic fungi, free-living fungi and green algae, cyanobacteria and heterotrophic bacteria.

Composition (%)[a]	Linnaeus Terrace		Mount Fleming			
	A856-100[b]	A867-110[c]	A834-576[c]	A845-523[c]	A856-82f[c]	ECL[d]
n-Alkane (short)	12.16	10.38	8.14	10.14	16.09	
12:0	0.00	0.00	0.00	0.15	0.77	–
13:0	0.14	0.00	0.12	0.23	2.98	–
14:0	0.16	0.00	0.24	0.29	2.33	–
15:0	0.69	0.15	0.49	0.30	0.74	–
16:0	0.82	0.56	0.57	0.51	0.79	–
17:0	2.40	1.88	1.09	1.42	1.84	–
18:0	2.34	2.81	1.71	2.11	1.77	–
19:0	5.61	4.98	3.92	5.13	4.87	–
n-Alkane (long)	48.15	78.33	60.86	63.53	40.38	
20:0	3.11	7.32	3.08	3.98	2.38	–
21:0	4.22	9.89	4.48	5.13	3.12	–
22:0	4.69	11.22	5.80	5.28	3.00	–
23:0	5.75	11.03	7.65	6.94	3.87	–
24:0	6.11	10.84	6.20	7.70	4.86	–
25:0	7.75	9.28	8.04	9.29	5.89	–
26:0	6.05	5.99	7.57	8.45	5.59	–
27:0	7.00	7.30	9.85	9.21	6.20	–
28:0	1.58	1.52	2.92	2.79	2.14	–
29:0	0.95	1.24	2.12	1.86	1.35	–
30:0	0.28	0.72	0.81	0.60	0.41	–
31:0	0.23	0.71	0.65	0.51	0.41	–
32:0	0.21	0.48	0.59	0.74	0.41	–
33:0	0.14	0.37	0.45	0.51	0.32	–
34:0	0.09	0.32	0.40	0.35	0.29	–
35:0	0.00	0.10	0.13	0.11	0.15	–
36:0	0.00	0.00	0.11	0.06	0.00	–
n-Alkene	3.00	0.28	7.25	0.45	0.59	
17:1	1.51	0.00	0.49	0.00	0.00	–
17:2	1.49	0.22	6.76	0.45	0.59	–
Anteiso	25.95	9.56	21.61	20.44	23.66	
20:0	0.43	0.00	0.30	0.34	0.37	19.71
21:0	0.69	0.00	0.35	0.54	0.68	20.71
22:0	1.43	0.29	0.94	1.22	1.21	21.71
23:0	1.97	0.57	1.38	1.83	1.80	22.70
24:0	3.78	1.14	2.69	3.16	3.13	23.70
25:0	4.16	1.62	3.34	4.17	3.68	24.71
26:0	6.10	2.47	5.78	6.58	5.10	25.72
27:0	2.34	1.43	1.98	2.33	2.09	26.71
28:0	4.79	2.04	4.36	0.28	4.65	27.71
29:0	0.25	0.00	0.25	0.00	0.68	28.71
30:0	0.00	0.00	0.24	0.00	0.27	29.70

TABLE I (*continued*)

Composition (%)[a]	Linnaeus Terrace		Mount Fleming			
	A856-100[b]	A867-110[c]	A834-576[c]	A845-523[c]	A856-82f[c]	ECL[d]
Isoprenoid	10.73	1.45	2.14	5.44	19.28	
16:0	0.14	0.00	0.16	0.18	0.74	–
18:0	0.40	0.28	0.28	0.20	0.52	–
19:0	1.39	0.57	0.45	1.28	1.55	–
20:0	2.18	0.61	0.33	0.30	0.37	–
20:1a[e]	1.26	0.00	0.16	0.79	4.51	–
20:1b[e]	1.89	0.00	0.33	1.36	4.29	–
20:1c[e]	3.47	0.00	0.42	1.33	7.31	–
Content (μg/g of dry sample)	1.2	0.045	0.11	0.20	0.31	

[a] Carbon chain length:number of double bonds.
[b] Living community.
[c] Fossil community.
[d] Equivalent carbon chain length values of *anteiso*-alkanes for the DB-5 column.
[e] Structures were not determined.

TABLE II

FATTY ACID COMPOSITIONS AND CONTENTS FOR ROCK SAMPLES COLONIZED BY CRYPTOENDOLITHIC LICHEN-DOMINATED MICROBIAL COMMUNITIES, ANTARCTICA

Communities as defined in Table I.

Composition (%)[a]	Linnaeus Terrace		Mount Fleming			
	A856-100[b]	A867-110[c]	A834-576[c]	A845-523[c]	A856-82f[c]	ECL[d]
n-Alkanoic (short)	18.95	54.63	22.92	16.33	19.27	
9:0	1.04	0.32	0.83	0.49	0.53	–
10:0	0.28	0.31	0.28	0.26	0.17	–
11:0	0.09	0.15	0.10	0.08	0.04	–
12:0	0.37	2.34	0.30	0.30	0.16	–
13:0	0.09	0.36	0.13	0.14	0.05	–
14:0	0.67	5.87	3.09	1.02	0.74	–
15:0	0.32	3.03	0.98	0.53	0.41	–
16:0	9.66	24.65	13.28	8.09	10.48	–
17:0	0.34	1.75	0.30	0.50	0.39	–
18:0	5.29	14.67	3.19	4.16	5.36	–
19:0	0.81	1.19	0.45	0.78	0.94	–
n-Alkanoic (long)	21.55	34.68	22.29	34.93	35.78	
20:0	6.62	2.47	3.55	5.92	7.46	–
21:0	0.83	2.20	0.73	1.40	1.34	–
22:0	1.61	3.64	1.31	3.19	2.54	–
23:0	0.92	3.87	1.42	1.78	1.64	–
24:0	1.44	5.87	2.43	3.19	2.82	–
25:0	1.36	4.66	2.15	2.85	2.82	–
26:0	3.29	4.91	3.02	5.86	5.90	–
27:0	1.70	2.58	2.48	3.78	3.86	–
28:0	3.17	3.77	4.05	5.29	5.77	–
29:0	0.30	0.47	0.71	1.06	0.91	–
30:0	0.17	0.25	0.41	0.61	0.56	–
31:0	0.09	0.00	0.03	0.00	0.04	–
32:0	0.06	0.00	0.00	0.00	0.11	–

(Continued on p. 274)

TABLE II (*continued*)

Composition (%)[a]	Linnaeus Terrace		Mount Fleming			
	A856-100[b]	A867-110[c]	A834-576[c]	A845-523[c]	A856-82f[c]	ECL[d]
n-Alkenoic	44.49	2.88	40.23	27.94	25.25	
16:1	1.86	0.00	0.38	1.74	0.50	–
17:1	0.58	0.00	0.66	2.57	0.00	–
18:1	10.65	1.53	11.96	8.62	8.98	–
18:2	17.86	1.35	19.91	6.98	10.00	–
18:3	13.54	0.00	7.32	8.03	5.77	–
Iso	1.00	1.30	0.24	2.64	0.45	
12:0	0.00	0.00	0.00	0.11	0.00	11.63
13:0	Trace	0.00	0.00	0.02	0.00	12.63
14:0	0.12	0.46	0.06	0.42	0.05	13.63
15:0	0.58	0.28	0.05	1.12	0.19	14.63
16:0	0.30	0.45	0.13	0.88	0.21	15.64
17:0	0.00	0.12	0.00	0.09	0.00	16.63
Anteiso (short)	0.87	1.00	0.86	2.15	0.72	
13:0	Trace	0.09	0.00	0.05	0.00	12.73
15:0	0.46	0.54	0.41	1.31	0.37	14.73
17:0	0.24	0.36	0.11	0.65	0.18	16.74
19:0	0.16	0.00	0.34	0.15	0.17	18.74
Anteiso (long)	11.69	4.71	11.76	13.53	17.43	
20:0	0.18	0.00	0.12	0.20	0.20	19.74
21:0	0.10	0.12	0.07	0.11	0.16	20.73
22:0	0.18	0.14	0.90	0.23	0.23	21.74
23:0	0.37	0.24	0.30	0.40	0.51	22.73
24:0	0.81	0.24	0.57	0.72	1.00	23.74
25:0	2.35	0.51	1.57	2.17	2.84	24.74
26:0	1.56	0.55	2.01	1.97	2.80	25.75
27:0	4.37	1.28	3.65	4.71	5.86	26.75
28:0	0.53	0.59	0.78	0.86	1.09	27.75
29:0	1.25	1.06	1.72	2.08	2.67	28.75
30:0	0.00	0.00	0.06	0.10	0.08	29.74
Branched[e]	1.45	0.81	1.71	2.48	1.09	
15:0	0.10	0.21	0.11	0.19	0.11	–
16:0	0.14	0.00	0.17	0.25	0.17	–
17:0	0.75	0.24	0.41	1.01	0.26	–
18:0	0.11	0.36	0.11	0.43	0.11	–
19:0	0.36	0.00	0.91	0.50	0.43	–
Content (μg/g of dry sample)	79	0.31	5.4	14	58	

[a] Carbon chain length:number of double bonds.
[b] Living community.
[c] Fossil community.
[d] Equivalent carbon chain length values of *iso*- and *anteiso*- alkanoic acids for the DB-5 column.
[e] Structures were not determined.

ty acids were fairly low, less than 1.2 and 79 μg per gram of dry sample (Tables I and II), probably because of the low biomass in the harsh natural environment of the Ross Desert.

Sources of long-chain anteiso-alkanes and long-chain anteiso-alkanoic acids

Anteiso-alkanes are uncommon in the plant kingdom but are found in certain vascular plants. For

instance, long-chain *anteiso*-alkanes having even-carbon numbers (*a*-C_{28} to *a*-C_{34}) are detected in various tobaccos with a predominance of *a*-C_{32} [21,22]. Even-carbon-numbered long-chain *anteiso*-alkanes (*a*-C_{24} to *a*-C_{32}) are also found in a number of insects [23,24]. They are usually accompanied by *n*- and other methyl-branched alkanes. Odd-carbon-numbered *anteiso*- alkanes (*a*-C_{15} to *a*-C_{29}) at a peak of *a*-C_{27} and odd-carbon-numbered *anteiso*-alkanoic acids (*a*-C_{13} to *a*-C_{31}) at a peak of *a*-C_{25} were detected in a wool wax by GC together with *n*- and *iso*-isomers of various compounds, including 2- and ω-hydroxy acids [25]. Vascular plants, insects and sheep do not occur in the sampling sites in the Ross Desert, and are unlikely sources of these *anteiso* compounds. No long-chain *anteiso*-alkanes and long-chain *anteiso*-alkanoic acids were detected in any lake sediment, pond sediment or soil sample in the Ross Desert or elsewhere in Antarctica, although long-chain alkanes and long-chain *anteiso*-alkanes are often major components in these samples [18,26–29]. These *anteiso* compounds were also not present in uncolonized Beacon Supergroup rock samples [30,31]. Hence long-chain *anteiso*-alkanes and long-chain *anteiso*-alkanoic acids are characteristic compounds of some cryptoendolithic microbial communities.

Cryptoendolithic micribial communities are fairly simple, composed of microalgae and cyanobacteria as primary producers, black and colorless fungi as consumers and heterotrophic bacteria as decomposers [2]. No secondary consumers are present as in the case of lakes in the McMurdo Dry Valleys [32]. Long-chain *anteiso*-alkanes and long-chain *anteiso*-alkanoic acids were found in the three microbial communities (lichen-dominated, red *Gloeocapsa* and *Hormathonema–Gloeocapsa* communities), but not in every sample (unpublished results). No long-chain *anteiso*-alkanes or long-chain *anteiso*-alkanoic acids were found in samples of granite or Koettlitz marble colonized by algae and lichens of the Ross Desert, and they were not detected in Nubian sandstone samples from the Negev Desert colonized by cryptoendolithic cyanobacteria (unpublished results).

These results can best be explained by microbial origin of long-chain *anteiso*-alkanoic acids and long-chain *anteiso*-alkanes, as they are characteristic of Antarctic cryptoendolithic microbial communities but not present in all samples. These organisms have adapted to a wide range of environments and to water and pH conditions (3.7–8.2) that vary widely [4], but analysis of organisms isolated from the rocks colonized by cryptoendolithic microbial communities (including five algae, four cyanobacteria, one lichen-forming fungus, three parasymbiotic black fungi, one yeast and sixteen bacteria) could not detect the presence of these compounds (unpublished results). *Anteiso*- and *iso*-alkenes ranging form *a*-C_{23} to *a*-C_{32} are found with the most predominant *anteiso*-alkanes of *a*-$C_{25:1}$, *a*-$C_{27:1}$ or *a*-$C_{29:1}$ in some bacteria [20,33,34]. Hence they may be derived from other organisms, *e.g.*, heterotrophic bateria that have not yet been isolated in culture [35]. The presence of short-chain *iso*- and *anteiso*-C_{12}–C_{17}-alkanoic acids (Table II), in addition to hopanoids ranging from C_{27} to C_{35} with a predominance of C_{30} (unpublished results), supports a considerable contribution of heterotrophic bacteria to these rock samples.

However, it is also possible that these unusual long-chain *anteiso* compounds arise from symbiotic processes rather than a single microorganism, as lichenic acids are only produced by lichens (symbiotic processes with green algae and fungi).

The coexistence of long-chain *anteiso*-alkanes and long-chain *anteiso*-alkanoic acids strongly suggests that long-chain *anteiso*-alkanes are derived from long-chain *anteiso*-alkanoic acids through microbial decarboxylation in the microbial communities [36]. The biosynthetic pathways of these *anteiso* compounds are not yet clear.

Long-chain *anteiso*-alkanoic acids and long-chain *anteiso*-alkanes are well preserved in rock samples with fossilized communities so they will probably be useful as biomarkers in environmental and geochemical studies. The long-chain *anteiso*-alkanoic acids may be important sources of long-chain *anteiso*-alkanes found in various geological environments. The long-chain *anteiso*-compounds also suggest the existence of a unique biosynthetic pathway in microorganisms. Further detailed studies using carbon isotopes (^{14}C or ^{13}C) are needed.

CONCLUSIONS

Hydrocarbons and fatty acids in rocks occupied by living and fossilized cryptoendolithic microbial

communities from the Ross Desert of Southern Victoria Land, Antarctica, were analyzed by capillary GC–MS. Long-chain *anteiso*-alkanes and long-chain *anteiso*-alkanoic acids were found in many samples, together with long-chain *n*-alkanes and *n*-alkanoic acids. These unusual compounds are probably derived from unidentified heterotrophic bacteria or formed through symbiotic processes in unique cryptoendolithic microbial communities. Long-chain *anteiso*-alkanes are probably derived from long-chain *anteiso*-alkanoic acids through microbial decarboxylation in the microbial communities. These *anteiso* compounds may be useful as new biomarkers in environmental and geochemical studies.

ACKNOWLEDGEMENTS

This work was partly supported by NSF grant DPP83-14180 and by NASA grant NSG-7337 to E.I.F. Comments by Dr. A. B. Thistle improved the presentation.

REFERENCES

1 E. I. Friedmann and R. Ocampo, *Science (Washington, D.C.)*, 193 (1976) 1247.
2 E. I. Friedmann, *Science (Washington, D.C.)*, 215 (1982) 1045.
3 J. A. Nienow, C. P. McKay and E. I. Friedmann, *Microb. Ecol.*, 16 (1988) 253.
4 E. I. Friedmann, M. Hua and R. Ocampo-Friedmann, *Polarforschung*, 58 (1988) 251.
5 E. I. Friedmann and R. Weed, *Science (Washington, D.C.)*, 236 (1987) 703.
6 E. I. Friedmann and A. M. Koriem, *Adv. Space Res.*, 9, No. 6 (1989) 167.
7 K. A. Kvenvolden, *Nature (London)*, 209 (1966) 573.
8 J. Han, M. Calvin, *Nature (London)*, 224 (1969) 576.
9 P. R. Mackenzie, S. C. Brassell, G. Eglinton and J. R. Maxwell, *Science*, 217 (1982) 491.
10 J. K. Volkman and J. R. Maxwell, in R. B. Johns (Editor), *Methods in Geochemistry and Geophysics 24. Biological Markers in the Sedimentary Record*, Elsevier, Amsterdam, 1986, p. 1.
11 R. B. Johns, T. Belsky, E. D. McCarthy, A. L. Burlingame, P. Haung, H. K. Schnoes, W. Richter and M. Calvin, *Geochim. Cosmochim. Acta*, 30 (1966) 1191.
12 A. L. Chaffee, D. S. Hoover, R. B. Johns and F. K. Schweighardt, in R. B. Johns (Editor), *Methods in Geochemistry and Geophysics 24, Biological Markers in the Sedimentary Record*, Elsevier, Amsterdam, 1986, p. 311.
13 E. J. Ledet and J. L. Laseter, *Science (Washington, D. C.)*, 186 (1984) 261.
14 P. E. Kolattukudy, *Lipids*, 5 (1970) 259.
15 A. P. Tulloch, in P. E. Kolattukudy (Editor), *Chemistry and Biochemistry of Natural Waxes*, Elsevier, Amsterdam, 1976, p. 235.
16 W. M. O'Leary, in A. I. Laskin and H. A. Lechevalier (Editors), *CRC Handbook of Microbiology. Vol. 4. Microbial Composition: Carbohydrates, Lipids, and Minerals*, CRC Press, Boca Raton, FL, 1982, p. 391.
17 P. J. Barrett and R. A. Kyle, in K. S. W. Campbell (Editor), *Gondowana Geology*, Australian National University Press, Canberra, 1975, p. 333.
18 G. Matsumoto, T. Torii and T. Hanya, *Mem. Natl. Inst. Polar Res. Special Issue*, 13 (1979) 103.
19 G. I. Matsumoto, K. Watanuki and T. Torii, *Hydrobiologia*, 172 (1989) 291.
20 T. G. Tornabene, E. Gelpi and J. Oró, *J. Bacteriol.*, 94 (1967) 333.
21 J. D. Mold, R. K. Stevens, R. E. Means and J. M. Ruth, *Biochemistry*, 2 (1963) 605.
22 A. P. Tulloch, in P. E. Kolattukudy (Editor), *Chemistry and Biochemistry of Natural Waxes*, Elsevier, Amsterdam, 1976, p. 235.
23 C. L. Soliday, G. J. Blomquist and L. L. Jackson, *J. Lipid Res.*, 15 (1974) 399.
24 L. L. Jackson and G. J. Blomquist, in P. E. Kolattukudy (Editor), *Chemistry and Biochemistry of Natural Waxes*, Elsevier, Amsterdam, 1976, p. 201.
25 D. T. Downing, Z. H. Kranz and K. E. Murray, *Aust. J. Chem.*, 13 (1960) 80.
26 G. Matsumoto, T. Torii and T. Hanya, *Nature (London)*, 290 (1981) 688.
27 J. K. Volkman, H. R. Burton, D. A. Everitt and D. I. Allen, *Hydrobiologia*, 165 (1988) 141.
28 G. I. Matsumoto, *Hydrobiologia*, 172 (1989) 265.
29 G. I. Matsumoto, A. Hirai, K. Hirota and K. Watanuki, *Org. Geochem.*, 16 (1990) 781.
30 G. I. Matsumoto, M. Funaki, T. Machihara and K. Watanuki, *Mem. Natl. Inst. Polar Res.*, 43 (1986) 149.
31 G. I. Matsumoto, T. Machihara, N. Suzuki, M. Funaki and K. Watanuki, *Geochim. Cosmochim. Acta*, 51 (1987) 2663.
32 B. C. Parker, G. M. Simmons, Jr., F. G. Love, R. A. Wharton and K. G. Seaburg, *BioScience*, 31 (1981) 656.
33 T. G. Tornabene, S. J. Morrison and W. E. Kloos, *Lipids*, 5 (1970) 929.
34 P. W. Albro, in P. E. Kolattukudy (Editor), *Chemistry and Biochemistry of Natural Waxes*, Elsevier, Amsterdam, 1976, p. 419.
35 D. M. Ward, R. Weller and M. Bateson, *Nature (London)*, 345 (1990) 63.
36 P. E. Kolattukudy, *Science (Washington. D.C.)*, 159 (1968) 498.

Journal of Chromatography, 598 (1992) 277–285
Elsevier Science Publishers B.V., Amsterdam

CHROM. 24 047

Kinetics of acrylamide photopolymerization as investigated by capillary zone electrophoresis

Cecilia Gelfi, Patrizia De Besi, Angela Alloni and Pier Giorgio Righetti*

Chair of Biochemistry and Department of Biomedical Sciences and Technologies, University of Milan, Via Celoria 2, Milan 20133 (Italy)

Tatyana Lyubimova and Vladimir A. Briskman

Institute of Continuous Media Mechanics of Urals Branch, USSR Academy of Sciences, 1 Akad. Korolyov Street, Perm 614061 (Russia)

(First received November 21st, 1991; revised manuscript received January 23rd, 1992)

ABSTRACT

Riboflavin-mediated photopolymerization of acrylamide had been investigated earlier and found to give a poor conversion of the monomer into the polymeric phase (barely 60% with standard 1-h light exposure at room temperature with a 12-W neon source). The kinetics of such a process were re-examined by using capillary zone electrophoresis and it was found that the efficiency could be augmented to >95% (even higher than in peroxodisulphate polymerization) under the following conditions: by conducting the photopolymerization process at 70°C for 1 h, instead of at room temperature, alternatively, by using a 105-W UV-A lamp, having a radiation spectrum extending also in the UV region, instead of the standard 12-W neon bulbs, and by increasing the amount of catalyst (riboflavin 5′-phosphate) from 6 to 12 ppm. In all instances, it was found that atmospheric oxygen would act as a retarder, the lag time being *ca.* 17 min at an oxygen partial pressure of 35 mmHg and increasing progressively to >70 min at >200 mmHg. However, even at a partial pressure as high as 900 mmHg (as obtained by oxygen insufflation from a tank), once the retarder had been consumed a conversion of monomers into the polymer chains of >92% was still obtained. In contrast, oxygen acts as an inhibitor in peroxodisulphate polymerization: from an incorporation efficiency of *ca.* 92% at 25 mmHg oxygen partial O_2 pressure, the conversion is lowered to only 40% at 900 mmHg.

INTRODUCTION

In the last few years, we have conducted an extensive investigation of the properties of Immobilines, the acrylamido weak acids and bases used for generating insolubilized pH gradients for isoelectric focusing (see ref. 1 for a review). Such research was prompted by the availability of capillary zone electrophoresis (CZE), which seems ideally suited for studying small molecules for which electrophoretic techniques in gel slabs do not have much to offer. We then continued such studies on a novel series of neutral acrylamido derivatives, both mono- and bifunctional, which we have recently synthesized [2]. In this work, we reinvestigated the kinetics of riboflavin polymerization of polyacrylamide gels.

The use of riboflavin for gel polymerization had been suggested as early as 1957 by Oster *et al.* [3] and was subsequently recommended by Davis [4] in disc electrophoresis for casting the two segments of sample and spacer gel. Later, the use of riboflavin 5′-phosphate (FMN) instead of riboflavin was proposed [5].

There are some distinct advantages in photopolymerization: riboflavin, which can be used at very low concentrations (6 ppm, as opposed to 400 ppm for peroxodisulphate), does not seem to oxidize or denature proteins entrapped in the sample gel [6],

0021-9673/92/$05.00

and allows ample control of the start of the polymerization, as gelation is only initiated by fluorescent light. Some aspects of photopolymerization have been elucidated. Thus, it appears that photopolymerization requires traces of oxygen in order to take place [7]. Photodecomposition of riboflavin, with the consequent reoxidation of leucoflavin and production of free radicals, can occur only if molecular oxygen is initially present. The standard technique for photopolymerization has been to subject the gelling solution to a 1-h light exposure with a 12- or 16-W neon bulb at level of 6 ppm riboflavin 5′-phosphate. However, when we followed the kinetics of this polymerization process [8], we found only 60% conversion under these conditions and reported that light exposure for at least 8 h was required to achieve >90% efficiency, as is customary in peroxodisulphate polymerization [9]. We had therefore favoured chemical initiation with the standard redox couple peroxodisulphate and N,N,N′,N′-tetramethylethylenediamine (TEMED) over the use of photopolymerization.

In this work, we studied photopolymerization again and report here conditions that allow conversion efficiencies of better than 95%, *i.e.*, even more favourable than in peroxodisulphate polymerization.

EXPERIMENTAL

Materials

Acrylamide, N,N′-methylenebisacrylamide (Bis), TEMED and ammonium peroxodisulphate were obtained from Bio-Rad Labs. (Richmond, CA, USA). The p*K* 9.3 Immobiline, used as an internal standard in CZE runs, was purchased from Pharmacia–LKB (Uppsala, Sweden).

Gel preparation

All gels were prepared at a concentration of 6%T and 4%C[a] in 5 m*M* phosphate buffer (pH 6.0). TEMED was always added at a concentration of 0.4 μl per ml of gelling solution. In photopolymerization, 6 μl/ml of a 1 mg/ml FMN solution were added, corresponding to $1.16 \cdot 10^{-5}$ mmol/ml of gel, whereas for chemical polymerization (peroxodisulphate) $1.4 \cdot 10^{-3}$ mmol/ml of gelling solution were used. Gel polymerization was conducted in spectrophotometric cuvettes of 5 mm thickness. No difference in incorporation efficiency was found between glass and quartz cuvettes. Photopolymerization was conducted either with a 12-W neon bulb (at a distance of 10 cm from the slab) or with a 105-W UV-A lamp. Standard conditions in both instances were 1 h at 25°C, but 50 and 70°C were also tried and some kinetic experiments were prolonged up to 24 h. In both instances, gelling solutions were either degassed with a mechanical or a water pump, or gassed for up to 120 s with pure oxygen. We also explored the effect of different levels of FMN in solution, from the standard value ($1.16 \cdot 10^{-5}$ mmol/ml of gel) up to 1.5× and 2× concentration.

Measurements of incorporation efficiencies

In all instances described above, 5 ml of acrylamide–Bis solution (6%T, 4%C) in 5 m*M* phosphate buffer (pH 6.0) were polymerized. The gel was then extruded, minced and extracted with an equal volume of methanol. After filtering the gel debris, the methanol was evaporated, the solution reconstituted to the original volume and p*K* 9.3 Immobiline was added as internal standard (2.0 m*M* final concentration). The amount of unreacted monomers was assessed by CZE, as described below, with a calibration graph consisting of eight dilutions of pure acrylamide covering the range 0.025–0.1 m*M*.

Capillary zone electrophoresis (CZE)

CZE was performed in a Beckman (Palo Alto, CA, USA) instrument (P/ACE System 2000) equipped with a fused-silica capillary (having an untreated inner surface) of 57 cm × 75 μm I.D. from Polymicro Technologies (Phoenix, AZ, USA). Runs were performed at 25°C in a thermostated environment in 0.1 *M* borate buffer (pH 9.0). In all instances the migration direction was toward the negative electrode. The samples were injected into the capillary by pressure (80 p.s.i.), usually for 10 s. The calibration graph for each acrylamido derivative analysed was constructed with the Beckman Gold integration system. In each run p*K* 9.3 Immobiline (2.0 mM) was used as an internal standard. Runs were usually performed at 15 kV and 50 μA with the detector set at 254 nm.

[a] C = g Bis/%T; T = g acrylamide + g Bis per 100 ml of solution.

Kinetics of riboflavin degradation

In order to follow the degradation kinetics of riboflavin during exposure to light for gel polymerization, a 2 m*M* solution of FMN in 5 m*M* phosphate buffer (pH 6.0) was irradiated with the 12-W neon bulb at time intervals up to 24 h at both 25 and 70°C. The irradiated samples were then analysed by CZE, as above, by using the p*K* 9.3 Immobiline (2.0 m*M*) as internal standard. The CZE analysis was done in a 57 cm × 75 μm I.D. capillary in 0.1 *M* phosphate buffer (pH 7.0) at 10 kV and 100 μA.

Inhibition/retardation curves

In order to check the effect of oxygen on riboflavin- *vs.* peroxodisulphate-polymerized gels, the two series of gels were prepared under the following conditions: (a) degassed for 30 min with a mechanical pump; (b) degassed for 30 min with a water pump; (c) control, non-degassed; (d) gassed with pure oxygen from a tank for 15, 30, 60 or 120 s. Polymerization was then conducted at 70°C and aliquots were collected at different time intervals. After extraction in methanol, the efficiency of incorporation was assessed by CZE as described above. The oxygen partial pressure in solution was determined by haemo-gas analysis in an ABL 330 instrument from Radiometer (Copenhagen, Denmark).

Polymerization lag

In order to check the effect of oxygen partial pressure on the lag time (*i.e.*, the time between the start of light exposure and onset of polymerization), a series of gels were photopolymerized at 25, 50 and 70°C, either under degassing conditions or after oxygen insufflation, as above. The onset of polymerization was assessed either by measuring the heat of polymerization with a differential thermocouple (copper–constantan with a sensitivity of 40 μV/°C) [9] or by shaking the gelling solution at regular time intervals.

RESULTS

Conversion efficiency as a function of time and temperature

For photopolymerization, it has been customary in the past to subject the gelling solution to a 1-h light exposure at room temperature [8], usually in front of neon lamps of 12 or 16 W, placed at a distance of *ca.* 10 cm from the gel cassette. However, under these conditions, the incorporation efficiency, as measured previously [8] by permanganate titration of unreacted double bonds, was barely 60%. We have repeated these measurements determining unreacted monomers, after extraction from the gel, by CZE. Fig. 1 gives an example of the kind of separations obtained; p*K* 9.3 Immobiline was always added as internal standard for quantification purposes. As shown in Fig. 2, the conversion at 1 h was *ca.* 70% and an 8-h exposure time was required to obtain an incorporation of *ca.* 95%, in agree-

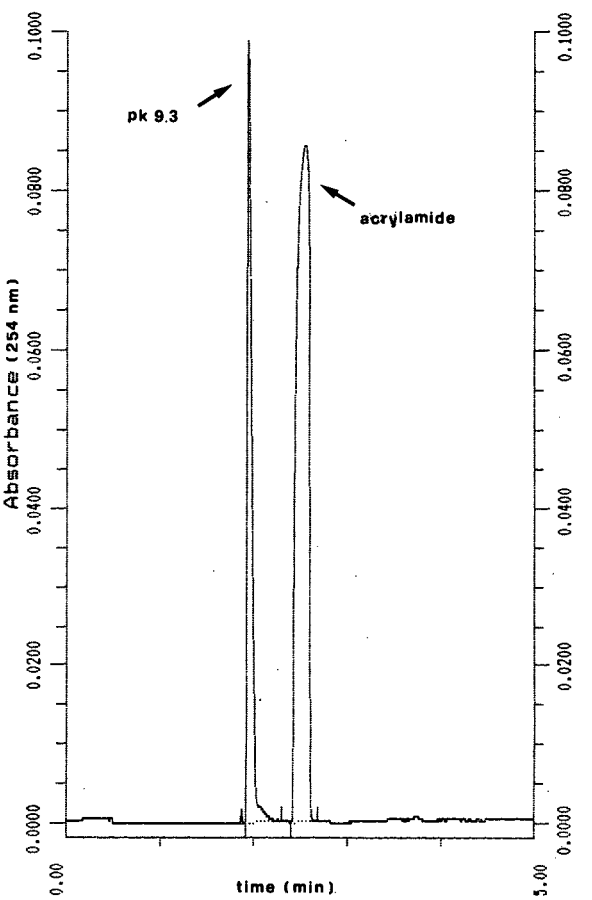

Fig. 1. Example of a CZE determination of unreacted acrylamide after gel polymerization. To the unreacted monomer, extracted from the gel, was added an internal standard (2.5 m*M* p*K* 9.3 Immobiline) and the mixture was run in a Beckman P/ACE 2000 at 15 kV and 50 μA in 100 m*M* borate buffer (pH 9.0) (cathodic migration). Capillary, 57 cm × 75 μm I.D.; detection at 254 nm.

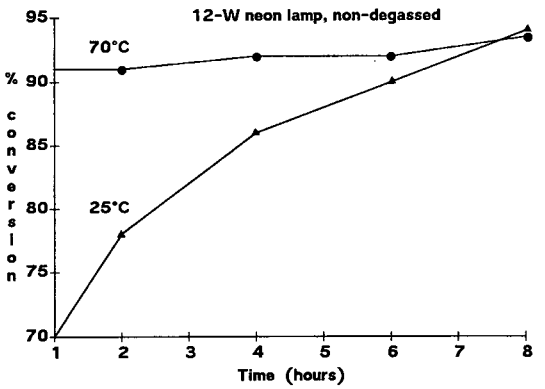

Fig. 2. Conversion efficiency as a function of time and temperature. Solutions of 6%T, 4%C monomers in 5 m*M* phosphate buffer (pH 6.0) were photopolymerized with FMN ($1.16 \cdot 10^{-5}$ mmol/ml of gelling solution) at either 25 or 70°C for up to 8 h. The solutions were not degassed and a 12-W neon bulb was used as a light source. At the given time intervals, 5-ml tubes were collected, the gels minced and extracted in methanol and ungrafted monomers determined after CZE in a P/ACE 2000 instrument in 100 m*M* borate buffer (pH 9.0) at 15 kV and 50 μA and 25°C. Capillary 57 cm × 75 μm I.D.; detection at 254 nm.

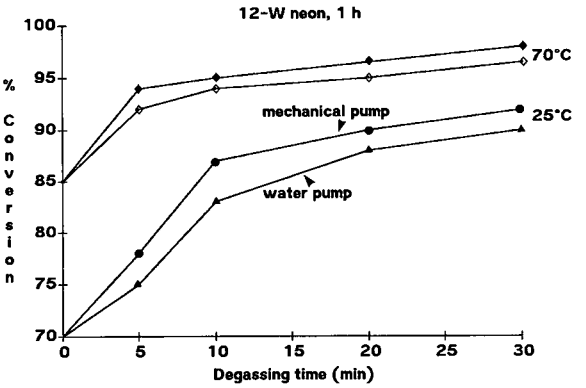

Fig. 3. Polymerization efficiency as a function of degassing method. Solutions of 6%T, 4%C monomers in 5 m*M* phosphate buffer (pH 6.0) were photopolymerized with FMN ($1.16 \cdot 10^{-5}$ mmol/ml of gelling solution) at either 25 or 70°C for 1 h in front of a 12-W neon bulb. The solutions were degassed for the times indicated either with a mechanical pump (giving a 35 mmHg oxygen partial pressure after 30 min) or with a water pump (65 mmHg). Ungrafted monomers were determined by CZE as in Fig. 2.

ment with the previous work [8]. However, in the past, there have been no reports on the effect of temperature on such a polymerization process. We had already reported in 1984 that, for casting Immobiline gels, good conversion in peroxodisulphate polymerization was only obtained by 1-h polymerization at 50°C [10]. Based on these observations, we tried the photopolymerization at 70°C; as shown in Fig. 2, at the end of the standard 1-h period, a conversion of >92% was obtained and essentially no "ripening" of the gel was noted if light exposure was prolonged up to 8 h.

Conversion efficiency as a function of oxygen partial pressure

The role of oxygen dissolved in solution has never been well elucidated in photopolymerization. We prepared different series of gels degassed either with a mechanical or with a water pump and polymerized them at either 25 or 70°C. As shown in Fig. 3, dissolved oxygen always inhibits, to some extent, the incorporation of monomers into the growing polymer, the effect being much less pronounced at 70 than at 25°C however. As shown in the graphs, a minimum degassing time of 10 min is required to minimize oxygen retardation. The oxygen partial pressure also has a strong effect on the lag time, *i.e.*, on the time of polymerization onset after starting light irradiation. As shown in Fig. 4, whereas at room temperature the lag time is *ca.* 30 min in the

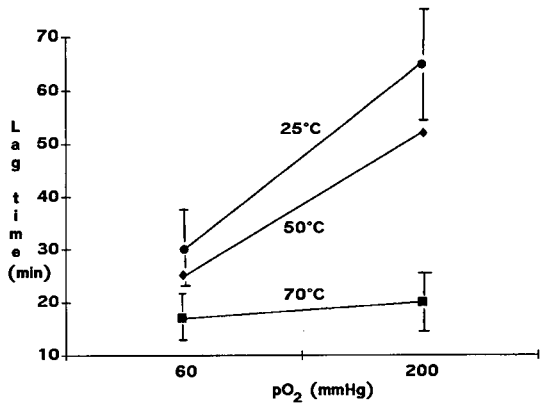

Fig. 4. Lag time of photopolymerization as a function of oxygen partial pressure (pO_2) and temperature. Solutions of 6%T, 4%C monomers in 5 m*M* phosphate buffer (pH 6.0) were photopolymerized with FMN ($1.16 \cdot 10^{-5}$ mmol/ml of gelling solution) at either 25, 50 or 70°C for 1 h in front of a 12-W neon bulb. The lag time was measured at two values of pO_2, corresponding to degassing with a water pump (65 mmHg) and to control, undegassed solutions (200 mmHg). The onset of polymerization was assessed either with a differential thermocouple (25°C) or by shaking the gelling solutions at regular time intervals.

presence of 60 mmHg of oxygen, it becomes 65–70 min at 200 mm Hg of oxygen. The lag time, however, is progressively decreased at gradually higher temperatures: thus, at 70°C, it is only 17 min at 60 mmHg and increases slightly to only 20 min at 200 mmHg oxygen partial pressure. There is, however, a large standard deviation, so that controlling the lag time still remains one of the most difficult tasks in photopolymerization.

What exactly the role of oxygen is in photopolymerization, as opposed to peroxodisulphate polymerization, is shown in Fig. 5. Both reactions were conducted at 70°C for a standard 1-h period, so as to minimize the lag time and ensure high conversions. In photopolymerization, it is seen that, on going from 200 mmHg (the oxygen partial pressure in control, undegassed solutions) to 900 mmHg (the oxygen partial pressure after gassing a solution for 120 s), the conversion efficiency is essentially unaffected, and remains at a constant, high level of >90% (the lag time will be strongly affected, however; see below). Conversely, with peroxodisulphate initiation, progressively increasing levels of oxygen are associated with a gradual decrease in conversion efficiency, from 94% at 200 mmHg down to barely 40% at 930 mmHg of oxygen (Fig. 5).

The different role played by oxygen in the two catalyst systems is further elucidated in Fig. 6; we

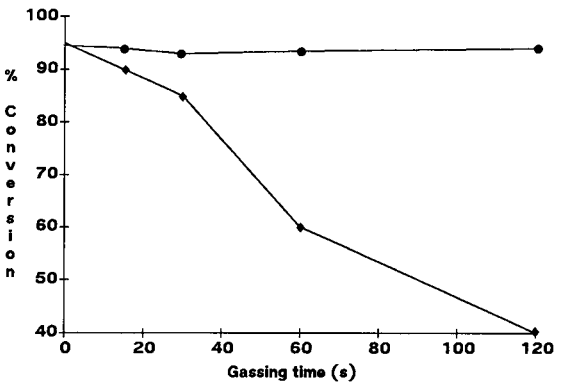

Fig. 5. Polymerization efficiency as a function of pO_2. Solutions of 6%T, 4%C monomers in 5 m*M* phosphate buffer (pH 6.0) were either photopolymerized with FMN ($1.16 \cdot 10^{-5}$ mmol/ml of gelling solution) at 70°C for 1 h in front of a 12-W neon bulb (●) or initiated with peroxodisulphate (1 h, 70°C) (◆). The solutions were either controls (200 mmHg pO_2) or gassed with pure oxygen from a tank (930 mmHg pO_2 at 120 s of gassing). Ungrafted monomers were determined by CZE as in Fig. 2.

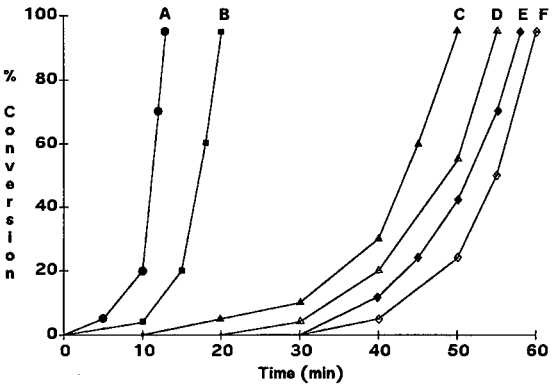

Fig. 6. Retardation curves as a function of pO_2. Solutions of 6%T, 4%C monomers in 5 m*M* phosphate buffer (pH 6.0) were photopolymerized with FMN ($1.16 \cdot 10^{-5}$ mmol/ml of gelling solution) at 70°C for 1 h in front of a 12-W neon bulb. The solutions contained from 35 mmHg pO_2 (curve A, degassed for 30 min with a mechanical pump) up to 930 mmHg pO_2 (curve F, gassed for 120 s with oxygen). Ungrafted monomers were determined by CZE as in Fig. 2.

have measured the lag time before polymerization onset as a function of oxygen partial pressure, from 35 mmHg (in solutions degassed for 30 min with a mechanical pump) up to 930 mmHg (in solutions gassed with pure oxygen for 120 s) (see Table I). It is seen that, in photopolymerization, oxygen has a strong influence only on the lag time, not on the final conversion efficiency, which is good (>90%) in all instances. In other words, whereas in photopolymerization oxygen acts only as a "retarder", with no effect on the final gel product, in perox-

TABLE I

OXYGEN PARTIAL PRESSURE IN DEGASSED, CONTROL AND GASSED GELLING SOLUTIONS

pO_2 measured in 5 m*M* phosphate buffer (pH 6.0)

Type of solution	pO_2 (mmHg)[a]
Degassed, mechanical pump (30 min)	35 ± 5
Degassed, water pump (30 min)	63 ± 12
Control	205 ± 4
15 s O_2 gassing	860 ± 39
30 s O_2 gassing	900 ± 35
60 s O_2 gassing	910 ± 40
120 s O_2 gassing	927 ± 45

[a] Mean values ± standard deviations for ten determinations.

odisulphate polymerization oxygen acts as an "inhibitor", impeding the incorporation of free monomers in the growing chains (see Discussion).

Another way to control the lag time (and the incorporation efficiency) is by using a stronger light source. When the gels are polymerized not in front of a 12-W neon source but in front of a 105-W UV-A lamp, the lag time, which at room temperature is 60 min, is reduced to barely 17 min (Fig. 7). The 105-W lamp also dramatically increases the incorporation efficiency: in fact, whereas at 25°C, with a 12-W bulb, barely a 70% conversion is achieved in a 1-h illumination period, under the same conditions the incorporation efficiency with the 105-W UV-A lamp is increased to >90% (Fig. 7), *i.e.*, to the same conversion that would have required, under the former conditions, an 8-h illumination period (see also Fig. 2).

Conversion as a function of riboflavin concentration

It has been customary, up to now, in photopolymerization to use a fixed level of FMN of the order of $1.16 \cdot 10^{-5}$ mmol/ml (standard conditions). We investigated whether a better conversion could be obtained by increasing the level. As shown in Table II, 1.5× and 2× concentration levels do offer a slight increase in incorporation efficiencies at all temperatures investigated. However, no effect was visible at higher concentrations (not shown). Therefore, a 2× FMN level is recommended in photopolymerization.

TABLE II

CONVERSION (%) AS A FUNCTION OF RIBOFLAVIN CONCENTRATION AND TEMPERATURE

Temperature (°C)	[Riboflavin][a]		
	1×	1.5×	2×
25	70 ± 12	70 ± 11	73 ± 15
50	76 ± 9	84 ± 9	88 ± 11
70	84 ± 6	88 ± 5	92 ± 8

[a] The standard riboflavin concentration (1×) was $1.16 \cdot 10^{-5}$ mmol/ml of gelling solution. Conversion results are mean values ± standard deviations for ten determinations.

The fate of riboflavin on illumination was investigated by light exposure at 25 and 70°C for up to 24 h. The sample was then injected into the CZE system and the remaining FMN peak was measured. As shown in Fig. 8, higher temperatures, at all times, produce a more rapid destruction of FMN; this could explain the much higher incorporation efficiencies at 70°C as opposed to 25°C.

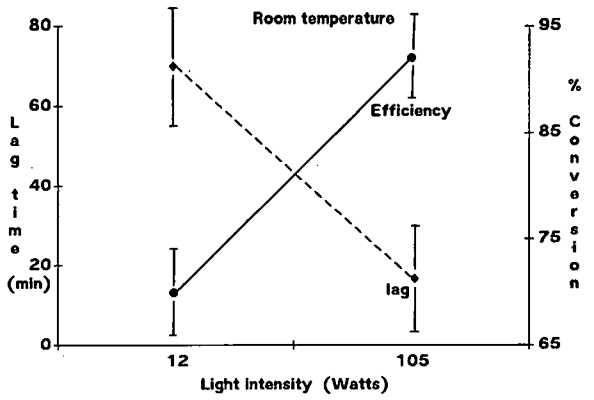

Fig. 7. Lag time and efficiency of incorporation as a function of wattage of the light source. Solutions of 6%T, 4%C monomers in 5 m*M* phosphate buffer (pH 6.0), were photopolymerized with FMN ($1.16 \cdot 10^{-5}$ mmol/ml of gelling solution) at 25°C for 1 h either in front of a 12-W neon bulb or by irradiation with a 105-W UV-A lamp. The onset of polymerization was assessed with a differential thermocouple, whereas the conversion efficiency was measured by CZE as in Fig. 2.

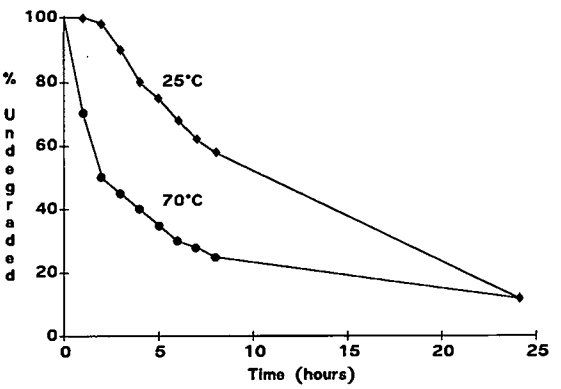

Fig. 8. Kinetics of riboflavin degradation as a function of temperature. FMN ($1.16 \cdot 10^{-5}$ mmol/ml) dissolved in 5 m*M* phosphate buffer (pH 6.0) was irradiated with a 12-W neon bulb at either 25 or 70°C. At the times indicated, aliquots were collected and analysed by CZE in 50 m*M* phosphate buffer (pH 7.0) at 100 μA and 10 kV (25°C).

DISCUSSION

Ten years ago, when we made our first thorough investigation of the kinetics of photopolymerization [8], we concluded that such a process was not attractive for producing polyacrylamide gels, because under standard conditions (1-h exposure, as also used in peroxodisulphate initiation), only 60% conversion could be achieved (*vs.* >90% with peroxodisulphate). In order to achieve the same incorporation efficiency, photopolymerization had to be protracted for at least 8 h, a much too slow process to be of practical interest in routine work. However, as we are planning a series of polymerization experiments in microgravity, photopolymerization became attractive, as the gel cassettes could be prepared on earth and polymerization activated in space simply by light irradiation: this basic need prompted the present investigation. We therefore established conditions which allow ample conversion of the monomers into the polymers within the standard 1-h exposure time by: (a) using a conventional neon bulb (12–16 W) but at 70°C or (b) using a strong light source (105-W UV-A, a domestic lamp used for indoor sun-tanning) at room temperature. The latter process is definitely preferable, because in the first instance both the light source and the gel cassette have to be placed in an oven. We have also demonstrated that it is possible to control the lag time by controlling the oxygen partial pressure in solution: when the latter is reduced to only 35 mmHg, the lag time is reduced from 60 min to only 15–17 min. It is tempting to suggest that, perhaps, in the total absence of oxygen, the lag time could be reduced to a vanishing value, but preparing a completely anaerobic solution (*e.g.*, by passing it through insolubilized ascorbic oxidase or another oxygen scavenger) would be too demanding in routine laboratory practice. There are, nevertheless, some important conclusions of our research which are discussed below.

Inhibitors vs. retarders

Inhibitors and retarders are substances which, when added to polymerization reactions in very low concentrations, produce large decreases in rate by, *e.g.*, deactivation of initiating centres of interruption of propagating chains. The terms retardation and inhibition tend nowadays to be used interchangeably, an inhibitor being considered to be a powerful retarder that cuts off chain growth at a very early stage and so effectively prevents significant polymerization. In classic chain kinetics, however, the two terms have specific and different meanings: inhibitors react very rapidly with initial active centres and so prevent initiation, whereas retarders destroy propagating species and thus reduce the rate of reaction. Obviously the distinction becomes tenuous when the similarity in reactivity between initiating and propagating species is close, and this is the situation with many free-radical polymerizations. Nonetheless, the difference between these two concepts is important for kinetics reasons. It is clear from our data (see Fig. 5 and 6) that oxygen acts in a completely different manner during peroxodisulphate as opposed to riboflavin polymerization. In the former instance, oxygen behaves as a true inhibitor or terminator, *i.e.*, it brings about the cessation of growth of a propagating radical, by a process of chain transfer [11]. This phenomenon is easily appreciated in routine laboratory practice: when gels are polymerized in an open-ceiling cassette, the top liquid layer, in contact with atmospheric oxygen, never polymerizes, unless it is protected by, *e.g.*, a layer of butanol. Conversely, with retardation, as in photopolymerization, only the onset of polymerization is shifted along the time axis (see Fig. 5); when the retarder initially present is completely consumed by reaction with primary radicals, the rate of polymerization assumes its uninhibited value, and the final gel product is indistinguishable from the unretarded controls.

Chemistry of the flavin radicals

The behaviour of flavin radicals has been elegantly elucidated by Hemmerich's group [12]. Basically, free flavin can produce radicals (by simultaneous abstraction of a proton and an electron) according to the scheme depicted on the next page.

At the pH prevailing during gel polymerization (in general pH 6–8), the blue radical is formed, with a high absorption maximum (560 nm). This radical is also zwitterionic, as it bears a proton on N–5 and has the adjacent oxygen ionized. If the pH in solution is lowered, a red, cationic radical is produced ($pK = 2.3$, absorption maxima at 470, 400 and 375 nm). At alkaline pH, a new red radical is produced ($pK = 8.4$), characterized by being anionic (one net

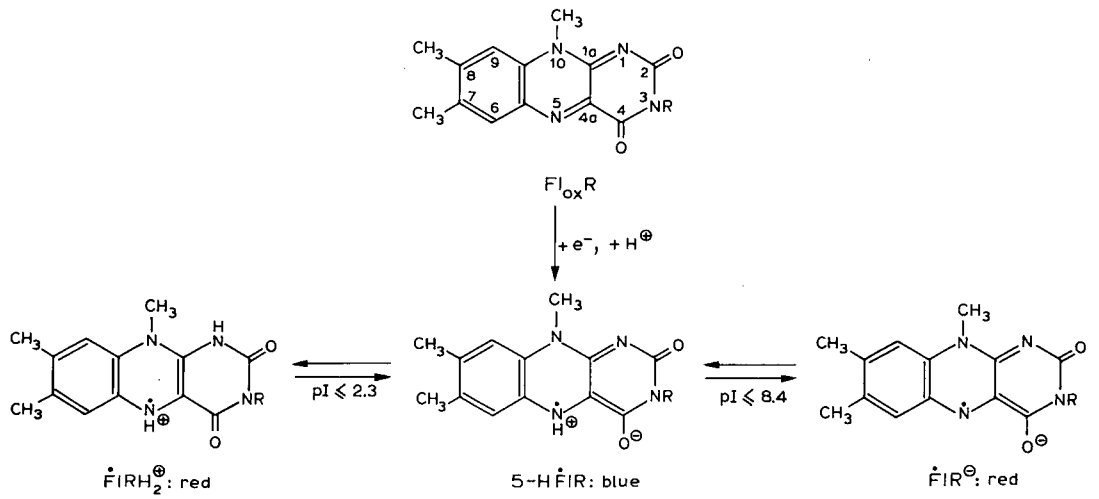

negative charge). At neutral pH, it is the zwitterionic radical that initiates and propagates the chain growth by adding to the acrylamide double bond. What is important, in riboflavin polymerization, is that, during the process of radical formation, there is no production of oxygen radicals which, in addition to propagating chain growth, act as oxidizing agents. This is in fact what happens in peroxodisulphate polymerization: our group has demonstrated that, in all polymerization processes initiated by peroxodisulphate, oxidation of all buffer components (especially primary to tertiary amines) is a common event. In immobilized pH gradients gels, at an appropriate pH, the Immobiline chemicals form N-oxides [13]; in conventional focusing gels, the carrier ampholyte bufers are also oxidized [14]. These N-oxide species remain in the gel matrix (whereas excess of peroxodisulphate is discharged at the anode in a pre-run) and are able to readily oxidize –SH groups in proteins to cystine residues, thus introducing an artefactual heterogeneity [15]. This phenomenon (a residual oxidizing power inherent to peroxodisulphate-polymerized gels) is totally absent in photopolymerized matrices [16].

CONCLUSIONS

Photopolymerization appears now to be a well controlled and highly efficient process: very high conversion rates (>95%) can be obtained by either carrying the process at 70°C for 1 h with a standard 12-W neon bulb or by using a high wattage source (105 W UV-A lamp) at room temperature. The role of oxygen as a retarder has been elucidated, and the lag time can be accurately controlled at low oxygen partial pressures (< 35 mmHg). A unique feature of photopolymerization appears to be the lack of oxidizing power, always present in peroxodisulphate-initiated chain growth.

ACKNOWLEDGEMENTS

This work was supported in part by grants from the Agenzia Spaziale Italiana (Rome) and from ESA–ESTEC for gel polymerization in space.

REFERENCES

1 M. Chiari, M. Giacomini, C. Micheletti and P. G. Righetti, *J. Chromatogr.*, 558 (1991) 285–295.
2 C. Gelfi, P. De Besi, A. Alloni and P. G. Righetti, *J. Chromatogr.*, submitted for publication.
3 J. K. Oster, G. Oster and G. Prati, *J. Am. Chem. Soc.*, 79 (1957) 595–598.
4 B. J. Davis, *Ann. N.Y. Acad. Sci.*, 121 (1964) 404–427.
5 C. J. Brackenridge and H. S. Bachelard, *J. Chromatogr.*, 41 (1969) 242–249.
6 K. H. Fantes and I. G. S. Furminger, *Nature* (London), 215 (1967) 750–751.
7 A. H. Gordon, in T. S. Work and E. Work (Editors), *Laboratory Techniques in Biochemistry and Molecular Biology*, Elsevier, Amsterdam, 1975.
8 P. G. Righetti, C. Gelfi and A. Bianchi-Bosisio, *Electrophoresis*, 2 (1981) 291–295.

9 P. G. Righetti and A. Bianchi-Bosisio, in J. P. Arbuthnott and J. A. Beeley (Editors), *Isoelectric Focusing*, Butterworths, London, 1975, pp. 114–131.
10 P. G. Righetti, K. Ek and B. Bjellqvist, *J. Chromatogr.*, 291 (1984) 31–42.
11 P. J. Flory, *J. Am. Chem. Soc.*, 59 (1937) 241–250.
12 F. Müller, P. Hemmerich and A. Ehrenber, in H. Kamin (Editor), *Flavins and Flavoproteins*, University Park Press, Baltimore, 1971, pp. 107–122.
13 P. G. Righetti, M. Chiari, E. Casale and C. Chiesa, *Theor. Appl. Electr.*, 1 (1989) 115–121.
14 G. Cossu, M. G. Pirastru, M. Satta, M. Chiari, C. Chiesa and P. G. Righetti, *J. Chromatogr.*, 475 (1989) 283–292.
15 M. Chiari, C. Chiesa, P. G. Righetti, M. Corti, T. Jain and R. Shorr, *J. Chromatogr.*, 499 (1990) 699–711.
16 M. Chiari, C. Micheletti, P. G. Righetti and G. Poli, *J. Chromatogr.*, 598 (1992) 287–297.

Journal of Chromatography, 598 (1992) 287–297
Elsevier Science Publishers B.V., Amsterdam

CHROM. 24 038

Polyacrylamide gel polymerization under non-oxidizing conditions, as monitored by capillary zone electrophoresis

Marcella Chiari, Claudia Micheletti and Pier Giorgio Righetti*

Chair of Biochemistry and Department of Biomedical Sciences and Technologies, University of Milan, Via Celoria 2, Milan 20133 (Italy)

Giovanni Poli

Department of Organic and Industrial Chemistry, University of Milan, Via Venezian 21, Milan 20133 (Italy)

(First received November 27th, 1991; revised manuscript received January 23rd, 1992)

ABSTRACT

It has been established that, during peroxodisulphate-catalysed polyacrylamide gel polymerization, there is a concomitant oxidation of all amino buffers present in the mixture, with the formation of N-oxides. This is deleterious in conventional isoelectric focusing and immobilized pH gradients because, even after discharging excess of peroxodisulphate at the anode, a residual oxidizing power remains in the matrix. When focusing proteins under mildly alkaline conditions, a redox reaction occurs during migration, and free SH groups are oxidized to –S–S– bridges, giving rise to spurious bands. The kinetics of riboflavin-catalysed gel polymerization have been reinvestigated and conditions were elucidated that allow >95% conversion of monomers into the growing chains, full control of the lag phase and short polymerization times, as typical of peroxodisulphate catalysis. It was demonstrated, by capillary zone electrophoresis and direct NMR analysis, that there is an additional unique advantage in photopolymerization, namely that even in a large excess of catalyst, no traces of oxidizing power can be found. The gel matrix thus generated is unable to induce any oxidation of proteins during gel electrophoresis.

INTRODUCTION

Peroxodisulphate-catalysed polyacrylamide gel polymerization has been a standard protocol since the inception of gel electrophoresis, as first reported by Raymond and Weintraub [1]. A notable exception is the use of riboflavin for gelation of the sample and spacer gel segments in disc electrophoresis, as proposed by Davis [2]. The reasons for using photopolymerization, however, were stated [2] to be only the convenience in controlling the onset of polymerization (as light exposure is required) and because "the pore size of riboflavin catalysed gel is larger than that of a peroxodisulphate catalyzed gel". However, the situation is more complex than that. In 1967 Fantes and Furminger [3] observed a loss of biological activity of interferon and ribonuclease under the influence of peroxodisulphate. Similar peroxodisulphate-induced inactivation was reported by Mitchell [4] in clostridial peptidase B, while Brewer [5] observed both inactivation and formation of protein cleavage products in yeast enolase. In the last report, peroxodisulphate attack of sulphydryl groups and of tyrosine and tryptophan residues was also proposed. In order to eliminate such peroxodisulphate-induced artifacts, Brewer [5] suggested addition of thioglycolate to the cathodic chamber, so as to have a reducing buffer boundary migrating in front of the proteins.

Our group has been recently able fully to verify and quantify this hypothesis of a potential oxidizing power of peroxodisulphate. When working with immobilized pH gradients (IPG) (the most powerful variant of isoelectric focusing, IEF) [6], we detected

0021-9673/92/$05.00

a pH-dependent oxidation of the four alkaline Immobilines (the acrylamide weak acids and bases used as buffers for maintaining the pH gradient in the gel) by peroxodisulphate during the polymerization process, with the formation of N-oxides. These $R–N^+O^-$ species are in turn strongly oxidizing and attack Cys residues in proteins by transforming them into –S–S–bridges. For alkaline proteins, this often results in spurious, additional bands existing in two possible equilibria: –SH and –S–S–. In the case of human α-globin chains, the formation of an inter-chain –S–S– bridge produces an intense band with a higher isoelectric point [7]. Not even the carrier ampholytes (the soluble, amphoteric buffers guaranteeing the pH gradient in conventional IEF) [8] are immune from this attack: they are also oxidized by peroxodisulphate, generating N-oxides able to oxidize –SH groups in proteins [9]. Hence the precaution of pre-running the gel for discharging harmful peroxodisulphate to the anode is ineffective, as new oxidizing species (N-oxides) remain in the gel, either because they seek an isoelectric point or because they are grafted to the matrix, as in the IPG technique. In a model system, where free Cys was incubated with isoelectric IPG beads at pH 9.0, 100% oxidation to cystine could be demonstrated in a 12-h period [10]. The situation appeared to be so dramatic that we even endeavoured to synthesize new types of acrylamido buffers for IPG resistant to oxidation by peroxodisulphate; one such a chemical was acryloylhistamine [2-(4-imidazolyl)ethylamine-2-acrylamide] [11].

We have recently reinvestigated riboflavin-catalysed gel polymerization, a technique which has not had many followers. In fact, in 1981, when we performed the first studies on photopolymerization, our conclusions were negative, because during the standard time allotted for polymerization (1 h at room temperature) barely 60% conversion of monomers into the growing chains could be obtained [12]. Given the fact that free, unreacted monomers are neurotoxic and can easily add to free –SH groups [13], we pursued the use of peroxodisulphate catalysis, because an efficiency of >90% can be easily elicited [14]. However, in a recent investigation [15], we established conditions allowing an efficiency of >95%, full control of the lag time and short polymerization times, as typical of peroxodisulphate catalysis. As is reported here, photopolymerization appears to offer another unique advantage, namely the complete absence of oxidizing power, even at higher catalyst levels than are customary.

EXPERIMENTAL

Aminopropylmorpholine and acetic anhydride were obtained from Aldrich-Chemie (Steinheim, Germany), pyridine, hydrogen peroxide and sodium dodecyl sulphate (SDS) from Merck (Darmstadt, Germany), riboflavin 5′-phosphate from Carlo Erba (Milan, Italy), ammonium peroxodisulphate from Bio-Rad Labs. (Richmond, CA, USA) and Immobiline p*K* 9.3 buffer from Pharmacia–LKB, (Uppsala, Sweden).

Capillary zone electrophoresis (CZE)

CZE was performed on a Waters Quanta 4000 (Millipore, Milford, MA, USA) in a 50 cm × 75 μm I.D. capillary from Polymicro Technologies (Phoenix, AZ, USA). All runs were made at 25°C in 50 m*M* phosphate buffer (pH 7.0) containing 50 m*M* SDS and 10% methanol (micellar electrokinetic chromatography) [16]. All runs were in the cathodic direction at 10 kV and 66 μA. Samples were loaded for 10 s by the "hydrostatic injection" method. Sample zones were revealed at 214 nm.

Nuclear magnetic resonance (NMR) spectroscopy

^1H and ^{13}C NMR spectra were recorded with a Bruker AC-200 instrument in the Fourier transform mode with tetramethylsilane as internal standard and D_2O as solvent.

Thin-layer chromatography (TLC) and column chromatography

TLC was performed on silica gel $60F_{254}$ plates from Merck, using chloroform–methanol (7:3, v/v) as eluent. The spots were revealed with 3.5% molybdophosphoric acid in ethanol. Preparative chromatography was performed in columns of silica gel 60 (230–400 mesh) from Merck (with chloroform–methanol (9:1) as eluent.

Synthesis of N-Acetylamino-n-propylmorpholine

In order to study the capability of photo- or peroxodisulphate polymerization to induce N-oxides,

analogues of the Immobiline buffers, lacking the double bond, were prepared, so that during exposure to these catalysts no production of a gel phase would ensue. An analogue of the p*K* 7.0 Immobiline was prepared as follows: 7.2 g (7.34 ml, 0.05 mol) of 4-(3-aminopropyl)morpholine were dissolved in 28 ml of pyridine. After adding 14.14 ml (0.13 mol) of acetic anhydride, the reaction was allowed to proceed overnight at room temperature. A 50-ml volume of a 10% solution of K_2CO_3 was then added while keeping the pH above 8.5 and then the mixture was extracted with ethyl acetate (3 × 50 ml). The organic phase, dried over Na_2SO_4, was evaporated *in vacuo*, then the excess of pyridine was eliminated by two treatments with toluene (the latter being then eliminated *in vacuo*). A yellow, oily product was recovered (3.9 g, 41% yield), which was then purified on a silica gel column (with a 1:40 ratio of product to silica) and eluted with chloroform–methanol (9:1). ^{1}H NMR (D_2O): δ 1.45 (m, 2H), 1.4 (s, 3H), 2.18 (m, 2H), 2.30 (bt, J = 5.0 Hz, 4H), 2.92 (t, J = 7.0, 2H), 3.50 ppm (bt, J = 4.5 Hz, 4H). ^{13}C NMR (D_2O): δ 21.15, 27.26, 39.93, 54.8, 57.7, 68.42 ppm. The formula is thus

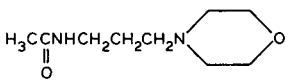

Synthesis of N-acetylamino-n-propylmorpholine-N-oxide

In order to prove the formation of N-oxides with peroxodisulphate catalysis, we synthesized such compounds to be used as reference standards according to VanRheenen *et al.* [17]. To 0.7 g (0.03 mol) of acetylamino-*n*-propylmorpholine, stirred in a flask, were added dropwise 0.426 ml (0.03 mol) of H_2O_2 (30% solution) during 2 h. The reaction temperature was kept at 70–75°C for 4 h with the aid of a thermostat. After cooling to room temperature, the flask was kept under stirring for 24 h. After adding 10 ml of ice-cooled ethyl acetate, a hygroscopic precipitate was formed. After elimination of the solvent, the precipitate was dissolved in 2 ml methanol and 59 mg of activated charcoal (Darco) and 59 mg of Celite were added. After filtering, methanol was evaporated; the colourless oil remaining was dissolved in hot acetone and precipitated by adding hexane (95:5). A 200-mg amount of a white oil was recovered. ^{1}H NMR (D_2O): δ 1.70 (s, 3H), 1.80 (m, 1H), 2.85–3.35 (8H), 3.52 (d, J = 12 Hz, 2H), 3.86 ppm (t, J = 12 Hz, 2H). ^{13}C NMR (D_2O): δ 23.56, 24.18, 33.82, 63.55, 65.69, 70.38 ppm. The formula is thus

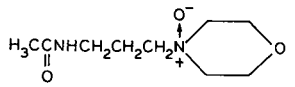

Oxidation of N-acetylamino-n-propylmorpholine by ammonium peroxodisulphate

Oxidation was carried out in three different ways, as follows.

(a) To a 100 m*M* solution of acetylamino-*n*-propylmorpholine in 200 m*M* phosphate buffer (pH 8.0) was added ammonium peroxodisulphate to a final concentration of 1.2%.

(b) The same solution as in (a) was first degassed for 20 min with a water pump prior to the addition of peroxodisulphate.

(c) To a 100 m*M* solution of acetylamino-*n*-propylmorpholine in 200 m*M* borate buffer (pH 9.0) was added ammonium peroxodisulphate to a final concentration of 1.2%.

In all three solutions, on progress of the reaction for 1 h at 50°C, the pH decreased spontaneously, to 6.2 in (a) and (b) and to 7.5 in (c). In order to quantify the reaction products, the above three solutions were diluted 1:10 in 50 m*M* phosphate buffer (pH 7.0), 0.25 m*M* Immobiline p*K* 9.3 was added as internal standard and the mixture was analysed by CZE in the Waters Quanta 4000 instrument.

Incubation of N-acetylamino-n-propylmorpholine with riboflavin 5′-phosphate

This was carried out in three different ways, as follows. (a) To a 200 m*M* solution of acetylamino-*n*-propylmorpholine in 300 m*M* phosphate buffer (pH 8.0) was added riboflavin 5′-phosphate to a final concentration of 1 m*M*. (b) To a 200 m*M* solution of acetylamino-*n*-propylmorpholine in 300 m*M* phosphate buffer (pH 8.0) was added riboflavin 5′-phosphate to a final concentration of 8 m*M*. (c) The same solution as in (b) was first degassed for 20 min with a water pump prior to the addition of riboflavin 5′-phosphate.

All the solutions were then irradiated at 70°C with a 12-W neon lamp for 1 h in spectrophoto-

metric cuvettes of 5 mm thickness. No difference in reactivity was found between glass and quartz cuvettes. In order to quantify the reaction products, the above three solutions were diluted 1:20 in 50 m*M* phosphate buffer (pH 7.0), 1 m*M* Immobiline p*K* 9.3 was added as internal standard and the mixture was analysed by CZE in the Waters Quanta 4000 instrument.

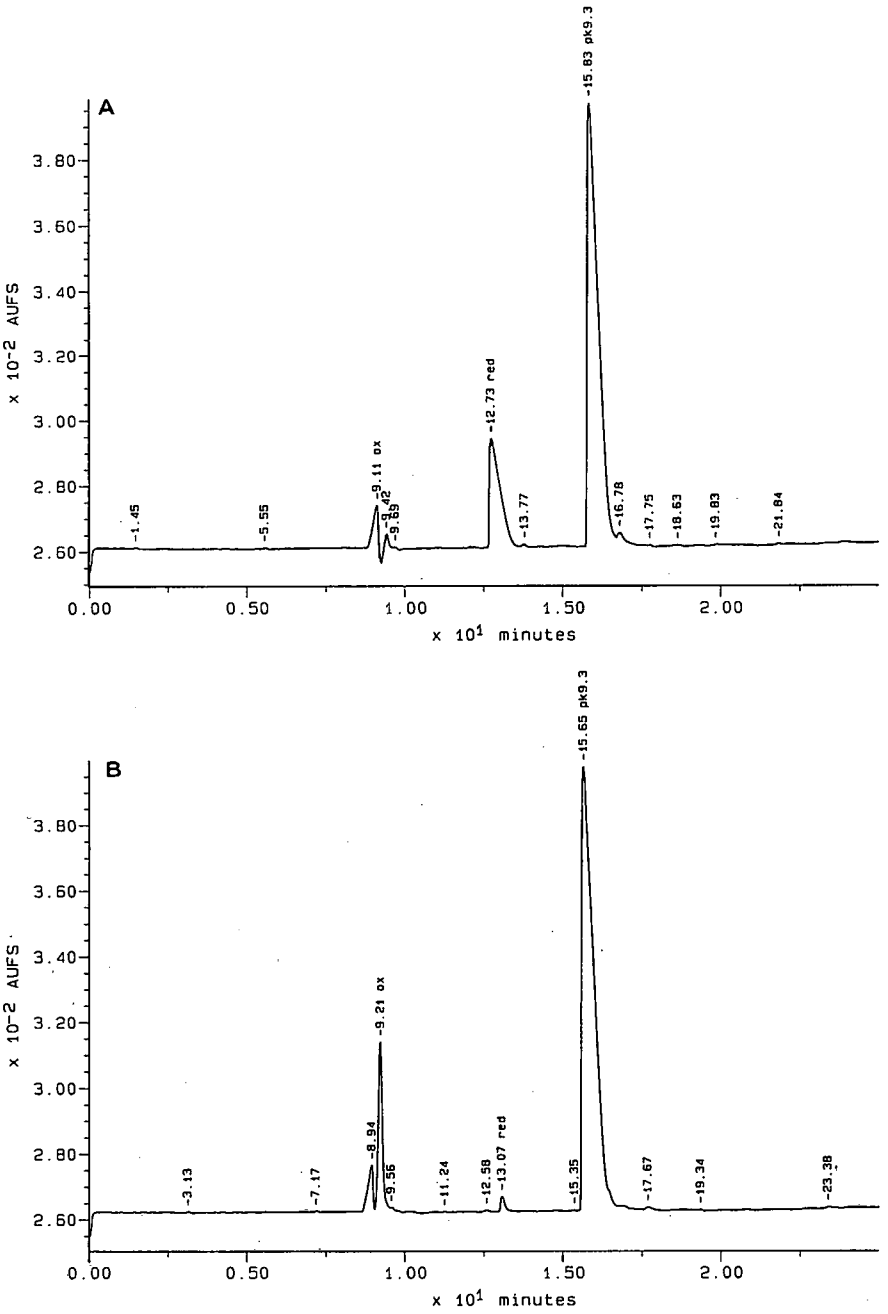

Fig. 1.

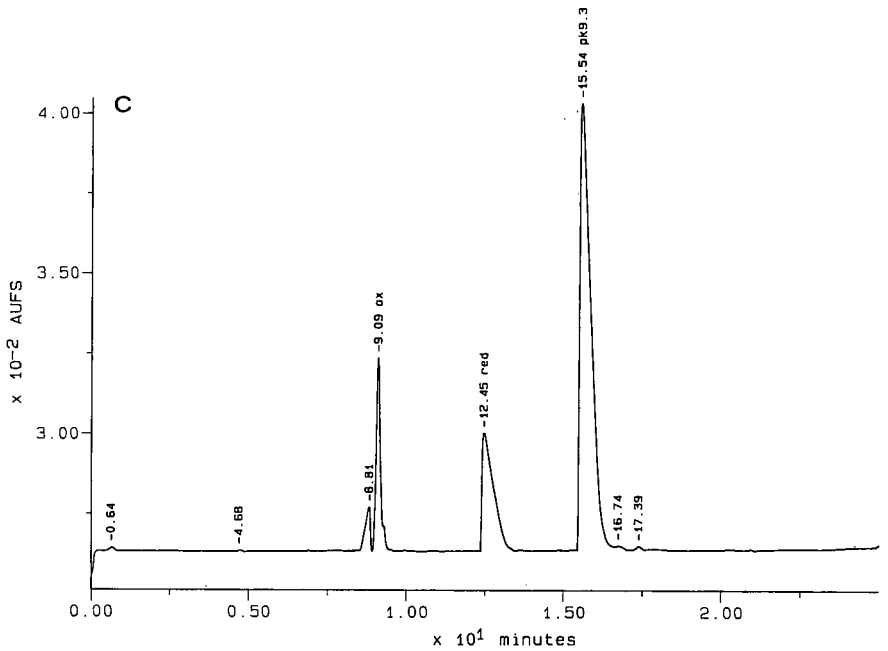

Fig. 1. CZE analysis of reduced and oxidized acetylamino-*n*-propylmorpholine. CZE was performed with a Waters Quanta 4000 instrument in a 50 cm × 75 μm I.D. capillary. All runs were at 25°C in 50 m*M* phosphate buffer (pH 7.0) containing 50 m*M* SDS and 10% methanol. Migrations were in the cathodic direction at 10 kV and 66 μA. Samples were loaded for 10 s by the "hydrostatic injection" method and were revealed at 214 nm. A = control, reduced sample with p*K* 9.3 internal standard added; B = oxidized, synthetic acetylamino-*n*-propylmorpholine with internal standard; C = mixture of reduced and oxidized species and of p*K* 9.3 standard.

RESULTS

Fig. 1 shows typical electropherograms of CZE separations of N-acetylamino-*n*-propylmorpholine and its derivatives. Fig. 1A shows an analytical run with a mixture of this compound with the internal standard (p*K* 9.3 Immobiline). When the corresponding N-oxide, synthesized as described above, is run instead, the peak of the reduced species disappears and a faster migrating component appears (Fig. 1B). When a 1:1 mixture of the reduced and oxidized standards is run (together with the internal standard), the peaks appear in the expected positions, indicating the capability of the CZE system to separate these two compounds. As the separation is done by micellar electrokinetic chromatography, such behaviour suggests that the N-oxide is more hydrophilic than the reduced species, and as such it is less incorporated in the SDS micelles.

Fig. 2 shows the results of incubating N-acetylamino-*n*-propylmorpholine with ammonium peroxodisulphate, the most common catalyst for inducing polyacrylamide gel polymerization. As shown in Fig. 2A, on incubation for 1 h at 50°C at pH 8.0, the reduced species appears to be in equilibrium with the N-oxide form (the latter representing 13%). When the same compound is incubated under the same conditions but at pH 9.0, the conversion to the N-oxide is of the order of 25% (Fig. 2B), but a number of other minor peaks are now also visible. They are tentatively identified as products of β-elimination of the N-oxide, as described in the literature (see Discussion) [18].

We next investigated the fate of the N-acetylamino-*n*-propylmorpholine standard when incubated with riboflavin 5′-phosphate under light irradiation, as in photopolymerization. Fig. 3A shows the CZE separation of the above product in presence of 1 m*M* riboflavin 5′-phosphate; no N-oxide peaks are visible. Even when the product is incubated in 8 m*M* riboflavin 5′-phosphate (a large excess in comparison with the 1 m*M* concentration required for

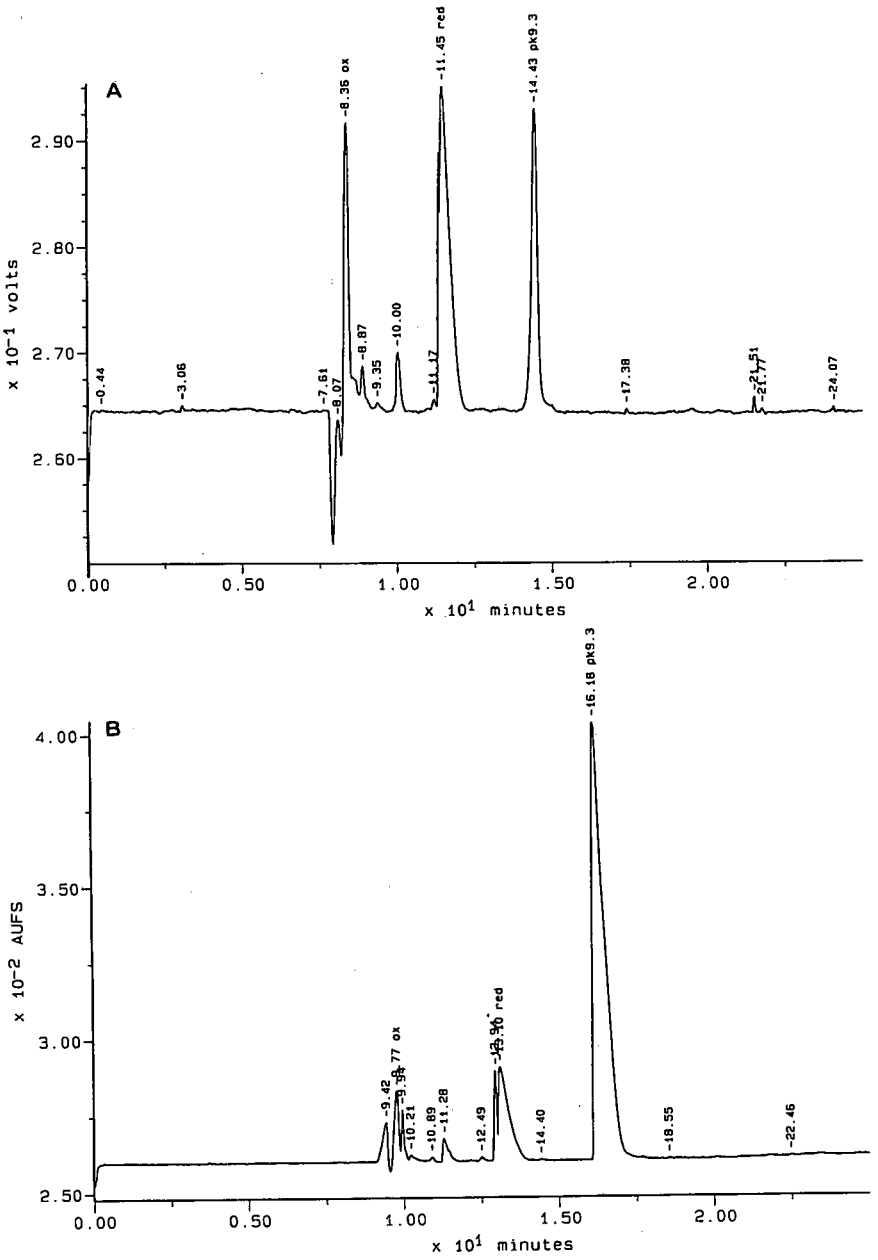

Fig. 2. CZE analysis of acetylamino-*n*-propylmorpholine incubated with peroxodisulphate. A = after incubation with 1.2% ammonium peroxodisulphate for 1 h at 50°C and pH 8.0; B = after incubation with 1.2% ammonium peroxodisulphate for 1 h at 50°C and pH 9.0 (borate buffer). Note the additional, minor peaks, attributed to products of β-elimination. All other experimental conditions as in Fig. 1.

photopolymerization) again no peaks resulting from oxidation are visible (Fig. 3B). When the latter mixture is degassed for 20 min prior to exposure to light and then analysed by CZE, the N-oxide peak is still absent (Fig. 3C).

We repeated the above experiments with light irradiation in the presence of riboflavin 5′-phosphate and with peroxodisulphate treatment and analysed all the reaction products also by TLC. Fig. 4 summarizes the results: in Fig. 4A, a chromatogram of

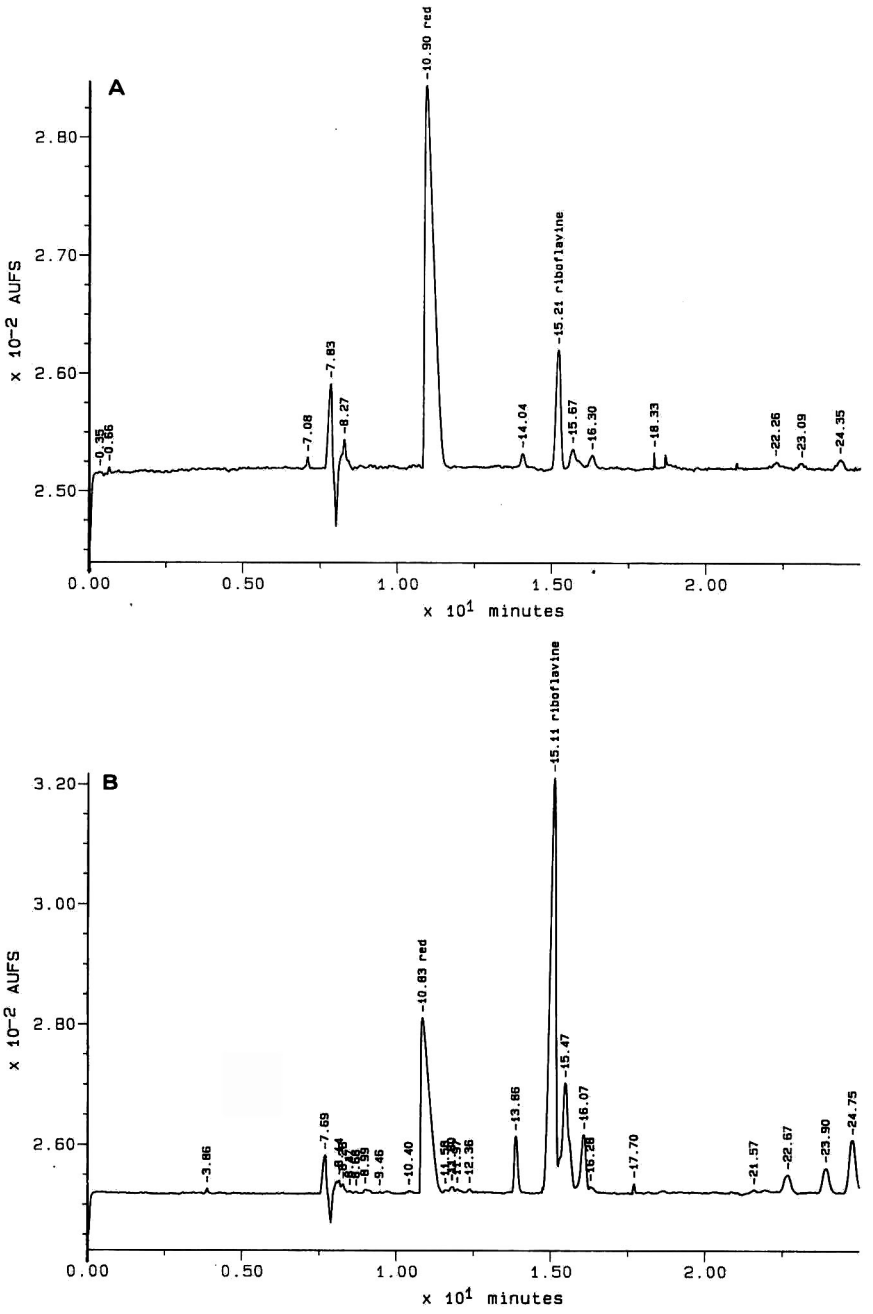

Fig. 3.

(Continued on p. 294)

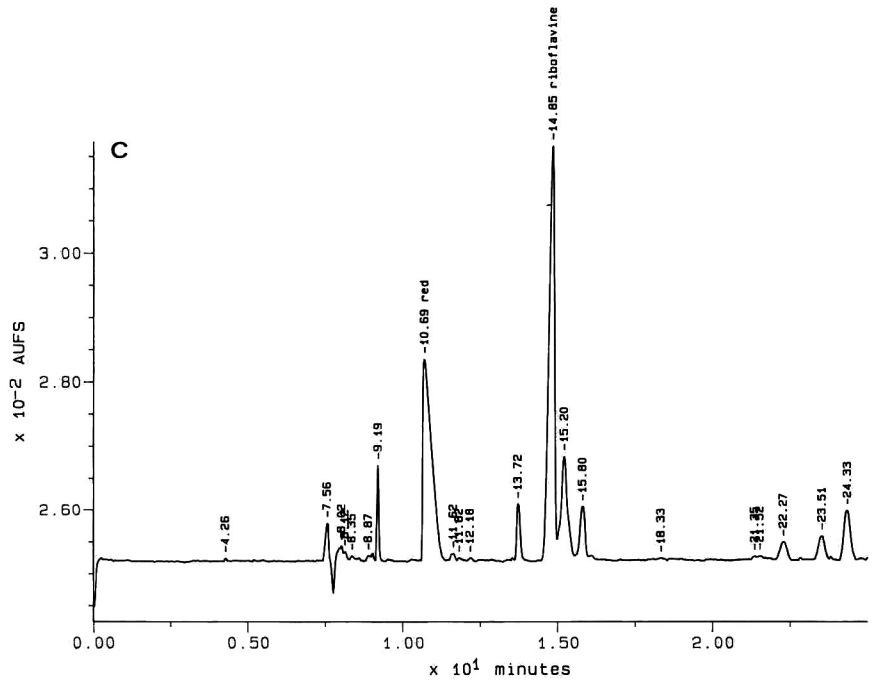

Fig. 3. CZE analysis of acetylamino-*n*-propylmorpholine incubated with riboflavin 5′-phosphate. A = reduced product incubated with 1 m*M* riboflavin 5′-phosphate; B = same as A but in the presence of 8 m*M* riboflavin 5′-phosphate (undegassed sample); C = same as B, but after degassing for 20 min with a water pump. Note in all instances the absence of the N-oxide peak.

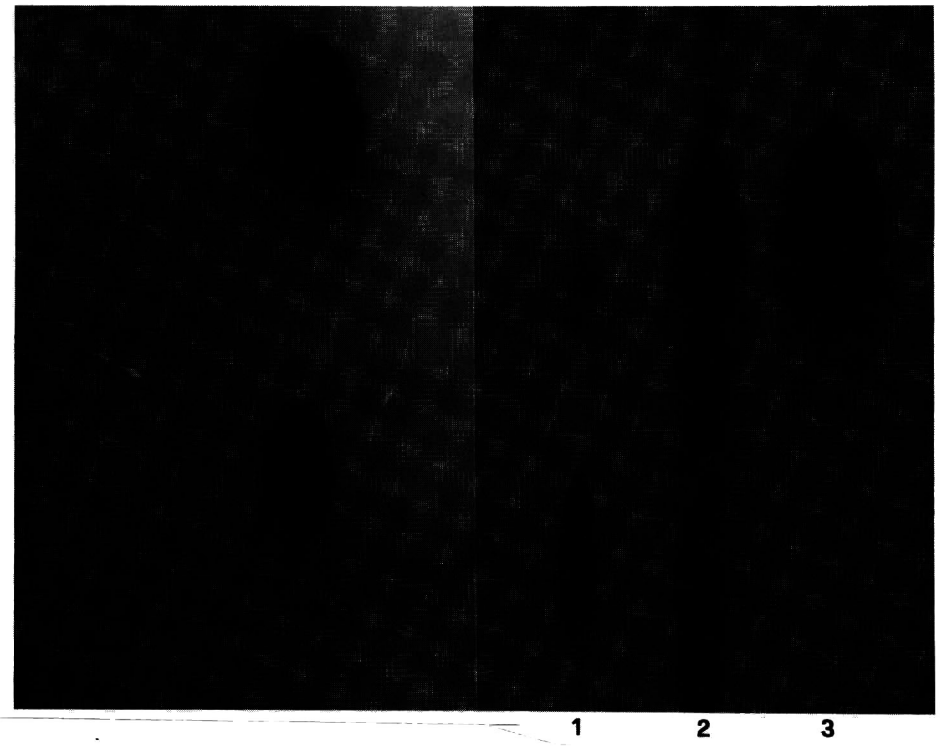

Fig. 4. TLC of reduced and oxidized acetylamino-*n*-propylmorpholine. A = 1:1 mixture of reduced (upper spot) and oxidized (lower spot) species; B: track 1 = purified N-oxide (note traces of reduced acetylamino-*n*-propylmorpholine with higher R_F); track 2 = peroxodisulphate-oxidized sample (1 h at 50°C in the presence of 3.2% peroxodisulphate); track 3 = purified, reduced acetylamino-*n*-propylmorpholine. The horizontal arrow heads with the letter O indicate the sample application line. The solvent front line is not visible on the upper part as this photograph is a close-up of the thin-layer plate.

an equimolar mixture of acetylamino-*n*-propylmorpholine and its N-oxide is shown. In Fig. 4B, the tracks are (1) the pure N-oxide (which is seen to contain traces of the reduced species), (2) the reduced compound treated with ammonium peroxodisulphate (a mixture of reduced and N-oxide species is clearly visible, with a few minor components tentatively identified as products of β-elimination) and (3) the standard of N-acetylamino-*n*-propylmorpholine.

DISCUSSION

The results indicate univocally, for the first time, the oxidizing power of peroxodisulphate during gel polymerization and, in contrast, the lack of such oxidizing power in photopolymerization with riboflavin and light. Whereas in previous papers we had clearly indicated the presence of N-oxides in all four Immobiline chemicals (p*K* 6.2, 7.0, 8.5 and 9.3), such a presence had been inferred from UV–visible spectra and indirect evidence. Here, in contrast, such species were identified from NMR spectra of the synthetic N-oxide product, followed by separation of the reduced and oxidized forms using both, CZE and TLC. We feel that this is an important advance as it finally clears years of debate on whether peroxodisulphate could or could not oxidize and modify proteins and what, on the contrary, would be the role of riboflavin in photopolymerization. From the present data, it is now clear that photopolymerization is totally unable to induce the formation of N-oxides, even when used in large excess and even in the presence of O_2 in the polymerizing solution (undegassed samples). In the light of the present results, photopolymerization now appears to be a very attractive alternative to peroxodisulphate catalysis. In fact, whereas formerly we had found poor conversion efficiencies in photopolymerization [12], we have recently reported very high conversions (>95%), obtained by either photopolymerizing at 70°C for 1 h with the standard 12-W neon lamp, or by photopolymerizing at room temperature but with a 105-W UV-A source.

In recent work [15], we also investigated the role of pO_2 during the polymerization process; oxygen acts as a retarder in photopolymerization, whereas it plays the role of a true inhibitor in peroxodisulphate catalysis. Even with very high levels of dissolved oxygen (pO_2 > 900 mmHg) one can still obtain a final product, in photopolymerization, identical with gels photopolymerized in only 35 mmHg of pO_2. Conversely, in peroxodisulphate polymerization, such high levels of oxygen in the gelling solution produce an irreversible inhibition of gelation.

It is of interest to note the coincident profiles of peaks in TLC and CZE: the spectrum of zones obtained in Fig. 2B is essentially identical with the series of spots in Fig. 4B (track 2). This further underlines the concept of Terabe [16] that in micellar electrokinetic chromatography the primary separation parameter is a chromatographic one, the electric field applied being merely a stronger field than a hydraulic pressure, and thus simply accelerating the separation process. From this point of view, it would appear that CZE would rather compete with high-performance liquid chromatography than with conventional electrophoretic techniques in gel slabs, such as isoelectric focusing and immobilized pH gradients.

When performing peroxodisulphate incubation at pH 9.0, we had assumed that this would increase the formation of N-oxide of N-acetylamino-*n*-propylmorpholine, as we had demonstrated [7] that such an oxidation is strongly pH dependent, as it depends on the availability of a free electron pair on the nitrogen atom. When such a nitrogen is extensively protonated (*e.g.*, at *ca.* 2 pH units below the p*K* value), oxidation is completely abolished [7]. However, a series of new peaks appear in both the CZE profile (Fig. 2B) and in TLC (Fig. 4B). Tentatively, we assume that these additional minor components are products of β-elimination, by which a double bond is formed at the N-oxide site, according to the following reaction:

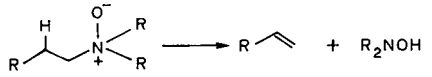

Although we have no direct proof of this, in previous studies we had noted a marked increase in UV chromophores after peroxodisulphate oxidation [7], in agreement with formation of UV-absorbing double bonds. Such a process of β-elimination has been well described [18]. Unfortunately, the amount of product was so minute as to defy any attempt at purification and further chemical characterization.

Chemistry of flavin radicals

The behaviour of flavin radicals has been elegantly elucidated by Hemmerich's group [19]. Basically, free flavin can produce radicals (by simultaneous abstraction of a proton and an electron) according to the scheme depicted below:

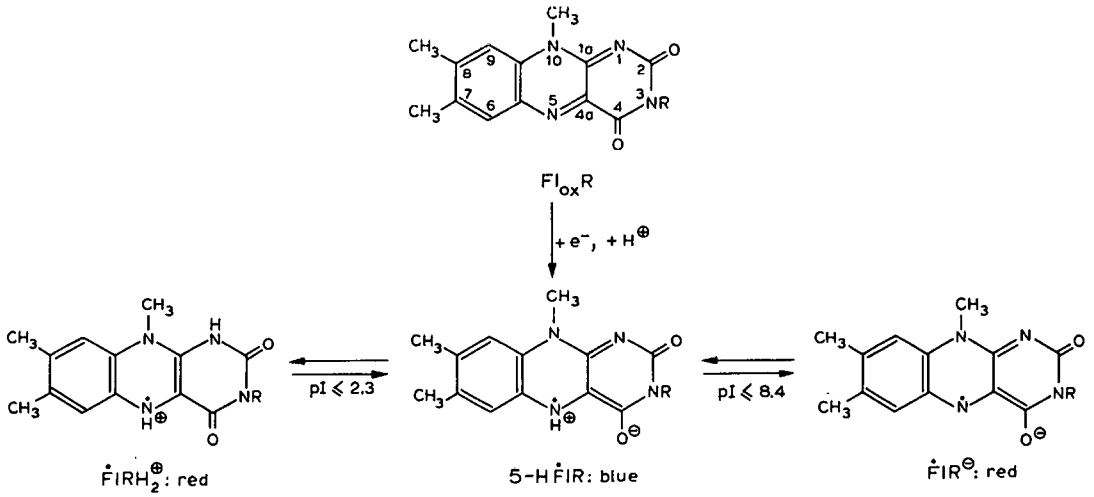

At the pH prevailing during gel polymerization (in general pH 6–8), the blue radical is formed, with a high absorption maximum (560 nm). This radical is also zwitterionic, as it bears a proton on N-5 and has the adjacent oxygen ionized. If the pH in solution is lowered, a red, cationic radical is produced (pK = 2.3, absorption maxima at 470, 400 and 375 nm). At alkaline pH, a new red radical is produced (pK = 8.4), characterized by being anionic (one net negative charge). At neutral pH, it is the zwitterionic radical that initiates and propagates the chain growth by adding to the acrylamide double bond. What is important, in riboflavin polymerization, is that, during the process of radical formation, there is no production of oxygen radicals which, in addition to propagating chain growth, act as oxidizing agents. Thus, the lack of oxidizing power is a unique feature of photopolymerization, whereas peroxodisulphate catalysis is simultaneously an oxidation event, as nascent oxygen radicals are produced by decomposition of peroxodisulphate.

CONCLUSIONS

Photopolymerization appears now to be a well controlled and highly efficient process: very high conversion rates (>95%) can be obtained by either carrying the process at 70°C for 1 h with a standard 12-W neon bulb or by using a high wattage source (105 W UV-A lamp) at room temperature. A unique feature of photopolymerization appears to be the lack of oxidizing power, always present in peroxodisulphate-initiated chain growth.

ACKNOWLEDGEMENTS

This work was supported in part by grants from the Agenzia Spaziale Italiana (Rome) and from ESA–ESTEC for gel polymerization in space.

REFERENCES

1 S. Raymond and L. Weintraub, *Science (Washington, D.C.)*, 130 (1959) 711–712.
2 B. J. Davis, *Ann. N. Y. Acad. Sci.*, 121 (1964) 404–427.
3 K. H. Fantes and I. G. S. Furminger, *Nature (London)*, 215 (1967) 750–751.
4 W. M. Mitchell, *Biochim. Biophys. Acta*, 147 (1967) 171–175.
5 J. M. Brewer, *Science (Washington D.C.)*, 156 (1967) 256–257.
6 P. G. Righetti, *Immobilized pH Gradients: Theory and Methodology*, Elsevier, Amsterdam, 1990.
7 P. G. Righetti, M. Chiari, E. Casale and C. Chiesa, *Appl. Theor. Electr.*, 1 (1989) 115–121.
8 P. G. Righetti, *Isoelectric Focusing: Theory, Methodology and Applications*, Elsevier, Amsterdam, 1983.
9 G. Cossu, M. G. Pirastru, M. Satta, M. Chiari, C. Chiesa and P. G. Righetti, *J. Chromatogr.*, 475 (1989) 283–292.
10 M. Chiari, C. Chiesa, P. G. Righetti, M. Corti, T. Jain and R. Shorr, *J. Chromatogr.*, 499 (1990) 699–711.
11 M. Chiari, M. Giacomini, C. Micheletti and P. G. Righetti, *J. Chromatogr.*, 558 (1991) 285–295.

12 P. G. Righetti, C. Gelfi and A. Bianchi-Bosisio, *Electrophoresis*, 2 (1981) 291–295.
13 M. Chiari, A. Manzocchi and P. G. Righetti, *J. Chromatogr.*, 500 (1990) 697–704.
14 P. G. Righetti and A. Bianchi-Bosisio, in J. P. Arbuthnott and J. A. Beeley (Editors), *Isoelectric Focusing*, Butterworths, London, 1975, pp. 114–131.
15 C. Gelfi, P. De Besi, A. Alloni, P. G. Righetti, T. Lyubimova and V. A. Briskman, *J. Chromatogr.*, 598 (1992) 277–285.
16 S. Terabe, *Trends Anal. Chem.*, 8 (1989) 129–134.
17 V. VanRheenen, R. C. Kelly and D. Y. Cha, *Tetrahedron Lett.*, 23 (1976) 1973–1976.
18 A. C. Cope and E. Ciganek, *Org. Synth., Coll. Vol.*, 4 (1963) 612–615.
19 F. Müller, P. Hemmerich and A. Ehrenber, in H. Kamin (Editor), *Flavins and Flavoproteins*, University Park Press, Baltimore, 1971, pp. 107–122.

Journal of Chromatography, 598 (1992) 298–302
Elsevier Science Publishers B.V., Amsterdam

CHROM. 24 044

Short Communication

Separation and determination of trace amounts of vanadium(V), chromium(III) and iron(III) with 2-(2-thienylazo)-5-diethylaminophenol chelates by high-performance liquid chromatography

Shaopu Liu*, Mingqiao Zhao and Chuanyue Deng

Department of Chemistry, Southwest China Teachers University, Chongqing 630715 (China)

(First received March 5th, 1991; revised manuscript received January 28th, 1992)

ABSTRACT

A reversed-phase high-performance liquid chromatographic method for the separation and the determination of vanadium(V), chromium(III) and iron(III) with 2-(2-thienylazo)-5-diethylaminophenol chelates on a C_{18}-bonded stationary phase by using methanol–tetrahydrofuran–water (20:15:65, v/v/v) containing 0.05 *M* lithium sulphate and 0.04 *M* acetate buffer (pH 5.5) as mobile phase and with spectrophotometric detection at 570 nm was developed. The method has high sensitivity, the detection limits being 0.5 ppb for vanadium(V), 2 ppb for chromium(III) and 1 ppb for iron(III). Under the optimum conditions, most other metal ions did not interfere, *e.g.*, up to 1000 μg of magnesium(III), cadmum(II), zinc(II), lead(II), maganese(II), calcium(II), barium(II), tin(II, IV) and tungsten (VI), 400 μg of thorium(IV), 200 μg of iron(II), bismuth(III), zirconium(IV), 150 μg of gallium(III) and 120 μg of lanthanum(III) in the determination of 2.5 μg of iron(III) and chromium(III) and 1 μg of vanadium(V). The method can be applied to the simultaneous determination of trace amounts of vanadium(V), chromium(III) and iron(III) in water, tea leaves and rice samples.

INTRODUCTION

High-performance liquid chromatography (HPLC) is extensively applied to the separation and determination of inorganic ions. Most studies involve the reversed-phase (RP) HPLC of metal ion chelates, because the methods are rapid, convenient, highly sensitive and allow the selective determination of metal ions. In these methods, the most commonly used chelating agents include sodium diethyldithiocarbamate (DDTC) [1], dithizone [2], 8-hydroxyquinoline [3], β-diketones [4], pyridylazo dyes such as PAR [5] and 5-Br-PAPS [6] and others [7], azo compounds of chromotropic acid [8,9] and porphyrins [10].

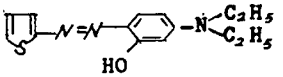

TADAP

The colour reaction of 2-(2-thienylazo)-5-diethylaminophenol (TADAP) with metal ions and their analytical application have not previously been reported. We found that it can form red or violet-red chelates of maximum absorption wavelength between 520 and 600 nm with vanadium(V), chromium(III), iron(III), cobalt(II), nickel(II), gallium(III), indium(II), titanium(IV), zirconium(IV), bismuth(III), copper(II), etc. The colour reactions

0021-9673/92/$05.00

have high sensitivity, but showed poor selectivity in the determination of metal ions by using spectrophotometry because of mutual interferences.

In this work it was found that the RP-HPLC determination of vanadium(V), chromium(III) and iron(III) with TADAP chelates has very good selectivity and the usual metal ions and anions do not interfere in the determination. The method can be applied to the determination of trace amounts of vanadium(V), chromium(III) and iron(III) in water, tea leaves, rice and other samples.

EXPERIMENTAL

Apparatus

The HPLC system consisted of a Model LC-6A pump (Shimadzu, Kyoto, Japan), a Rheodyne (Cotati, CA, USA) Model 7125 injection valve (20-μl sample loop), a Model C-R3A chromatographic data processor (Shimadzu), a column packed with 9–11-μm YWG-C_{18} ODS (250 × 4.0 mm I.D.) (Dalian Institute of Chemical Physics, Academia Sinica, China), a Model SPD-6AV UV-VIS spectrophotometric detector (Shimadzu) and a Model U-3400 spectrophotometer (Hitachi, Kyoto, Japan). A Model SA-720 pH meter (Orion, Cambridge, MA, USA), a Model CQ-50 ultrasonicator for degassing the mobile phase (Shanghai Ultrasonic Instrument Factory, Shanghai, China) and a Model 800 centrifuge (Shanghai Operating Apparatus Factory, Shanghai, China) were used.

A Model WF-1A atomic absorption spectrometer (Beijing Second Optical Instrument Factory, Beijing, China) was used for the determination of chromium and vanadium using a Model WF-4A graphite furnace and for the determination of iron using an air–acetylene flame.

Reagents

All solutions were prepared with analytical-reagent grade chemicals and all water used was doubly distilled.

TADAP (analytical-reagent grade, Beijing Chemical Factory, Beijing, China) was prepared as a 0.1% solution in ethanol.

Stock standard solutions of various metal ions of concentration 1 mg/ml were prepared by the usual method from highly pure metal oxides or salts. Working standard solutions of concentration 1–10 μg/ml were prepared by dilution with water.

The mobile phase was methanol–tetrahydrofuran–water (20:15:65, v/v/v) containing 0.05 *M* lithium sulphate and 0.04 *M* acetate buffer (pH 5.5). The mobile phase was filtered through a 0.45-μm membrane filter and degased using a Model CQ-50 ultrasonic bath before use.

General procedure

Amounts of 1 μg of vanadium(V), 2.5 μg of chromium(III) and 2.5 μg of iron(III) were placed in a 25-ml volumetric flask, 2.0 ml of acetic acid–sodium acetate buffer solution (pH 5.5), 4.0 ml of ethanol and 2.0 ml of 0.1% ethanolic TADAP solution were added and mixed and diluted to about 20 ml with water. After heating in a water-bath at 80–90°C for 10 min, the solution was cooled to room temperature, diluted to the mark with water and centrifuged for 3 min at 3000 rpm.

An aliquot of 20 μl of the solution was injected into the chromatograph with the 20-μl loop injector. The flow-rate of the mobile phase was 0.9 ml/min and the elutes were monitored at 570 nm with an SPD-6AV UV-VIS spectrophotometric detector. The sensitivity was set at 0.08 a.u.f.s. The amounts of metal ions eluted were determined from the peak areas.

Determination of vanadium(V), chromium(III) and iron(III) in water

A clean, filtered 15.0-ml water sample was placed in a 25.0-ml volumetric flask, then vanadium(V), iron(III) and chromium(II) were determined as described under *General procedure*.

Determination of vanadium(V), chromium(III) and iron(III) in tea leaves and rice

A 1.000-g amount of oven-dried tea leaves or rice was weighed into a crucible, covered and ashed in an electric oven at 750°C for 3 h. The ash was dissolved nitric acid (1:1) and the solution was evaporated nearly to dryness. The residue was dissolved in and diluted to 52.0 ml with water. A 15.0-ml volume of this solution was placed in a 25-ml volumetric flask for the determination of vanadium(V) and chromium(III), but 0.5 ml of the solution for the determination of iron(III). The determination was then carried out as described under *General procedure*.

RESULTS AND DISCUSSION

Absorption spectra of the chelates

The characteristics of the chelates of TADAP with vanadium(V), chromium(III) and iron(III) and their absorption spectra are shown in Table I and Fig. 1. The composition ratios of the chelates were established by Job's method and the equilibrium shift method. Under similar conditions, TADAP also forms sensitive coloured chelates with titanium(IV), zirconium(IV), bismuth(III), gallium(III), cobalt(II), nickel(II), copper(II) and some noble metals. Their maximum absorption wavelength are all between 520 and 600 nm. However, trace amounts of vanadium(V), chromium(III) and iron(III) can be satisfactorily separated and determined in the presence of the above-mentioned interfering ions by RP-HPLC with spectrophotometric detection at 570 nm.

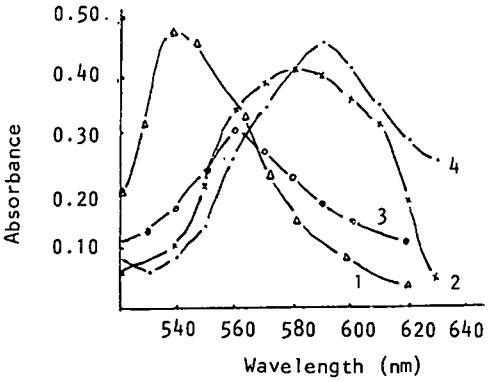

Fig. 1. Absorption spectra of TADAP and its chelates with metal ions (5 μg/25 ml). pH, 5.5. 1 = TADAP against water; 2 = V(V) against reagent blank; 3 = Cr(III) against reagent blank; 4 = Fe(III) against reagent blank.

Effect of the composition and pH of the mobile phase

A number of combinations of organic solvents and water such as methanol–water, methanol–acetonitrile, methanol–acetonitrile–water and methanol–tetrahydrofuran–water were investigated as mobile phases. The methanol–tetrahydrofuran–water mixture was found to be the best because it gives better peak shapes and a more effective separation of vanadium(V), chromium(III) and iron(III) than the other mixtures, and it was adopted in subsequent work.

The retention times of the chelates of chromium(III) and iron(III) decrease with increase in the tetrahydrofuran concentration in the mobile phase, but the effect is smaller with the vanadium(V) chelate. The best separation was obtained using methanol–tetrahydrofuran–water (20:15:65, v/v/v) as the mobile phase.

Using the methanol–tetrahydrofuran–water system in the absence of any counter ions, the peaks of chromium(III) and iron(III) chelates are slow to appear and are low, flat and tailing, although that for the vanadium(V) chelate is good. When different inorganic salts such as lithium sulphate, sodium sulphate, sodium dihydrogenphosphate, sodium bromide, potassium nitrate and potassium iodide were added, it was found that lithium sulphate gave the greatest improvement in chromatographic characteristics, and led to very satisfactory separations of all three chelates, but the effect of the other compounds was not remarkable. The suitable concentration range of lithium sulphate is between 0.04 and 0.08 *M*. If the anions of the inorganic salts have complexing ability or are strongly reducing, *e.g.*, PO_4^{3-}, I^- or Br^-, they will lead to a decrease in sensitivity for the determination of iron(III). In subsequent experiments we chose 0.05 *M* lithium sulphate.

The effect of the pH of the mobile phase on the retention time was investigated. At pH >6.0 or <4.0 the peak areas decrease, but at pH >6.5 the retention time was prolonged. Therefore, the optium pH range is between 5.0 and 6.0. In subsequent experiments acetic acid–sodium acetate buffer solution (pH 5.5) was used.

TABLE I

COLOUR REACTION CHARACTERISTICS OF TADAP CHELATES WITH VANADIUM(V), CHROMIUM(III) AND IRON(III)

Metal ion	λ_{max} (nm)	pH	Temperature (°C)	Composition ratio (M:L)
V(V)	585	4.2–6.7	25	1:1
Cr(III)	560	3.0–6.2	80–90 (10 min)	1:2
Fe(III)	590	4.2–6.8	25	1:2

TABLE II

DETERMINATION OF VANADIUM, CHROMIUM AND IRON IN WATER, TEA LEAVES AND RICE

Sample	Element		Content determined	Average content	Standard deviation	Relative standard deviation (%)	AAS[a] method
Tap water	V	(ppb)	0.62, 0.65, 0.63	0.63	0.015	2.4	0.59
	Cr	(ppb)	23.3, 22.8, 23.2	23.1	0.264	1.1	24.2
	Fe	(ppm)	0.24, 0.238, 0.238	0.24	0.001	0.5	0.242
Spring water	V	(ppb)	1.32, 1.28, 1.30	1.30	0.02	1.5	1.30
	Cr	(ppb)	9.83, 9.70, 10.22	9.92	0.27	2.7	10.3
	Fe	(ppm)	0.126, 0.125, 0.127	0.126	0.001	0.7	0.127
Tea leaves	V	(ppb)	650, 680, 680	670	17	2.6	664
	Cr	(ppb)	260, 272, 268	267	6	2.3	273
	Fe	(ppm)	78.9, 176.8, 178.4	178.0	1.1	0.6	182
Rice	V	(ppb)	135, 138, 138	137	1.7	1.3	134
	Cr	(ppb)	84.8, 85.3, 84.4	84.5	0.6	0.7	85.6
	Fe	(ppm)	23.4, 22.6, 23.4	23.1	0.46	1.9	23.3

[a] Atomic absorption spectrometric.

Effect of foreign ions

The effect of foreign ions on the determination of 2.5 μg of iron(III) and chromium(III) and 1 μg of vanadium(V) was studied under the optimum conditions. Most other ions do not interfere (relative error ≤5%), *e.g.*, to 1000 μg of magnesium(II), cadmium(II), zinc(II), lead(II), molybdenum(VI), manganese(II), calcium(II), tin(II, IV), tungsten(VI) and barium(II), 400 μg of thorium(IV), 200 μg of iron(II), bismuth(III) and zirconium(IV), 150 μg of gallium(III), 120 μg of lanthanum(III), 80 μg of indium(III), 30 μg of copper(II) and nickel(II) and 25 μg of cobalt(II). Hence the method has high selectivity.

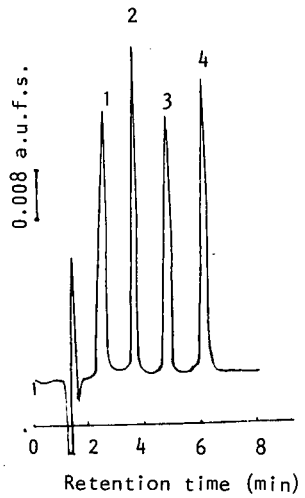

Fig. 2. Standard chromatogram. V(V), 1 μg in 25 ml; Cr(III), 2.5 μg in 25 ml; Fe(III), 2.5 μg in 25 ml. Peaks: 1 = V(V); 2 = TADAP; 3 = Cr(III); 4 = Fe(III).

Calibration graph and detection limits

Calibration graphs of peak area *versus* metal ion concentration were linear in the concentration ranges 0–200 ppb for vanadium(V), 4–400 ppb for chromium(III) and 5–400 ppb for iron(III).

The detection limits, calculated as the concentrations that gave a signal twice the background noise (signal-to-noise ratio = 2), were 0.5 ppb for vanadium(V), 2 ppb for chromium(III) and 1 ppb for iron(III). A standard chromatogram is shown in Fig. 2.

Results of analysis of samples

The results for the determination of vanadium, chromium and iron in water, tea leaves and rice are shown in Tables II and III. The relative standard deviations are between 0.7% and 2.7% (n = 8) and the recoveries are between 94.2% and 100.5%.

TABLE III

RECOVERY OF DETERMINATION OF V(V), Cr(III) AND Fe(III)

Sample	Element	Amount determined (ng)	Amount added (ng)	Total amount determined (ng)	Recovery (%)
Tap water	V	9.45	100.0	109.5	100.5
	Cr	364.5	100.0	437.4	97.4
	Fe	3.63×10^3	$10.0 \cdot 10^3$	$13.42 \cdot 10^3$	94.2
Tea leaves	V	670	100.0	772.0	100.3
	Cr	267	100.0	358	96.6
	Fe	178.0×10^3	$100.0 \cdot 10^3$	$276.0 \cdot 10^3$	98.9

REFERENCES

1 R. M. Smith and L. E. Yankey, *Analyst (London)*, 107 (1982) 74.
2 K. Ohashi, S. Iwai and M. Horiguchi, *Bunseki Kagaku*, 31 (1982) E 285.
3 B. Wenclawiak, *Fresenius' Z. Anal. Chem.*, 308 (1981) 120.
4 J. D. Willett and M. M. Knight, *J. Chromatogr.*, 237 (1982) 99.
5 H. Hoshino, T. Yotsuyanagi and K. Aomwar, *Bunseki Kagaku*, 27 (1978) 315.
6 Y. Shijo and T. Shimizu, *Analyst (London)*, 113 (1988) 1201.
7 H. Wada, S. Nezu, T. Ozawa and G. Nakazwa, *J. Chromatogr.*, 295 (1984) 413.
8 X. X. Zhang, M. S. Wang and J. K. Cheng, *Anal. Chem.*, 60 (1988) 1670.
9 X. X. Zhang, M. S. Wang and J. K. Cheng, *J. Chromatogr. Sci.*, 26 (1988) 517.
10 K. Saitoh, M. Kobayashi and W. Suzuki, *J. Chromatogr.*, 243 (1982) 291.

Journal of Chromatography, 598 (1992) 303–308
Elsevier Science Publishers B.V., Amsterdam

CHROM. 24 026

Short Communication

Simple method for collecting volatile compounds from single insects and other point sources for gas chromatographic analysis

Miklós Tóth*

Plant Protection Institute, Hungarian Academy of Sciences, P.O. Box 102, H-1525 Budapest (Hungary)

Hans-Rudolf Buser

Swiss Federal Research Station, CH-8820 Wädenswil (Switzerland)

(First received September 19th, 1991; revised manuscript received January 21st, 1992)

ABSTRACT

A simple method is described for trapping airborne volatile compounds in the ng range for their subsequent gas chromatographic–mass spectrometric analysis. Volatile compounds are trapped on the inner surface of glass capillaries. The trapped compounds are extracted by rinsing the capillaries with 2–3 μl of solvent, and the extracts are directly analysed. As examples, pheromones are analysed. The method may also be suitable for the collection of volatile compounds from other point sources.

INTRODUCTION

The collection of airborne pheromones and other volatile compounds has been one of the key issues in semiochemical research. In most instances volatile compounds emitted from living organisms have been trapped on Porapak Q, Tenax, active carbon, glass-wool or glass beads [1–6], and then washed off with a relatively large volume (several hundred microlitres or more) of solvent. This necessitates an evaporation stage to remove most of the solvent before analysis, which can result in contamination or loss of components of the volatile compounds trapped. This problem can be overcome by collecting the volatile compounds in glass capillary tubes, which will allow desorption with small volumes of solvents [7,8]. Based on this technique, we describe here a simple, flexible and convenient collection method which makes possible the qualitative analysis of pheromone-like effluents from single insects or other point sources, and which can be carried out also under field conditions. The application of the method to four different compound classes of pheromones is described.

EXPERIMENTAL

Insects

The insect cultures of *Mamestra brassicae* L., *Mamestra oleracea* L., *Heliothis armigera* L. (Lepidoptera, Noctuidae) and *Chiasma clathrata* L. (Lepidoptera, Geometridae) were derived from eggs of female moths collected from the wild. The pupae reared were sexed and the sexes were held separately

0021-9673/92/$05.00

under a reversed 18 h–6 h light–dark photoregime at 25°C in the laboratory. Emerging adults were collected daily and were transferred to 1-l glass jars where they were supplied with a 5% honey solution on cotton-wool. Female moths exhibiting calling behaviour were collected, and deep-frozen at −65°C until used. For performing collections of volatile compounds from live insects, female moths were placed singly in wire containers (100 × 100 × 100 mm) one day prior to collection. The front wall of the container was removable to allow free access to the calling female.

Extracts of volatile compounds

Volatile compounds from calling female moths held at ambient room temperature (20–25°C) were collected in two 20-μl disposable micropipettes (Rudolf Brand, Wertheim, Germany) connected firmly in series by a small piece of PTFE tubing. Air (50 ml/min) was drawn through this set-up using a commercial aquarium pump. The open end of the first capillary was held at a distance of 1–2 mm from the pheromone gland surface of the calling moth. To prevent a possible breakthrough of the volatile compounds collected, the walls of the second capillary were cooled by placing a piece of ice on the outside of the capillary. After a collection period of 20–30 min the capillaries were rinsed with 2–3 μl of solvent by letting the plug of solvent pass two or three times along the total length of the capillaries. The remaining volume of solvent was then taken out from the end of the capillary with a Hamilton microsyringe and was either injected directly into the gas chromatograph or combined with further rinsings and stored for later analysis in a glass ampoule sealed with a flame. A simultaneous blank collection was conducted in a similar way by holding the open end of the capillary at a distance of several centimetres from the calling moths.

Collection of volatile compounds from the pheromone glands of dead females was conducted in a similar manner. The pheromone gland of a dead female moth was artificially held in an exposed position by a pair of fine forceps and the open end of the capillary was held at a distance of 1–2 mm from the gland surface.

For preparation of direct pheromone gland extracts, the terminal segments of the abdomina of females were excised and extracted in small volumes (5 μl per female) of *n*-pentane or *n*-hexane (analytical-reagent grade; Merck, Darmstadt, Germany) for 15 min.

Analysis

Extracts obtained from *M. brassicae* and *H. armigera* were analysed by gas chromatography with flame ionization detection (GC–FID). An HP-5890 gas chromatograph (Hewlett-Packard, Avondale, PA, USA) equipped with an SP-2340 (Supelco, Bellefonte, PA, USA) fused-silica capillary column (30 m × 0.32 mm I.D.) was used. This column was temperature programmed as follows: 60°C for 2 min isothermal, increased at 10°C/min to 100°C, then at 5°C/min to 220°C, followed by an isothermal hold at this temperature. Splitless injections at 210°C were made in 2μl of solvent.

Extracts of *M. oleracea* and *C. clathrata* were analysed by GC–mass spectrometry (MS) using a VG Tribrid double-focusing magnetic sector mass spectrometer (VG Analytical, Manchester, UK) operating in the electron impact (EI) ionization mode (70 eV, 180°C). EI mass spectra (*m/z* 35–485, 1.16 s per scan) were recorded at nominal resolution. In this instance an SE-54 high-resolution fused-silica GC column (25 m × 0.32 mm I.D.) was used and temperature programmed as follows: 60°C for 2 min isothermal, increased at 20°C/min to 140°C, then at 5°C/min to 280°C, followed by an isothermal hold at this temperature. The samples (2 μl in *n*-hexane or *n*-pentane) were injected on-column at 60°C. Data acquisition was started at 140°C and retention times were measured from this point.

RESULTS AND DISCUSSION

In *H. armigera* the major component in direct gland extracts and collections of volatile compounds from live or dead females (Fig. 1A, B and D) had a retention time identical with that of synthetic (*Z*)-11-hexadecenal. Likewise, small peaks (2–5% of the major component) were detected at the retention times of (*Z*)-9-hexadecenal and hexadecanal in all of the above samples. These three components have been reported as sex pheromone components of *H. armigera* in similar ratios [9].

The major component in both the gland extract and of volatile collection compounds from dead females in *M. brassicae* (Fig. 2A and D) had a reten-

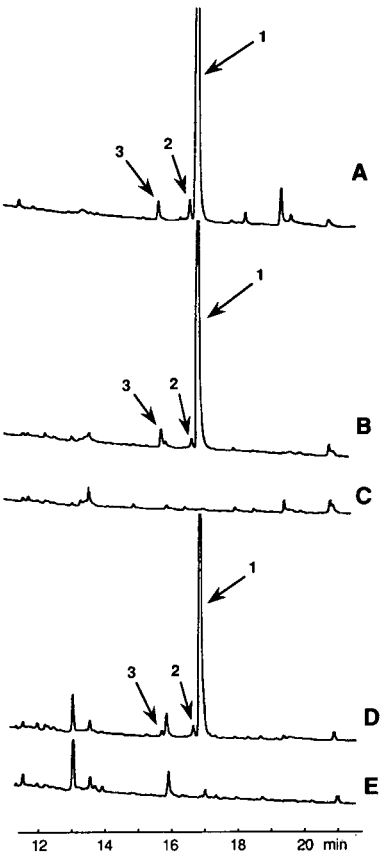

Fig. 1. Chromatograms (FID) of extracts obtained from *H. armigera* females. (A) 0.5 FE (female equivalent) of direct pheromone gland extract; (B) 1 FHE (female hour equivalent) of volatile collection from living females; (C) corresponding blank collection; (D) 0.3 FHE of collection of volatile compounds from dead females; (E) corresponding blank collection. Peaks 1, 2 and 3 coincided with respect to retention time with synthetic (*Z*)-11-hexadecenal, (*Z*)-9-hexadecenal and hexadecanal, respectively.

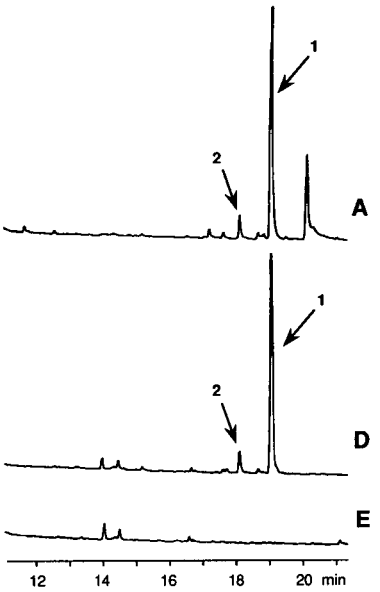

Fig. 2. Chromatograms (FID) of extracts obtained from *M. brassicae* females. (A) 0.7 FE of direct pheromone gland extract; (D) 0.2 FHE of collection of volatile compounds from dead females; (E) corresponding blank collection. Peaks 1 and 2 coincided with respect to retention time with synthetic (*Z*)-11-hexadecenyl acetate and hexadecyl acetate, respectively.

tion time identical with that of (*Z*)-11-hexadecenyl acetate. A smaller peak (*ca.* 5%) was detected at the retention time of hexadecyl acetate. Both compounds have been described as sex pheromone components in this species [10].

In *M. oleracea* (Fig. 3A and D), the presence of (*Z*)-11-hexadecenyl acetate and (*Z*)-11-hexadecenol was verified by comparison of the retention times and mass spectra in both the gland extract and the collection of volatile compounds from dead females. The acetate-to-alcohol ratios were 4:1 and 1.6:1 in the gland extract and in the collection of volatile compounds, respectively. The same two compounds have been reported as sex pheromone components of *M. oleracea* [11].

The presence of (6*Z*,9*Z*)-6,9-*cis*-3,4-epoxyheptadecadiene, previously identified as the main component of the sex pheromone of *C. clathrata* [12], was detected by GC–MS analysis of both gland extracts and collections of volatile compounds from living females (Fig. 4A and B).

In all four species studied the presence of known pheromone components was detected in both collections of volatile compounds and direct gland extracts. The only significant qualitative difference observed was that some peaks present in the gland extracts were not found in the collections of volatile compounds (Figs. 1A, B and D; 2A and D and 4A and B). The four species studied produce four different molecular types of pheromones: long-chain monounsaturated acetates (*M. brassicae, M. oleracea*), alcohols (*M. oleracea*), aldehydes (*H. armigera*) and epoxides derived from polyunsaturated hydrocarbons (*C. clathrata*). The present method for the collection of volatile compounds seems to be

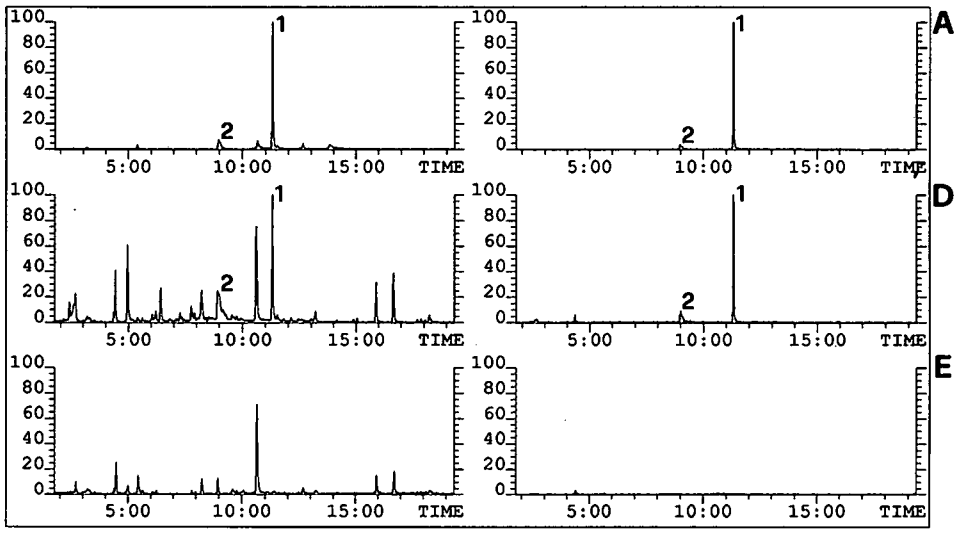

Fig. 3. Reconstructed total ion chromatograms (left) and mass chromatograms (*m/z* 222) selective for hexadecenyl acetates ($M^+ - 60$) and alcohols ($M^+ - 18$) (right) of extracts obtained from *M. oleracea* females. (A) 0.7 FE of direct pheromone gland extract; (D) 1.0 FHE of collection of volatile compounds from dead females; (E) corresponding blank collection. Peaks 1 and 2 coincided with respect to retention time and mass spectrum with synthetic (*Z*)-11-hexadecenyl acetate and (*Z*)-11-hexadecenol, respectively. Time in min.

capable of collecting pheromones with all these structures.

Gland extracts similar to those analysed here are frequently used in identification projects of unknown pheromones. In this study, comparable amounts of the main pheromone components were collected from collections of volatile compounds from living or dead females, and gland extracts (Table I). Consequently, extracts collected in capillaries by the present method could be used for the analysis

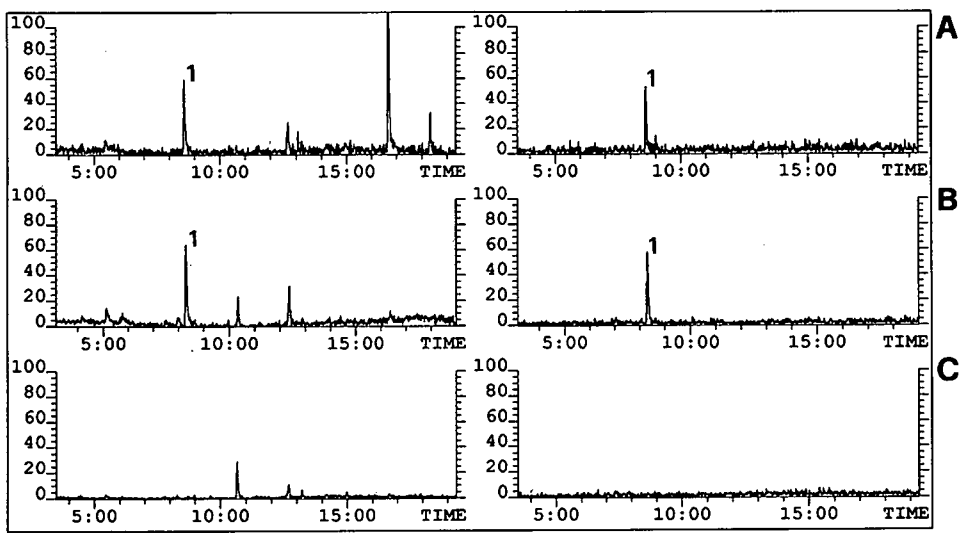

Fig. 4. Reconstructed total ion chromatograms (left) and mass chromatograms (*m/z* 178) selective for (6*Z*,9*Z*)-6,9-*cis*-3,4-epoxyheptadecadiene (right) of extracts obtained from *C. clathrata* females. (A) 1.0 FE of direct pheromone gland extract; (B) 1 FHE of collection of volatile compounds from living females; (C) corresponding blank collection. Peak 1 coincided with respect to retention time and mass spectrum with synthetic (6*Z*,9*Z*)-6,9-*cis*-3,4-epoxyheptadecadiene. Time in min.

TABLE I

AMOUNTS OF MAJOR PHEROMONE COMPONENTS IN GLAND EXTRACTS, AND IN COLLECTIONS OF VOLATILE COMPOUNDS FROM LIVING OR DEAD FEMALE MOTHS OF FOUR LEPIDOPTERAN SPECIES

Species	Collection of volatile compounds		Gland extract (ng/FE)[a]
	From living females (ng/FHE)[a]	From dead females (ng/FHE)[a]	
H. armigera	7.1 ($n=3$)	15.0 ($n=1$)	8.1 ($n=5$)
M. brassicae	24.7 ($n=4$)	24.9 ($n=9$)	63.8 ($n=6$)
M. oleracea	n.a.	5.9 ($n=6$)	16.0 ($n=6$)
C. clathrata	4.9 ($n=3$)	n.a.	3.2 ($n=5$)

[a] Amounts for (*Z*)-11-hexadecenal, (*Z*)-11-hexadecenyl acetate and (6*Z*,9*Z*)-6,9-*cis*-3,4-epoxyheptadecadiene are given for *H. armigera*, the two *Mamestra* species and *C. clathrata*, respectively. FE = Female equivalent; FHE = female hour equivalent; n.a. = not analysed; n = number of females analysed.

of unknown pheromones. Such extracts may represent more reliably the actual ratios of pheromone components released. In this study there was a clear difference between the ratios of (*Z*)-11-hexadecenyl acetate and the corresponding alcohol in extracts obtained by collection of volatile compounds and by gland extraction (Fig. 3A and D). The difference observed may reflect the difference in volatilty of an acetate *vs.* an alcohol. It is interesting that in *H. armigera* or *M. brassicae*, where all pheromone components are aldehydes or acetates, respectively, no significant difference in ratios was observed between collections of volatile compounds and gland extracts (Figs. 1A, B and D and 2A and D).

Peaks in the collections of volatile compounds originating from contaminants in the laboratory atmosphere did not seem to interfere severely with the analysis of the pheromone components (Figs. 1–4B *vs.* C and D *vs.* E). This is possible because the volatile compounds are collected in the close vicinity of their source, and their concentration in the air sampled (ng/l) is therefore likely to exceed the concentration of general contaminants present in the atmosphere. In instances where such contamination hinder the analysis, a curtain of clean air in the vicinity of the source of volatile compounds may be of advantage.

In this study, we did not detect a significant breakthrough of compounds past the cooled part of the micropipette. When collecting more volatile compounds, it may be advantageous to cool the micropipette with dry-ice. On the other hand, this may lead to plugging of the pipette with ice, as water vapour from the air sampled condenses and freezes [7].

The main advantages of the present collection method are its ease of use and simplicity. From a biological viewpoint, it is very advantageous that the insects are not enclosed in small and sometimes sophisticatedly built containers, which could interfere with their normal behaviour, as in earlier methods [7,8]. By directly observing the behaviour of the insects, collection bouts can be restricted to well defined periods, thereby making it possible to analyse volatile compounds emitted while the insects exhibit different types of behaviour.

Although so far the method has been applied only under laboratory conditions, it should easily adaptable to field conditions, if a transferable electric source is provided for the pumps. This would allow collections of volatile compounds from insects in their natural habitats, which would facilitate the interception and identification of chemical messages in natural contexts of their release and reception.

The small volumes of solvents used to rinse off the volatile compounds collected will allow the direct analysis of samples from single insects, and collected in a relatively short period of time.

Apart from collecting volatile compounds from insects, the proposed method could also be used for the monitoring of components emitted from artificial sources, *e.g.*, rubber septa, which are most frequently used as pheromone dispensers in commer-

cial attractant traps. In a preliminary test we collected volatile compounds from a rubber septum treated with a 100-μg dose of a mixture of (*Z*)-7-dodecenyl acetate and (*Z*)-9-tetradecenyl acetate. Whereas the stock solution of these compounds applied to the rubber septum contained 84.7% of the tetradecenyl acetate (as compared with the amount of the dodecenyl compound), rinses of the capillaries contained only 28.9%; such a change to a lower percentage of the less volatile tetradecenyl compound was to be expected. A more accurate knowledge of ratios emitted can help in, among others, optimization of blend ratios of artificial attractants.

The main disadvantage of the proposed collection method is that in its present form it yields only qualitative results. As it operates as an open system, only a portion of the volatile compounds emitted can be collected. The method may be improved by introducing an internal standard, *i.e.*, a volatile source which emits a compound at a known release rate.

Despite the above drawbacks, the proposed method for the collection of volatile compounds is recommended for use first of all in pheromone identification projects, supplementing other sample collection methods, *e.g.*, solvent extraction of glands, GC with solid-sample injection of single pheromone glands [13,14] or in other areas where rapid qualitative monitoring of emitted compounds is required.

Recently, the application of adsorption traps with activated charcoal particles embedded on the inside surface of glass capillary tubes and of capillary traps containing films of a non-polar stationary phase has been described for use in the headspace detection of volatile organic compounds in gas samples [15]. Such capillary traps will evidently have a greater trapping capacity than the empty capillaries used in this study. However, for the time being the application of such adsorption traps will possibly be limited to the few laboratories with the expertise and instrumentation needed for their complicated preparation and use.

ACKNOWLEDGEMENTS

Technical assistance in providing insect material by A. Suvada is gratefully acknowledged. This research was partially supported by grants OTKA of the Hungarian Academy of Sciences and of the Swiss National Science Foundation.

REFERENCES

1 T. C. Baker, L. K. Gaston, M. Mistrot Pope, L. P. S. Kuenen and R. S. Vetter, *J. Chem. Ecol.*, 7 (1981) 961.
2 L. B. Bjostad, L. K. Gaston and H. H. Shorey, *J. Insect Physiol.*, 26 (1980) 493.
3 K. J. Byrne, W. E. Gore, G. T. Pearce and R. M. Silverstein, *J. Chem. Ecol.*, 1 (1975) 1.
4 M. Ma, H. E. Hummel and W. E. Burkholder, *J. Chem. Ecol.*, 6 (1980) 597.
5 D. Morse, R. Szittner, G. G. Grant and E. A. Meighen, *J. Insect Physiol.*, 28 (1982) 863.
6 J. H. Tumlinson, R. R. Heath and P. E. A. Teal, in B. A. Leonhardt and M. Beroza (Editors), *Insect Pheromone Technology: Chemistry and Applications* (*ACS Symposium Series*, No. 190), American Chemical Society, Washington, DC, 1982, pp. 1–27.
7 A. Shani and M. J. Lacey, *J. Chem. Ecol.*, 10 (1984) 1677.
8 P. Witzgall and B. Frérot, *J. Chem. Ecol.*, 15 (1989) 707.
9 M. Kehat and E. Dunkelblum, *J. Insect Behav.*, 31 (1990) 75.
10 D. L. Struble, H. Arn, H. R. Buser, E. Städler and J. Freuler, *Z. Naturforsch. C*, 35 (1979) 45.
11 C. Descoins, E. Priesner, M. Gallois, H. Arn and G. Martin, *C.R. Acad. Sci. Sér. D*, 286 (1978) 77.
12 M. Tóth, G. Szöcs, C. Löfstedt, B. S. Hansson, F. Schmidt and W. Francke, *Z. Naturforsch. C*, 46 (1991) 257.
13 A. B. Attygalle, M. Herrig, O. Vostrowsky and H. J. Bestmann, *J. Chem. Ecol.*, 13 (1987) 1299.
14 E. D. Morgan, *Anal. Chim. Acta*, 236 (1990) 227.
15 B. V. Burger, M. Le Roux, Z. M. Munro and M. E. Wilken, *J. Chromatogr.*, 552 (1991) 137.

Journal of Chromatography, 598 (1992) 309–312
Elsevier Science Publishers B.V., Amsterdam

CHROM. 24 011

Short Communication

Intra-injector formation of methyl esters from phenoxy acid pesticides

Ilia Brondz*,☆

Research Department, National Institute of Occupational Health, Umeå (Sweden)

Ingar Olsen

Department of Microbiology, Dental Faculty, University of Oslo, Oslo (Norway)

(First received August 20th, 1991; revised manuscript received January 14th, 1992)

ABSTRACT

Trimethylanilinium hydroxide was used as a derivatization agent for a broad range of phenoxy acids. Derivatization took place inside the injector immediately before gas chromatographic analysis, thereby minimizing the chance of exposing the operator to trimethylanilinium hydroxide. The reproducibility and sensitivity of the derivatization procedure were high. Maximum sensitivity for 19 phenoxy acids was 0.1–0.3 ppm. Derivatization was quantitative and did not produce by-products. The procedure required a minimum of time and effort compared with other derivatization methods in current use and is recommended for routine determinations of phenoxy acids.

INTRODUCTION

Phenoxy acids are widely used in forestry and agriculture as regulators of plant growth [1]. As an example, herbicides represent 80% of the crop protection chemicals used in Sweden, and phenoxy acids account for 65% of these herbicides [2]. An important characteristic of phenoxy acids is their selectivity. Phenoxy acids affect most of the dicotyledonous plants, whereas monocotyledonous plants and cereals are not influenced by the concentrations used in agriculture. Unfortunately, phenoxy acids are not sufficiently stable or volatile to be determined by gas chromatography (GC) without derivatization.

Several methods have been used for the derivatization of such acids. Cochrane [3] reviewed esterification and transesterification of phenoxy acids: 2,4-dichlorophenoxypropionic acid (2,4-D), 2,4,5-trichlorophenoxypropionic acid (2,4,5-T) and 4-chloro-2-methylphenoxyacetic acid (MCPA) have been esterified with sulphuric acid–*n*-propanol and 2,4-D and 2,4,5-T with sulphuric acid–methanol. Solutions of boron trifluoride in methanol, *n*-butanol or 2-chloroethanol have been applied to esterify 2,4-D, picloram, 2,4,5-T and other herbicidal acids. Further, diazomethane has been used to esterify 2,4-D, dicamba, MCPA, picloram and 2,4,5-T. Overall, diazomethane is the most frequently used derivatization agent for phenoxy acids but, because of the toxicity, carcinogenicity and explosiveness of

☆ Present address: Department of Herbology, Norwegian Plant Protection Institute, Box 70, 1432 Ås-NLH, Norway.

0021-9673/92/$05.00

this substance, alternative compounds are being sought.

In a previous study [4], we introduced trimethylanilinium hydroxide (TMAH) as a derivatization agent in the clinical laboratory for free fatty acids extracted from bateria. The aim of this study was to examine whether TMAH can be used for the derivatization of a broad range of phenoxy acids, and to see if this derivatization procedure can be carried safely out inside the injector. Phenoxy acids, which are derivatives from formic, acetic, propionic and butyric acids, undergo the same chemical reactions as do fatty acids [4–6].

EXPERIMENTAL

Chemicals

The phenoxy acid standards included in this study, their sources and their retention times (t_R) in the gas chromatograph used are given in Table I. MethElute methylating agent (Pierce Europe, Oud Beijerland, Netherlands), containing 0.2 *M* TMAH in anhydrous methanol, was also applied.

Sample preparation

Standards of phenoxy acids were dissolved in anhydrous methanol at concentrations of 1–2 ppm. Of this solution 100 μl were transferred using a Hamilton syringe to a glass vial and dried with nitrogen. The vial was closed and 100 μl of TMAH in methanol (see *Chemicals*) were injected into the vial after perforation of its closing rubber membrane. GC and GC–mass spectrometry (GC–MS) were performed immediately after derivatization and after storage of the derivatized phenoxy acids for 4 days.

GC of derivatized phenoxy acids

A Model 8700 gas chromatograph (Perkin-Elmer, Norwalk, CT, USA) was used with a fused-silica capillary column (15 m × 0.25 mm I.D.) with a film thickness of 0.25 μm of the stationary phase CP-Sil 5 methylphenylsilicone (Chrompack, Middelburg, Netherlands). Helium served as the carrier gas at a flow-rate of 2.0 ml/min. The temperature of the injector was 240°C and that of the flame ionization detector was 275°C. The column temperature programme was 90°C, held for 1 min, and then increased from 90 to 290°C at 6°C/min. The attenuator was set at 8. The chart paper speed was 10 mm/min. The sample (2 μl) was delivered as a splitless injection.

GC–MS

The instrument used for GC–MS consisted of a Model 8700 gas chromatograph furnished with an ion-trap detector (Perkin-Elmer). For the chromatographic conditions, see the previous section.

The derivatization procedure was controlled using 1 ppm of MCPA and MCPA methyl ester (Pestanal; Riedel-de Häen, Seelze, Germany). The reaction products were determined by GC–MS.

RESULTS AND DISCUSSION

The retention time of the TMAH reagent was less than 10 min (Fig. 1). Thereafter, the derivatized

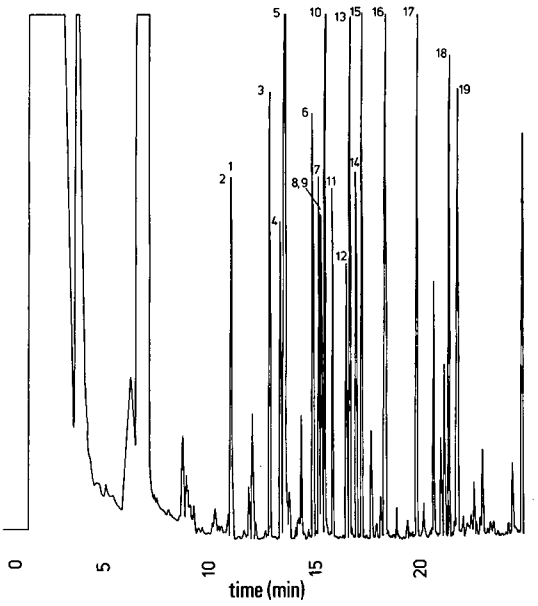

Fig. 1. Gas chromatogram of TMAH derivatized phenoxy acid standards. For conditions, see text. Peaks: 1 = 2-phenoxypropionic acid; 2 = *p*-fluorophenoxyacetic acid; 3 = 2-methylphenoxyacetic acid; 4 = 3-methylphenoxyacetic acid; 5 = 4-methylphenoxyacetic acid; 6 = 2-formylphenoxyacetic acid; 7 = 2,5-dimethylphenoxyacetic acid; 8 = 2-(4-chlorophenoxy)propionic acid; 9 = 2,4-dimethylphenoxyacetic acid; 10 = 2-methoxyphenoxyacetic acid; 11 = 4-phenoxybutyric acid; 12 = 3-methoxyphenoxyacetic acid; 13 = 4-methoxyphenoxyacetic acid, 14 = 2-(4-chloro-2-methylphenoxy)propionic acid; 15 = 4-chloro-2-methylphenoxyacetic acid; 16 = 2,4-dichlorophenoxypropionic acid; 17 = 4-iodophenoxyacetic acid; 18 = α-(2,4,5-trichlorophenoxy)propionic acid; 19 = 2,4,5-trichlorophenoxyacetic acid.

phenoxy acid standards appeared at various intervals (Table I, Fig. 1). The reproducibility of the TMAH derivatization procedure was high, as was its sensitivity. Based on five parallel measurements with a 1 ppm solution of MCPA (see under *GC–MS*), the S.D. was 3%. The maximum sensitivity for the nineteen phenoxy acids shown in Fig. 1 was 0.1–0.3 ppm. When only those phenoxy acids most frequently used in agriculture were considered, the sensitivity was 0.1–0.2 ppm. There was no difference in the chromatographic pattern of the immediately injected reaction mixture and the pattern of that injected after 4 days.

GC–MS fragmentation of the methyl ester from MCPA is shown in Fig. 2. The GC–MS fragmentation pattern agreed with that of the authentic standard. Derivatization with TMAH was quantitative and did not produce any by-products. Similar results were achieved with free fatty acids [4,6].

In order to test the methylphenylsilicone stationary phase, 300 injections were made into the column. No broadening of peaks or changes in retention values were observed. The chance of exposing the operator to TMAH was minimal as the derivatization occurred inside the injector immediately before GC.

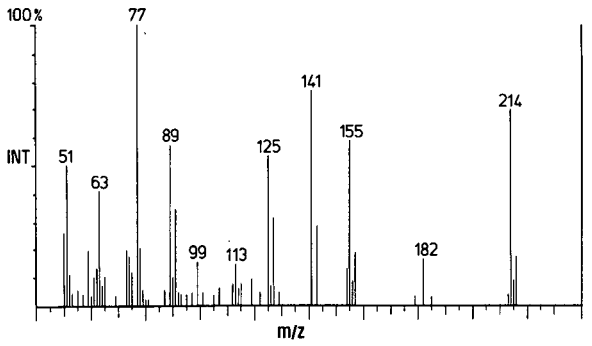

Fig. 2. Electron impact mass spectrum of the methyl ester from MCPA.

We have suggested "intra-injector derivatization" as a more appropriate term for this mode of

TABLE I

SOURCES AND RETENTION TIMES OF PHENOXY ACID STANDARDS EXAMINED BY GAS CHROMATOGRAPHY

Acid	Source	Retention time (min)
2-Phenoxypropionic	Janssen[a]	11.11
p-Fluorophenoxyacetic	Janssen	11.16
2-Methylphenoxyacetic	Ventron[b]	13.00
3-Methylphenoxyacetic	Ventron	13.45
4-Methylphenoxyacetic	Ventron	13.60
2-Formylphenoxyacetic	Ventron	14.85
2,5-Dimethylphenoxyacetic	Ventron	15.00
2-(4-Chlorophenoxy)propionic	Janssen	15.25
2,4-Dimethylphenoxyacetic	Ventron	15.30
2-Methoxyphenoxyacetic	Ventron	15.60
4-Phenoxybutyric	Ventron	15.90
3-Methoxyphenoxyacetic	Ventron	16.70
4-Methoxyphenoxyacetic	Ventron	16.85
2-(4-Chloro-2-methylphenoxy)propionic	Aldrich-Chemie[c]	17.05
4-Chloro-2-methylphenoxyacetic	Aldrich-Chemie	17.30
2,4-Dichlorophenoxypropionic	Sigma[d]	18.30
4-Idophenoxyacetic	Ventron	19.90
α-(2,4,5-Trichlorophenoxy)propionic	Sigma	21.40
2,4,5-Trichlorophenoxyacetic	Aldrich-Chemie	21.80

[a] Janssen Chemica, Beerse, Belgium.
[b] Ventron, Karlsruhe, Germany.
[c] Aldrich-Chemie, Steinheim, Germany.
[d] Sigma, St. Louis, MO, USA.

derivatization than "on-column derivatization" [4]. TMAH in methanol has, according to our information, not previously been used for the derivatization of a broad range of phenoxy acids. The procedure requires a minimum of time and effort compared with other derivatization methods in current use [3] and is recommended for routine determinations of phenoxy acids.

ACKNOWLEDGEMENT

We thank the Swedish Medical Research Council (stipend K 90-16F-9251-01) for financial support.

REFERENCES

1 M. E. Synerholm and P. W. Zimmerman, *Contrib. Boyce Thompson Inst.*, 14 (1945) 91.
2 M. Åkerblom, B. Kolmodin-Hedman and S. Höglund, in J. Miyamoto *et al.* (Editors), *IUPAC Pesticide Chemistry. Human Welfare and the Environment*, Pergamon Press, Oxford, 1983, pp. 229–232.
3 W. P. Cochrane, *J. Chromatogr. Sci.*, 17 (1979) 124.
4 I. Brondz and I. Olsen, *J. Chromatogr.*, in press.
5 J. J. Bailey, *Anal. Chem.*, 39 (1967) 1485.
6 B. S. Middleditch and D. M. Desiderio, *Anal. Lett.*, 5 (1972) 605.

Journal of Chromatography, 598 (1992) 313–315
Elsevier Science Publishers B.V., Amsterdam

CHROM. 24 082

Short Communication

Flame-photometric detection of nitrous oxide in addition to phosphine

Guenter Gassmann*

Biologische Anstalt Helgoland, Zentrale Hamburg, Notkestrasse 31, D-2000 Hamburg 52 (Germany)

Sven Dahlke

Biologische Station Hiddensee, Universität Greifswald, D-2346 Kloster (Germany)

(First received November 21st, 1991; revised manuscript received February 4th, 1992)

ABSTRACT

Nitrous oxide can be separated from phosphine in a short (10 m) capillary column coated with a porous layer of Porapack Q, and determined under phosphorus-sensitive flame-photometric detection (P-FPD) conditions at 526 nm. The detection limits of nitrous oxide depend on the detector gas flows. A high oxygen/hydrogen ratio (0.8) is favourable to the nitrous oxide determination with a detection limit of $20 \cdot 10^{-12}$ m^3. The specificity of P-FPD remains at the 100:1 ratio in favour of phosphine.

INTRODUCTION

During experiments aimed at detecting traces of phosphine in marine sediments by gas chromatographic (GC) separation and flame-photometric detection (FPD), nitrous oxide gave positive detector responses under phosphorus-selective conditions. These very disturbing results caused us to investigate in more detail the detectability of nitrous oxide by phosphorus-selective FPD (P-FPD), since the specific detection of nitrous oxide under phosphorus-selective conditions was hitherto unknown. Generally, nitrogen-containing compounds show a weak emission of NH_2 bands between 440 and 700 nm and of CN bands between 385 and 388 nm [1] (see also ref. 2).

Nitrous oxide is a conservative constituent of the atmosphere. The ambient concentration is about 300 mm^3 m^{-3}. The most sensitive method of detecting nitrous oxide involves high-temperature electron capture detection [3,4]. The detection limit is about $10 \cdot 10^{-15}$ m^3. Phosphine, used in the food industry and by electronic chip manufacturers as a fumigant and as a dopant, respectively, can be selectively detected by flame photometry [5,6] at a wavelength of 526 nm with a detection limit of $0.5 \cdot 10^{-15}$–$1 \cdot 10^{-15}$ m^3.

MATERIALS AND METHODS

Phosphine (0.5%, v/v) in nitrogen and nitrous oxide were obtained from Messer-Griesheim. A Carlo Erba GC 2900 gas chromatograph equipped with a phosphorus (526 nm) flame photometric detector (Model SSD-250) and a Hitachi-Merck recording integrator (Model D-2500) were used. The gaseous samples were introduced from a pressurized 1-dm^3 glass flask through a fused-silica capil-

0021-9673/92/$05.00

lary trap (3 m × 0.1 mm) cooled with liquid nitrogen into a capillary column (Chrompack Poraplot Q, 10 m × 0.32 mm × 10 μm). The sample gas flow and volume were measured by a flow meter and a gas burette connected between the capillary trap and analytical column by a three-way capillary valve (Gerstel GC 02943-31). The GC conditions were: carrier gas, hydrogen; pressure, 10^5 Pa (2.8 cm^3 min^{-1}); oven temperature, 313 K, detector temperature, 448 K; detector gases, hydrogen 0.8 · 10^5–1.3 · 10^5 Pa (20–45 cm^3 min^{-1}), air 2.5 · 10^5–3.5 · 10^5 Pa (90–130 cm^3 min^{-1}).

RESULTS

Two sets of experiments with constant chromatographic but variable detector conditions were carried out. For the first set (indicated by a Roman numeral I in Fig. 1) we chose a detector gas flow of hydrogen (20 cm^3 min^{-1}) and air (90 cm^3 min^{-1}) just at the point where the flame would be extinguished by increasing air flow or decreasing hydrogen flow. These were very unfavourable conditions for the detection of phosphorus compounds. Therefore, phosphine can only be detected in the 200 · 10^{-15}–600 · 10^{-15} m^3 range. For the detection of nitrous oxide, these gas flows are highly favourable. Nitrous oxide can be detected in the 20 · 10^{-12}–400 · 10^{-12} m^3 range (see also Fig. 2). The detection limit for phosphine is 200 · 10^{-15} m^3 and for nitrous oxide 20 · 10^{-12} m^3. Obviously, the specificity of the detector remains at the 100:1 ratio in favour of the phosphorus compound at the detection limits.

In the second set of experiments (indicated by the Roman numeral II in Fig. 1), the detector gas flows (45 cm^3 min^{-1} for hydrogen and 130 cm^3 min^{-1} for air) were increased in order to establish a level of flame stability whereby small changes in both flows would not significantly change the detector signal. The detection of phosphine increases drastically (to the 5 · 10^{-15}–100 · 10^{-15} m^3 range), while the detector response of nitrous oxide turns out to be ambiguous. The detector response for higher mass flows increases while lower mass flows are less detectable. The detection limit for phosphine in this case was 5 · 10^{-15} m^3 and for nitrous oxide 100 · 10^{-12} m^3. The detector specificity for phosphorus over nitrous oxide turns in favour of phosphine to 20 000:1.

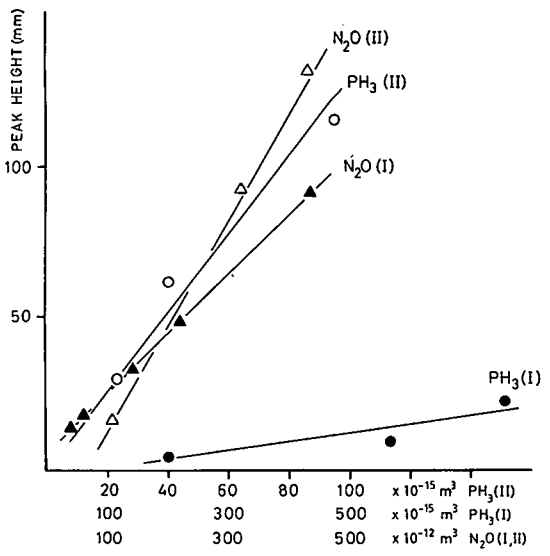

Fig. 1. Peak heights *versus* different amounts of nitrous oxide (N_2O) and phosphine (pH 3) depending on detector gas flows: I = 20 cm^3 min^{-1} hydrogen and 90 cm^3 min^{-1} air; II = 45 cm^3 min^{-1} hydrogen and 130 cm^3 min^{-1} air.

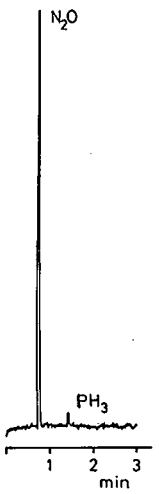

Fig. 2. Nitrous oxide (540 · 10^{-12} m^3) and phosphine (275 · 10^{-15} m^3) separated on a Poraplot Q capillary column (10 m × 0.32 mm × 10 μm) and detected by P-FPD with detector gas flows of 20 cm^3 min^{-1} hydrogen and 90 cm^3 min^{-1} air.

DISCUSSION

The detection limits of phosphine and nitrous oxide shown in these experiments are not at all impressive. Other flame photometric detectors exhibit a much better performance for the detection of phosphine. FPD of nitrous oxide is 2000 times less sensitive than electron-capture detection. Nevertheless, it is very disturbing that nitrous oxide may interfere with the phosphine determination in cases where a complete chromatographic separation has not been achieved. In such cases, the presence of a phosphorus compound might be presumed where in fact only higher levels of nitrous oxide are present. As the discussion on the presence or absence of phosphine in nature has intensified [7], the demonstration of a positive P-FPD response to nitrous oxide shows that the interpretation of this signal as "phosphorus"-containing or even as "phosphine" must be regarded with caution.

ACKNOWLEDGEMENTS

The financial support by the BMFT Project No. 03F0564 is gratefully acknowledged.

REFERENCES

1 R. S. Braman, *Anal. Chem.*, 38 (1966) 734.
2 W. A. Aue, B. Millier and Xun-Yun Sun, *Anal. Chem.*, 63 (1991) 2951.
3 W. E. Wentworth and R. R. Freeman, *J. Chromatogr.*, 79 (1973) 322.
4 R. A. Rasmussen, J. Krasnec and D. Pierotti, *Geophys. Res. Lett.*, 3 (1976) 615.
5 B. Berk, W. E. Westlake and F. A. Gunther, *J. Agr. Food Chem.*, 18 (1970) 143.
6 H. Nozoye and K. Someno, *Bunseki Kagaku*, 34 (1985) 508.
7 I. Devai, L. Felföldy, I. Wittner and S. Plosz, *Nature (London)*, 333 (1988) 343.

Journal of Chromatography, 598 (1992) 316
Elsevier Science Publishers B.V., Amsterdam

CHROM. 24 136

Book Review

Eucalyptus leaf oils: use, chemistry, distillation and marketing, edited by D. J. Boland, J. J. Brophy and A. P. N. House, ACIAR/CSIRO Inkata Press, Melbourne, Sydney, 1991, 252 pp., price A$ 65.00.

This timely update comes thirty years after the last comprehensive work on the chemistry and utilisation of *The Eucalypts* (Penfold and Willis [1]). Division into three two-chapter parts separates discussion on the history and biology of oil production (Part I) from reference lists of eucalyptus oil constituents (Part II) and commercial aspects of distillation and marketing (Part III).

The history of eucalyptus oil research and development in Australia in the context of the current world market situation is outlined in Chapter 1. Chapter 2 begins with a summary of oil uses and then discusses the biology and biochemistry of eucalyptus oil formation. High-quality, informative photographs of leaf surfaces and oil glands along with a summary of current thinking on the role of constituents make this a highly readable chapter. Some definitive conclusions about progeny trials are reached but generally the need for more basic research and more carefully controlled experiments is stated. Chapters 3 and 4 are useful reference sections suggesting alternative sources of cineole and list eucalyptus as a source of compounds such as nerolidol, tasmanone, methyl cinnamate, benzaldehyde, geranyl acetate, jensenone etc. (see also Appendix 4). Half of the bulk of the book is contained in Chapter 3 which lists 111 eucalypts using a one-page-per-taxa format with tree description, range of leaf oil constituents, record of oil yield and use along with a species distribution map. The following chapter constitutes a table updating Penfold and Willis's 1961 data with the Chapter 3 data and information from the literature. This compilation of 300 taxa (over 400 entries) now supersedes all earlier lists (Penfold and Morrison [2], Penfold and Willis [1] and becomes the authoritative eucalyptus oil constituent reference collection. Australian distillation procedures provide an excellent basis for Chapter 5 which describes still design and distillation practise with such detailed diagrammatic explanations that basic processing plants could be built using this chapter alone. Practical aspects of marketing oils are outlined in Chapter 6 and several appendices give useful data (*e.g.*, collection locations, chemical structures) for specialised interests.

The production is remarkably free from error except for the occasional textual error (*e.g.*, isopentyl in Fig. 2.4) and a few more obvious type print misalignments. A general index in addition to the species index would have been helpful. Lodging voucher specimens for the Chapter 3 study may have enabled future workers to avoid the lack-of-reference problems encountered by the present contributors (*cf.*, Chapter 4). Photographs are informative in black and white. The explanatory note on the Chapter 3 maps could have been better positioned and contributors deserve more prominent credit by name at the commencement of each chapter. A good cover design is spoilt by choice of colour —the silver on green is illegible in some lighting conditions.

The Editors' Preface statement that the book was prepared primarily for use in developing countries does not do justice to a book that should be mandatory reading for all who deal with, or intend to deal with, eucalypts at the phytochemical, taxonomic, production, quality control or marketing level. The eucalyptus oil story also provides a convenient model for the development of other essential oils.

Wollongbar (Australia) Ian Southwell

1 A. R. Penfold and J. L. Willis, *The Eucalypts*, World Crop Series, Leonard Hill, London, and Interscience Publishers, New York, 1961, pp. 264–278.
2 A. R. Penfold and F. R. Morrison, in E. Guenther (Editor), *The Essential Oils*, Vol. 4, D. van Nostrand, New York, 1950, pp. 437–525.

Author Index

PUBLICATION SCHEDULE FOR 1992

Journal of Chromatography and *Journal of Chromatography, Biomedical Applications*

MONTH	O 1991–F 1992	M	A	M	J	
Journal of Chromatography	Vols. 585–593	594/1 + 2 595/1 + 2	596/1 596/2 597/1 + 2	598/1 598/2 599/1 + 2 600/1 600/2	602/1 + 2	The publication schedule for further issues will be published later.
Cumulative Indexes, Vols. 551–600					[a]	
Bibliography Section		610/1			610/2	
Biomedical Applications	Vols. 573 and 574	575/1 575/2	576/1	576/2 577/1	577/2	

[a] Cumulative Indexes will be Vol. 601, to appear early 1993.

INFORMATION FOR AUTHORS

(Detailed *Instructions to Authors* were published in Vol. 558, pp. 469–472. A free reprint can be obtained by application to the publisher, Elsevier Science Publishers B.V., P.O. Box 330, 1000 AH Amsterdam, The Netherlands.)

Types of Contributions. The following types of papers are published in the *Journal of Chromatography* and the section on *Biomedical Applications:* Regular research papers (Full-length papers), Review articles and Short Communications. Short Communications are usually descriptions of short investigations, or they can report minor technical improvements of previously published procedures; they reflect the same quality of research as Full-length papers, but should preferably not exceed five printed pages. For Review articles, see inside front cover under Submission of Papers.

Submission. Every paper must be accompanied by a letter from the senior author, stating that he/she is submitting the paper for publication in the *Journal of Chromatography*.

Manuscripts. Manuscripts should be typed in double spacing on consecutively numbered pages of uniform size. The manuscript should be preceded by a sheet of manuscript paper carrying the title of the paper and the name and full postal address of the person to whom the proofs are to be sent. As a rule, papers should be divided into sections, headed by a caption (*e.g.*, Abstract, Introduction, Experimental, Results, Discussion, etc.). All illustrations, photographs, tables, etc., should be on separate sheets.

Introduction. Every paper must have a concise introduction mentioning what has been done before on the topic described, and stating clearly what is new in the paper now submitted.

Abstract. All articles should have an abstract of 50–100 words which clearly and briefly indicates what is new, different and significant.

Illustrations. The figures should be submitted in a form suitable for reproduction, drawn in Indian ink on drawing or tracing paper. Each illustration should have a legend, all the *legends* being typed (with double spacing) together on a *separate sheet*. If structures are given in the text, the original drawings should be supplied. Coloured illustrations are reproduced at the author's expense, the cost being determined by the number of pages and by the number of colours needed. The written permission of the author and publisher must be obtained for the use of any figure already published. Its source must be indicated in the legend.

References. References should be numbered in the order in which they are cited in the text, and listed in numerical sequence on a separate sheet at the end of the article. Please check a recent issue for the layout of the reference list. Abbreviations for the titles of journals should follow the system used by *Chemical Abstracts.* Articles not yet published should be given as "in press" (journal should be specified), "submitted for publication" (journal should be specified), "in preparation" or "personal communication".

Dispatch. Before sending the manuscript to the Editor please check that the envelope contains four copies of the paper complete with references, legends and figures. One of the sets of figures must be the originals suitable for direct reproduction. Please also ensure that permission to publish has been obtained from your institute.

Proofs. One set of proofs will be sent to the author to be carefully checked for printer's errors. Corrections must be restricted to instances in which the proof is at variance with the manuscript. "Extra corrections" will be inserted at the author's expense.

Reprints. Fifty reprints of Full-length papers and Short Communications will be supplied free of charge. Additional reprints can be ordered by the authors. An order form containing price quotations will be sent to the authors together with the proofs of their article.

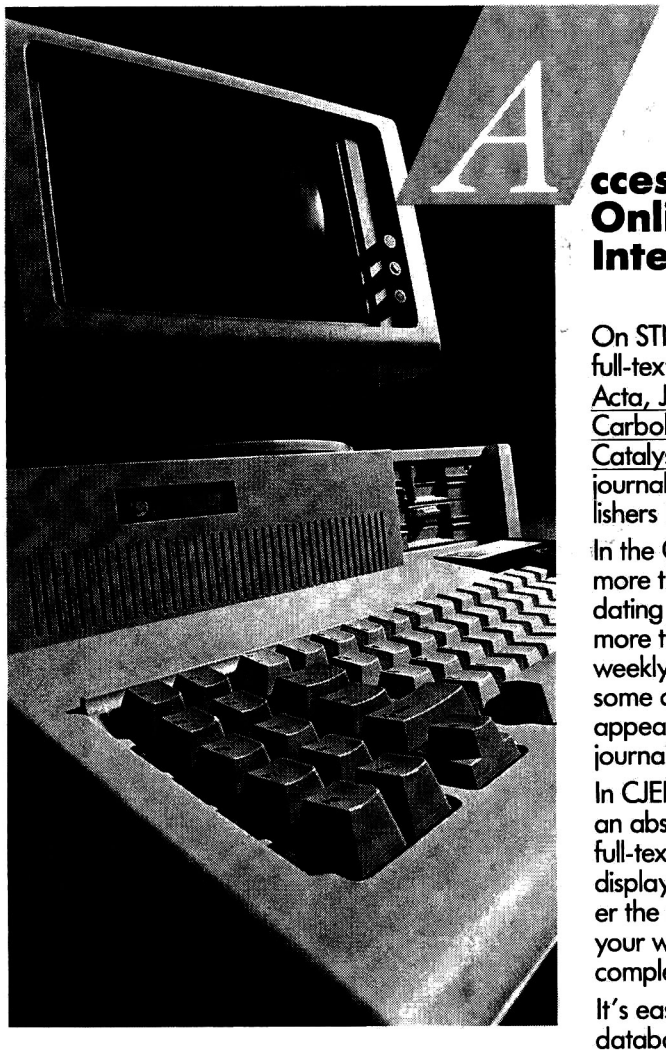

Access Elsevier Journals Online on STN International® !

On STN International, you can now access full-text articles from Analytica Chimica Acta, Journal of Organometallic Chemistry, Carbohydrate Research, and Applied Catalysis, four of the leading chemistry journals published by Elsevier Science Publishers B.V.

In the CJELSEVIER database, you'll find more than 2,400 citations added yearly, dating from 1990 to the present, with more than 50 new articles appearing weekly. The information in CJELSEVIER is some of today's most current — updates appear within the database BEFORE the journals are available!

In CJELSEVIER, you don't have to rely on an abstract or on keywords. On STN, the full-text articles are both searchable and displayable. You can quickly decide whether the material in the article is important to your work. In CJELSEVIER, you're getting complete information right from the start!

It's easy to begin searching the CJELSEVIER database on STN. Simply fill out the attached coupon. We will send you a complete packet of information on all the full-text chemistry databases on STN and an STN sign-up kit.

☐ **YES! I'd like further information on full-text chemistry searching on STN. Please rush my information kit to me.**

Name _____

Title _____

Organization _____

Address _____

_____

Telephone _____

Mail to: STN International, c/o CAS® Marketing Dept. 39990, P.O. Box 3012, Columbus, OH 43202 USA.

STN®
INTERNATIONAL
The Scientific & Technical Information Network